

Calcium signalling, pacing and rhythmic cell activity

D.F. van Helden, School of Biomedical Sciences, University of Newcastle, NSW 2308, Australia.

My interest in this area first arose while studying mesenteric veins in young guinea pigs. The mesentery is also replete with striking arrays of lymphatic vessels, demarcated into chambers by frequently occurring unidirectional valves. A feature that really caught my attention was that the lymphatic chambers at times exhibited spontaneous rhythmical contractions that acted as “primitive” hearts to propel lymph. This phenomenon was so intriguing that the recording microelectrodes, while intended for the small veins, often “magically” strayed to record electrical activity from the lymphatic smooth muscle.

The venous studies were being made to investigate spontaneous transient depolarizations (STDs), an activity reminiscent of transient depolarizations termed “bumps” that had been reported in photoreceptors. STDs also paralleled spontaneous transient hyperpolarisations that had been reported in neurons and smooth muscle, differing primarily in their polarity. We investigated these events, providing evidence that they were generated by spontaneous release of Ca^{2+} from intracellular Ca^{2+} stores and finding that the underlying currents, which we termed spontaneous transient inward currents (STICs), were likely to be generated by Ca^{2+} -activated Cl^- channels. The significance of these events took on a whole new dimension once microelectrode recordings were made in lymphatic chambers, which indicated that lymphatic smooth muscle not only exhibited STDs but that they, or summations thereof, were responsible for driving rhythmical lymphatic constrictions. This was most surprising, as prior to this pacemaking was considered to be generated by voltage-dependent channels in the cell membrane, as had been first described for heart pacemaking. The fact that Ca^{2+} stores might also act as a pacemaker introduced a very different mechanism, one operated by an intracellular pacemaker “clock” set by the release-refill cycle of Ca^{2+} stores.

The mechanism soon proved to be more widespread, having roles in other pacemaker activities such as vasomotion and gastrointestinal contractions. However, there remained a significant question, as to how the mechanism operated, given that individual Ca^{2+} release events are small and could not activate sufficient current to drive pacemaking. The key to solving this came with the realisation that stores had the capacity to interact as coupled oscillators and so coordinate their activity. A simple example of a coupled oscillator system is an array of pendulums interconnected by springs, which entrain their cycles when randomly activated. In the case of stores, coupling between stores is mediated by both diffusion of store activators between stores (*e.g.* Ca^{2+}) and by voltage coupling. The latter is mediated through transmission of membrane depolarization causing enhancement of store activators and hence store cycling. It provides some 500 fold stronger coupling between stores than does diffusion of activators. Evidence for the latter has been provided by studies on blood vessels and strips of gastric smooth muscle.

The same coupled oscillator-based mechanism can generate long-range chemical/electrical signalling within cells and cellular syncytia. The mechanism subserves a similar role as sequentially conducting action potentials, but is very different depending on Ca^{2+} stores interacting as coupled oscillators and not voltage dependent channels in the cell membrane. Importantly, while coupling between Ca^{2+} stores may lead to near synchronous local chemical/electrical signalling, substantial phase delays develop between oscillators over longer distances giving the impression of a propagating wave. We refer to such propagation as Ca^{2+} phase waves. This mechanism is likely to underlie propagation of slow waves in the gastrointestinal system and hence is of considerable importance.

Biology continues to astonish even in well-studied areas such as heart pacemaking, as it has now been shown that Ca^{2+} store-based pacemaking is also a player in the generation of heartbeats. Thus two “clocks” mediate heart pacemaking, the “classical” pacemaker in the cell membrane and the intracellular Ca^{2+} store “clock”. These interact symbiotically to produce robust heart pacemaking. Interestingly, lymphatic pacemaking under certain conditions may also be mediated by both these mechanisms and hence lymphatic “hearts” may not be as primitive as previously thought. The existence of store pacemaking and Ca^{2+} phase waves provides new therapeutic directions for treatment of various pathologies (*e.g.* arrhythmias). In case of the lymphatics, targeting the mechanism may lead to better treatments of disorders such as lymphedema. On the flip side, inhibiting the lymphatic pump may also provide a new first aid treatment for snakebite, as venoms usually first transit the lymphatic system. This subject is of some significance, as snakebite remains a world health problem with ~100,000 deaths and 400,000 amputations per year. Fortunately, this approach may have merit, as we find that lymphatic transport is considerably slowed by topical application of an agent that inhibits lymphatic pacemaking.

Perspectives on multidrug resistance in membrane transporters

A.M. George, Department of Medical and Molecular Biosciences, Faculty of Science, University of Technology Sydney, PO Box 123, Broadway, NSW 2007, Australia.

Membrane proteins constitute about 30% of all proteins and among these are a large cohort of transporters, receptors, and enzymes. Membrane transporters have become the subject of intense research over the past two decades, chiefly because many of them are responsible for a process known as drug efflux in which the drug is captured at the cell membrane and extruded to the outside, thereby protecting the cell from the action of the drug. This is best and most simply illustrated by the resistance of many bacteria to antibiotics by drug efflux. Though this is one of many mechanisms of cellular resistance to drugs, it is perhaps the most perplexing as it most often appears in the guise of multidrug resistance. In all, there are five major classes or families of membrane drug transporters, namely, the Major Facilitator Superfamily (MFS), Small Multidrug Resistance (SMR), Multidrug and Toxin Extrusion (MATE), Resistance Nodulation Division (RND), and ATP-Binding Cassette Transporter (ABC) families.

The failure of cancer chemotherapy in humans is a noted example of efflux-mediated resistance. A most insidious feature of multidrug resistance is that it is often triggered by exposure to a single drug. For example, if human tumours are treated with a cytotoxic drug, the drug will bring about unbridled expression of an ABC transporter called P-glycoprotein. Though this protein has seen only one drug, it elaborates an efflux mechanism for all known cytotoxic drugs thereby rendering chemotherapy irrelevant as a curative treatment for cancerous tumours. A single membrane transporter is capable of extruding a large number of unrelated drugs, making the cells multidrug resistant. That this mechanism is ubiquitous among all phyla makes it a major investigative topic. It was thought that recent resolved structures of some of these transporters would quickly yield the mechanistic details of multidrug resistance, but the reality is less promising. However, some important studies have given clues about the way in which specific transporters are able to extrude a diverse range of drugs.

Molecular determinants of MRP1/ABCC1 expression and transport

S.P.C. Cole, Division of Cancer Biology & Genetics, Queen's University Cancer Research Institute, Kingston, ON K7L 3N6, Canada.

The 190-kDa Multidrug Resistance Protein 1 (MRP1/ABCC1), first cloned by our group in 1992 from a drug resistant lung cancer cell line (Cole *et al.*, 1992), is a member of the 'C' branch of the ATP-binding cassette (ABC) superfamily of polytopic membrane proteins. MRP1 belongs to a subset of ABCC proteins comprising five domains: 3 membrane spanning domains (MSDs), containing 5, 6, and 6 transmembrane (TM) α -helices, respectively, and two cytoplasmic nucleotide binding domains (NBDs) (Leslie, Deeley & Cole, 2005). In addition to its drug efflux properties, MRP1 mediates the ATP-dependent transport of a broad array of exogenous and endogenous organic anions, including the cysteinyl leukotriene C₄ (LTC₄), an eicosanoid derivative that mediates inflammation and is involved in human bronchial asthma (Leslie, Deeley & Cole, 2005; Cole & Deeley, 2006). Thus MRP1 plays important roles in the cellular efflux of physiologically important signalling molecules as well as participating in the tissue disposition and elimination of drugs and their conjugated metabolites (Leslie, Deeley & Cole, 2005; Cole & Deeley, 2006). A substantial number of individual amino acids in different regions of MRP1 have been demonstrated to be critical for its substrate specificity and transport activities, as well as its stable expression in the plasma membrane. While some mutation-sensitive residues are found in the cytoplasmic loops (CLs) of MRP1, many are in, or are closely associated with, the TM helices of the core region of the transporter that likely forms part of a substrate/inhibitor binding pocket and/or substrate translocation pathway through the membrane. Particularly crucial for LTC₄ binding and transport are Lys332 in TM6 (Haimeur, Deeley & Cole, 2002; Haimeur *et al.*, 2004; Maeno *et al.*, 2009). Current evidence suggests that TM6-Lys332 is involved in the recognition of the γ -Glu portion of LTC₄ and other substrates/modulators containing GSH or GSH-like moieties (Maeno *et al.*, 2009). These and other data indicate that MRP1 has at least three substrate binding pockets. In contrast, residues involved in the proper assembly and/or structural stability of MRP1 have thus far been found in the CLs that mediate the coupling of the ATPase activity at the NBDs to the substrate translocation through the MSDs. Thus non-conservative substitutions of several ionizable amino acids in CL7 in MSD1 (Conseil, Deeley & Cole, 2006) and CL5 in MSD1 (Iram & Cole, 2010) profoundly diminish the levels of MRP1 at the plasma membrane of mammalian cells. Many (but not all) of these residues are predicted by homology models of MRP1 to be located in an environment where they could form bonding interactions with residues in the opposing NBD. We propose that these and other interdomain interactions are critical to the proper assembly and trafficking of MRP1 to the plasma membrane of mammalian cells.

Cole SP, Bhardwaj G, Gerlach JH, Mackie JE, Grant CE, Almquist KC, Stewart AJ, Kurz EU, Duncan AM, Deeley RG. (1992) *Science* **258**, 1650-4.

Cole SP, Deeley RG. (2006) *Trends Pharmacological Sciences* **27**, 438-46.

Conseil G, Deeley RG, Cole SP. (2006) *Journal of Biological Chemistry* **281**, 43-50.

Leslie EM, Deeley RG, Cole SP. (2005) *Toxicology and Applied Pharmacology* **204**, 216-37.

Haimeur A, Conseil G, Deeley RG, Cole SP. (2004) *Molecular Pharmacology* **65**, 1375-85.

Haimeur A, Deeley RG, Cole SP. (2002) *Journal of Biological Chemistry* **277**, 41326-33.

Iram S, Cole SPC. (2010) unpublished observations

Maeno K, Nakajima A, Conseil G, Rothnie A, Deeley RG, Cole SP. (2009) *Drug Metabolism and Disposition* **37**, 1411-20.

Supported by the Canadian Institutes of Health Research

Drug translocation by P-glycoprotein: how do topographical changes in transmembrane helices assist?

R. Callaghan,¹ R.M. McMahon,¹ E. Crowley,¹ M. O'Mara² and I.D. Kerr;³ ¹Nuffield Department of Clinical Laboratory Sciences, John Radcliffe Hospital, University of Oxford, Oxford, OX3 9DU, United Kingdom, ²Molecular Dynamics Group, School of Chemistry and Molecular Biosciences, University of Queensland, Brisbane, QLD 4072, Australia and ³Centre for Biochemistry and Cell Biology, School of Biomedical Sciences, University of Nottingham, Queen's Medical Centre, Nottingham, NG7 2UH, United Kingdom.

Background: Resistance to chemotherapy is a major causative factor in the frustratingly poor success rate of chemotherapeutic management in cancer. The resistant phenotype is multifactorial involving both cellular and tissue architectural factors. One of the most prevalent, and effective, resistance pathways involves drug efflux pumps from the ATP-Binding Cassette (ABC) superfamily of transport proteins. The efflux proteins confer resistance by ensuring that cancer cells accumulate insufficient concentrations of anti-cancer drugs and thereby evade their cytotoxic actions. P-glycoprotein (a.k.a P-gp or ABCB1) is an archetypal ABC drug efflux pump and is known to confer resistance in a variety of cancer types including colon, liver, breast and a host of haematological disorders. P-gp is known to bind and transport over 200 pharmacological agents; hence it is referred to as a multi-drug transporter. This property remains a biological enigma and remains poorly understood. P-gp comprises four domains, two intramembranous (TMD) and two cytoplasmic (NBD). The TMDs are known to bind drug substrates and provide the translocation pore whilst the NBDs hydrolyse ATP to power the active transport. The TMD and NBDs are linked during translocation to ensure that drug binding and ATP hydrolytic events are efficiently coupled.

Objective: The process of coupling remains undefined, although two transmembrane helices (TM6 & TM12) appear to be intimately involved. As part of an ongoing investigation we aim to provide molecular details on the coupling process and the involvement of these two TM helices. The present investigation describes the role of TM12 in mediating coupling and the conformational changes it undergoes during the translocation process.

Strategy: The investigative strategy involves the mutagenesis based insertion of cysteine residues into various positions along TM12 using the fully functional cysteine-less isoform of P-gp as a template. The single cysteine mutant isoforms were expressed in insect cells with a recombinant baculovirus and purified using affinity chromatography. The purified, reconstituted mutant isoforms were assessed for function to ascertain the functional involvement of the targeted residue positions. In the second phase of investigation, the introduced cysteine residues were measured for their accessibility to covalent modification by a variety of thiol-reactive probes. Using probes with varying biophysical properties, differential labelling would reveal the local environment at each position. Finally, the isoforms were "trapped" in different conformations to assess the changes in local environment and thereby reveal the topography alterations during the translocation process.

Results: This cytosolic region undergoes a shift from a hydrophilic to hydrophobic environment during ATP hydrolysis. Overall the carboxy-proximal region of TM12 appears more responsive to changes in the catalytic state of the protein compared to its amino-proximal region. Thus, the carboxy-proximal region is suggested to be responsive to nucleotide binding and hydrolysis at the NBDs and therefore directly involved in inter-domain communication. These data can be reconciled with an atomic scale model of human ABCB1.

Conclusion: Taken together, these results indicate that TM12 plays a key role in the progression of the ATP hydrolytic cycle in ABCB1, in particular coordinating conformational changes between the NBDs and TMDs.

The malaria parasite's chloroquine resistance transporter: a multidrug resistance carrier?

R.E. Martin,^{1,2} R.L. Summers,¹ M. Nash,¹ R.V. Marchetti,¹ T.J. Dolstra¹ and K. Kirk,¹ ¹Research School of Biology, The Australian National University, Canberra, ACT 0200, Australia and ²School of Botany, The University of Melbourne, Parkville, VIC 3010, Australia.

Malaria remains a major infectious disease in many parts of the world; an effective vaccine is not yet available and the parasite has developed resistance to most of the antimalarial drugs currently in use. When it was introduced in the 1940s, the affordability, low toxicity, and effectiveness of chloroquine (CQ) caused a revolution in the control of the disease. Around 15 years later, however, chloroquine-resistant (CQR) parasites had emerged and by the 1990s resistant strains were prevalent in most regions where malaria is endemic. CQR parasites accumulate much less CQ than do their CQ-sensitive (CQS) counterparts and it is this marked decrease in drug accumulation that underlies the phenomenon of CQ resistance. CQ resistance has been attributed primarily to mutations in the chloroquine resistance transporter (PfCRT), an integral membrane protein localised to the parasite's internal digestive vacuole (believed to be the site of CQ action) and a member of the Drug/Metabolite Transporter (DMT) Superfamily. Furthermore, mutations in this protein also modulate the parasite's susceptibility to a number of other clinically important drugs. However, the mechanism by which mutant PfCRT confers reduced drug accumulation within the digestive vacuole, and hence resistance, has been unclear.

We have expressed PfCRT in *Xenopus* oocytes, achieving a robust heterologous system for the functional characterization of this protein. Achieving expression was not straightforward; the coding sequence was codon-harmonised to facilitate correct folding of the protein and a number of putative trafficking motifs were removed to prevent its retention at internal membranes. Without these changes, PfCRT was not expressed at significant levels in the oocyte plasma membrane. Using this system, we undertook direct measurements of [³H]CQ transport *via* PfCRT and provided a clear demonstration that the resistance-conferring form of PfCRT (PfCRT^{CQR}) has the ability to transport CQ out of the digestive vacuole whereas the sensitive form of the protein (PfCRT^{CQS}) does not (Martin *et al.*, 2009). We also showed that the transport of CQ *via* PfCRT^{CQR} is inhibited by verapamil, a drug long-recognised for its ability to reverse CQ-resistance *in vitro*. Moreover, CQ uptake was inhibited by a number of quinoline antimalarials (including quinine and amodiaquine) as well as the antiviral agent amantadine (which exhibits some antimalarial activity *in vitro*, particularly against CQR parasites). By contrast, piperazine and artemisinin (both clinically effective against CQS and CQR strains) were without effect. A focus of our recent work has been on determining whether verapamil, quinine, or amodiaquine are also transported *via* mutant forms of PfCRT.

There has been some conjecture as to whether PfCRT behaves as a channel or a carrier (*e.g.* Sanchez *et al.*, 2007). We found that the transport of CQ *via* PfCRT^{CQR} is saturated by low (clinically relevant) concentrations of the drug (the apparent K_m (CQ) was 245 μ M; Martin *et al.*, 2009). To place this in context, the addition of 100 nM CQ to the extracellular solution is estimated to result in a CQ concentration of around 2 mM in the digestive vacuole of CQS parasites and 200 to 500 μ M in the digestive vacuole of CQR parasites - due to the accumulation of the drug *via* 'weak-base trapping' in this acidic compartment. A characteristic of saturable transport is the ability of unlabelled substrate to *cis*-inhibit the uptake of a radiolabelled substrate. We observed *cis*-inhibition of [³H]CQ transport by unlabelled CQ in oocytes expressing PfCRT^{CQR} and likewise found that the inhibition of PfCRT^{CQR} by a number of different compounds, including quinine, verapamil, and amantadine, was concentration-dependent. Furthermore, we have recently shown that CQ uptake in oocytes expressing PfCRT^{CQR} displays another hallmark of carrier-mediated transport - a marked dependence on temperature (Summers & Martin, 2010). Taken together, the saturability and strong temperature-dependence of CQ transport *via* PfCRT^{CQR}, along with the placement of the protein within the DMT superfamily of carrier proteins, support the view that PfCRT is a carrier. Moreover, the interaction of mutant forms of the protein with a number of different drugs suggests that PfCRT can function as a multidrug resistance carrier. The finding that PfCRT^{CQR} behaves as a carrier has significant implications for the treatment of CQR parasites with CQ or CQ-like drugs. In particular we relate this to the example of Guinea-Bissau, where high doses of CQ are routinely used to cure CQR malaria (Ursing *et al.*, 2007).

Martin RE, Marchetti RV, Cowan AI, Howitt SM, Bröer S & Kirk K (2009) *Science* **325**, 1680-2.

Sanchez CP, Stein WD & Lanzer M (2007). *Trends in Parasitology* **23**, 332-9.

Summers RL & Martin RE (2010) *Virulence* **1**, 304-308.

Ursing J, Schmidt BA, Lebbad M, Kofoed PE, Dias F, Gil JP & Rombo L (2007) *Infection, Genetics, and Evolution* **7**, 555-61.

Antimicrobial resistance in staphylococci: Molecular architecture of a multidrug binding site

M.H. Brown, School of Biological Sciences, Flinders University, Bedford Park, SA 5042, Australia.

A significant mechanism of bacterial resistance is the active export of antimicrobials from cells by broad specificity multidrug efflux systems. The export of antiseptics and disinfectants in staphylococci, mediated by the plasmid-encoded determinant *qacA*, is an example of such a multidrug efflux system (Brown & Skurray, 2001). QacA is a 514-amino acid membrane protein, containing 14 transmembrane segments (TMS), and is a member of the Major Facilitator Superfamily (MFS) of transport proteins. QacA confers resistance to more than 30 different monovalent and bivalent cationic, lipophilic antimicrobial compounds from 12 different chemical families *via* a proton motive force-dependent efflux mechanism. Transport and competition studies have indicated that QacA interacts with monovalent and bivalent compounds at two distinct substrate-binding sites (Mitchell *et al.*, 1999). Mutagenesis of the aspartic acid residue at position 323 in TMS 10 of the QacA protein has been shown to radically alter the substrate specificity of the transporter. Cysteine-scanning mutagenesis of 35 residues within and surrounding TMS 10 delineated the extents of the TMS and identified residues within the substrate-binding site; TMS 10 appears to play an integral role in the formation of the substrate-binding site of QacA (Xu *et al.*, 2006). Interestingly, the location of key negatively-charged residues in QacA has an influence on the subset of bivalent cations recognised (Hassan *et al.*, 2007).

To date there is no high resolution structure of a 14-TMS transport protein. However, since QacA possesses a number of amino acid sequence motifs conserved within the MFS protein family, it is practical to extrapolate the known structures of related 12-TMS transport proteins, such as GlpT and LacY? An alternative way of obtaining information on the structure of multidrug binding exporters, in particular their binding pockets, is to analyse other multidrug-binding proteins that may be more amenable to crystal structure analyses (Grkovic *et al.*, 2002). One such protein, the QacR transcriptional repressor, negatively regulates the expression of *qacA* and is induced by interaction with antimicrobials which are substrates of QacA; binding of these compounds conformationally modifies QacR such that it can not bind to the *qacA* DNA operator sequence (Schumacher *et al.*, 2002). Crystal structures of QacR complexed to a number of chemically- and structurally-different cationic compounds have shed light on the induction mechanism of QacR and also illustrate the versatility of the substrate-binding domain of this protein, revealing separate, but linked ligand-binding sites within a single protein (Schumacher *et al.*, 2001; Brooks *et al.*, 2007). Recent mutagenic studies have focused on the four glutamic acid residues, identified from these structures, that line and surround the QacR ligand binding pocket (Peters *et al.*, 2008). Biochemical analyses and examination of crystal structures have revealed that these acidic residues do not appear to play a role in charge neutralisation of cationic substrates but may be involved in substrate discrimination through affecting the positioning of the drugs within the binding pocket. This only serves to provide further evidence of the promiscuous nature of the binding pocket of multidrug binding proteins.

Brooks BE, Piro KM & Brennan RG. (2007) *Journal of the American Chemical Society* **129**: 8389-8395.

Brown MH & Skurray RA. (2001) *Journal of Molecular Microbiology and Biotechnology* **3**: 163-170.

Grkovic S, Brown MH & Skurray RA. (2002) *Microbiology and Molecular Biology Reviews* **66**: 671-701.

Hassan KA, Skurray RA & Brown MH. (2007) *Journal of Bacteriology* **189**: 9131-9134.

Mitchell BA, Paulsen IT, Brown MH & Skurray RA. (1999) *Journal of Biological Chemistry* **274**: 3541-3548.

Peters KM, Schuman JT, Skurray RA, Brown MH, Brennan RG & Schumacher MA. (2008) *Biochemistry* **47**: 8122-8129.

Schumacher MA, Miller MC, Grkovic S, Brown MH, Skurray RA & Brennan RG. (2001) *Science* **294**: 2158-2163.

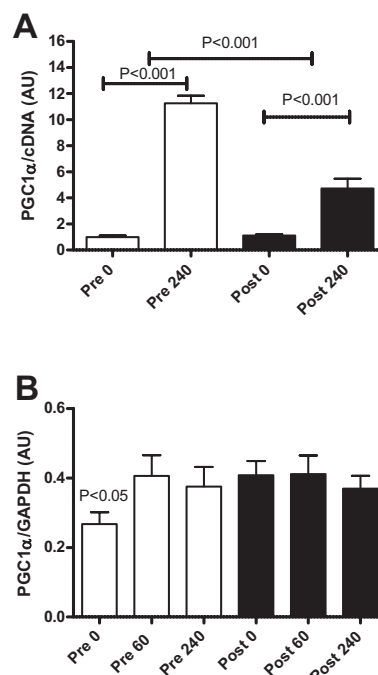
Schumacher MA, Miller MC, Grkovic S, Brown MH, Skurray RA & Brennan RG. (2002) *EMBO Journal* **21**: 1210-1218.

Xu Z, O'Rourke BA, Skurray RA & Brown MH. (2006) *Journal of Biological Chemistry* **281**: 792-799.

Reduced mitochondrial biogenesis activation during exercise after short-term training

N.K. Stepto,^{1,2} G. Wadley,³ B. Benziane,⁴ A.V. Chibalin,⁴ B.J. Canny⁵ and G.K. McConell,¹ ¹Institute of Sport Exercise and Active Living, Victoria University, Melbourne, VIC 8001, Australia, ²School of Sport and Exercise Science, Victoria University, Melbourne, VIC 8001, Australia, ³School of Exercise and Nutrition Sciences, Deakin University, Burwood, VIC 3152, Australia, ⁴Department of Physiology and Pharmacology, Karolinska Institutet, Stockholm, Sweden, and ⁵Department of Physiology, Monash University, Clayton, VIC 3800, Australia.

Mitochondrial biogenesis and function are important for energy production in cells and tissues. Aberrant mitochondrial function, specifically reduced volume not function, has been implicated as a cause or at least a contributor to lifestyle diseases including insulin resistance, obesity and diabetes. It is also well established that mitochondrial function and biogenesis is promoted by physical activity and exercise. In this study we investigated whether mitochondrial biogenesis was maintained in response to acute exercise after 10d of intensive cycle training despite the reduction of AMPK activity. Nine untrained, healthy participants (mean \pm SEM; 23 \pm 5 years of age, BMI: 24.9 \pm 1 kg.m⁻² VO_{2peak} 44.1 \pm 7.2 ml.kg⁻¹.min⁻¹) provided written informed consent. These participants performed a 60 min bout of cycling exercise at 164 \pm 9 W (~70% pre-training VO_{2peak}), muscle biopsies were taken from the *vastus lateralis* muscle under local anesthesia at rest, immediately and 3h after exercise. Within 7 days the participants then underwent 10d of intensified cycle training including 4 days of high-intensity interval training. Three days after the final training session participants repeated the pre-training exercise trial with biopsies at the same absolute work load (~164 W). Protein and mRNA were extracted from muscle for analysis by immunoblotting or RT QPCR respectively. AMPK Thr172 phosphorylation increased by 15 fold and 4 fold during exercise before and after training respectively ($p < 0.05$). PGC1- α gene expression was increased by 11 and 4 fold ($p < 0.001$; Figure A) 3 h after the exercise bout before and after training.



PGC1- α protein expression increased 1.5 fold ($p < 0.05$; Figure B) in response to exercise pre-training with no further increases occurring after the post-training exercise bout. COXIV gene expression was increased by training only (1.6 fold; $p < 0.0001$). On the other hand COXIV protein expression increased (1.5 fold; $p < 0.05$) but demonstrated a 20% reduction ($p < 0.01$) in response to acute exercise before and after training. The nuclear co-repressor RIP140 and COXI protein expression was influenced by acute exercise only. Specifically, protein expression of RIP140 increased by ~5.5 fold ($p < 0.01$) and COXI decreased ~2 fold ($p < 0.01$) in response to acute exercise before and after training. These data demonstrate that short-term intensified training promotes gene and protein expression for mitochondrial biogenesis, and that acute exercise after training at the same absolute intensity results in reduced gene expression responses.

30 days of normobaric hypoxia increases mitochondrial respiration

D.J. Bishop,¹ A. Ferri,^{1,2} I. Rivolta,² A. Panariti,² A. Zaza² and G. Miserocchi,² ¹Institute of Sport, Exercise and Active Living (ISEAL) and School of Sport and Exercise Science, Victoria University, Melbourne, VIC 8001, Australia and ²Dipartimento di Medicina Sperimentale, Università degli Studi di Milano-Bicocca, Monza, Italy.

Contrasting increases in cytochrome c oxidase and decreases in mitochondrial volume have been reported in response to stays at high altitude (Hoppeler & Vogt, 2001). However, none of these studies directly measured mitochondrial respiration and all can be criticised for a lack of control for changes in physical activity. The purpose of this study was to investigate the effects 30 days of hypoxia on directly-measured, mitochondrial respiration. Twenty Wistar rats were randomly assigned to 30 days of either normobaric normoxia (CON; 21% O₂) or hypoxia (HYP; 10% O₂). Both submaximal (0.1 mM ADP) and maximal (2 mM ADP) ADP-stimulated mitochondrial respiration were determined on both isolated mitochondria (from lungs) and permeabilised muscle fibres from the left (LV) and right ventricle (RV), and the *soleus* (SOL) and EDL. Results were analysed using one-way ANOVA ($p < 0.05$). Both submaximal and maximal ADP-stimulated respiration was significantly greater in HYP for SOL and LV, and tended to be higher for RV ($p = 0.06$). There were no significant differences for the EDL. The significantly greater mitochondrial respiration in the LV of HYP (26%; $p < 0.05$) was similar to a previous study (16%, ns) (Novel-Chaté *et al.*, 1998). The non-significantly greater mitochondrial respiration in the RV of HYP is also consistent with previous research (Novel-Chaté *et al.*, 1998) and can probably be attributed to significantly greater mass of the RV. We have shown for the first time however, that there is a greater mitochondrial respiration in the *soleus* of rats exposed to 30 days of hypoxia.

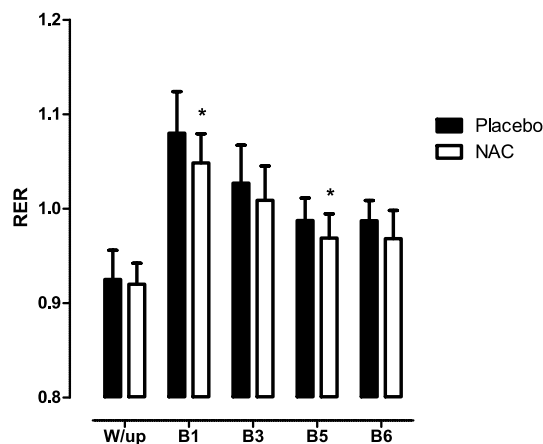
Hoppeler, H. & Vogt, M. (2001). Muscle tissue adaptations to hypoxia. *Journal of Experimental Biology* **204**, 3133-3139.

Novel-Chaté, V., Mateo, P., Saks, V.A., Hoerter, J.A. & Rossi, A. (1998). Chronic exposure of rats to hypoxic environment alters the mechanism of energy transfer in myocardium. *Journal of Molecular and Cellular Cardiology* **30**, 1295-1303.

3-day oral N-acetyl-cysteine supplementation alters metabolism but not performance of high intensity aerobic exercise in trained cyclists

A. Trewin,¹ F. Billaut,^{1,2} A. Petersen,^{1,2} B.D. Perry,¹ E. Goff,¹ T. Atanasovska¹ and N.K. Stepto,^{1,2} ¹School of Sport and Exercise Science, Victoria University, Melbourne, VIC 8001, Australia and ²Institute of Sport Exercise and Active Living, Victoria University, Melbourne, VIC 8001, Australia.

Redox homeostasis is essential for proper functioning of biological systems. Oxidative stress impairs contractile activity in skeletal muscle, and contributes to muscular fatigue during heavy exercise (Barclay & Hansel, 1991; Reid *et al.*, 1992). Accordingly, antioxidant supplements may assist endogenous antioxidants to prevent deleterious effects associated with oxidative stress (Medved *et al.*, 2004; Kelly *et al.*, 2009). In this study we investigated the effect of oral N-acetyl-cysteine (NAC) supplementation on metabolism and high intensity cycling performance. Nine well-trained male cyclists (mean \pm SD; 27 ± 6 years of age, $\text{VO}_{2\text{peak}} 69.4 \pm 5.8 \text{ ml}\cdot\text{kg}^{-1}\cdot\text{min}^{-1}$) provided written informed consent. In a randomized, double-blind crossover design, subjects performed a 6×5 min High Intensity-Interval Training (HIT) cycling session at 82.5% of peak sustained power output, followed by a 10 minute self-paced Time Trial (TT) on two occasions 7 d apart. Prior to one session subjects consumed $5 \times 750\text{ml}$ doses (2×2 d, 2×1 d, 1×1 hr pre-trial) of sports drink each containing $100\text{mg}\cdot\text{kg}^{-1}$ NAC, which was repeated for the other session, but without NAC. Metabolic, electromyographic (EMG), performance data, and blood/plasma samples were collected for analysis before, during, and after the 6×5 min HIT bouts and subsequent TT. Respiratory Exchange Ratio (RER) was decreased in the NAC condition throughout HIT exercise, and was significant at bouts 1 and 5 ($p < 0.05$) as shown in The Figure. Compared to placebo, NAC decreased blood lactate during TT and recovery ($p < 0.05$). Both pH ($p < 0.01$), and HCO_3^- ($p < 0.05$) were reduced throughout exercise and recovery with NAC. In contrast NAC resulted in higher blood glucose concentration during HIT ($p < 0.05$). EMG median frequency of the *vastus lateralis* decreased in HIT bout 6 in the NAC condition ($p < 0.05$). No significant difference was observed in the total work performed in the 10-min TT ($p = 0.16$). These data indicate that NAC does not change performance in a self-paced 10-min TT, but induces a shift in muscle fibre-type recruitment and alters metabolism during high intensity interval exercise, which may provide a glycogen-sparing effect during prolonged exercise.

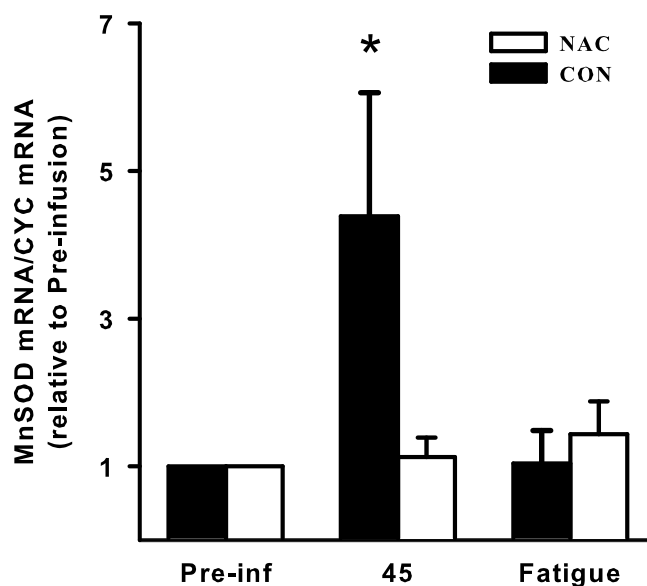


- Barclay, J. & Hansel, M. (1991) Free radicals may contribute to oxidative skeletal muscle fatigue. *Canadian Journal of Physiology and Pharmacology*, **69**, 279-284.
- Kelly, M., Wicker, R., Barstow, T. & Harms, C. (2009) Effects of N-acetylcysteine on respiratory muscle fatigue during heavy exercise. *Respiratory Physiology & Neurobiology*, **165**, 67-72.
- Medved, I., Brown, M.J., Bjorksten, A.R., Murphy, K.T., Petersen, A.C., Sostaric, S., Gong, X. & McKenna, M.J. (2004) N-acetylcysteine enhances muscle cysteine and glutathione availability and attenuates fatigue during prolonged exercise in endurance-trained individuals. *Journal of Applied Physiology*, **97**, 1477-1485.
- Reid, M., Haack, K., Franchek, K., Valberg, P., Kobzik, L. & West, M. (1992) Reactive oxygen in skeletal muscle. I. Intracellular oxidant kinetics and fatigue in vitro. *Journal of Applied Physiology*, **73**, 1797.

Actions of the antioxidant *N*-acetylcysteine on cell signaling response to exercise in human skeletal muscle

A.C. Petersen,^{1,2,3} M.J. McKenna,³ I. Medved,² K.T. Murphy,² M.J. Brown,⁴ P. Della Gatta¹ and D. Cameron-Smith,¹ ¹School of Exercise and Nutrition Sciences, Deakin University, Melbourne, ²School of Sport and Exercise Science, Victoria University, Melbourne, VIC 8001, Australia, ³Institute of Sport, Exercise and Active Living, Victoria University, Melbourne, VIC 8001, Australia and ⁴Department of Anaesthesia, Royal Melbourne Hospital, Melbourne, VIC 3050, Australia.

Production of reactive oxygen species (ROS) in skeletal muscle is markedly increased during exercise and may be essential for exercise adaptation. We therefore investigated the effects of infusion with the antioxidant *N*-acetylcysteine (NAC) on exercise-induced activation of signaling pathways and genes involved in exercise adaptation in human skeletal muscle. Subjects completed two exercise tests, 7 days apart, with saline (control, CON) or NAC infusion before and during exercise. Exercise tests comprised of cycling at 71% $\text{VO}_{2\text{peak}}$ for 45 min, then 92% $\text{VO}_{2\text{peak}}$ to fatigue with *vastus lateralis* biopsies at pre-infusion, after 45 min cycling and at fatigue. Analysis was conducted on the mitogen-activated protein kinase (MAPK) signaling pathways, which are involved in growth, metabolism, differentiation, transcription, translation, and remodeling and also nuclear factor- κB (NF κB) signaling, which is a major stimulator of genes involved in inflammation and muscle protein turnover. We found that exercise increased phosphorylation of the MAP kinases c-Jun N-terminal kinase (JNK), p38 MAPK, and extracellular signal regulated kinases 1 and 2 (ERK 1/2), and that NAC had no effect on these kinases. NF- κB p65 phosphorylation was unaffected by exercise; however it was reduced in NAC at fatigue by 14% ($p < 0.05$) compared to pre-infusion. Additionally, we analysed expression of exercise and/or ROS sensitive genes involved in stress-response (heat shock protein 70, HSP70), inflammation (interleukin-6, IL-6; monocyte chemotactic protein-1), anti-oxidant defense (manganese superoxide dismutase, MnSOD) and mitochondrial biogenesis (peroxisome proliferator-activated receptor coactivator-1 α , PGC-1 α). Exercised induced mRNA expression was ROS dependent for MnSOD (Figure), but not PGC-1 α , interleukin-6, MCP-1, or heat-shock protein 70. These results suggest that inhibition of ROS attenuates some skeletal muscle cell signaling pathways and gene expression involved in adaptations to exercise.



Rigour or rigor mortis: a challenge for physiology

P. Poronnik, Health Innovations Research Institute, School of Medical Sciences, RMIT University, Bundoora, VIC 3083, Australia.

The education sector is in ongoing turmoil with debates around the “difficulty” of the proposed national curriculum in maths and science with potential flow-on effects to the tertiary sector. Physiology as an independent discipline is also under ongoing threat, often seen as primarily service teaching for medicine related courses. Together with the massification of the tertiary sector and fiscal pressures, does this lead to dilution and less rigorous teaching in physiology? The mantra of multidisciplinary is also a potential threat in that it may encourage a shallower-broader educational approach rather than directing disciplinary depth. Is physiology just too hard for the “average” science student? Or do the current methods of physiology delivery simply fail to engage and excite the students to strive for academic excellence through an inherent curiosity about how the body works? In response to the 2003 BIO2010 report on undergraduate biology curriculum, Dee Silverthorn issued a “call to action” to restore physiology to its true place in the science curriculum as “the integrative discipline in biology”. Since then, there has been an increasing recognition within the physiology family of these issues. Our challenge is to capitalize on the forward movement in this area and enact this essential change. We need to build critical mass to reinvigorate the physiology curriculum in a way that recognizes and contextualizes prior knowledge and challenges students to actively participate in the learning around the fundamental concepts that are the foundations of modern physiology. Encouragement, tangible support, teamwork and academic output and recognition are key enablers that will place physiology in the centre of biomedical curriculum of the future.

Committee on Undergraduate Biology Education to Prepare Research Scientists for the 21st Century. BIO 2010: Transforming Undergraduate Education for Future Research Biologists. Washington DC: National Academy Press, 2003.

Silverthorn DU. (2003) Restoring physiology to the undergraduate biology curriculum: a call for action. *Advances in Physiology Education* **27**: 91-6.

Using the Finapres to teach cardiovascular physiology to second year science students

Y.M. Hodgson and J. Choate, Department of Physiology, Monash University, VIC 3800, Australia.

There are many ways of teaching cardiovascular physiology to university science students, but few of these directly demonstrate or measure cardiac output and total peripheral resistance, concepts which are fundamental to an understanding of cardiovascular physiology. The Physiology Department at Monash University has been trialling the use of a finger pressure cuff, the *Finapres* system, in the cardiovascular practical classes. This abstract reports on the initial findings from a study of 220 second year physiology students undertaking a practical class on exercise and cardiovascular physiology using the *Finapres* system.

During the practical class students worked in groups of 5, with one student performing graded levels of exercise on a cycle ergometer. The exercise workload was increased every 3 minutes by increments of 50 watts, until the subject reached 75% of their maximum HR. The *Finapres* finger cuff, together with *Beatscope* software, were used to continuously measure and record blood pressure (BP). Heart rate (HR) and cardiac output (CO) were triggered from the pulse rate and the pulse waveform, respectively. The students were asked to calculate the stroke volume (SV) and the total peripheral resistance (TPR).

To determine if the *Finapres* practical class had improved student learning and understanding of cardiovascular physiology and exercise, pre- and post-tests were given to the students at the beginning and end of the practical class. The questions tested the students understanding of cardiovascular physiology during rest and exercise. Statistical analysis of student performance for the individual questions indicated that there was a significant improvement for two questions following the practical class. The first question required a calculation of the CO. On the pre-test 75.81% of students answered this correctly. This rose to 84.5% on the post-test. A similar increase (78% to 84%) was seen for a multiple choice question about the sympathetic cardiac response to exercise. However, there was no significant difference in the overall pre- and post-test results, suggesting that the *Finapres* practical had a positive, but narrow, effect on learning.

A questionnaire using a five point Likert scale, similar to that used by Rodriguez-Barbero (2008), was used to evaluate the student experience of the *Finapres* system. The findings showed that students: i) appreciated the immediacy of the recording of cardiovascular responses (4.17 ± 0.85 , mean \pm SD); ii) felt that they gained a better understanding of how to record physiological data (4.06 ± 0.89); iii) enjoyed the practical class (4.17 ± 0.96); and iv) would recommend the *Finapres* to other students (4.12 ± 0.97). Given this positive student feedback, we have subsequently used the *Finapres* system to teach Physiotherapy and third year Physiology (Science) students about circulatory reflex responses to perturbations in the cardiovascular system. The ability of the *Finapres* system to continuously record and calculate BP, HR, CO, SV, and TPR during the experimental protocols provides students with immediate feedback and, we believe, improves their understanding of cardiovascular physiology.

Rodríguez-Barbero, A. & López-Novoa, J.M. (2008) Teaching integrative physiology using the quantitative circulatory physiology model and case discussion method: evaluation of the learning experience. *Advances in Physiology Education*, **32**: 304-311.

The KISS approach: How to develop an effective self directed e-learning application

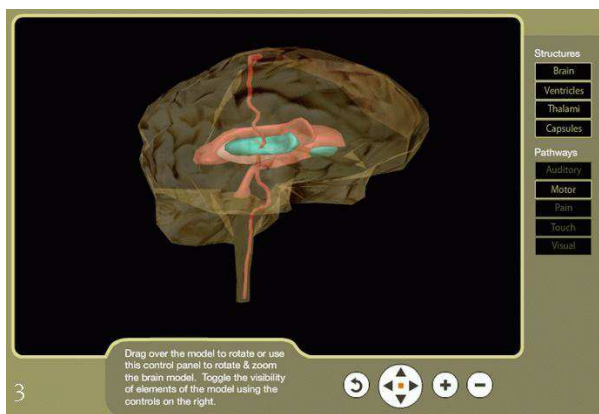
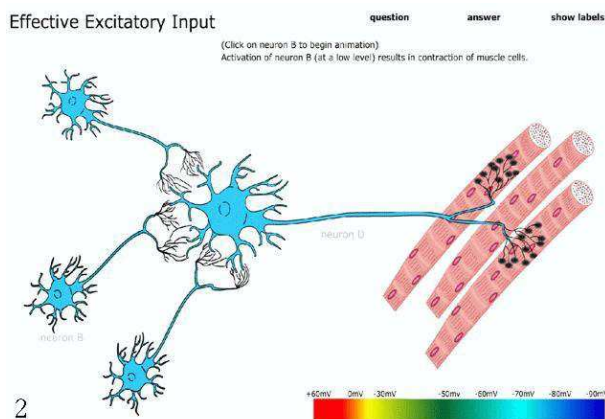
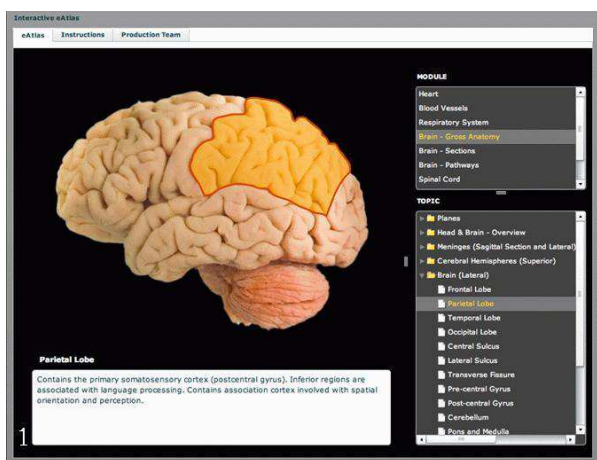
R. Guy,¹ H. Pisani,² P. Rich,¹ G. Mandarano,¹ C. Leahy,² T. Molyneux² and R. Davidson,¹ ¹School of Medical Sciences, RMIT University Bundoora, Bundoora, VIC 3083, Australia and ²School of Health Sciences, RMIT University, Bundoora, VIC 3083, Australia.

An Interactive e Atlas of functional anatomy (IeA) has been developed to provide support for large class teaching and to encourage engagement in the study area (Figure 1). The IeA provides general support for introductory anatomy & physiology courses and also forms a component of blended learning and distance education.

The KISS approach (keep it simple for students) was used during development of atlas content and structure. Best practice principles and cognitive load theory were used to provide effective interactivity, flexibility, options and feedback.

Two other online applications (Neuronal Physiology animation Figure 2; Glass Brain Figure 3) have also been developed using best practice principles.

Preliminary evaluations indicate a good student response to the applications. The KISS approach may be useful in facilitating student engagement in e-learning environments.



--

Lecture attendance, learning style and assessment outcome in physiology students

D.A. Saint, D.M. Horton and S.D. Wiederman, *Discipline of Physiology, School of Medical Sciences, The University of Adelaide, Adelaide, SA 5005, Australia.*

It seems self-evident that students attendance at lectures should predict their performance in exams and other assessments. This has been shown in some studies, for example in dental students (El Tantawi, 2009) but the correlation is often weak. Some authors have suggested that provision of alternative learning materials, such as online lectures, may be detrimental to student performance because it reduces attendance at "conventional" lectures (Fernandes, Male & Cruickshank, 2008). Students have varied learning styles, or combinations of styles, assessed by VARK (visual, auditory, reading/writing and kinaesthetic), and this has been shown in some cases to predict academic outcomes (Dobson, 2009). However, the interaction between lecture effectiveness and student learning styles is poorly understood. Here, we have investigated the correlation between lecture attendance and student performance in different assessment tasks, and the influence of the students' learning style on this. We hypothesised that the degree of correlation of lecture attendance with academic performance will be different for students with different VARK profiles.

Second year students for the combined Biomedical, Health and Science 2009 cohort (n=120) completed a questionnaire in which they self-reported their lecture attendance and the time they spent using alternative resources to supplement their learning. Self-reported lecture attendance in the first semester of 2009 was 73 ± 2%. Correlations between lecture attendance and grade outcome are shown the Table.

Grade Component	Combined Male/Female n=120	Male Only n=49	Female Only n=71
Practical	r=0.29, p<0.002	r=0.32, p<0.03	r=0.20, p<0.10, ns
Tutorials	r=0.35, p<0.0005	r=0.29, p<0.05	r=0.33, p<0.005
Exam	r=0.21, p<0.02	r=0.29, p<0.04	r=0.10, ns
Combined Grade	r=0.31, p<0.001	r=0.35, p<0.01	r=0.20, p<0.10, ns

95 students completed the VARK assessment. For these students, a greater percentage score of "R" (i.e. use read/writing as a method of learning by VARK analysis) predicted: Exam Mark (r=0.22, p<0.03), Tutorial mark (r=0.20, p<0.05), Practical Mark (r=0.19, p<0.07), Overall Mark (r=0.26, p<0.02). Females had a higher proportion of "R" compared to males (Females =0.29 ± 0.01, n=63; Males =0.25 ± 0.01, n=32; P<0.03).

We conclude that lecture attendance and learning styles interact in predicting overall mark, but the details, and the causal relationships, require more investigation.

El Tantawi MMA, (2009) *Journal of Dental Education* **73(5)**: 614-623.

Fernandes L, Maley M, Cruickshank C (2008) *Journal of the International Association of Medical Science Educators (JIAMSE)* **18(2)**: 62-70.

Dobson JL (2009) *Advances in Physiology Educudation* **33**: 308-314,

The Human Physiology Writing Centre: Task-based building of student capacity

S. Wiederman,¹ J. Miller² and C. Habel,² ¹Discipline of Physiology, School of Medical Sciences, and ²Centre for Learning & Professional Development, The University of Adelaide, Adelaide, SA 5005, Australia.

Students studying second year Human Physiology write a literature review in the first semester and a critical evaluation in the following semester. Generally, students are asked to complete such writing tasks, without any established teaching procedures. Therefore, these assessments can be difficult, particularly for 'English as an Additional Language' (EAL) students. As an aid, we provide a detailed assessment criteria sheet, however the interpretation of this information can in itself be a challenge. To remedy this situation, we established the Human Physiology Writing Centre, providing tutoring to the students for the specific writing task. The students were provided with two individual 30-minute sessions (one week apart) with a writing tutor (trained Psychology PhD students). The tutors provided guidance with the purpose of the task and an explanation of the assessment criteria. Working with the students and their drafts, they helped with logical flow and structure; as well as grammar and style. The tutors were not familiar with the underlying content (Physiology), which maintained a focus on writing. Qualitatively, the students have reported overwhelming support for this program (*via* student evaluations).

This 'task-specific' approach introduces the students to other 'writing' resources available within the University (the Writing Centre). This mentorship encourages student engagement with improving their writing *via* both intrinsic (context) and extrinsic (assessment) motivators. Importantly, we are providing the resources required to meet the student learning objectives of improved scientific writing.

Effect of hypoxia on the dynamic response of leg blood flow during exercise

S. Green and J. Donnelly, Department of Physiology, University of Otago, Dunedin 9013, New Zealand.

Systemic hypoxia increases the muscle hyperaemic response during steady-state exercise. However, the effect of hypoxia on dynamic response characteristics of muscle blood flow is not known. To test this effect, eight subjects performed eight exercise trials while breathing a normoxic ($F_{I}O_2 = 0.2094$) or hypoxic ($F_{I}O_2 = 0.105$) gas mixture. Exercise consisted of five minutes of intermittent contractions of the left calf muscle (3s duty cycle) at a low intensity (20% MVC) during which leg blood flow (LBF) and mean arterial pressure (MAP) were measured between each contraction. Four sets of LBF responses were averaged for each subject under normoxia and hypoxia and fitted using a multiphasic exponential function. This enabled amplitudes and temporal parameters of a fast and slow growth phase, as well as a rapid decay phase, to be estimated. Hypoxia did not significantly affect MAP at rest but resulted in a 7% lower value by the end of exercise ($p < 0.05$). In contrast, hypoxia increased the change in LBF from the start to end of exercise by 13% ($p = 0.07$) and the amplitude of the rapid growth phase of the LBF response by 16% ($p < 0.001$). Hypoxia also increased the amplitude of the slow growth phase by 24% ($p = 0.08$) but it had no effect on the decay phase. These results suggest that the effect of hypoxia on exercise hyperaemia is targeted at rapid and slow phases of the response.

Citrulline supplementation does not prevent atrophy during limb-casting in mice

R. Koopman, D. Ham, B.G. Gleeson and G.S. Lynch, Basic and Clinical Myology Laboratory, Department of Physiology, The University of Melbourne, VIC 3010, Australia.

Essential amino acids, particularly the branched-chain amino acids, have been shown to play a major role in the regulation of muscle protein synthesis and breakdown (Koopman, 2007). Thus, ingestion of specific amino acids (AAs) could be an effective therapeutic strategy to attenuate the muscle wasting and weakness common in many disease states and conditions. Although studies have indicated that supplementation with non-proteinogenic amino acids such as citrulline, can manipulate the anabolic response, their application for treating muscle wasting has received little attention. Interestingly, oral administration of citrulline to old malnourished rats enhanced muscle protein synthesis (Osowska *et al.*, 2006). Citrulline can be converted to arginine in the kidneys and thus plays an important role in protein homeostasis, controlling urea production and arginine availability. We hypothesized that citrulline administration increases muscle protein synthesis thereby preventing skeletal muscle wasting during limb-casting. Our aims were to establish the stimulating/protective properties of citrulline *in vitro* on muscle cell hypertrophy and atrophy, and to examine whether citrulline could attenuate the loss of muscle function during casting.

Atrophy was induced in cultured C2C12 myotubes by switching the medium to HBS, with or without the addition of 2.5 mM citrulline. After 6h of treatment, cells were fixed in 3.7% formaldehyde and reacted with myosin antibodies to determine myotube diameter, or prepared for western blot and RT-PCR analyses. Mice (n=24) were subjected to unilateral limb-casting. Mice were anaesthetised with an intraperitoneal (*i.p.*) injection of Ketamine/Xylazine (100 mg/kg Ketamine; 10 mg/kg Xylazine) so there was no response to tactile stimulation. The left hindlimb was wrapped in a special veterinary plaster with the foot positioned in plantar flexion to induce maximal atrophy of the gastrocnemius and other hindlimb muscles. Mice received citrulline (n=12, 1 g/kg/day) or alanine (n=12, control) during the 2 weeks of limb-casting. At the end of the treatment, mice were anaesthetised and *tibialis anterior* (TA) muscle function was assessed *in situ* (Murphy *et al.*, 2010). Mice were killed by cardiac excision while anaesthetised deeply. Muscles were analysed for changes in muscle fibre cross sectional area, fibre type distribution and oxidative capacity.

C2C12 myotubes incubated in HBS for 6h had a 40% reduction in myotube diameter. Incubation with citrulline partly prevented this wasting, with citrulline incubated myotubes being 18% bigger than the HBS or HBS-alanine treated myotubes ($p<0.05$). Incubation with citrulline did not enhance the phosphorylation status of p70-S6K1 or Akt. Two weeks of unilateral limb-casting resulted in 25% reductions ($p<0.05$) in quadriceps and TA muscle mass, and 33% and 15% reductions in peak and specific force, respectively, of TA muscles. These changes in muscle mass and function were associated with a specific atrophy of the type IIB/x fibres, without changes in the size of type IIA muscle fibres. Citrulline treatment during limb-casting did not attenuate muscle wasting.

Although citrulline administration reduced muscle wasting *in vitro*, it was unable to counteract muscle wasting *in vivo*. Citrulline does not exert its effect on skeletal muscle *via* the classical amino acid-induced increase in Akt/mTOR signalling.

Koopman R. (2007). *International Journal of Sports Nutrition and Exercise Metabolism* **17**: S47-S57.

Murphy KT, Koopman R, Naim T, Leger B, Trieu J, Ibebunjo C & Lynch GS. (2010). *FASEB Journal* doi:10.1096/fj.10-159608

Osowska S, Duchemann T, Walrand S, Paillard A, Boirie Y, Cynober L & Moinard C. (2006). *American Journal of Physiology. Endocrinology and Metabolism* **291**: E582-586.

Supported by the Ajinomoto Amino Acid Research Program (Japan)

Inhibition of the renin-angiotensin system enhances whole body and skeletal muscle function in healthy and tumour-bearing mice

K.T. Murphy,¹ A. Chee,¹ A.M. Allen² and G.S. Lynch,¹ ¹Basic and Clinical Myology Laboratory, Department of Physiology, The University of Melbourne, VIC 3010, Australia and ²Central Cardiovascular Regulation Group, Department of Physiology, The University of Melbourne, VIC 3010, Australia.

Cancer cachexia describes the progressive skeletal muscle wasting and weakness in many cancer patients. Cancer cachexia impairs mobility, causes severe fatigue, and accounts for >20% of cancer-related deaths. The mechanisms underlying cancer cachexia are multifactorial and current treatments have proved ineffective as they have only targeted one of these mechanisms (Murphy & Lynch, 2009). Renin-angiotensin system (RAS) inhibition has typically been used in the treatment of hypertension, but recent evidence indicates that stimulation of RAS may contribute to skeletal muscle breakdown by a myriad of mechanisms, including inducing inflammation, causing insulin resistance, inducing skeletal muscle apoptosis, reducing protein synthesis and enhancing protein degradation. RAS inhibition may therefore preserve or enhance skeletal muscle strength and function and consequently, represents a potential therapeutic strategy for counteracting the skeletal muscle wasting and weakness associated with conditions such as cancer cachexia. We tested two hypotheses: i) that life-long RAS inhibition would enhance whole body and skeletal muscle function in healthy mice; and ii) that acute RAS inhibition would enhance whole body and skeletal muscle function in a commonly used murine model of cancer cachexia.

All experiments were approved by the Animal Experimental Ethics Committee of The University of Melbourne and conducted in accordance with the current codes of practice of the National Health and Medical Research Council (Australia). Animals were anaesthetised with sodium pentobarbitone (Nembutal, 60 mg/kg, *i.p.*) prior to assessment of muscle contractile properties and were later killed as a consequence of cardiac excision while anaesthetised deeply.

In study 1, 12 week old wild-type control mice ($n=13$) and those lacking the angiotensin type 1A receptor ($AT_{1A}^{-/-}$, $n=15$) were tested for whole body strength (grip strength) and function (rotarod), glucose sensitivity during a glucose tolerance test and maximum tetanic force production and fatiguability *in situ* of the *tibialis anterior* (TA) muscle (Murphy *et al.*, 2010). Compared with controls, $AT_{1A}^{-/-}$ mice exhibited a 17% higher grip strength ($p<0.01$) and a 49% prolonged latency-to-fall during a rotarod test ($p<0.01$). Glucose sensitivity was improved by 23-26% in $AT_{1A}^{-/-}$ mice ($p<0.01$). Maximum *in situ* forces (normalised to CSA) of TA muscles was higher by 25% in $AT_{1A}^{-/-}$ mice ($p<0.05$), but the force decline during fatiguing intermittent stimulation was not different between groups.

In study 2, 15 week old CD2F1 (Balb/c \times DBA) mice bearing Colon-26 (C-26) tumour cells were treated for 14 days with the ACE inhibitor, Perindopril (4 mg/kg/day, $n=4-7$) *via* the drinking water. Control mice were given water alone ($n=4-6$). Perindopril prevented the decline in body mass in C-26 tumour-bearing mice ($p<0.01$), enhanced grip strength by 29% ($p<0.05$) and prolonged the latency-to-fall during a rotarod test by 56% ($p<0.05$). Glucose sensitivity was improved with Perindopril ($p<0.01$). Perindopril had no effect on maximum force of TA muscles *in situ* or of diaphragm muscle strips *in vitro*, but attenuated the decline in force during fatiguing intermittent stimulation in both TA muscles and diaphragm muscle strips ($p<0.01$).

RAS inhibition enhanced whole body and skeletal muscle function, and improved glucose sensitivity in healthy mice and in mice bearing C-26 tumours. These findings highlight the therapeutic potential of RAS inhibition for cancer cachexia and other diseases associated with skeletal muscle wasting and weakness.

Murphy KT & Lynch GS. (2009) *Expert Opinion on Emerging Drugs* : 619-632.

Murphy KT, Koopman R, Naim R, Léger B, Trieu J, Ibebunjo C & Lynch GS. (2010) *FASEB Journal* In Press (Jul 12, 2010) doi:2010.1096/fj.2010-158741.

Voltage-dependent and -independent Ca²⁺ entry into skeletal muscle during excitation-contraction coupling

B.S. Launikonis, School of Biomedical Sciences, The University of Queensland, Brisbane, QLD 4072, Australia.

Excitation-contraction coupling (EC coupling) is the process that links the activation of the surface membrane of a muscle to the force response produced. This process is reliant on a rapid and large change in cytoplasmic [Ca²⁺] ([Ca²⁺]_{cyto}) due to release activated from the internal Ca²⁺ store, the sarcoplasmic reticulum (SR). The change in [Ca²⁺]_{cyto} regulates the movement of the contractile proteins in the muscle to produce force. Also, during EC coupling there can be an input of Ca²⁺ across the surface membrane, or from the invagination of this membrane, the tubular (t-) system. In skeletal muscle, this influx of Ca²⁺ is not strictly required for a contracture to occur, but its importance may be in the longer-term regulation of function or may indeed have more subtle, immediate consequences that are not clear from present measurements. Several pathways can be responsible for an influx of Ca²⁺ into skeletal muscle fibres during EC coupling. These can be voltage-dependent, including L-type Ca²⁺ current, action potential-activated Ca²⁺ current (APACC) and excitation-coupled Ca²⁺ entry (ECCE); or voltage-independent, including store-operated Ca²⁺ entry (SOCE), stretch-activated Ca²⁺ entry or otherwise activated to enter through transient receptor protein (TRP) channels. It should be noted that the conditions that prevail under bouts of EC coupling are the conditions that activate voltage-dependent and -independent Ca²⁺ entry during EC coupling in skeletal muscle (Allen *et al.* 2005; Launikonis *et al.*, 2010).

The nature of these voltage-dependent and -independent pathways in skeletal muscle have been examined by a number of groups using either fully differentiated fibres or myotubes. A problem that does arise here is that properties derived on myotubes are often assumed to be very similar to that in the fully differentiated muscle. There are significant differences in myotube and adult fibre physiology and membrane ultrastructure, making extrapolation of results derived on one cell to other not a simple matter. The examination of Ca²⁺ currents in myotubes may have been necessary in some instances because conventional electrophysiological methods are difficult or do not have the sensitivity to measure such tiny Ca²⁺ currents in adult fibres. Furthermore, the use of pharmacological agents commonly used to block Ca²⁺ entry pathways are, unfortunately, non-specific in most cases. A combination of these factors may have lead to a misrepresentation of certain pathways existing in myotubes or adult fibres.

In adult, mammalian skeletal muscle fibres it has been possible to image Ca²⁺ in the lumen of the t-system using a low-affinity Ca²⁺-sensitive fluorescent dye. The dye is trapped in the t-system of skinned fibres, where the surface membrane has been removed by microdissection. With this preparation, Ca²⁺ movement across the t-system membrane is visualized as a net change in the Ca²⁺-dependent fluorescence signal emitted from the t-system lumen. This can be monitored in conjunction with a spectrally separate Ca²⁺-sensitive dye in the cytoplasm to monitor changes in [Ca²⁺]_{cyto}, which will be predominately due to fluxes across the SR membrane. This preparation has allowed the identification and characterization of SOCE during voltage-independent Ca²⁺ release and also APACC, which has been identified and observed to occur during single and trains of action potentials in adult mammalian skeletal muscle fibres.

Allen DG, Whitehead NP, Yeung EW. (2005) *Journal of Physiology*, **567**: 723-735.

Launikonis BS, Murphy RM, Edwards JN. (2010) *Pflügers Archiv*, **460**: 813-823.

Coupling and uncoupling of the DHPRs and Ca²⁺ release channels in skeletal muscle fibres

T.L. Dutka, Department of Zoology, La Trobe University, VIC 3086, Australia.

This study focused on the importance of transverse tubular (T)-system potential on excitation-contraction (E-C) coupling and the consequences of disrupted dihydropyridine receptor (DHPR)-ryanodine receptor (RyR) coupling on sarcoplasmic reticulum (SR) Ca²⁺ handling. Male Long-Evans hooded rats were killed by anaesthetic overdose (4 % v:v isoflurane) and EDL muscles swiftly excised and immersed in paraffin oil at resting length. Individual fibres were mechanically skinned, connected to a force transducer (stretched to 120 %) and immersed in a standard K-HDTA-based solution. All solutions contained as follows (in mM); 1 free Mg²⁺, 8 ATP; 10 creatine phosphate, 55, 66 or 126 K⁺, at pH 7.1, and were equilibrated to room temperature (~23°C). Single fibres were electrically stimulated (75 V cm⁻¹, 1 ms pulse) to produce twitch or tetanic (50 and 100 Hz) force responses. Additionally, paired pulses with differing intervals (0-50 ms) were applied to determine the repriming period of sodium channels in the T-system membrane (Dutka & Lamb, 2007a).

The importance of T-system membrane potential. Partial long-lasting depolarization of the T-system membrane (achieved by lowering the cytoplasmic [K⁺]) reduces tetanic force by impairing AP repriming and preventing the generation of APs in quick succession thus reducing DHPR-mediated Ca²⁺ release through RyR1. This reduced muscle excitability was not due to DHPR inactivation because lowering the frequency of stimulation partly ameliorated the effect. Furthermore, when fibres were chronically partially depolarized, PCr/CK ATP regeneration system was not optimal and slowed the repriming period of T-system Na⁺ channels. Addition of Phospho(enol) pyruvate (PEP) hastened AP repriming and hence, improved T-system excitability (Dutka & Lamb, 2007b) implying Na⁺/K⁺-ATPases function better when ATP is produced glycolytically in the triad junction instead of by PCr/CK elsewhere.

The importance of strict DHPR-RyR1 coupling. Disruption of the interaction between DHPRs and RyR1 appears to cause an irreversible Ca²⁺-leak from the SR through RyR1. When DHPR are in there *in situ* state they have been shown to suppress RyRs activity (*i.e.* Ca²⁺ spark) at rest in cultured mammalian muscle (Zhou *et al.*, 2006). Similarly, Weiss *et al.*, (2004) showed that a mutation in the DHPR cytoplasmic III-IV loop of alpha (1S) subunit (R1086H) greatly enhanced RyR1 sensitivity to activation by voltage/caffeine, indicating that DHPRs had a negative allosteric modulatory effect on RyR1. Furthermore, high Ca²⁺-induced uncoupling of DHPRs from RyRs has also been shown to cause a similar irreversible SR Ca²⁺ leak in mechanically-skinned fibres (Lamb & Cellini, 1999). In the experiments described here, immediate application of S-nitrosoglutathione GSNO_{imm} (a reactive oxygen and nitrogen species) to the fibres reduced twitch and tetanic force responses (15 and 10 % respectively) even though it caused an ~0.1 pCa unit increase in contractile Ca²⁺-sensitivity. These reductions to AP-mediated force responses were due to impaired DHPR-RyR coupling and concomitantly GSNO_{imm} treatment also caused Ca²⁺ leakage through RyRs, which was not reversible with DTT. The Ca²⁺ leak through RyRs was substantially blocked by raising the free [Mg²⁺] from 1 to 10 mM. The irreversible Ca²⁺ leak caused by DHPR uncoupling observed by others (Lamb & Cellini, 1999; Weiss *et al.*, 2004; Zhou *et al.*, 2006) is strikingly similar to that observed here caused by exposure to GSNO_{imm}, which might help explain the ROS-mediated loss of signal transduction observed during prolonged low frequency fatigue (Bruton *et al.*, 2008).

Bruton JD, Place N, Yamada T, Silva JP, Andrade FH, Dahlstedt AJ, Zhang SJ, Katz A, Larsson NG & Westerblad H. (2008). *Journal of Physiology* **586**, 175-184.

Dutka TL & Lamb GD. (2007a). *American Journal of Physiology. Cell Physiology* **292**, C2112-2121.

Dutka TL & Lamb GD. (2007b). *American Journal of Physiology. Cell Physiology* **293**, C967-977.

Weiss RG, O'Connell KM, Flucher BE, Allen PD, Grabner M & Dirksen RT. (2004). *American Journal of Physiology. Cell Physiology* **287**, C1094-1102.

Zhou J, Yi J, Royer L, Launikonis BS, Gonzalez A, Garcia J & Rios E. (2006). *American Journal of Physiology. Cell Physiology* **290**, C539-553.

One is enough: RyR1 allele-specific gene silencing in mouse models of central core disease (CCD) and malignant hyperthermia (MH)

R.T. Dirksen, R.E. Loy, J.D. Lueck and M. Mostajo-Radji, University of Rochester, Department of Pharmacology and Physiology, Rochester, NY 14642, USA. (Introduced by Angela Dulhunty)

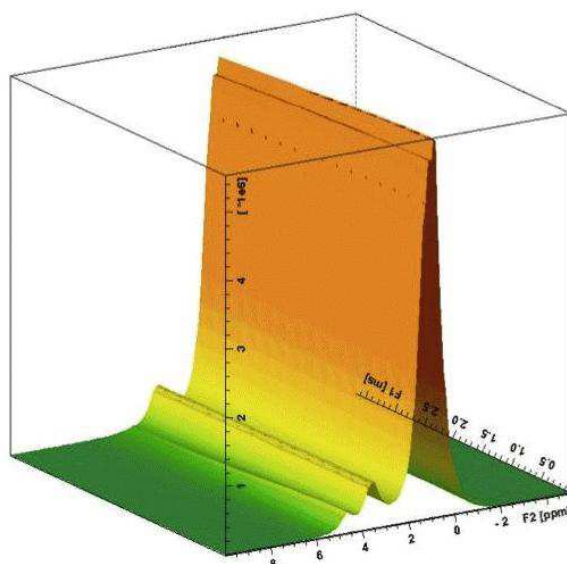
Central Core Disease (CCD) and Malignant Hyperthermia (MH) are linked to single amino acid substitutions in the skeletal muscle Ca^{2+} release channel, the type 1 ryanodine receptor (RyR1). We focus on two autosomal dominant (AD) RyR1 mutations, Y522S (YS) and I4898T (IT), which cause MH and CCD, respectively. The AD mode of inheritance and data indicating knock-out of one RyR1 allele is well-tolerated in mice led us to hypothesize that allele-specific gene silencing (ASGS) of the mutant allele would rescue RyR1 functional defects in skeletal muscle cells from YS and IT knock-in mice.

We evaluated the functional consequences of allele-specific silencing in YS and IT muscle cells using short interfering RNAs (siRNAs). To screen potential siRNAs for relative knockdown efficacy and allele specificity, we generated cDNAs encoding fusion proteins derived from wild type (WT) (Venus-Exons-3XFLAG) and either YS or IT mutation-containing (Cherry-Exons-3XHA) exons. Simultaneous transfection of these cDNAs and siRNAs into HEK293 cells and subsequent evaluation of mRNA (semi-quantitative RT-PCR) and protein levels (fluorescence microscopy and western blotting) was used to determine knockdown efficacy and allele-specificity prior to functional rescue experiments. Myotubes derived from heterozygous YS mice (YS/+) exhibit ~4-fold increase in caffeine sensitivity (EC_{50} values were 0.5mM and 2.3mM for YS/+ and WT, respectively). Treatment of YS/+ myotubes with a YS-selective siRNA, normalized caffeine sensitivity ($\text{EC}_{50} = 2.5\text{mM}$) without decreasing peak caffeine-induced release. Similarly, YS-selective siRNA treatment rescued the increased voltage sensitivity of Ca^{2+} release in YS/+ myotubes determined in perforated-patch clamp experiments ($\text{VF}_{1/2}$: WT = -18mV, YS/+ scrambled = -35mV, YS/+ YS-selective = -18mV). These results indicate that ASGS represents a promising approach for normalization of RyR1 function in MH and CCD. Similar functional rescue experiments in adult skeletal muscle fibres are currently underway.

Small molecule diffusion in inverse cubic phase lipid systems

S. Fraser,^{1,2} R. Mulder,² J. Cosgriff,² X. Mulet,² F. Separovic¹ and A. Polyzos,³ ¹School of Chemistry, Bio21 Institute, The University of Melbourne, VIC 3010, Australia, ²Ian Wark Laboratories, CSIRO CMSE, Clayton North, VIC 3165, Australia and ³Department of Chemistry, University of Cambridge, Cambridge, United Kingdom.

The cubic phases formed by amphiphiles are an important class of nanostructured self-assembled material. Colloidally stable, particulate dispersions of the inverse cubic phase, termed cubosomes, are of particular interest due to their thermal stability, large surface-area to volume ratio (up to 400m².g⁻¹ of cubic gel), their ability to incorporate functional molecules, and a viscosity approximately equal to that of water. In such structurally complex, multi-component systems, diffusion NMR is a powerful technique for measuring small molecule diffusion within cubosomes and, importantly, allows simultaneous acquisition of diffusion coefficients for free molecules in solution or bound to a receptor embedded in the lipid matrix. The model system used here is the biotin-Neutravidin system ($K_D = \sim 10^{-15}$ M), with the biotin chemically attached to a lipid incorporated into the cubosomes, whilst the Neutravidin is added in solution. The results reported here indicate a multi-component diffusion of water and proteins through the pores of cubosomes. NMR diffusion measurements show signal attenuation in the water and protein resonances whilst the lipid components of the system remain unaffected (Figure). The decrease in diffusion constants for water and protein in the cubosome system in comparison to free solution indicates that diffusion is dependent on the porous nature of the cubosome and protein binding.



DOSY proton NMR spectra of the phytantriol inverse cubic phase at 25°C.

Detection of proteins in the pathological deposits in Pseudoexfoliation syndrome using Atomic Force Microscopy

R. Creasey,¹ C. Gibson,¹ S. Sharma,¹ J.E. Craig,¹ T. Becker,² P. Hinterdorfer³ and N.H. Voelcker,¹ ¹Flinders University of South Australia, GPO Box 2100, Adelaide, SA 5001, Australia, ²Nanochemistry Research Institute, Curtin University, GPO Box U1987, Perth, WA 6845, Australia and ³Institute for Biophysics, Johannes Kepler University Linz, Altenberger St. 69, Linz 4040, Austria.

Protein aggregation is of significant interest to various disciplines; it can be the cause of debilitating diseases, or the foundation of advanced nanomaterials. One ocular disease hallmarked by protein aggregation is known as Pseudoexfoliation Syndrome (PEX). This condition is caused by the formation of insoluble aggregates, and is characterised by deposition of fibrillar proteinaceous material on the anterior lens capsule. PEX deposits in the eye block the aqueous outflow mechanisms, which can lead to an elevation in intraocular pressure and subsequent glaucoma. Glaucoma is the second leading cause of irreversible blindness worldwide, and PEX is the most common known risk factor for glaucoma.

Proteomic analyses have revealed an association of various genetic markers and protein expression with PEX; however a complete explanation for disease susceptibility is not yet available. As the aggregates are a complex arrangement of proteins, the ultrastructure is poorly characterised and many protein constituents of the aggregates remain unknown. This study addresses the critical issue of determining the molecular nature of PEX on lens capsules in their native state by atomic force microscopy (AFM) based antibody recognition imaging. The particular focus of this study is on a type of AFM methodology referred to as topography and recognition imaging (TREC). Proteins identified by proteomic data as being implicated in the PEX pathophysiology, such as clusterin and LOXL1, are detected by an AFM probe modified with the appropriate antibody. Topographical AFM images and antibody recognition images are obtained simultaneously to determine the specific location of proteins in and around PEX aggregates on the lens capsule anterior surface. These data, combined with data from alternative antibody-recognition imaging techniques, proteomic and genetic analyses, are leading to an improved understanding of the pathophysiological basis of PEX. A more complete understanding of the pathophysiological basis for the disease will lead to the development of earlier detection methods and treatments that target the disease instead of the subsequent glaucoma.

Visualisation of bacterial hydrodynamics

J.L. Flewelling, University of Oxford, Clarendon Laboratory, Parks Road, Oxford, OX1 3PU, England.

Bacteria and other microorganisms live in an aqueous, low-Reynolds number environment where viscous forces dominate. The means by which many microorganisms propel themselves through such an environment are not well understood. Additionally, understanding the way in which fluid couples physical interactions between micro-scale objects and surfaces has received increasing attention in a number of biological and technological fields over recent years. The traditional approaches to investigating these problems are mathematical simulations and particle image velocimetry (PIV) experiments. While modeling can be done in three dimensions, the vast majority of experimental investigations have been restricted to only two. This is primarily due to the reduced depth of field available at the high magnifications required to see microorganisms.

I have used some novel approaches to investigating hydrodynamic interactions on the micro-scale, specifically in the context of the bacterial flagellar motor. I have adapted in-line holographic PIV techniques (Cheong *et al.*, 2009) for use in a biological environment under high magnification. Assays of motile *Escherichia coli* are seeded with microsphere tracer particles and illuminated with a collimated laser beam. The coherent light scattering off a microsphere interferes with non-scattered light and results in a characteristic interference pattern. From this pattern, microsphere positions in three dimensions can be determined. This technique allows for greater depth of field than other techniques, and, when combined with high-speed video microscopy, can generate a full three-dimensional map of a flow field in a dynamic micro-system.

Independently, microspheres can also be used as passive detectors of dynamic behaviour. In a separate experiment, a microsphere is held in an optical trap in close proximity to a second microsphere attached to the motor of an immobilised bacterium. The resulting hydrodynamic interactions are recorded through video microscopy. The ultimate aim of this approach is to develop a non-contact method of detecting the motion of dynamic systems which are invisible under normal microscopy.

These methods hold promise for exploring and visualising not only bacterial systems, but any dynamic, aqueous micro-scale environment.

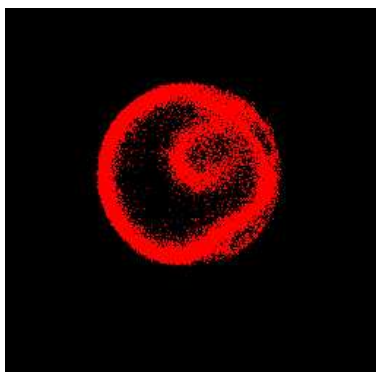
Cheong, FC, Sun, B, Dreyfus, R, Amato-Grill, J, Xiao, K, Dixon, L & Grier, DG (2009). Flow visualization and flow cytometry with holographic video microscopy. *Optics Express*, **17**(15), 13071–13079.

Shedding light on liposomes: Using lipid-mimetic metal complexes for fluorescent labeling

A. Mechler, M. S. Huda, E. Doevan and C. Hogan, Department of Chemistry, La Trobe University, VIC 3086, Australia

For the study of biophysical systems involving phospholipid membranes, such as membrane lysis by antimicrobial peptides, supported membrane deposition, or liposome size and shape studies, it is often desired to apply a fluorescent label to the lipid phase. However, lipid membranes are dynamic systems that are highly dependent on the strength of headgroup interactions, internal pressure and lipid mobility. If either of these factors is changed, the properties of the membrane (surface tension, liposome diameter, ability to attach to surfaces) might change as well, compromising the measurements. Unfortunately, fluorescent labeled lipids and membrane-specific dyes typically do change the physicochemical properties of the membrane. Our aim was to develop a fluorescent dye that is similar to the lipid molecules in shape and size, and to use it for liposome imaging.

Two metal complexes, $(\text{Ru}(2,2\text{-bipyridine})_2(4,4\text{-dinonyl-2,2-dipyridyl})(\text{PF}_6)_2)$ and $(\text{Ir}(2\text{-phenylpyridine})_2(4,4\text{-dinonyl-2,2-dipyridyl})(\text{PF}_6))$ have been synthesized, both with the same molecular structure: a "head group" made of the metal coordinated by bpy and ppy, respectively, and a "tail group" with two alkane chains. The lipid-mimetic complexes have been successfully reconstituted into DMPC liposomes. Importantly, when making the liposomes, extrusion was omitted; only a gentle vortexing and 30 s weak sonication was employed and the liposome size distribution was left to evolve. As a result, liposomes of a relatively broad size distribution were created, tending towards a bimodal distribution containing small unilamellar liposomes (SUV; $\sim 100\text{nm}$ of diameter) and large (up to micron size) liposomes, as revealed by DLS measurements. Importantly, the size distribution of the liposomes labeled with the metal complexes is very similar to DMPC liposomes without the fluorescent label, thus the presence of the complex does not alter significantly the physicochemical properties of the membrane. It is regularly assumed that if larger liposomes form they must be multilamellar "onion" structures with an SUV core. However, confocal microscopic imaging of the metal complex labeled liposomes shows hollow structures with occasional encapsulated smaller liposomes. The figure shows an example of a confocal microscopic cross-section picture of a large liposome enclosing a smaller one. Remarkably, the metal complexes suffer minimal, practically negligible photobleaching, making longer time lapse studies feasible. The two metal complexes fluoresce at different wavelengths opening the door for dichroic measurements with this new labeling method.



A liposome- in- liposome system, labeled with $\text{Ru}(\text{bpy})_2$ dinone. The diameter of the outer liposome is $\sim 3.5\mu\text{m}$.

Shedding light on neurodegeneration: small angle X-ray scattering and misfolded proteins

C.C. Curtain, Mental Health Research Institute, The University of Melbourne, Melbourne, VIC 3010, Australia.

The misfolding pathways that lead to cytotoxic species vary between diseases such as Alzheimer's (AD), Huntington's and Parkinson's but there is a common link in that they all involve some form of oligomeric species, in contrast to the extra- or intra-cellular fibrillar deposits of aggregated protein that are regarded as end products of the pathological process (Villemagne *et al.*, 2010). To elucidate possible folding pathways for the amyloid β peptide of AD (A β) we made time-resolved, stopped-flow SAXS measurements at the Australian Synchrotron on A β 1-40 and A β 1-42 peptides in dilute NaOH (13mM) that were rapidly mixed with pH 6.9 phosphate buffered saline containing Cu²⁺ ions. These showed that protofibril formation occurred in less than one second in either control or Cu²⁺-containing buffer and that evolution of the fibrils in subsequent seconds followed a non-linear pattern. Static measurements on the peptides that had been reacted with sub-micellar concentrations of the lipid mimetic, N-lauroylaminopropyl-N',N'- dimethylamine oxide (LDAO) and a dipeptide formed of tyrosine 10 cross-linked A β 1-40 (Kok *et al.*, 2009), however, gave a stable well-defined "Y" shaped structure for both the di-tyrosine linked peptide and LDAO- associated A β 1-42. The "Y" shape is reminiscent of the Fc antibody fragment. Since the di-tyrosine linked peptide is neurotoxic, as in the case of cytotoxic antibodies, its two arms may carry ligands able to cross-link cell membrane receptors to initiate a cytotoxic cascade.

Villemagne VL, Perez KA, Pike KE, Kok WM, Rowe CC, White AR, Bourgeat P, Salvado O, Bedo J, Hutton CA, Faux NG, Masters CL, Barnham KJ (2010) *Journal of Neuroscience* **30**: 6315-22.

Kok WM, Scanlon DB, Karas JA, Miles LA, Tew DJ, Parker MW, Barnham KJ, Hutton CA (2009) *Chemical Communications (Cambridge, England)* **7**: 6228-30.

Integrating peripheral and central mechanisms that regulate growth hormone (GH) secretion during periods of altered food consumption

F.J. Steyn, J.W. Leong and C. Chen, School of Biomedical Sciences (SBMS), The University of Queensland, St. Lucia, QLD 4067, Australia.

Growth hormone (GH) has gained most of its recognition for its role in stimulating linear growth. However it is also a key anabolic hormone in the regulation of energy balance; in this role GH stimulates muscle growth and bone density, and also regulates body fat mass and lipid metabolism. Somewhat reciprocally, body composition and meal pattern are both major determinants of GH secretion in that the central and peripheral peptides normally involved in the regulation of food intake mediate GH secretion. As a result, nutritional status impacts the regulation of the GH axis culminating in reduced or increased levels of GH secretion during periods of excessive or restricted energy consumption, respectively.

To fully understand the impact of energy flux on GH secretion, one must consider interactions between multiple endocrine systems and their integration with the central mechanisms that drive GH secretion. At its core, central regulation of GH secretion from the anterior pituitary gland is modulated by stimulating GH releasing hormone (GHRH) and inhibitory somatostatin (SRIF) neurons. These neurons are dispersed between populations of orexigenic (primarily NPY and AgRP expressing neurons) and anorexigenic neurons (including neurons expressing POMC and CART). Despite the fact that direct interactions between hypothalamic appetite regulatory neurons and those regulating GH secretion are still under investigation, clear relationships between peripheral factors coupled to food intake and GH secretion have been established. For example, ghrelin - a potent orexigenic hormone secreted by the stomach - stimulates both NPY/AgRP neurons and GH secretion.

The endogenous cannabinoid system has gained favour as a central regulator of appetite. Treatment with cannabinoid receptor subtype-1 (CB1) agonist result in a biphasic response in food intake; low dosages stimulate food consumption whereas high dosages have an inhibitory effect. Of particular importance regarding GH secretion and food intake is the potential role of the endogenous cannabinoid system in integrating peripheral with central mechanisms that are involved in mediating GH secretion. Early observations suggest that activation of the CB1 receptor by exogenous cannabinoids result in suppression of GH secretion. These studies do not take into account the biphasic effects of CB1 receptor activation, and consequently do not address potential stimulatory or inhibitory effects of cannabinoids on GH secretion. Furthermore, as fasting stimulates the endogenous cannabinoid system, early attempts do not address the potential interaction of cannabinoids on GH secretion during periods of reduced food intake.

Our recent observations confirm that central activation of the CB1 receptor suppresses the initial fasting-induced increase in GH secretion. Gene analysis studies confirm that these effects are mediated *via* an interaction with GHRH neurons. It should be noted, however, that the impact of fasting and the mechanisms that drive GH secretion during early periods of food restriction differ from those regulating pulsatile GH secretion during times of adequate food consumption. In this scenario we observe a differential impact following CB1 activation, where low levels of cannabinoid treatment (0.5mg/kg IP) resulting in increased food intake is coupled with an increase in GHRH mRNA within the arcuate nucleus. In contrast, elevated dosages (1.0mg/kg IP) of cannabinoid treatment do not affect food intake nor do they induce any alterations in GHRH mRNA expression. This finding was surprising considering that the same dosage (1.0mg/kg IP) was sufficient to inhibit the initial fasting-induced increase observed in GHRH mRNA. We are currently extending these observations to determine whether the differential impact on GHRH neurons relates to changes in peripheral GH secretion. Overall, our observations suggest that the endogenous cannabinoid system may prove to be yet another mechanism involved in the already complicated array of integrated systems that regulate GH secretion during periods of altered food consumption.

Control of energy balance by nutrient sensing neurons

M.A. Cowley, Department of Physiology, Monash University, Clayton, VIC 3800, Australia.

Obesity confers significant health risks, and rates of obesity continue to rise within the developed and developing world. The Cowley lab has discovered how Proopiomelanocortin (POMC) neurons in the brain detect levels of leptin, which signals adipose stores. This signal allows the brain to regulate food intake and energy expenditure to maintain homeostasis. We have also discovered that the melanocortin circuits transduce the appetite reducing actions of the gut hormone PYY3-36, and the appetite stimulating actions of ghrelin. This suggests that the melanocortin circuits are a major neural center for processing signals of energy status to regulate long term body weight. More recently the lab has discovered how the brain becomes resistant to leptin, and how leptin resistance is a hallmark of obesity. The lab has developed several therapies that bypass leptin resistance and regulate food intake and energy expenditure to reduce adipose stores and cause weight loss. One of these therapies has recently completed Phase 3 trials.

Regulation of hypothalamic GHRH neuronal activity by ghrelin and obestatin

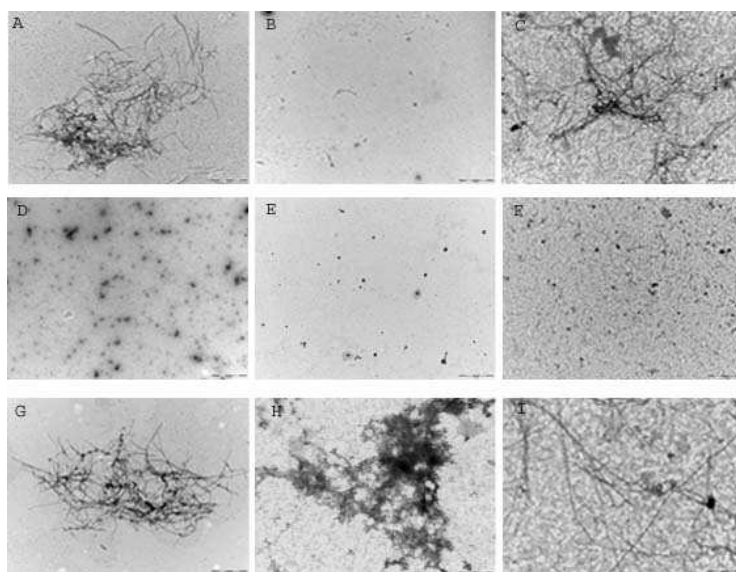
J. Epelbaum, Center for Psychiatry & Neuroscience, UMR-S894 Inserm, Faculté de Médecine, Université Paris Descartes, 75006 Paris, France. (Introduced by Chen Chen)

Ghrelin, a natural ligand of the Growth Hormone Secretagogue Receptor (GHS-R), is synthesized in the stomach but it may also be expressed in lesser quantity in the hypothalamus where the GHS-R is located on Growth Hormone Releasing Hormone (GHRH) neurons. Obestatin, a 23 amino acid peptide derived from the same precursor as ghrelin, antagonizes ghrelin-induced increase of Growth Hormone (GH) secretion *in vivo* but it is not active on pituitary explants *in vitro*. Thus, the blockade of ghrelin-induced GH release by obestatin is likely mediated at the hypothalamic level within the neuronal network which controls pituitary GH secretion. Ghrelin increased GHRH and decreased somatostatin (somatotropin releasing inhibitory factor, SRIF) release from hypothalamic explants while obestatin only reduced ghrelin-induced increase of GHRH release. Thus, the effect of ghrelin and obestatin is targeted to GHRH neurons. Patch-clamp recordings on mouse GHRH-eGFP neurons indicate that ghrelin and obestatin do not affect glutamatergic synaptic transmission. In sharp contrast, ghrelin decreases GABAergic synaptic transmission, an effect which is blocked in the presence of the GHS-R antagonist BIM-28163. Ghrelin also stimulates the firing rate of GHRH neurons. Obestatin blocks the effects of ghrelin on GABAergic synaptic transmission. These data suggest that 1) ghrelin increases GHRH neurons excitability by increasing their action potential firing rate and decreasing the strength of GABA inhibitory inputs, thereby leading to an enhanced GHRH release and 2) obestatin can counteract ghrelin actions. Such interactions between metabolic regulatory neuropeptides on GHRH neurons are likely to participate in the control of GH secretion.

Electron microscopic study of the effect of p75NTR extracellular domain on the amyloid β protein assembly

J.J. Lu, M. Yang, Y. Lim, J.H. Zhong, Y.J. Wang and X.F. Zhou, Department of Physiology, Flinders University of South Australia, Bedford Park, SA 5042, Australia.

Accumulation of toxic amyloid- β in the cerebral cortex and hippocampus is a major pathological feature of Alzheimers disease (AD). The p75 neurotrophin receptor (p75NTR) is the common receptor for neurotrophins which can mediate cell death and neurite degeneration. Previous studies showed that the expression of p75NTR is increased in AD brain and activation of p75NTR by A β and nerve growth factor (NGF) does not always promote neuronal death but can promote survival of human neurons (Zhang *et al.*, 2003). In this study, we investigated the effect of p75NTR extracellular domain fused with Fc fragment of human IgG (p75/Fc) on the A β assembly using transmission electron microscopy (TEM). A β peptide purchased from American Peptide (Sunnyvale,CA) was dissolved in DMEM at the final concentration of 22 μ mol/l. Samples were divided into 4 experimental groups and incubated at 4°C and 37°C respectively for 24 hours: 1, A β prepared immediately after dissolution without incubation; 2, A β incubated alone; 3, A β incubated with p75NTR (molar ratio 1:0.5) and 4, A β incubated with human IgG (molar ratio 1:0.5).



Electron micrographs of samples of incubates. Scale bars 1 μ m.

We found that A β prepared immediately after dissolution without incubation showed only amorphous material under TEM. After A β was incubated alone at 37°C for 24 hours, numerous fibrils were seen (Figure A). However, when A β was incubated together with p75/Fc, only short fibrils can be observed and the number of fibrils remarkably reduced (Figure B). Addition of Human Ig G into the A β solution did not alter the morphology and number of fibrils obviously (Figure C). After incubation at 4°C, numerous oligomers formed (Figure D). Addition of p75/Fc to the A β remarkably reduced the number of oligomers (Figure E) but addition of human IgG did not change the morphology and number of oligomers (Figure F). We further investigated whether the p75/Fc can disaggregate the preformed A β fibrils. When preformed A β fibrils were incubated with p75/Fc for additional 3 days, most fibrils disassembled and became aggregates, but these fibrils showed no change when incubated with human IgG (Figure H). In conclusion, p75/Fc can inhibit the oligomerization and fibrillation of A β . Furthermore, p75/Fc can also disaggregate the preformed A β fibrils. Thus, p75 NTR may be a potential therapeutic agent for AD.

Zhang Y, Hong Y, Bounhar Y, Blacker M, Roucou X, Tounekti O, Vereker E, Bowers WJ, Federoff HJ, Goodyer CG, LeBlanc A. (2003) p75 neurotrophin receptor protects primary cultures of human neurons against extracellular amyloid beta peptide cytotoxicity, *Journal of Neuroscience* **23**: 7385-7394.

Superoxide dismutase 2 in human brain: A marker for mitochondria and mitochondrial dysfunction in Parkinson's disease and dementia with Lewy bodies

O. Barnes and J.H.T. Power, Department of Human Physiology, School of Medicine, Flinders University, Bedford Park, SA 5042, Australia.

Mitochondrial dysfunction and oxidative stress are regarded as two of the main mechanisms associated with the pathogenesis of Parkinson's disease (PD) and Dementia with Lewy body disease (DLB). Both PD and DLB are neurodegenerative diseases termed synucleinopathies characterized by the formation of intracellular inclusions termed Lewy bodies. Lewy bodies are aggregations of lipid and protein within the dopaminergic neurones within the substantia nigra in PD and within cortical neurones in DLB. There is still debate as to whether Lewy bodies are protective or are detrimental to neurones, although there are several reports that they generate hydrogen peroxide. Cellular antioxidant enzymes offer protection against reactive oxygen species, including free radicals and peroxides, produced as a by-product of oxidative phosphorylation. The mitochondrial antioxidant enzyme superoxide dismutase 2 (SOD2) is a key enzyme in mitochondrial defences as it inactivates the superoxide radical to form hydrogen peroxide during oxidative phosphorylation. Several other enzymes such as glutathione peroxidase 4 (GPx4) and the more recently identified peroxiredoxin 3 and peroxiredoxin 5 inactivate mitochondrial derived hydrogen peroxide. These antioxidants are vital to protect mitochondria from oxidative damage to DNA, lipids and proteins. This project is focussed on the distribution of SOD2 in human brain and the profile of oxidative damage in PD and DLB.

Human brain proteins from PD, DLB and control tissue were separated using PAGE and the molecular forms of SOD2 were determined using Western blotting. The general distribution of SOD2 was examined using light immunohistochemistry and the specific cellular distribution with confocal immunofluorescence with specific cellular markers. SOD2 was co-localized with the Lewy body marker α -synuclein to determine if there was a relationship between Lewy body pathology and mitochondria since we have previously observed mitochondrial components in Lewy bodies using electron microscopy. In addition, SOD2 was co-localized with a marker of oxidative DNA damage (8-hydroxy-2-deoxyguanosine) to determine if mitochondrial or nuclear DNA damage was present in these diseases. A SOD2 ELISA was set up to determine if the level of this enzyme was up or down regulated in PD or DLB.

Western blotting indicated that SOD2 was an abundant enzyme in white and gray matter of all brain regions examined with a molecular weight of 22kD, the predicted molecular weight of SOD2. Light immunohistochemistry indicated that SOD2 was present in most cells with a granular staining consistent with mitochondrial staining. There appeared to be stronger staining in the control brain tissue with the large cortical neurones particularly prominent. A network of granular staining was observed in all tissues consistent with mitochondrial staining in axons. Confocal immunohistochemistry with cellular markers indicated that neurones, astrocytes, microglia and oligodendrocytes were all positive for SOD2, consistent with this enzyme being essential in all cells. White matter in diseased tissue was well stained and many astrocytes were large and activated.

Confocal immunohistochemistry co-localizing α -synuclein and SOD2 in PD and DLB showed that mitochondria were sequestered into Lewy bodies in a progressive manner. Lewy bodies were seen to be surrounded with SOD2 positive mitochondria. In neurons with advanced Lewy bodies mitochondrial fragments and SOD2 were present but the mitochondrial integrity appeared to be lost. ELISA results indicated that the level of SOD2 was highest in normal control brain indicating that SOD2 was not upregulated in these diseases. This is in contrast to the cellular antioxidants peroxiredoxin 6 and glutathione peroxidase 1 in these diseases. Staining with a DNA oxidative marker showed that neurones with Lewy bodies did not exhibit mitochondrial nuclear damage. Interestingly, surrounding glial cells showed marked oxidative damage as shown by the nuclear staining.

In conclusion these results show that SOD2 is an abundant antioxidant enzyme in human brain and present in most cells and is an excellent marker for mitochondria. The finding that mitochondria are sequestered into Lewy bodies may have serious implications for neuronal survival. The loss of cellular energy production may be the mechanism of cell death in these diseases.

The relationship between fibrillin and Marfan's syndrome

Y. Lu,¹ R. Jeremy,² M. Kekic¹ and B.D. Hambly,¹ ¹Discipline of Pathology, Bosch Institute, University of Sydney, NSW 2006, Australia and ²Central Clinical School, Cardiology, Royal Prince Alfred Hospital, University of Sydney, NSW 2006, Australia.

Fibrillin is a 350kDa calcium-binding glycoprotein that is vital for the formation of elastic and non-elastic fibers in connective tissue. It is secreted into the extracellular matrix by fibroblasts and becomes incorporated into insoluble microfibrils, which provide a scaffold for deposition of elastin. Mutations in fibrillin are associated with several different connective tissue diseases, especially Marfan's syndrome (MFS). The initial hypothesis has been that mutations in fibrillin result in defective microfibrils. However, fibrillin-1 also interacts with latent transforming growth factor- β binding proteins and controls TGF- β bioavailability; dysregulation of TGF- β activation and signalling has been demonstrated in the diseased tissues of an MFS-affected mouse model. Therefore, one or both mechanisms of dysfunction may result in the MFS phenotype. The human FBN gene consists of repeating EGF (epidermal growth factor) domains and TB (transforming growth factor β -binding protein) domains. The majority of EGF domains contain a Ca^{2+} binding consensus sequence and are known as cbEGF domains (43/47 cbEGF domains in FBN1 and FBN2; 42/44 cbEGF domains in FBN3). Ca^{2+} confers structural rigidity to the fragment, producing a rod-like conformation by structural and dynamic studies of tandem repeats of cbEGF domains. TB domains exist uniquely in the microfibril protein family, locating in extracellular matrix fibrils; the major function is involved in extracellular matrix construction and storage of latent TGF- β . All TGF- β isotypes are over expressed in MFS. We have examined the locations of over 600 mutations in fibrillin-1 that cause MFS, then correlated and classified the mutations in terms of their structural and functional consequences. We have shown that in some case Ca^{2+} -binding is impaired (EGF domain structural defect) and in other cases storage of latent TGF- β is predicted to be altered due to TB domain structural perturbations.

Oxytocin depolarizes mitochondrial membrane in freshly isolated myometrial cells

F.S. Gravina,¹ P. Jobling,¹ R.B. de Oliveira,¹ K.P. Kerr,¹ H. Parkinson² and D.F. van Helden,¹ ¹School of Biomedical Sciences and Pharmacy, University of Newcastle, NSW 2308, Australia and ²Department of Physiology, Monash University, VIC 3800, Australia.

Oxytocin is a peptide hormone involved in reproduction, including stimulation of uterine contractions and lactation. Even though oxytocin agonists and antagonists have been used for the induction and prevention of labour, the mechanism of action on uterine smooth muscle is not fully understood. It is known that oxytocin increases intracellular Ca^{2+} , stimulating Ca^{2+} entry and Ca^{2+} release from the sarcoplasmic reticulum (SR). The SR also interacts closely with mitochondria and we have previously shown that mitochondria play an important role in uterine activity. The aim of this study is to investigate whether and if so how mitochondria respond to oxytocin. Female Swiss mice (6-10 weeks) were euthanased by overexposure to the inhalation anaesthetic isoflurane (5-10%) followed by exsanguination, a procedure approved by the Animal Care and Ethics Committee at the University of Newcastle. Uteri were dissected out and the endometrium removed by fine dissection. Isolated cells were obtained by placing myometrial strips into an enzymatic solution containing 0.1% collagenase, 0.03% elastase and 0.3% hyaluronidase for 50 minutes, followed by trituration. To evaluate changes in mitochondrial membrane potential, myometrial cells were loaded with $5\mu\text{g/ml}$ 5,5',6,6'-tetrachloro-1,1',3,3'-tetraethylbenzimidazolocarboxyanide iodide (JC-1) for 1 hour and then were perfused for 30 minutes with Hepes buffer prior to experiments. JC-1 J-aggregates (complexes formed in high mitochondrial membrane potential) were visualized with excitation/emission of 488/585 nm, while JC-1 monomers were detected at 488/522 nm. Application of 0.1nM and 1nM oxytocin, perfused for 11 minutes, decreased mitochondrial membrane potential (Ψm) to $92 \pm 2\%$ ($n=5$ cells) and $73 \pm 4\%$ ($n=9$ cells, different from control, $p<0.001$) of control respectively. As a positive control, 1 μM carbonylcyanide 3-chlorophenylhydrazone (CCCP) was perfused and caused a large decrease in Ψm , this being $58 \pm 9\%$ of control ($p<0.001$). To understand the mechanisms involved in this mitochondrial depolarization, oxytocin 1nM was applied in combination with 2-APB (an inhibitor of IP3 receptors and store-operated Ca^{2+} entry), in Ca^{2+} free (0.5mM EGTA) solution, or with 2 mM nifedipine (L-type Ca^{2+} channel blocker). When decreasing intracellular Ca^{2+} , either by inhibiting Ca^{2+} entry or SR Ca^{2+} release, the effect of oxytocin on mitochondrial depolarization was diminished. In the presence of 2-APB, the mitochondrial depolarization evoked by 1nM oxytocin was $88 \pm 3\%$ of control ($n=8$ cells), in Ca^{2+} free (EGTA) solution it was $91 \pm 2\%$ of control ($n=8$ cells) and with nifedipine it was $87 \pm 5\%$ of control. These results were not significantly different from control ($p>0.05$), suggesting that Ca^{2+} has a substantial role in mediating the oxytocin-induced change in Ψm . It is concluded that oxytocin depolarizes the mitochondrial membrane and this mechanism is in part dependent on intracellular $[\text{Ca}^{2+}]$.

Intrauterine growth restricted fetuses have increased blood flow to the adrenals and decreased blood flow to the heart but no difference in brain blood flow

R. Poudel, I.C. McMillen, S. Dunn and J.L. Morrison, Early Origins of Adult Health Research Group, Sansom Institute, University of South Australia, Adelaide, SA 5000, Australia.

Intrauterine growth restriction (IUGR) refers to the inability of a fetus to grow to its genetically determined potential size. IUGR fetuses are known to have an increased risk of cardiovascular disease in later life. The most common cause of IUGR is placental insufficiency, which is associated with a reduction in delivery of oxygen and/or nutrients to the fetus. It is well established that in response to acute hypoxemia, fetuses redistribute their cardiac output to maintain adequate perfusion of key organs including the brain, heart and adrenal glands at the expense of peripheral tissues. It is not known, however, whether the redistribution of cardiac output persists in chronically hypoxemic IUGR fetuses. The surgical removal of uterine caruncles (placental attachment sites) in the non-pregnant ewe results in the restriction of placental growth (PR) and chronic fetal hypoxemia. We hypothesize that exposure of the fetus to PR and chronic hypoxemia results in increased blood flow to the brain, heart and adrenals in late gestation. At 123 ± 1 d gestation, vascular catheters were implanted in the fetuses to measure fetal blood gases, blood pressure (BP) and heart rate (HR). Blood flow studies were conducted at 130 ± 1 d of gestation, using fluorescent labelled microspheres. At 133 ± 1 d gestation (term 150 ± 3 d), ewes and fetuses were humanely killed and fetal weights recorded. The fetal tissues including brain, heart and adrenals were dissected and weighed. Microspheres were harvested by tissue digestion and the amount of fluorescence in each organ was then quantified to measure blood flow. Fetuses were allocated into two groups: control (C) (n=6) and IUGR (n=5) according to their mean gestational PaO₂ and fetal weight. Fetal weight (C, 3.7 ± 0.1 kg; IUGR, 2.7 ± 0.1 kg) and mean gestational PaO₂ (C, 21.8 ± 1.4 mmHg; IUGR, 15.4 ± 0.2) were significantly reduced in the IUGR group. There was no difference in baseline MAP and HR between the control and IUGR fetuses. There was no difference in blood flow to brain between the two groups, however IUGR fetuses had a significantly higher blood flow to the adrenals and significantly lower blood flow to the heart compared to control fetuses. Reduction in heart blood flow in IUGR fetuses may be responsible for changes in cardiomyocyte and blood vessel development and increase the risk of cardiovascular disease in their adult life. Whereas the increase in blood flow to the adrenal may be necessary to support the increase in plasma cortisol concentrations in IUGR fetuses. The lack of change in brain blood flow in the IUGR fetus, who exhibits brainsparing is an unexpected finding but may reflect differences in substrate delivery, extraction or consumption in the brain of the IUGR fetus.

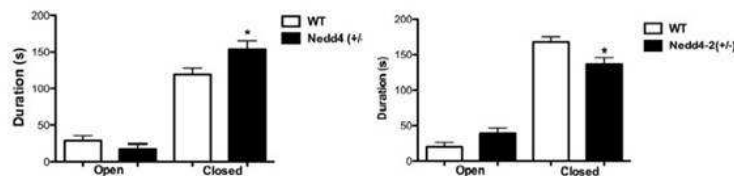
Nedd4 and Nedd4-2 heterozygosity leads to opposing anxiety behaviour in mice

D. Bongiorno,^{1,2} N. Boase,³ S. Kumar³ and P. Poronnik,^{1,2} ¹School of Medical Sciences, RMIT University, Bundoora 3083, ²Health Innovations Research Institute (HIRi), RMIT University, Bundoora 3083 and ³Centre for Cancer Biology, SA Pathology, Frome Road, Adelaide 5000.

Introduction: Nedd4 and Nedd4-2 (Neural precursor cell Expressed Developmentally Down-regulated 4 and 4-2) are two closely related ubiquitin ligases (E3) that have distinct substrates within the central nervous system (CNS) (Yang and Kumar, 2010). The absolute physiological implications of which have yet to be determined. Therefore it is not surprising that Nedd4 and Nedd4-2 knockout mice are not viable and die shortly after birth due to developmental or physiological defects. In this study we investigated whether a single copy deletion of either Nedd4 or Nedd4-2 (by using heterozygous mice) is sufficient to alter anxiety related behaviours *in vivo*. We hypothesize that although Nedd4 and Nedd4-2 are closely related E3s, they are likely to be functionally different due to unique substrate profiles, and that their loss may have differential effects on animal behaviour.

Method: Elevated plus maze (EPM) was used to assess anxiety in adult (8-12 week old) Nedd4 heterozygous (+/-, n=14), Nedd4-2 heterozygous (+/-, n=8) and wild type (WT) littermate controls (n=8 for each group). The EPM is composed of two open and two closed arms, and mice are given 5 minutes to explore the maze. The proportion of time spent in the open versus closed arm is an indicator of anxiety. For example, increase in duration spent in closed over open arm indicates increased anxiety, and conversely a decrease in time spent in open over closed arm indicates decreased anxiety.

Results:



Results from this study show that when a single copy of the gene encoding for Nedd4 or Nedd4-2 is deleted, significant alterations in anxiety is produced. Interestingly, as shown in the figure, Nedd4 heterozygous mice spend a significantly longer duration in the closed arm of the maze compared to wild-type littermate controls, suggesting increased anxiety. Conversely, Nedd4-2 heterozygous mice spend significantly less time in the closed arm, and subsequently increase the time spent exploring the open arm suggesting reduced anxiety in these mice compared to wild type littermate controls.

Conclusion: Nedd4 and Nedd4-2 may modulate neuronal function by targeted degradation of specific substrates that may contribute to the observation in anxiety changes. Further investigations are required to define precise E3 substrates that modulate anxiety behaviours in these mice.

Yang, B. and S. Kumar (2010). "Nedd4 and Nedd4-2: closely related ubiquitin-protein ligases with distinct physiological functions." *Cell Death and Differentiation* **17**(1): 9.

Parvalbumin-immunoreactive neurons in the rat ventral respiratory column receive close appositions from galanin-immunoreactive axons

K.L. Jung,¹ D.R. McCrimmon,² G.F. Alheid,² G.M. Etelvino¹ and I.J. Llewellyn-Smith,¹ ¹Cardiovascular Medicine, Physiology and Centre for Neuroscience, Flinders University, Bedford Park, SA 5042, Australia and ²Physiology, Feinberg School of Medicine, Northwestern University, Chicago, IL 60208, USA.

The neurochemistry of neurons in the ventral respiratory column (VRC) correlates with their function (Feldman *et al.*, 2003; Alheid & McCrimmon, 2008). Galanin (GAL) influences breathing when injected into the VRC (Abbott *et al.*, 2009) and occurs in about 40% of chemosensitive neurons in the retrotrapezoid nucleus (RTN), which lies ventral and caudal to the facial nucleus (Stornetta *et al.*, 2009). Two-thirds of large VRC neurons with spinally-projecting axons contain the calcium binding protein, parvalbumin (Parv; Alheid *et al.*, 2002). In the VRC, the neurokinin 1 receptor (NK1R) occurs in small neurons of the PreBötzinger (PreBöt) group and in larger bulbospinal neuron that occur caudal to the PreBöt neurons (Guyenet *et al.*, 2002). In this study, we used peroxidase immunohistochemistry to investigate whether GAL-immunoreactive axons innervate Parv-immunoreactive VRC neurons and to characterize the neurochemistry of a new group of GAL-immunoreactive neurons that we identified in the caudal ventral respiratory group (cVRG).

Male and female Sprague-Dawley rats were anesthetized with pentobarbitone (60 mg/kg i.p.) and perfused transcardially with phosphate-buffered 4% formaldehyde. Each perfused medulla was cut on a cryostat at 30 µm into 4 series of sections. In some series of sections, GAL-immunoreactivity was visualized alone using a black peroxidase reaction product. A second set of sections was stained to reveal Parv with a brown peroxidase reaction product and GAL with a black peroxidase reaction product. In a third set of sections, NK1R-immunoreactivity was detected with a black reaction product; and GAL, with a brown product.

We identified two groups of GAL-immunoreactive somata in the ventral medulla. The rostral group, which are the RTN neurons, lay medial and ventral to the caudal end of the facial nucleus. A second GAL-positive group was located more caudally, immediately ventral and slightly lateral to the column of Parv neurons. In a 1:4 series of sections, there were on average 56 ± 12 neurons (n=8) in this caudal GAL-containing group. The location of the second group suggested that these might be PreBöt neurons and therefore might contain NK1R. Some of the caudal GAL-immunoreactive neurons were NK1R-immunoreactive as well as GAL-immunoreactive. However, these NK1R-positive neurons were too big to be PreBöt neurons. In the VRC, occasional black GAL-immunoreactive axons closely apposed some large brown Parv-immunoreactive cell bodies.

These observations indicate that GAL occurs in a population of bulbospinal neurons in cVRG as well as in some RTN neurons. The data also suggest that GAL may influence respiration at two sites within central respiratory circuitry. RTN neurons may release GAL onto Parv-immunoreactive VRC neurons, which innervate spinal motor neurons that control respiratory pump muscles. Bulbospinal cVRG neurons may also release GAL directly onto spinal motor neurons innervating pump muscles.

- Abbott SB, Burke PG, Pilowsky PM. (2009) Galanin microinjection into the PreBotzinger or the Botzinger Complex terminates central inspiratory activity and reduces responses to hypoxia and hypercapnia in rat. *Respiratory Physiology and Neurobiology* **167**: 299-306
- Alheid GF, Gray PA, Jiang MC, Feldman JL, McCrimmon DR. (2002) Parvalbumin in respiratory neurons of the ventrolateral medulla of the adult rat. *Journal of Neurocytology* **31**: 693-717.
- Alheid GF, McCrimmon DR. (2008) The chemical neuroanatomy of breathing. *Respiratory Physiology and Neurobiology* **164**: 3-11.
- Feldman JL, Mitchell GS, Nattie EE. (2003) Breathing: rhythmicity, plasticity, chemosensitivity. *Annual Review of Neuroscience* **26**: 239-266.
- Guyenet PG, Sevigny CP, Weston MC, Stornetta RL. (2002) Neurokinin-1 receptor-expressing cells of the ventral respiratory group are functionally heterogeneous and predominantly glutamatergic. *Journal of Neuroscience* **22**: 3806-3816.
- Stornetta RL, Spirovski D, Moreira TS, Takakura AC, West GH, Gwilt JM, Pilowsky PM, Guyenet PG. (2009) Galanin is a selective marker of the retrotrapezoid nucleus in rats. *Journal of Comparative Neurology* **512**: 373-383.

Mechanism underlying distension-evoked peristalsis in guinea-pig distal colon: is there a role for enterochromaffin (EC) cells?

*N.J. Spencer, L. Robinson, S.J. Gregory, M. Kyloh, V. Zagorodnyuk, H. Peiris, S. Brookes and D.J. Keating,
Department of Human Physiology, Flinders University of South Australia, Bedford Park, SA 5042, Australia.*

Background: The mechanism underlying distension-induced peristalsis in the large intestine is unknown. Studies have suggested that the initiation of peristalsis is due to release of 5-hydroxytryptamine (5-HT) from enterochromaffin (EC) cells in the mucosa, which activates neighbouring sensory nerve endings. However, no direct evidence to support this hypothesis exists, since real time recordings of 5-HT release from EC cells have not been made during colonic peristalsis.

Methods: Real time amperometric recordings with video imaging of colonic movements were used to determine whether 5-HT release from EC cells was required for distension-evoked peristalsis in guinea-pig colon.

Results: Amperometric recordings revealed a basal and transient release of 5-HT from EC cells during peristalsis. This was evident when the carbon fibre electrode, lowered to within 100 μ m of the mucosal border, recorded an ambient release of 5-HT of 22 μ M (N=5). However, removal of the mucosa and submucosal plexus abolished all release of 5-HT (0.0 μ M; N=5), but did not prevent, nor inhibit the initiation of peristalsis, nor propulsive force generated during peristalsis. The propagation velocity of fecal pellets along the colon of dissected (mucosa-free) preparations (1.7 ± 0.2 mm/s; N=14) was significantly reduced compared to control intact preparations (2.6 ± 0.2 mm/s; N=25). This reduction in propagation velocity occurred even though there was no reduction in propulsive force generated during peristalsis in preparations devoid of mucosa and submucosal plexus. Maintained distension by fecal pellets generated cyclical peristaltic waves, which also persisted following removal of the mucosa and submucosal plexus, albeit with a reduced pacemaker frequency.

Conclusions: The initiation of colonic peristalsis evoked by physiological distension and the propagation of physiological colonic content does not require any release of 5-HT from EC cells, the submucosal plexus, nor activation of sensory nerve endings in the mucosa, as previously hypothesized. Our data lead to the inescapable conclusion that the mechanoreceptors activated by radial distension and sensory neurons which initiate peristalsis lie in the myenteric plexus and/or *muscularis externa*. Moreover, the pattern generator underlying cyclical generation of peristaltic waves in response to maintained distension also does not require release of 5-HT from the mucosa, or neural activity from within the submucosal plexus.

Identification of the pacemaker mechanism underlying migrating motor complexes in mouse small intestine

L. Beech, S. Gregory, M. Kyloh and N.J. Spencer, Department of Human Physiology, Flinders University of South Australia, Bedford Park, SA 5042, Australia

Introductions: Migrating motor complexes (MMCs) are spontaneous contractions of the small intestine, which occur cyclically and propagate over large lengths of intestine, leading to the propulsion of intestinal content. Although the mechanism underlying MMC generation is unknown, there has been a resurgence of interest in the mechanisms underlying the pacemaker or "clock" that generates spontaneous MMCs. This is because in human patients with diarrhea-predominant IBS (D-IBS) the frequency of MMC is altered and thought to be responsible for the abdominal pain and discomfort underlying the disease. Data obtained from a number of laboratories strongly suggests that the activity of the MMC pacemaker involves release of serotonin (5-HT) from the intestinal epithelium (mucosa), since antagonists of the 5-HT₃ receptor slow the MMC pacemaker and prolong intestinal transit, making these drugs effective in relieving the symptoms of D-IBS. What is not clear, is how or where the release of 5-HT from EC cells acts to control the MMC pacemaker, or whether EC cells themselves even form part of the MMC pacemaker mechanism. Greater than 90% of all the 5-HT in the body is made and released specifically by EC cells in the intestinal mucosa, so an understanding of whether EC cells and 5-HT release from EC cells is involved in the MMC pacemaker mechanism is of supreme importance to clinical treatment of D-IBS. Although the location of the pacemaker that generates MMC rhythmicity is unknown, it must lie within the small intestine itself, since MMCs still occur in an isolated ileum.

Aim: To determine the role of the mucosa and submucosal plexus (and hence endogenous serotonin release from EC cells) in the generation and propagation of spontaneous MMCs.

Methods: Spontaneously occurring MMCs were recorded from isolated intact segments of mouse ileum at 36°C. Simultaneous mechanical recordings were made from three sites along the ileum to determine the propagation velocity and direction of velocity of MMCs. The primary aim was to determine whether MMCs would still occur if the mucosa and submucosal plexus were removed from the ileum and if so, how are their properties different from control preparations with mucosa present.

Results: In intact preparations of ileum, regular MMCs were recorded, with a mean interval of 4.1 ± 0.1 min (n=5). To test whether the mechanisms underlying MMC generation required the mucosa, we sharply dissected off the mucosa, submucosa and submucosal plexus from the entire full length of ileum. Removal of these structures did not prevent the cyclical generation of MMCs. Surprisingly, the pacemaker frequency actually increased, such that the mean interval between MMCs after the removal of the mucosa, submucosa and submucosal plexus was 2.6 ± 0.2 min; n=5 ($p < 0.05$). There were no significant differences in MMC amplitudes (control: 0.5 ± 0.06 mN, *c.f.* without mucosa: 0.1 ± 0.01 mN; n=4; $p < 0.05$), or half durations (control: 29.7 ± 3.1 s *c.f.* without mucosa: 16.8 ± 1.3 s; n=4; $p < 0.05$). MMCs that persisted in dissected preparations consisting of only myenteric ganglia and smooth muscle were abolished by hexamethonium $200 \mu\text{M}$; n=3.

Conclusions: These results lead to the inescapable conclusion that in the small intestine, the pacemaker and pattern generator underlying the cyclical generation and propagation of MMCs is located within the myenteric plexus and/or *muscularis externa* and do not require the release of substances from the mucosa or neuronal activity within the submucosal plexus for their spontaneous activation.

The effects of amyloid precursor protein (APP) trafficking, processing and interaction with p75 in the presence of amyloid- β

K. Smith, M. Yang and X. Zhou, Department of Human Physiology, Flinders University, GPO Box 2100, Adelaide, SA 5001, Australia.

Alzheimer's disease (AD) is one of the most well known and most debilitating neurodegenerative diseases. Neurons die in AD due to toxic levels of amyloid beta ($A\beta$) proteins and tangled clusters of tau proteins within the cell. The $A\beta$ originates from cleavage of APP (amyloid precursor protein). APP has been shown to interact with p75NTR (the neurotrophin receptor), leading to cell death (Fombonne *et al.*, 2009). However, how APP interacts with p75NTR and whether the receptor ligands affect their interactions are not known. We propose that p75NTR ligands may affect APP-p75TR interactions and the interaction may participate in the development of AD.

In the present study we attempted to use FRET (fluorescence resonance energy transfer) analysis to characterize the nature of the APP-p75NTR interaction in HEK293 cells which were transfected with p75NTR-CFP and APP-YFP plasmids and controls. These cells were subjected to a range of neurotrophins, and $A\beta$, at differing concentrations. The FRET efficiency of APP-p75NTR was significantly higher than the negative control and comparable to the positive control, suggesting these two molecules are close to each other. All neurotrophins at least in a lower concentration triggered an increase in the FRET efficiency between p75NTR and APP, suggesting neurotrophins can enhance the interaction between p75NTR and APP. Interestingly, $A\beta$ at all concentrations triggered a dramatic increase in FRET efficiency, reaching over 3-fold of the positive control, suggesting that $A\beta$ can cause p75NTR-APP clumping together and trigger an aggressive interaction between these molecules. As $A\beta$ is the pathogenic agent for AD, the subsequent experiments had focused on the nature of the $A\beta$ induced interactions.

$A\beta$ time course of $A\beta$'s effect on p75NTR-APP interaction was undertaken. Results showed that the interaction increased dramatically within the first 1-3 minutes of the addition of $A\beta$ to the cells. $A\beta$ not only had a profound effect on p75NTR-APP interaction, but also its effect was almost immediate, suggesting a quick biochemical reaction. It is known that both p75NTR and APP have phosphorylation sites within their intracellular domains. We propose that a phosphorylation event may play a role in the interaction of p75NTR-APP upon addition of the ligand $A\beta$. When a phosphorylation inhibitor KT5720 was added to transfected cells with added $A\beta$, FRET efficiency dropped. Reciprocally, when a phosphorylation activator 8-Br-cAMP was added, FRET efficiency increased significantly. These data seem to support the idea that p75NTR-APP interaction is under the influence of a phosphorylation event. Furthermore we proposed that endogenous $A\beta$ may constitutively activate the interactions of p75NTR and APP. To test the idea, FRET efficiency dropped further by blocking endogenous $A\beta$ with an antibody 6E10, indicating endogenous $A\beta$ may increase the interaction of APP and p75NTR. Also, the preliminary data support that $A\beta$ increases APP transcription possibly *via* activation of the p75NTR-APP pathway. This could suggest that $A\beta$ may have a positive feed forward mechanism that increases APP transcription, which may in turn increase an output of $A\beta$. We conclude that p75NTR ligands, $A\beta$ and neurotrophins enhance the interaction of p75NTR-APP in a phosphorylation dependent manner, and the increased interaction of p75NTR-APP may participate in the pathogenesis of AD.

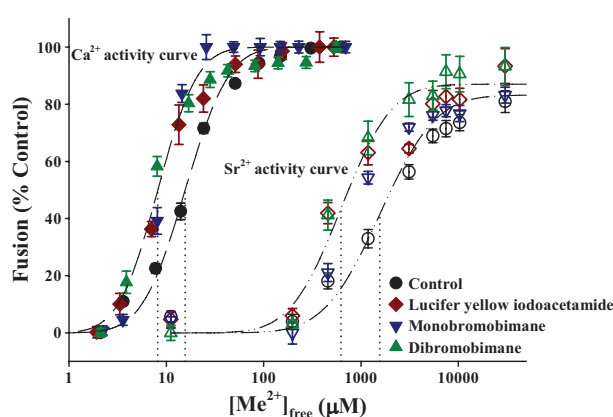
Fombonne J, Rabizadeh S, Banwait S, Mehlen P, Bredesen DE (2009) Selective vulnerability in Alzheimer's disease: amyloid precursor protein and p75(NTR) interaction. *Annals of Neurology* **65**: 294-303.

Thiol-reactivity: A small molecule approach to identifying proteins involved in regulating the calcium sensing steps of native membrane fusion

K.L. Furber¹ and J.R. Coorssen,² ¹Physiology & Pharmacology, Faculty of Medicine, University of Calgary, Calgary, AB T2N 4N1, Canada and ²Molecular Physiology, School of Medicine, University of Western Sydney, Campbelltown, NSW 1797, Australia.

In specialized cells, fusion of secretory vesicles with the plasma membrane enables release of biologically active molecules; this process is tightly regulated by intracellular Ca^{2+} . However, the identity of critical proteins involved in Ca^{2+} sensing and triggering of native membrane fusion remain speculative. Unlike other types of secretory vesicles, isolated cortical vesicles (CV) from unfertilized urchin eggs remain fully primed and fusion-ready providing a stage-specific preparation to quantitatively assess the native, Ca^{2+} -triggered fusion mechanism (Zimmerberg *et al.*, 2000). Thiol-reactivity offers an unbiased approach in studying proteins involved in Ca^{2+} -triggered membrane fusion. Furthermore, alkylating reagents are highly selective for, and bind irreversibly to, cysteine residues, providing important information about function while also tagging the proteins involved.

Previous work indicates that multiple thiol sites differentially regulate the ability of CV to fuse as well as the efficiency of fusion (*i.e.* Ca^{2+} sensitivity and kinetics) (Furber, Brandman & Coorssen, 2009; Furber, Dean & Coorssen, 2010). Iodoacetamides and bimanans have the unique ability to access a novel thiol site that potentiates the efficiency of fusion, presumably by altering the Me^{2+} sensing mechanism (Figure).



This may be due to a direct effect on a Ca^{2+} binding protein or disruption of a regulatory interaction in the fusion complex, yet delineating the exact nature of this mechanism first requires identification of the protein(s) being targeted. Initial studies coupling Lucifer yellow iodoacetamide treatment with 2-dimensional electrophoresis of CV membranes revealed that numerous proteins become labeled (Furber, Dean & Coorssen, 2010). Thus, several strategies have been employed to better focus on the labeled spots pertinent to mechanism: (i) comparison of labeling across multiple reagents and concentrations; (ii) prefractionation of cholesterol-enriched membranes to isolate proteins preferentially located at/near the fusion site; and (iii) third-

dimension electrophoretic separations for improved resolution.

Labeled proteins thus far identified include a variety of metabolic enzymes, cytoskeletal components (actin and tubulin), and several isoforms of Rab GTPases. Both the cytoskeleton and Rab proteins have defined roles in vesicle mobility and trafficking, but these data raise the possibility they may also act in later stages of exocytosis to regulate Ca^{2+} sensitivity and kinetics of secretion. Pharmacological experiments using cytoskeletal (de)stabilizing reagents in the stage-specific CV preparation rule out a direct role for actin (Hibbert, Butt & Coorssen, 2006) and tubulin (Furber *et al.*, unpublished) in the Ca^{2+} -triggering steps of membrane fusion. Nonetheless, there is evidence indicating a role for cytoskeletal components in fusion pore expansion and thus the kinetics of the release process (Berberian *et al.*, 2009; Doreian, Fulop & Smith, 2008; Larina *et al.*, 2007; Miklavc *et al.*, 2009). We are currently focusing on Rab proteins as prime candidates involved in the regulation of fusion efficiency, perhaps reminiscent of the synergistic effects between Ca^{2+} (C_E) and GTP (G_E) on secretion in other cell types (Coorssen, Davidson & Haslam, 1990; Howell, Cockcroft & Gomperts, 1987).

Berberian K, Torres AJ, Fang Q, Kisler K & Lindau M (2009) *Journal of Neuroscience*, **29**, 863-870.

Coorssen JR, Davidson MM & Haslam RJ (1990) *Cell Regulation*, **1**, 1027-1041.

Doreian BW, Fulop TG & Smith CB (2008) *Journal of Neuroscience*, **28**, 4470-4478.

Furber KL, Brandman DM & Coorssen JR (2009) *Journal of Chemical Biology*, **2**, 27-37.

Furber KL, Dean KT & Coorssen JR (2010) *Clinical and Experimental Pharmacology and Physiology*, **37**, 208-217.

Hibbert JE, Butt RH & Coorssen JR (2006) *International Journal of Biochemistry and Cell Biology*, **38**, 461-471.

Howell TW, Cockcroft S & Gomperts BD (1987) *Journal of Cell Biology*, **105**, 191-197.

Larina O, Bhat P, Pickett JA, Launikonis BS, Shah A, Kruger WA, Edwardson JM & Thorn P (2007) *Molecular Biology of the Cell*, **18**, 3502-3511.

Miklavc P, Wittekindt OH, Felder E & Dietl P (2009) *Annals of the New York Academy of Science*, **1152**, 43-52.

Zimmerberg J, Blank PS, Kolosova I, Cho MS, Tahara M, & Coorssen JR (2000) *Biochimie*, **82**, 303-314.

Spinal projections of medium sized sensory neurons that express Calcitonin Gene-Related Peptide but not Substance P in mice

G.R. Kestell, R.L. Anderson, J.N. Clarke, R.V. Haberberger and I.L. Gibbins, Centre for Neuroscience and Anatomy & Histology, Flinders University, GPO Box 2100, Adelaide, SA 5001, Australia.

Many small diameter sensory neurons in dorsal root ganglia (DRG) contain both calcitonin gene-related peptide (CGRP) and substance P (SP). These neurons generally have a nociceptive function. However, in DRG of mice, a population of medium diameter neurons express CGRP but not SP. The projections and functions of these neurons are not known. Therefore, we have combined *in vitro* axonal tracing with multiple-labelling immunohistochemistry to map the projections of these neurons to the cervical spinal cord.

Mice (C57/B16) were anaesthetised with inhaled isoflurane and exsanguination, prior to removal of the upper spinal cord with intact brachial plexus and dorsal root ganglia. Neurobiotin (NB) was applied to the C7 ventral ramus and the brachial plexus-DRG-spinal cord preparation was incubated for 4 hours. NB was subsequently detected with streptavidin-DTAF in spinal cord and DRG sections, which were also labelled for CGRP and SP.

The majority of the DRG neurons were filled with NB. Approximately one-third of the sensory neurons in C7 DRG expressed CGRP. 44% of these neurons did not contain detectable levels of SP and had an average soma size of $522 \pm 26 \mu\text{m}^2$. Within cervical spinal cord, terminals containing CGRP were prominent in the superficial dorsal horn (lamina I) and deeper dorsal horn (lamina IV). CGRP terminals lacking SP were most prominent in lateral areas of lamina I and in lamina IV. Surprisingly these terminals were only occasionally filled with NB. NB filled fibres mainly projected into the medial dorsal horn. These fibres included large myelinated fibres that extended into the ventral horn, and smaller diameter fibres that penetrated lamina IV. Some of these small diameter fibres in lamina IV contained CGRP and the majority of these lacked SP. Small diameter fibres filled with NB and CGRP were also present in laminae I and II. A subpopulation of these fibres did not contain SP.

Although the majority of sensory neurons in the DRG are filled with NB it appears that there is an under-representation of small diameter NB filled fibres in the spinal cord. A likely explanation is that these neurons of the C7 DRG project to other spinal segments rostro-caudal to the C7 segment. Our data show that 44% of the sensory neurons positive for CGRP do not contain detectable levels of SP. Based on their multiple somatotopic projections we propose that neurons containing CGRP without SP may represent a subpopulation of polymodal mechanoreceptors.

Activation of CB1 receptor inhibits fasting-induced increase in growth hormone (GH) secretion in mice

J.W. Leong, F.J. Steyn, L. Huang and C. Chen, School of Biomedical Sciences (SBMS), University of Queensland, St Lucia, QLD 4067, Australia.

The endocannabinoid system is one of the main regulators of energy homeostasis. While the mechanisms by which endocannabinoids regulate food intake are still under investigation, growing evidence supports a potential interaction with endocrine factors. Initial observations suggest that activation of cannabinoid receptor type 1 (CB1) by the cannabinoid Δ -9-tetrahydrocannabinol (Δ 9THC) results in suppression of the potent anabolic hormone growth hormone (GH). To address the impact of cannabinoids on GH secretion, we measured the effects of Δ 9THC (1.0mg/kg, IP) treatment on the activation of the GH axis following fasting. We isolated measures of peripheral hormones involved in the regulation of food intake and GH secretion, and correlated these to hypothalamic and pituitary gene expression of factors involved in the regulation of GH secretion. To characterise GH secretion we incorporated a newly developed and sensitive GH ELISA with repeated tail tip blood samples in 7-9 week old male C57 mice. Results confirm that fasting results in an initial increase and an eventual decrease in GH secretion. Addition of Δ 9THC treatment inhibits the fasting-induced increase in GH secretion. Immunofluorescent staining in GH-GFP transgenic mice confirms that somatotrophs do not express CB-1 receptors. Δ 9THC treatment does not change pituitary GH mRNA expression. Within the arcuate nucleus we observed an increase in growth hormone releasing hormone (GHRH) and somatotropin releasing inhibiting factor (SRIF) mRNA expression after fasting. This does not occur following Δ 9THC treatment. These changes appear to be independent of orexigenic and anorexigenic pathways as Δ 9THC does not impact fasting induced changes in NPY, AgRP, POMC or CART mRNA expression. We observed no changes in circulating levels of plasma leptin or active ghrelin in response to Δ 9THC treatment. Based on these results, the consequence of Δ 9THC treatment on fasting GH secretion is most likely mediated by hypothalamic mechanisms. This is consistent with prior reports confirming the expression of CB1 in the arcuate nucleus. Specifically, results suggest that CB1 activation inhibits the initial rise in GH secretion during fasting through an interaction with GHRH and SRIF neurons.

Characterising the impact of lipid-rich diets on the endocrine profile of C57 mice during progressive weight gain resulting in the development of obesity

T. Xie, F.J. Steyn, J.W. Leong and C. Chen, School of Biomedical Sciences (SBMS), University of Queensland, St Lucia, QLD 4067, Australia.

Obesity develops from an imbalance between energy consumption and energy output. While this addresses the overall change in energy homeostasis (resulting in weight gain), it does not consider physiological disruptions resulting in an inability to regulate energy demand or output. The endocrine system is central to the regulation of appetite, breakdown of dietary components for storage or use, and overall maintenance of body composition. Weight gain and obesity are associated with multiple disruptions in the normal endocrine profile. For example, secretion of ghrelin, growth hormone and adiponectin all decline with increased adiposity, whereas obesity is associated with prolonged elevation of leptin and the development of central leptin resistance. In order to characterize the impact of obesity on endocrine function it is necessary to first identify suitable animal models that closely correlate to endocrine disruptions associated with human obesity. In this study we assessed the effectiveness of three commercial diets (sourced from Specialty Feeds, Western Australia) in inducing obesity: a very high fat, low sucrose diet (VHFLS diet - 60% kcal contribution from fat, 106g/kg sucrose), a high fat moderate sucrose diet (HFMS diet - 23% kcal contribution from fat, 201g/kg sucrose), and a high fat high sucrose diet (HFHS diet - 23% kcal contribution from fat, 405g/kg sucrose). Four week old male C57 mice were fed on either diet for a period of 12 weeks, and analysis of weight gain and consequential effects on endocrine function were assessed at 4, 8 and 12 weeks of feeding. Age-matched control mice were maintained on standard mouse chow. Animals had free access to food and water for the duration of the experiment, with the exception of two days prior to sacrificing when animals were fasted overnight for a glucose tolerance test. We found that a diet rich in fat and sucrose is sufficient to induce obesity in mice by 12 weeks of feeding. By contrast, animals maintained on the VHFLS diet did not become obese. A characteristic shift in the endocrine profile was observed in all animals maintained on a high fat diet. However, development of glucose intolerance by week 12 of dietary intervention only occurred in HFHS diet-fed mice. These results confirm that a diet rich in fat and sucrose is essential to induce a characteristic shift in endocrine profile in C57 mice to that observed in human obesity. We will utilize this animal model to further characterize the impact of obesity on endocrine profile disruption.

Possible role of fatty acid GPCRs in endometrial cancer cell growth *in vitro*

K.W. Lee, F.J. Steyn and C. Chen, School of Biomedical Sciences (SBMS), University of Queensland, St. Lucia, QLD, 4072, Australia.

Endometrial cancer is one of the most common gynaecological tumours in developed countries, with a lifetime risk of 2-3%. Studies have revealed an association between obesity and the incidence of endometrial cancer. A high level of very low density lipoprotein (VLDL) is a common phenomenon in obesity along with high levels of free fatty acids (FFAs). GPR40 and GPR120, both G-protein coupled receptors, are functional receptors for medium- and long-chain FFAs, and implicated in the growth and development of different cell types. Gene analysis revealed that the human endometrial cancer cell lines used in this study, Ishikawa and HEC1A, predominantly expresses GPR120 and GPR40 respectively. In this study, we investigated the effects of long-chain fatty acids on Ishikawa and HEC-1A growth, as well as the contribution of GPR40 and GPR120 activation in this process. Using a tetrazolium-based proliferation assay we demonstrate that oleic acid (C18:1) significantly increased proliferation in both Ishikawa and HEC-1A cells within 72 hours in a dose dependent manner. A similar increase in Ishikawa cell proliferation occurs when cells are treated with the synthetic non-FFA GPR40 and GPR120 agonist, GW9508. This does not occur in the HEC-1A cells. To isolate the effects of the two receptors, Ishikawa cells were treated with a GPR40 antagonist, GW1100, in conjunction with GW9508. Results indicated that GW1100 had no effect on the stimulation of cell proliferation, suggesting all pro-proliferative effects of GW9508 are mediated through GPR120. These results suggest that GPR120 plays a more important role in the growth of endometrial cancer cell lines compared to GPR40. Further analysis of downstream pathways following GPR120 activation in Ishikawa cells using GW9508 along with antagonists for PI3K, PKC, PLC, and PKA were conducted. Results confirm a significant reduction in the pro-proliferative effects of GW9508 in cells treated with the PI3K, PKC, and PLC antagonists. Overall, results suggest that the pro-proliferative effects of OA may be mediated through pathways involving down-stream activation of PI3K, PKC, and PLC, following GPR120 activation.

The effect of maternal separation stress and high fat diet on tyrosine hydroxylase regulation in the rat adrenal gland

L. Bobrovskaya,¹ J. Maniam,² L.K. Ong,³ P.R. Dunkley³ and M.J. Morris,² ¹School of Pharmacy and Medical Sciences, University of South Australia, SA 5000, Australia, ²School of Medical Sciences, Faculty of Medicine, University of New South Wales, NSW 2052, Australia and ³School of Biomedical Sciences and Pharmacy, University of Newcastle, NSW 2308, Australia.

Background: Tyrosine hydroxylase (TH) is the rate-limiting enzyme in the synthesis of catecholamines. In the short term TH activity is regulated by its phosphorylation at specific serine residues most particularly Ser40, whereas in the longer term TH is regulated by increases in TH protein. Previous studies *in vivo* have shown altered expression of TH mRNA and TH protein in adrenal gland in response to different types of stress. Maternal separation stress is known to exert lasting effects on the HPA axis but the impact on the adrenomedullary hormonal system is not known.

Aims: In this study we aimed to investigate the effects of maternal separation stress and palatable high fat diet on the adrenomedullary TH protein and TH phosphorylation at Ser40 in male and female rats.

Methods: Male and female Sprague-Dawley rats were exposed to maternal separation for 15 minutes per day (S15, control non-stressed group), 180 minutes per day (S180, stressed group) or left non-handled (NH, non-handled control group) from postnatal days 2-14. At weaning, postnatal day 21, half of pups of each gender from each treatment group were assigned to standard laboratory chow (11 kJ/g, energy 12% fat, 21% protein, 65% carbohydrate- NH, S15, S180 groups) and half to high fat diet (15.3 kJ/g, energy 32% fat, 18% protein, and 50% carbohydrate-NH+HFD, S15+HFD, S180+HFD groups). At 19 weeks of age the pups were anaesthetised by halothane exposure and sacrificed. Adrenal glands were rapidly removed and TH phosphorylation at Ser40 and TH protein were analysed by western blotting.

Results: TH protein was not significantly changed between the treatment groups in male rats. However, pSer40TH was significantly increased in the S180+HFD group relative to the S180 group (2 fold, $p < 0.05$) in male rats. In contrast, in female rats TH protein was significantly increased (1.7 fold, $p < 0.01$) in the NH+HFD group relative to the NH group while pSer40TH was significantly reduced (by 60%, $p < 0.05$) in the S180 group relative to the NH group.

Conclusions: We provide evidence for the first time that the maternal separation stress decreases pSer40TH in female rats but not in male rats. We also show that high fat diet increases TH protein content in non-stressed female rats and pSer40TH in stressed male rats. These data suggest that in female rats the maternal separation stress leads to the decreased capacity of the adrenal gland to synthesise catecholamines by inhibiting pSer40TH. High fat diet leads to the increased capacity of the adrenal medulla to synthesise catecholamines by increasing TH protein content (in non-stressed female rats) or by increasing pSer40TH (in stressed male rats). The gender differences observed in these studies may suggest that gonadal steroids contribute to the regulation of TH in the adrenal gland in response to the maternal separation stress and high fat diet.

Fasting increases fat mobilisation and utilisation subsequent to high intensity intermittent exercise in healthy adults

M. Attardi, E. Rybalka, A. Hayes and C.G. Stathis, Metabolism, Exercise & Nutrition Unit, School of Biomedical & Health Sciences & Institute of Sport, Exercise science & Active Living (ISEAL), Victoria University, PO Box 14428, Melbourne City MC, VIC 8001, Australia.

Introduction: Although fat mobilisation and utilisation in response to fasting and exercise have been shown to increase, the effects of superimposing a high intensity intermittent exercise (HIIE) protocol on varying durations of fasting on fat oxidation have yet to be investigated. Thus the aim of this study was to determine the effect of increasing the duration of fasting on fat oxidation and physical and cognitive performance following HIIE in healthy, untrained males.

Methods: Five healthy, adult males completed a 12 h, 18 h and 36 h fast in random order prior to carrying out HIIE (3 times 50% VO_2 peak). This was followed by a 60 min recovery period, and a subsequent time to exhaustion test (TTE) (80% VO_2 peak). Cognitive tests were administered at the commencement of each trial and post-recovery.

Results: HIIE increased fat mobilisation and utilisation irrespective of fasting status. Fasting resulted in overall elevations in resting, exercise and recovery concentrations of plasma free fatty acids (FFA) (0.18 ± 0.08 , 0.28 ± 0.11 and 0.40 ± 0.14 mEq/L; at 12 h, 18 h and 36 h, respectively, $p < 0.05$) and glycerol (0.025 ± 0.02 , 0.037 ± 0.02 and 0.408 ± 0.02 mEq/L; at 12 h, 18 h and 36 h, respectively, indicating an increased reliance on fat mobilisation and utilisation with prolonged fasting. Fasting did not affect performance on a bout to exhaustion (TTE) (8.98 ± 6.67 , 9.28 ± 8.11 and 8.54 ± 6.75 min; at 12 h, 18 h and 36 h, respectively) or cognition, as measured by a Nintendo DS (219.72 ± 22.80 , 208.88 ± 27.04 and 226.42 ± 18.46 ; at 12 h, 18 h and 36 h, respectively). Participants reported increased appetite as the duration of fasting increased. However this was not reflected in the total amount of kilojoules consumed in the first meal following the trial or in the subsequent 24 h, which was equivalent between fasting trials.

Conclusions: An increased fasting duration of up to 36 h, increased fat mobilisation and utilisation as evidenced by plasma concentrations of FFA and glycerol at rest, during HIIE and during recovery, and was shown not to affect physical and cognitive performance variables.

Caffeine ingestion and high intensity intermittent exercise increases post exercise fat mobilisation and glycogenolysis in healthy individuals

T. Gerber, E. Rybalka, A. Hayes and C. Stathis, *Metabolism Exercise and Nutrition Unit, School of Biomedical and Health Sciences and Institute of Sport, Exercise science and Active Living (ISEAL), Victoria University, PO Box 14428, Melbourne City MC, VIC 8001, Australia.*

Introduction: Considering exercise for weight management, high intensity intermittent exercise (HIIE) elevates fat metabolism and is effective at reducing adiposity¹. By superimposing caffeine, a known lipolytic agent, we aimed to further increase fat metabolism with HIIE.

Methods: Six participants provided written informed consent and completed two exercise trials consisting of 30 min of HIIE (20s cycling at 150% $\text{VO}_{2\text{max}}$ with 40s rest), followed by a time to exhaustion (TTE) test at 150% $\text{VO}_{2\text{max}}$ with prior ingestion of 5 mg/kg of either caffeine or placebo (Caltrate) in randomised order. A matched paired students t-test, two-way repeated measures ANOVA and Tukeys *post hoc* analysis were employed to identify significant differences. Plasma was analysed for glycerol, free fatty acids, lactate, glucose and uric acid. All testing procedures were approved by the Victoria University Human Research Ethics Committee.

Results: During recovery from TTE, plasma glycerol was significantly increased with caffeine ($p<0.05$), with a similar trend for plasma FFA ($p=0.1$). VO_2 was significantly elevated in the caffeine trial compared to placebo after both HIIE and TTE exercise bouts ($p<0.05$), and plasma uric acid was significantly higher after caffeine following TTE ($p<0.05$).

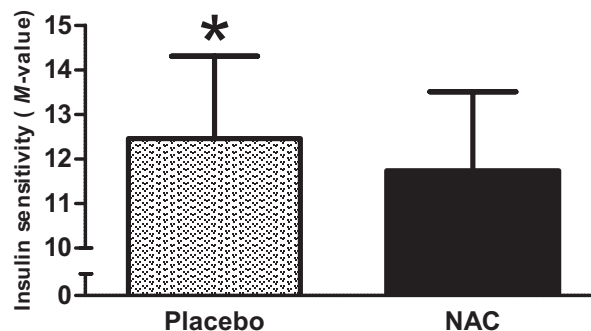
Conclusion: Caffeine and HIIE, with subsequent TTE exercise, may be an effective method at stimulating lipolysis for potential increased fat oxidation following exercise. Furthermore, enhanced energy expenditure following exercise suggests this protocol is beneficial for optimising energy deficit and potential use in weight management program.

Trapp EG, Chisholm DJ, Freund J, Boutcher SH. (2008) *International Journal of Obesity* **32**: 684-91.

N-acetylcysteine decreases insulin sensitivity after moderate intensity exercise

B.D. Perry,¹ I. Levinger,^{1,2} M.J. Brown,¹ M.J. McKenna¹ and N.K. Stepto,^{1,2} ¹School of Sport and Exercise Science Victoria University Melbourne Victoria and ²Institute of Sport Exercise and Active Living Victoria University Melbourne Victoria.

This study examined the effect of the antioxidant N-acetylcysteine (NAC) on acute insulin sensitivity after exercise in seven young, healthy participants. Moderate intensity aerobic exercise increases acute insulin sensitivity (Hawley & Lessard, 2008; Howlett *et al.*, 2008) and recent evidence has suggested that regular antioxidant supplementation ablates the increase in insulin sensitivity seen through a structured exercise program (Ristow *et al.*, 2009). This study thus seeks to test if an antioxidant can alter insulin sensitivity after a single bout of exercise. Seven untrained, healthy participants (22.1 ± 3.2 years of age, BMI: 24.8 ± 3 kg.m⁻², VO₂ peak, 50.6 ± 4 ml/kg/min) underwent a blind crossover study design, consisting of two identical trials separated by ~14 days. In each trial NAC or saline was intravenously infused before and during sub-maximal exercise for a total of 95 minutes (62.5 ml/kg/min for 15 min, followed by 25 ml/kg/min for 80 min). During this infusion time, the participant underwent 35 minutes of passive rest, followed 60 minutes of sub-maximal exercise (55 min at 68% VO₂ peak followed by 85% VO₂ peak for five min) on an electronically braked cycle ergometer. After three hours rest, a hyperinsulinemic euglycemic insulin clamp was used to determine insulin sensitivity *via* a modified M-value (glucose infusion rate/ mean insulin concentration). NAC infusion during exercise resulted in ~5.8% decrease in insulin sensitivity post-exercise (Figure, $p = 0.041$).



This research demonstrates that NAC alters insulin sensitivity after a single bout of intensified exercise. These data also suggest that reactive oxygen species produced during exercise have a role increasing post-exercise insulin sensitivity.

- Hawley, J. & Lessard, S. (2008) Exercise training-induced improvements in insulin action. *Acta Physiologica* **192**, 127-135.
- Howlett, K., Mathews, A., Garnham, A. & Sakamoto, K. (2008) The effect of exercise and insulin on AS160 phosphorylation and 14-3-3 binding capacity in human skeletal muscle. *American Journal of Physiology. Endocrinology and Metabolism* **294**, E401-7.
- Ristow, M., Zarse, K., Oberbach, A., Klötting, N., Birringer, M., Kiehntopf, M., Stumvoll, M., Kahn, C. & Blüher, M. (2009) Antioxidants prevent health-promoting effects of physical exercise in humans. *Proceedings of the National Academy of Sciences of the USA* **106**, 8665-70.

This study was funded by the VU Researcher Development Grant Scheme, 2009 (IL, NKS, MJM)

Role of phosphorylation in the Ca²⁺ regulation of Ca²⁺ release channels in skeletal muscle

K. Walweel, D.F. van Helden and D.R. Laver, School of Biomedical Sciences and Pharmacy, University of Newcastle and Hunter Medical Research Institute, Callaghan, NSW 2308, Australia.

During excitation contraction coupling, the action potential depolarises the voltage-dependent L-type Ca²⁺ channels in the sarcolemma and T-tubules, leading to a release of Ca²⁺ from the sarcoplasmic reticulum (SR, the main intracellular Ca²⁺ store) and a rise in cytoplasmic Ca²⁺ which stimulates muscle contraction. In skeletal muscle, the Ca²⁺ release channels in the SR (RyR1 isoform) are stimulated *via* a direct protein-protein interaction with the L-type Ca²⁺ channels whereas in cardiac muscle it is the inflow of Ca²⁺ into the cytoplasm through the L-type Ca²⁺ channels that activates the cardiac ryanodine receptors (RyR2). Cardiac and skeletal RyR isoforms are modulated differently by intracellular Ca²⁺. Cardiac RyRs have a complete reliance on Ca²⁺ for opening in which Ca²⁺ in the cytoplasm and SR lumen produce a synergistic activation of the channel (Laver & Honen, 2008). On the other hand, skeletal RyRs can open in the complete absence of Ca²⁺ or any other activating ligand and intracellular Mg²⁺ is required to inhibit RyR1 and prevent SR Ca²⁺ release during muscle relaxation (Laver *et al.*, 2004). In this study, we explore the effect of endogenous phosphorylation of RyR1 on its ability to open in the absence of Ca²⁺.

RyR1 was isolated from rabbit skeletal muscle as described previously (Laver *et al.*, 1995). RyRs were incorporated into artificial lipid bilayers and channel gating was measured by single channel recording. RyR open and closed times were measured in the presence various concentrations of cytoplasmic and luminal [Ca²⁺] and in the presence of cytoplasmic ATP or AMP-PCP (2 mmol/l). The effect of endogenous phosphorylation of RyR1 was assessed by incubating SR vesicles containing RyR1 with Protein Phosphatase1 (PP1, 20 units/mg SR protein) for 5 min at 30°C. PP1 removes phosphate groups from serine residues.

RyR1 in their endogenous phosphorylation state were quite active in the virtual absence of cytoplasmic and luminal Ca²⁺ (1 nmol/l cytoplasmic and < 10 µmol/l luminal). Under these conditions they had an opening rate of 100 ± 50 s⁻¹ (n=4). The opening rate showed no significant dependence on luminal [Ca²⁺] between 10 µmol/l and 2 mmol/l. The opening rate increased with increasing cytoplasmic [Ca²⁺] up to 1000 s⁻¹ with half activation at 1 µmol/l. RyR1 treated with PP1 had zero opening rate in the absence cytoplasmic and luminal Ca²⁺. Opening rates increased to 2 ± 0.5 s⁻¹ in the presence of 0.1 mmol/l luminal Ca²⁺ and 170 ± 80 s⁻¹ in the presence of 0.1 mmol/l cytoplasmic Ca²⁺.

The results indicate that endogenous phosphorylation is important for maintaining the level of activity of RyR1 in skeletal muscle. Interestingly, dephosphorylation of RyR1 makes them reliant on Ca²⁺ for their activation and in that regard makes them very similar cardiac RyRs. This suggests that a key functional difference between cardiac and skeletal muscle may depend on phosphorylation of a serine residue in RyR1.

Laver DR, Roden LD, Ahern GP, Eager KR, Junankar PR & Dulhunty AF. (1995). Cytoplasmic Ca²⁺ inhibits the ryanodine receptor from cardiac muscle. *Journal of Membrane Biology* **147**, 7-22.

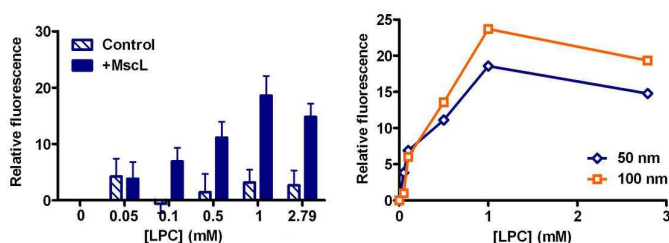
Laver DR, O'Neill ER, and Lamb GD (2004) Luminal Ca²⁺-regulated Mg²⁺ inhibition of skeletal RyRs reconstituted as isolated channels or coupled clusters. *Journal of General Physiology* **124**: 741-758

Laver DR, Honen BN (2008) Luminal Mg²⁺, a key factor controlling RyR2-mediated Ca²⁺ release: Cytoplasmic and luminal regulation modelled in a tetrameric channel. *Journal of General Physiology*, **132**: 429-446.

Ion channels as nanovalves for the controlled release of liposome-encapsulated particulates

M.J. Landsberg,¹ A.F.W. Foo,¹ A.R. Battle,^{1,2} B.J. Marsh,¹ B. Hankamer¹ and B. Martinac,² ¹Institute for Molecular Bioscience, The University of Queensland, St Lucia, QLD 4072, Australia and ²Victor Chang Cardiac Research Institute, Darlinghurst, NSW 2010, Australia.

The bacterial mechanosensitive channel of large conductance (MscL) acts as an osmotically-activated nanovalve, allowing bacteria to respond to hypo-osmotic stress by opening nanometer-size channel pores. Significant insights into the underlying mechanism of channel activation and opening by membrane tension have been obtained for individual MscL channels reconstituted into artificial liposomes using patch clamp, electron paramagnetic resonance (EPR) and fluorescence spectroscopy in combination with computational modeling of channel dynamics during channel opening (Perozo *et al.*, 2002; Corry *et al.*, 2005; Betanzos *et al.*, 2002). Given the relatively large size of the MscL pore (>25 Å), we have investigated its suitability for use as a nanovalve enabling controlled release of liposome-encapsulated particulates. Liposomes present one of the major forms of particulate drug carriers and provide an excellent method of encapsulation of highly toxic drugs, for example. In this study we have describe methods for generating small liposomes of uniform size based on a combination of liposome extrusion techniques and continuous sucrose gradient centrifugation. In addition, we demonstrate that MscL reconstituted into these liposomes may be used as a nanovalve for controlled release of small molecules including the self-quenching fluorescent dye 5,6-carboxyfluorescein (CF). CF release is regulated by the MscL-activating amphipath L- α -Lysophosphatidylcholine and exhibits a dependence on liposome size, amphipath concentration and protein-to-lipid ratio (see Figure).



Perozo E, Cortes DM, Sompornpisut P, Kloda A, Martinac B. (2002) Open channel structure of MscL and the gating mechanism of mechanosensitive channels. *Nature* **418**: 942-8.

Corry B, Rigby P, Liu ZW, Martinac B. (2005) Conformational changes involved in MscL channel gating measured using FRET spectroscopy. *Biophysical Journal* **89**: L49-51

Betanzos M, Chiang CS, Guy HR, Sukharev S. (2002) A large iris-like expansion of a mechanosensitive channel protein induced by membrane tension. *Nature Structural Biology* **9**:704-10.

Supported by the NHMRC project grant 635513.

The availability of Aquaporin 1 to function as a gated cation channel is regulated by tyrosine kinase signalling

E.M. Campbell and A.J. Yool, Medical School North, Department of Physiology, School of Health Science, University of Adelaide, Frome Road, SA 5005, Australia.

Aquaporins (AQPs) belong to the family of major intrinsic proteins, MIPs, found across all forms of life. AQPs commonly facilitate the rapid transport of water across cell membranes with some sub-types transporting other small molecules and ions. AQP1 also has been shown to function as an ion channel when activated by cGMP, although this finding is controversial as some research groups have not detected ion permeation, or have found only a small proportion of the water channel population is available to function as gated ion channels. Molecular dynamic simulation and electrophysiological analyses suggested that cations permeate AQP1 *via* the central pore formed by the tetrameric organisation of subunits, and that a conserved intracellular loop between the 4th and 5th transmembrane domains is required for cGMP-dependent gating (Yu *et al.*, 2006).

The purpose of this study was to use cysteine residues introduced into AQP1 by mutagenesis and probed with mercuric chloride to test the central pore hypothesis, and to evaluate the role of tyrosine phosphorylation in the carboxy (C)-terminal domain for controlling availability of AQP1 ion channels to be activated by cGMP.

Human AQP1 wild type or site-directed mutant cRNAs were injected singly or in combination into *Xenopus* oocytes and incubated for at least 48h prior to experimentation. AQP1 ion channels were stimulated by the addition of extracellular CPT-cGMP (20 μ M). Conductances were measured by two-electrode voltage clamp, and compared with non-AQP-expressing control oocytes. Tyrosine kinase inhibitor (1-Naphthyl PPI, 10 μ M) and tyrosine phosphatase inhibitor (bpV phen, 100 μ M) were applied to determine the phosphorylation states necessary for AQP1 ion channel activation. A functional AQP1 mutant lacking all four native cysteines was made and used as a template for the introduction of cysteine residues into the putative central pore region and the C-terminal domain phosphorylation sites. Mercury was applied to probe the effects of the cysteine residues on the activation of the ionic conductance.

Results to date indicate that tyrosine phosphorylation is a powerful modulator of AQP1 ion channel activity, and that introduced cysteines in AQP1 mutants are effective tools for demonstrating that the central pore region is involved in the permeation of ions through the channel, and that the C-terminal region modulates ion channel availability. Continuing work is testing the hypothesis that phosphorylation serves as a master switch that controls AQP1 responsiveness to cGMP.

The presence of hierarchical levels of regulation of AQP1 could explain the differences that have been reported in ion channel activity across various experimental preparations, demonstrating that an increase in cGMP level alone is not sufficient to guarantee ion channel activation. These findings offer insight into the possible resolution of an intriguing controversy in the aquaporin field, and expand our understanding of aquaporins as complex multifunctional channels.

Yu J, Yool AJ, Schulten K & Tajkhorshid E (2006). Mechanism of gating and ion conductivity of a possible tetrameric pore in aquaporin-1. *Structure* 14, 1411-1423.

Conformational changes associated with desensitisation in the ligand binding domain of the glycine receptor

Q. Wang, S.A. Pless and J.W. Lynch, *The Queensland Brain Institute, University of Queensland, St Lucia, QLD 4072, Australia.*

Glycine receptor chloride channels (GlyRs) belong to the Cys-loop ligand-gated ion channel receptor family. Synaptic GlyRs are responsible for mediating inhibitory neurotransmission in the spinal cord, brainstem and retina. Agonists binding to the extracellular ligand binding domain (LBD) induce local conformational changes that are propagated to the distant activation gate in the transmembrane domain to open the channel pore. Ligand-gated channels also display a phenomenon termed desensitisation, which is the progressive fading of the ionic flux in the prolonged presence of agonist. The rates of onset and recovery from desensitisation are important parameters governing the size and decay rate of synaptic currents. Despite the physiological and pathological importance of this process, very little is known about the conformational changes mediating desensitisation in Cys-loop receptors. Here we employed voltage clamp fluorometry (VCF) in an attempt to systematically map LBD conformational changes that accompany desensitization with a view to developing a structural model of this process.

Xenopus laevis frogs were anaesthetized in 1g/l ethyl-m-aminobenzoate according to procedures approved by the University of Queensland Animal Ethics Committee. Stage VI oocytes were removed and injected with 10 ng of wildtype or mutant $\alpha 1$ GlyR mRNA into the cytosol and incubated for 3-10 days at 18°C. For labelling, oocytes were placed into ice-cold ND96 saline solution containing 10 μ M sulforhodamine methanethiosulfonate (MTSR) for 25 s. Oocytes were then washed and stored in ND96 for up to 6 h before recording. For recording, oocytes were placed on the stage of an inverted fluorescence microscope. Fluorescence signals were recorded by a photomultiplier and membrane currents were recorded using conventional two-electrode voltage-clamp.

We have previously shown that the following LBD sites can be productively labelled with MTSR: A52C, Q67C, L127C, G181C, N203C, H201C, G221C, Q219C, L127C, S121C and M227C. In each case, agonist application results in non-desensitizing current and fluorescence responses. In order to induce fast current desensitization, we incorporated the intracellular A248L mutation in conjunction with each of the above mutations. Our aim was to determine whether fluorescence responses desensitized with the same time constant (τ) as the current response, or whether they remained non-desensitizing. A desensitizing fluorescence response would be taken as evidence that the label was detecting a local conformational change associated with desensitization. Incorporation of the A248L mutation resulted in fast desensitizing current responses ($\tau < 3000$ ms) at all double mutant receptors studied. However, labels attached to Q67C, G181C, N203C, H201C and G221C showed non-desensitizing fluorescence responses, indicating that these residues are not involved with conformational changes mediating desensitization. The loop 2 mutant, A52C, and the pre-M1 domain mutant, M227C, are both located near the transmembrane domain interface. We found the glycine-induced fluorescence signal of both residues had the same desensitization rate as the current (A52C: τ for current = 3500 ± 200 ms and τ for fluorescence = 3150 ± 360 ms; M227C: τ for current = 3250 ± 130 ms and τ for fluorescence = 3280 ± 350 ms).

We found no evidence for desensitization-induced conformational changes in the domains that form the glycine binding site or in the inner β -sheet domain of the LBD. However, we did find evidence that labelled sites in loop 2 and the pre-M1 domain did alter conformation during receptor desensitization. These sites are located close to the interface between the LBD and the transmembrane domain. Further experiments focused on these regions should help elucidate the structural changes that mediate desensitization in this important model receptor family.

Modelling the response of ion transporters to hyperosmotic shock in cells of salt-sensitive *Chara australis* and salt-tolerant *Lamprothamnium succinctum*

S. Al Khazaaly and M. Beilby, School of Physics, Biophysics, The University of NSW, NSW 2052, Australia.

We compared the response of salt-sensitive *Chara australis* and salt-tolerant *Lamprothamnium succinctum* to hyperosmotic shock. Media osmolarities were increased to 285 mOsmol/kg by adding sorbitol. Current-voltage scans were obtained as function of time in sorbitol medium. The data were modelled by a parallel combination of proton pump, inward and outward rectifiers and background currents (Beilby & Walker, 1996).

The response of *Lamprothamnium succinctum* was to increase the average membrane potential up to -151 ± 10 mV ($n=5$) after 148 ± 74 minutes (Al Khazaaly & Beilby, 2007). Modelling indicated increased rate of proton pumping. The half activation potential of the inward rectifier depolarized above the resting membrane potential, so K^+ ions could be imported into the cell, contributing to turgor regulation. In contrast to *Lamprothamnium succinctum*, most *Chara australis* cells became strongly depolarized, conductive and showed varying rate of plasmolysis. The *Chara australis* proton pump responded to osmotic shock, but did not maintain rates high enough to keep membrane potential negative. Eventually all cells became plasmolysed and their conductance increased considerably to 5.5 S.m^{-2} and higher. The failure of *Chara* to regulate turgor (Bisson & Bartholomew, 1984) appears to arise from insufficient activation of the proton pump to turgor decrease.

Al Khazaaly, S. & Beilby, M.J. (2007). Modeling ion transporters at the time of hypertonic regulation in *Lamprothamnium succinctum* (Characeae, Charophyceae). *Charophytes* **1(1)**: 28-47.

Beilby, M.J. & Walker, N.A. (1996). Modeling the current-voltage characteristics of *Chara* membranes. I. the effect of ATP and zero turgor. *Journal of Membrane Biology* **149**: 89-101.

Bisson, M. & Bartholomew, D. (1984). Osmoregulation or turgor regulation in *Chara*. *Plant Physiology* **74**: 252-255.

Ivermectin interacts with an intersubunit transmembrane domain of the glycine receptor

T. Lynagh, T.I. Webb and J.W. Lynch, Queensland Brain Institute, Building 79, The University of Queensland, St Lucia, QLD 4072, Australia.

Ivermectin is a widely-used anti-parasitic drug that is effective against nematodes and insects. It paralyzes and starves nematodes by activating inhibitory currents at glutamate-gated chloride channels (GluCl). It also activates other members of the Cys-loop ligand-gated ion channel superfamily including the human glycine receptors (GlyR). The location of the ivermectin binding site on these receptors is not known. Homomeric and heteromeric Cys-loop receptors are formed by five subunits that each contain a large N-terminal ligand-binding domain and four membrane-spanning helices (M1-M4). We recently showed that ivermectin sensitivity at GluCl and GlyRs depends on the amino acid identity at a particular location in the third transmembrane (M3) domain (GlyR Ala288). We hypothesized that tryptophan substitution of residues vicinal to Ala288 might also impair activation by ivermectin and provide a structural basis for understanding the binding interaction between ivermectin and GlyR.

We used site-directed mutagenesis to generate several GlyRs containing a bulky tryptophan residue in a domain formed by M3 (including Ala288) from one subunit and M1 from an adjacent subunit, according to the high-resolution structures of analogous proteins. HEK-293 cells were transfected with wild-type (WT) or mutant GlyR DNA and sensitivity to ivermectin was measured by recording ivermectin-mediated current magnitudes using whole cell patch clamp recording. Several mutants showed 2-4-fold shifts in EC_{50} values for activation by ivermectin. However, the M1 mutant Pro230Trp showed a 100-fold increase in ivermectin EC_{50} value ($p < 0.001$, $n = 4$). M3 Leu291Trp and M1 Leu233Trp were not activated by ivermectin at all ($n = 8$). Furthermore, at both of these mutants, ivermectin irreversibly inhibited responses to glycine, with 30 μ M ivermectin causing 100% inhibition of responses to saturating glycine concentrations ($n = 5$). Ala288Trp was poorly expressed but showed small responses to glycine and no responses to ivermectin.

Ala288, which is located in M3, is directly opposite Pro230, located in M1, in our model of the intersubunit transmembrane domain, and substitution of either residue for bulky amino acids decreases sensitivity to activation by ivermectin. M3 Leu291 is directly opposite M1 Leu233 in this domain, and mutation of either of these leucine residues for tryptophan converts ivermectin from an agonist to a ligand that antagonises activation by glycine. Since mutations in the upper part of this domain reduce the sensitivity to activation by ivermectin and mutations in the lower part reverse the effects of ivermectin, we conclude that while this domain might contribute to an ivermectin binding site, it certainly forms a crucial part in the agonist transduction pathway. This result provides an important insight into the binding and gating mechanisms of this important anti-parasitic drug.

How do mutations in the cytoplasmic PAS domain of hERG affect channel structure?

Y. Ke,¹ M. Hunter,¹ CA. Ng,¹ D. Stock² and JI. Vandenberg,¹ ¹Molecular Cardiology and Biophysics Division, Victor Chang Cardiac Research Institute, Lowy Packer Building, 405 Liverpool St, Darlinghurst NSW 2010, Australia and ²Structural and Computational Biology Division, Victor Chang Cardiac Research Institute, Lowy Packer Building, 405 Liverpool St, Darlinghurst NSW 2010, Australia.

The human *ether a go-go related gene* (hERG) encodes for a K⁺ channel predominately expressed in the heart. Mutations in this gene cause prolongation of the QT interval on the surface electrocardiogram and are associated with a marked increased risk of ventricular arrhythmias and sudden cardiac death. Over 300 mutations in hERG have been identified however only a small number of these have been characterized at the molecular level. Many mutant hERG proteins exhibit intracellular trafficking defect, in that they fail to exit from the ER and do not reach the cell surface.

The N-terminus of hERG contains a (PAS) domain, which is a hot spot for mutations. To investigate the molecular basis of the defect caused by these mutants, we have studied the biophysical properties of the isolated PAS domain for WT and 11 mutant constructs. The PAS domain constructs were evaluated for thermal stability (Table) and ability to form quaternary interactions with other domains in the channel. All but two mutants (R56Q and I42N) reduced the thermal stability of the PAS domain. 10/11 of the full-length PAS domain mutants of hERG expressed in HEK293 cells exhibited a trafficking defect. However, none of these mutants resulted in a dominant negative suppression when co-expressed with WT hERG channels.

Mutant/WT	Melt temp (°C)	Trafficking defective at 37°C	Rescued at 26°C
F29L	48.12	Yes	Yes
I42N	57.77	Yes	Yes
Y43C	40.08	Yes	No
R56Q	56.11	No	
C64Y	52.39	Yes	Yes
T65P	49.25	Yes	Yes
A78P	49.82	Yes	Yes
L86R	41.00	Yes	No
I96T	46.60	Yes	Yes
M124R	45.09	Yes	Yes
WT	57.20		

This suggests that PAS domain mutants will result in only a moderate clinical phenotype. This is consistent with recent clinical data from the International Long QT Syndrome registry showing that patients with mutations in the N-terminus (which includes the PAS domain) have a less severe phenotype than patients with mutations in the pore domain.

Charged residues involved in GABA_C receptor agonist selectivity

H-S. Tae¹ and B.A. Cromer,² ¹Ion Channels and Diseases Group, Howard Florey Institute, University of Melbourne, Parkville, VIC 3010, and ²Health Innovations Research Institute, School of Medical Sciences, RMIT University, Bundoora, VIC 3083, Australia.

The homopentameric $\rho 1$ γ -aminobutyric acid receptor (GABA_C) is a member of the Cys loop ligand-gated receptor family and closely related to the heteropentameric GABA_A receptors. The GABA binding sites are at the intersubunit interfaces of the N-terminal extracellular domains. Homology modeling of these receptors, based on recent structural information, has provided a reasonable view of the receptor structure but precise molecular details and the exact orientation of GABA and other agonists in the binding pocket remains unclear. In this study, we have used homology modeling to identify a series of conserved charged residues at the GABA-binding site that we hypothesized may be important for agonist sensitivity and selectivity. To test this hypothesis we used site-directed mutagenesis in combination with two-electrode voltage clamp recording of recombinant receptors expressed in *Xenopus* oocytes. Several of the mutants tested showed a reduced sensitivity to GABA compared to the wild type receptor, whilst at the same time showing an increase in sensitivity to other agonists. This altered agonist selectivity was particularly sensitive to the size or length of the ligand. Our results are consistent with our hypothesis and demonstrate the functional importance of these conserved charged residues in determining agonist selectivity of the GABA_C receptor and potentially other related receptors.

Characterisation of ASCT-mediated transport at low pH

A.J. Scopelliti, R.M. Ryan and R.J. Vandenberg, Department of Pharmacology, Blackburn Building D06, The University of Sydney, NSW 2006, Australia.

The alanine, serine and cysteine transporters (ASCT1 and 2) are electroneutral exchangers. They belong to the Solute Carrier Family 1, along with human and prokaryotic glutamate transporters (Excitatory Amino Acid Transporters - EAATs and Glt_{ph} respectively). Neutral amino acid exchange is coupled to only one Na^+ ion, as opposed to the three Na^+ , one H^+ ion and K^+ coupling required for acidic amino acid transport by the EAATs. Although amino acid exchange by ASCT is not H^+ -coupled, its substrate specificity is pH-dependent. Cysteate is a substrate at pH5.5, but not at neutral pH. Conversely, alanine and serine are substrates at neutral pH, but are lesser substrates at pH 5.5. We initiated a study of ASCT1 to provide more detailed comparisons with the well characterized EAATs so as to provide a better understanding of the molecular basis for similarities and differences between ASCT and the EAATs. ASCT1 was expressed in *Xenopus laevis* oocytes and the two electrode voltage clamp technique was used to characterize the pH dependence of amino acid exchange. In addition to coupled ion-substrate fluxes, ASCT1 also supports an uncoupled anion current, which is similar to that of the EAATs. As coupled amino acid-ion exchange is electroneutral, we monitored the generation of the uncoupled anion current as a measure of substrate flux. Using this method alanine and serine generate large uncoupled anion currents. We demonstrate that the acidic amino acids L-aspartate and L-cysteate are also substrates at pH5.5, but L-glutamate and D-aspartate are not substrates. While L-alanine and L-serine exchange at neutral pH can only be supported by Na^+ , we demonstrate that L-aspartate and L-cysteate exchange at low pH can be supported by a variety of cations, including Li^+ , K^+ and Cs^+ . To determine the molecular basis for these changes in substrate selectivity and cation coupling, we created and tested a range of mutations in the transport domain of ASCT1. Residues that have previously been implicated in substrate and/or cation coupling in the EAATs and are also different between the EAATs and ASCT1 were targeted for further investigation. One of these mutations, A382T, in transmembrane domain 7 was found to relax the substrate specificity towards acidic amino acids. This mutant allowed the transport of L-aspartate at pH7.5, although produced much smaller currents than L-alanine or L-serine. At pH5.5, L-aspartate and L-cysteate mediated currents were 3-4fold larger than those mediated by neutral amino acids, indicating a much larger anion flux when L-aspartate or L-cysteate are bound. Furthermore, D-aspartate, but not L-glutamate generated anion fluxes. Exploiting the apparent variation in transport mechanisms between acidic and neutral amino acids in ASCT may aid in furthering the understanding of transport mechanisms in the EAATs.

Rapid down-regulation of the rat glutamine transporter SNAT3 by a caveolin-dependent trafficking mechanism in *Xenopus laevis* oocytes

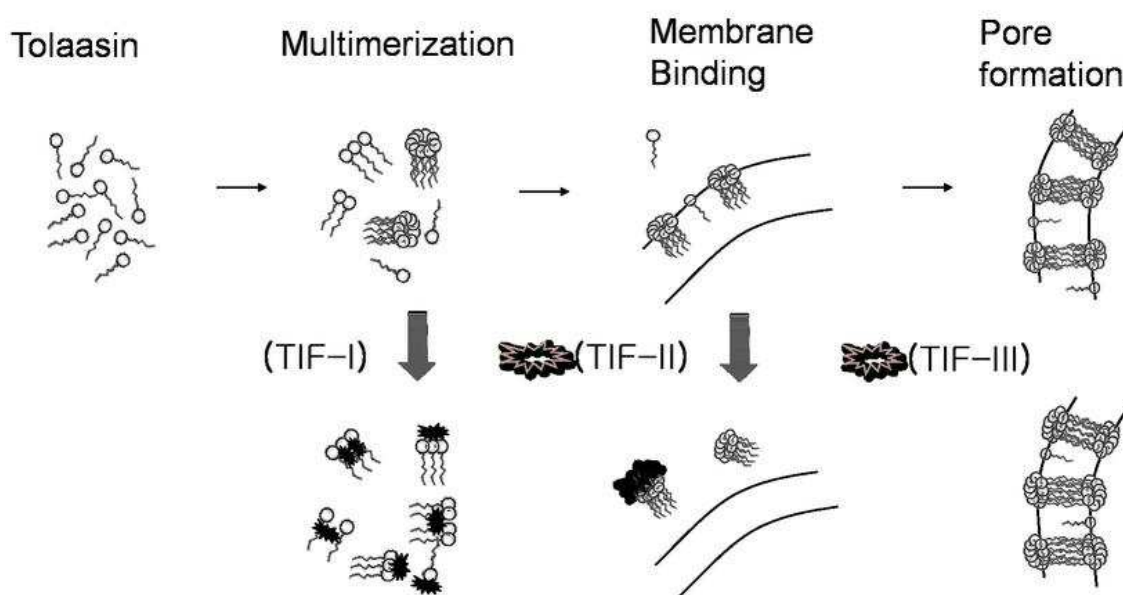
S. Balkrishna, A. Bröer, A. Kingsland and S. Bröer, Research School of Biology, Australian National University, Canberra, ACT 0200, Australia.

The glutamine transporter SNAT3 is involved in the uptake and release of glutamine in the brain, liver, and kidney. Substrate transport is accompanied by Na⁺ cotransport and H⁺ antiport. In this study, treatment of *Xenopus laevis* oocytes expressing rat SNAT3 with the phorbol ester PMA resulted in a rapid downregulation of glutamine uptake in less than 20 minutes. PMA treatment of oocytes co-expressing SNAT3 and the monocarboxylate transporter MCT1 reduced SNAT3 activity only, demonstrating the specificity of the regulatory mechanism. Single or combined mutations of seven putative phosphorylation sites in the SNAT3 sequence did not affect the regulation of SNAT3 by PMA. Expression of an EGFP-SNAT3 fusion protein in oocytes established that the downregulation was caused by the retrieval of the transporter from the plasma membrane. Co-expression of SNAT3 with dominant negative mutants of dynamin or caveolin revealed that SNAT3 trafficking occurs in a dynamin-independent manner and is influenced by caveolin. While System N activity was not affected by PMA in cultured astrocytes, a downregulation was observed in HepG2 cells.

Characterization of tolaasin inhibitory factors for the suppression of brown blotch

S.W. Park, M.H. Kim and Y.K. Kim, Department of Agricultural Chemistry, Chungbuk National University, Cheongju, Korea.

The brown blotch disease of cultivated oyster mushroom is evoked by tolaasin, a 1.9 kDa peptide. Tolaasin is produced by *Pseudomonas tolaasii* and forms pores in the cellular membranes of cultivated mushroom. Previously, we showed that the tolaasin-induced pore formation required the multimerization of tolaasin molecules and the multimerization of tolaasin was blocked by the treatment of various chemical compounds. These chemicals were named tolaasin-inhibitory factor (TIF) to prevent the brown blotch disease. Among different food additives, fatty acid derivatives blocked effectively the tolaasin-induced hemolysis. These compounds were effective at concentrations of 10-100 μM and sometimes even at 1 μM . TIF successfully inhibits the ion channel activities of tolaasin channel in artificial lipid bilayers. TIF activities were not dependent on temperature and pH, although haemolytic activity of tolaasin increased at higher temperature. Chemical properties of TIF were investigated to develop a commercial product for farmers. Since TIFs are unsaturated carbon compounds, they were sensitive to the air exposure and light irradiation. In nitrogen-filled air tight containers, TIFs were stable and less than 10% activity was decreased during a storage period of three months. However, more than 90% of TIF activity was suppressed by two weeks in the presence of oxygen. Room light also decreased the TIF activity by two times. Temperature did not show significant effects on the stability of TIFs, since storage at 5, 25, and 45°C did not show any difference. Therefore, in order to make the storage period of TIF longer, containers should be designed to oxygen-tight and light-free. Currently, the degradation products of various TIF are being identified by mass spectroscopy to analyze solution the structure of tolaasin and binding sites of TIF.



Ophiobolin A is an inhibitor of STIM1/Orai1-mediated current

M-S. To,^{1,2} J. Castro,³ B.P. Hughes,⁴ G.J. Barritt³ and G.Y. Rychkov,² ¹Department of Human Physiology, School of Medicine, Flinders University, Bedford Park, SA 5042, Australia, ²Discipline of Physiology, School of Medical Sciences, University of Adelaide, Adelaide, SA 5005, Australia, ³Department of Medical Biochemistry, School of Medicine, Flinders University, Bedford Park, SA 5042, Australia and ⁴School of Pharmacy and Medical Sciences, University of South Australia, Adelaide, SA 5000, Australia.

Store-operated Ca²⁺ entry (SOCE) plays a critical role in maintaining Ca²⁺ homeostasis and involves the activation of Ca²⁺ influx across the plasma membrane following depletion of Ca²⁺ from the endoplasmic reticulum (Feske, 2009; Putney, 2010). Two proteins, stromal interaction molecule 1 (STIM1) and Orai1 have been recently identified as essential components of Ca²⁺ release activated Ca²⁺ (CRAC) channel, the best characterised mediator of SOCE (Roos *et al.*, 2005; Prakriya *et al.*, 2006). STIM1 predominantly resides in the endoplasmic reticulum (ER) and acts as a Ca²⁺ sensor, while Orai1 has a plasma membrane (PM) localisation and comprises the channel pore. Upon store depletion, STIM1 and Orai1 redistribute in the ER and PM respectively, and co-localise at junctional ER, regions where the ER and PM are juxtaposed. The present study investigates the effects of the fungal toxin ophiobolin A (OphA), a known calmodulin (CaM) inhibitor, on the activation of CRAC current (I_{CRAC}) and distribution of STIM1 and Orai1 in liver cells.

The experiments were conducted on control H4IIE liver cells and H4IIE cells heterologously expressing STIM1 and Orai1. Fura-2 imaging has been used to measure cytoplasmic [Ca²⁺] and membrane currents were measured by whole cell patch clamping using a computer based patch-clamp amplifier (EPC-9, HEKA Elektronik) and PULSE software (HEKA Elektronik).

It was determined by patch-clamp recordings that OphA inhibited the activation of native I_{CRAC} in control H4-IIE cells stimulated with either inositol 1,4,5-trisphosphate (IP₃) or thapsigargin (TG). Fura-2 imaging revealed that OphA had no detectable effect on intracellular Ca²⁺ release secondary to TG application. However Ca²⁺ entry was entirely inhibited by OphA at a concentration of 20 μM. It is therefore likely that OphA acts *via* a mechanism independent of store depletion. As the biophysical properties of the I_{CRAC} mediated by heterologously expressed STIM1 and Orai1 depend on the relative expression levels of these proteins (Scrimgeour *et al.*, 2009), two transfection ratios between STIM1 and Orai1 containing plasmids were used (1:4 and 4:1 of Orai1:STIM1). When STIM1 was co-expressed in excess of Orai1, the resulting current was inhibited almost entirely by OphA. In contrast, the inhibition was reduced when cells were transfected with Orai1 in excess of STIM1. Confocal imaging also revealed differences in the redistribution of STIM1 and Orai1 following application of TG when OphA was present. When STIM1 was expressed alone, its response to TG in the presence of OphA was indistinguishable from control. However, when STIM1 was co-expressed in excess of Orai1, the redistribution of STIM1 was uninhibited whereas Orai1 maintained its contiguous distribution.

The results suggest that OphA is a novel inhibitor of I_{CRAC} and is likely to act by disrupting the interaction between STIM1 and Orai1.

Feske S. (2009). *Immunological reviews* **231**, 189-209.

Prakriya M, Feske S, Gwack Y, Srikanth S, Rao A & Hogan PG. (2006). *Nature* **443**, 230-233.

Putney JW. (2010). *Molecular Interventions* **10**, 209-218.

Roos J, DiGregorio PJ, Yeromin AV, Ohlsen K, Lioudyno M, Zhang S, Safrina O, Kozak JA, Wagner SL, Cahalan MD, Velicelebi G & Stauderman KA. (2005). *The Journal of Cell Biology* **169**, 435-445.

Scrimgeour N, Litjens T, Ma L, Barritt GJ & Rychkov GY. (2009). *Journal of Physiology* **587**, 2903-2918.

Characterization of a novel hERG potassium channel isoform upregulated in schizophrenia patients

J. Heide,^{1,2} S.A. Mann¹ and J.I. Vandenberg,^{1,2} ¹Victor Chang Cardiac Research Institute, Lowy Packer Building, 405 Liverpool Street, Darlinghurst, NSW 2010, Australia and ²Schizophrenia Research Institute, Lowy Packer Building, 405 Liverpool Street, Darlinghurst, NSW 2010, Australia .

Background: Recently, Weinberger and colleagues found an association between a single nucleotide polymorphism (SNP) in the second intron of the KCNH2 gene and schizophrenia (Huffaker *et al.*, 2009). The KCNH2 SNP results in increased expression of an alternatively spliced isoform of the human ether-a-go-go-related (hERG 1A) potassium channel (referred to as hERG 3.1) in the prefrontal cortex and hippocampus. Intriguingly, the vast majority of antipsychotics, which block dopamine receptors as their major therapeutic mechanism, also inhibit hERG K⁺ channels. This raises the possibility that, in patients who have increased levels of hERG 3.1, treatment with antipsychotics could exacerbate, or ameliorate, symptoms of the disease. Accordingly, the aim of this study was to characterize the gating properties of the novel hERG 3.1 isoform and investigate the effects of antipsychotic drugs on this isoform.

Methods: hERG K⁺ channel currents were recorded from CHO cells, stably expressing hERG 1A or transiently transfected with the hERG 3.1 isoform, using the whole-cell voltage clamp technique.

Results & Conclusions: hERG channels can exist in one of three main gating states, a closed state, an open state or an inactivated state. Transitions between these states are voltage dependent.

hERG 3.1 displays the same voltage dependence of channel activation as the 1A isoform, but has a voltage dependence of channel inactivation that is 8mV shifted to more positive potentials when compared to the hERG 1A isoform. While the rates of channel activation are not statistically different for both isoforms, the rates of deactivation are faster across the tested voltage range by almost an order of magnitude. This faster channel deactivation leads to an overall "loss of function" effect and less flux of potassium ions across the cell membrane. Applying of the known state dependent hERG blocker Haloperidol has a significantly lowered affinity for the 3.1 isoform compared to the 1A isoform.

The clinical significance of reduced hERG block in patients with increased levels of the hERG 3.1 isoform remains to be determined.

Huffaker SJ, Chen J, Nicodemus KK, Sambataro F, Yang F, Mattay V, Lipska BK, Hyde TM, Song J, Rujescu D, Giegling I, Mayilyan K, Proust MJ, Soghoyan A, Caforio G, Callicott JH, Bertolino A, Meyer-Lindenberg A, Chang J, Ji Y, Egan MF, Goldberg TE, Kleinman JE, Lu B, Weinberger DR. (2009) *Nature Medicine* **15**: 509-518.

Modeling of the open-channel structure of MscL using restrained simulations

E. Deplazes,¹ M. Louhivuori,² S.J. Marrink² and B. Corry,¹ ¹University of Western Australia, Perth, WA 6025 Australia and ²Rijksuniversiteit Groningen, 9700 AB Groningen, Netherlands.

Mechanosensitive channels are membrane proteins that act as safety valves to protect bacterial cells from sudden osmotic shock. The gating is induced by tension in the surrounding lipid bilayer and the channel undergoes a large conformational change during the transition from closed to open. The structure of the mechanosensitive channel of large conductance (MscL) in the closed state has been solved by XRD (Chang *et al.*, 1998). The protein has been characterized using EPR (Perozo *et al.*, 2002) and FRET (Corry *et al.*, 2005) spectroscopy but a detailed structure of the channel in the open state is still unknown. Computational modelling of MscL is challenging as the gating transition spans several time and lengths scales.

In this study we present a method for incorporating structural data from EPR and FRET experiments into a coarse grained model of the MscL. The simulations system consisted of a solvated MscL protein, embedded in a lipid bilayer, and was modelled using the MARTINI force field (Marrink *et al.*, 2007). Restraints based on solvent accessibility from EPR data were implemented by altering the interactions of specific residues with water and lipid particles. Distance restraints between specific residues were implemented using harmonic potentials. A series of MD simulations of at least 1 μ s with different combinations of restraints and membrane tension were carried out. Restraints were slowly introduced to induce the opening of the channel. The simulations produced a set of open channel structures that were analysed using a range of structural features such as pore radius and helix tilt.

Chang G, Spencer RH, Lee AT & Barclay MT (1998). Structure of the MscL homolog from mycobacterium tuberculosis: A gated mechanosensitive ion channel. *Science* **282**, 2220-2226

Corry B, Rigby P, Liu ZW & Martinac B (2005). Conformational changes involved in MscL channel gating measured using FRET spectroscopy. *Biophysical Journal* **89**, L49-L51

Marrink SJ, Risselada HJ, Yefimov S, Tieleman DP & deVries AH (2007). The MARTINI force field: coarse grained model for biomolecular simulations. *Journal of Physical Chemistry B* **111**, 7812-7824

Perozo E, Kloda A, Cortes DM & Martinac B (2002). Physical principles underlying the transduction of bilayer deformation forces during mechanosensitive channel gating. *Nature Structural Biology* **9**, 696-703

The Tyr-315 to Cys polymorphism in the P2X4 receptor causes loss of function and is associated with increased pulse pressure in humans

L. Stokes,¹ K. Scurrah,² J. Ellis,³ B. Cromer,⁴ K. Skarratt,¹ S. Harrap² and J. Wiley,^{1,4} ¹Sydney Medical School Nepean, University of Sydney, Level 5 South Block Nepean Hospital, Penrith, NSW 2751, Australia, ²Centre for Molecular, Environmental, Genetic and Analytic Epidemiology, University of Melbourne, Parkville, VIC 3052, Australia, ³Murdoch Childrens Research Institute, Royal Children's Hospital, Flemington Road, Parkville, VIC 3052, Australia and ⁴Florey Neurosciences Institute, University of Melbourne, Level 3 Alan Gilbert Building, 161 Barry St., South Carlton, VIC 3053, Australia.

The P2X4 receptor is expressed in endothelial cells where it is involved in shear stress-induced calcium signalling and generation of nitric oxide. We mutated an EGFP-tagged human P2X4 plasmid and expressed the constructs in HEK-293 cells. Electrophysiological studies showed that the Tyr315Cys mutation significantly reduced the peak amplitude of the ATP-induced inward current to 10.9% of wild-type P2X4 receptors (n = 4-8 cells, $p = 0.0002$). Co-transfection experiments to mimic a heterozygous state reduced the response to ATP to 40% of wild-type alone. Concentration-response curves for ATP showed that the Tyr315Cys P2X4 mutant caused a rightward-shift of the EC50 compared to the wild-type receptor. Further investigation using BzATP, a partial agonist at human P2X4 receptors, also showed a right-shifted dose-response and an increase in EC50 in the Tyr315Cys P2X4 receptor compared to the wild-type. Cell surface expression of the Tyr315Cys-P2X4 mutant was significantly reduced compared to wild-type P2X4 receptor. A single nucleotide polymorphism representing the Tyr315Cys P2X4 mutant was tested against supine systolic, diastolic and pulse pressures in 2864 subjects from the Victorian Family Heart Study. The mutant allele frequency was 1.4% (89 heterozygotes and 1 homozygote) and showed no evidence of population stratification ($p = 0.73$). In a variance components analysis with adjustments for age, sex and their interaction in parents and offspring separately we found significant association with pulse pressure ($p = 0.023$ for total association) such that 1 minor allele increased pulse pressure by 2.84 mmHg (95% CI 0.41 to 5.27). These data suggest that Tyr315Cys disrupts ATP binding to the P2X4 receptor and this is supported by modelling data using the recently published crystal structure of the zebrafish P2X4 receptor. The associated increase in pulse pressure might reflect reduced large arterial compliance as a result of impaired endothelium-dependent vasodilation in large arteries.

Brush-border peptidases alter the kinetic properties of neutral amino acid transporters B0AT1 and B0AT3

S. Fairweather, A. Bröer, T. Thayjogarah and S. Bröer, Research School of Biology, College of Medicine, Biology and Environment, Australian National University, Canberra, ACT 0200, Australia.

Protein digestion, absorption and re-absorption of the resulting amino acids are fundamental functions of the small intestine and kidneys. Until recently, the classic view of protein digestion was that no direct interaction between the brush-border peptidases and amino acid transporters occurred. However, the discovery that the carboxy-peptidase Angiotensin Converting Enzyme 2 (ACE2) is required for the trafficking of the neutral amino acid transporter B0AT1 to the cell surface *in vitro* and *in vivo* in the intestine has led to a re-evaluation of this traditional view. These discoveries raise the possibility that other brush border peptidases may play a functional role in neutral amino acid transport in the small intestine and/or kidney. It is now known that transporters other than B0AT1, especially B0AT3 (XT2), require ACE2 for trafficking to the cell surface.

Here, we show that the brush-border peptidases Aminopeptidase N (APN) and ACE2 regulate the kinetic properties of the neutral amino acid transporters B0AT1 and B0AT3, respectively. In both cases this regulation involves an increase in substrate affinity of the transporters. Co-expression of APN with B0AT1 resulted in a 2-fold increase in substrate affinity of the transporter for its neutral amino acid substrates. Co-expression of B0AT3 with ACE2 resulted in a 6-fold increase in the substrate affinity of B0AT3 for its main substrates alanine and glycine. Co-immunoprecipitation of B0AT1 and APN reveals that the two proteins form a complex in the apical membrane of the small intestine as do B0AT3 and ACE2 in the kidney. This suggests the formation of brush-border metabolons in both these organs. Site-directed mutagenesis and functional assays studies of APN suggests that the peptidase increases the substrate affinity of B0AT1 by creating a change in the local concentration of substrate that the transporter "sees" in the vicinity of the plasma membrane.

Inhibitory activity of plant extracts on *Plasmodium falciparum* aquaporin

J. Pei and A.J. Yool, Discipline of Physiology, School of Medical Sciences, University of Adelaide, SA 5005, Australia.

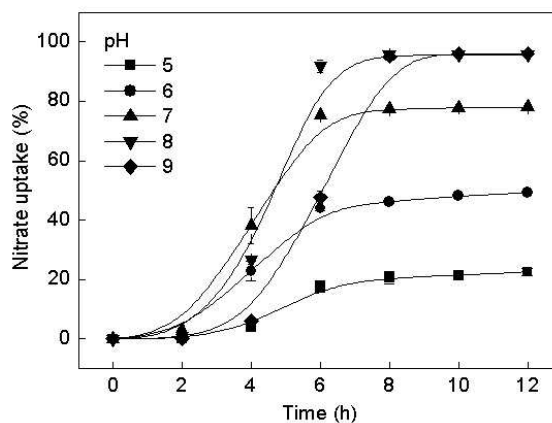
Malaria is one of the top three global infectious diseases that are life threatening. In 2002, there were about 300-600 million malaria cases recorded globally (Snow *et al.*, 2005). For humans, *Plasmodium falciparum* accounts for most of the severe and fatal malaria cases. *Plasmodium falciparum* aquaglyceroporin (PfAQP) is expressed on the parasite plasma membrane which is the major glycerol transporter (Beitz, 2007). Mice infected with PfAQP knockout parasites had a longer survival time compared with wildtype parasites (Promeneur *et al.*, 2007). Because the mutation rate of PfAQP gene is relatively low compared with the majority of the genome (Bahamontes-Rosa *et al.*, 2007), a PfAQP blocker could be a good goal for anti-malarial drug development. I hypothesized that these plants, Bacopa (*Bacopa monnieri.*), Rhubarb (*Rheum rhuababarum*), Ginseng (*Panax ginseng*) and Fuling (*Poria cocos*), that have been used as diuretics in traditional medicine have an inhibitory effect on PfAQP. *Xenopus laevis* oocytes that express PfAQP were used in the swelling-shrinking assays to test the inhibitory effect on PfAQP of selected plant extracts. Two hours incubation in three of the whole plant extracts (5mg mL⁻¹) decrease the glycerol swelling rate to 7.16%, 7.37% and 20.01% respectively compared with the swelling rates of untreated oocytes. Plant extracts were fractionated by reverse-phase chromatography using C18 silica column and mobile phase of 100% to 0% water in methanol. Six fractions were collected and dried down. Active fractions inhibited the glycerol permeability of PfAQP dose dependently and the inhibitory magnitude increased with time. Chemical analyses of the active components are in progress. The identification of first plant derived PfAQP blockers present exciting opportunities for the development of novel anti-malarial drugs.

- Bahamontes-Rosa N, Wu B, Beitz E, Kremsner PG, Kun JF. (2007) Limited genetic diversity of the *Plasmodium falciparum* aquaglyceroporin gene. *Molecular and Biochemical Parasitology* **156**: 255-257.
- Beitz E. (2007) Jammed traffic impedes parasite growth. *Proceedings of the National Academy of Sciences of the USA* **104**: 13855-13856.
- Promeneur D, Liu Y, Maciel J, Agre P, King LS, Kumar N. (2007) Aquaglyceroporin PfAQP during intraerythrocytic development of the malaria parasite *Plasmodium berghei*. *Proceedings of the National Academy of Sciences of the USA* **104**: 2211-2216.
- Snow RW, Guerra CA, Noor AM, Myint HY, Hay SI. (2005) The global distribution of clinical episodes of *Plasmodium falciparum* malaria. *Nature* **434**: 214-217.

Characterization of microbial nitrate uptake for the treatment of agricultural wastewater

Y.B. Yoon and Y.K. Kim, Department of Environmental & Biological Chemistry, Chungbuk National University, Cheongju, Korea.

Although nitrate is an essential nutrient for the growth and reproduction of all plants, the excess nitrate causes serious physiological problems in plant growth, known as 'salt stress'. In order to remove the excess amount of nitrate from cultivating soils, we have isolated soil microorganisms which have a high capacity of nitrate uptake. These microorganisms were found to be also useful for the removal of nitrate from wastewaters. The amount of wastewater, such as household sewage, livestock wastewater, and food wastewater, is increasing every year and regulations of ocean disposal become active at 2012 in Korea. Livestock wastewaters are required to be treated by wastewater treatment plants. To increase the efficiency of wastewater treatment, microorganisms were used for the removal of various chemicals, hydrocarbons, and heavy metals. Microbial applications were also useful for the removal of nitrogen compounds from the livestock wastewaters. In this study, microorganisms were isolated from livestock farms as well as upland soils and their nitrate uptake activities were investigated. We have isolated three microorganisms from a hog farm and four microorganisms from a poultry farm. Nitrate uptake activities of these microorganisms were excellent compared with those of soil microorganisms, *Enterobacter* species and *Bacillus* species. All these soil bacteria have been demonstrated to remove nitrate of 2,000-5,000 ppm. The characteristics of nitrogen metabolism were investigated and it was found that those isolated from wastewaters showed pH-dependence on the growth and nitrate uptake. In the range of pH 5 to 8, both bacterial growth and nitrate uptake were increased from 1,000 to 5,000 ppm. Interestingly, at pH 9, both were maximal but delayed by 2 h. At pH 9, both bacterial growth and nitrate uptake were suppressed for 4 h during the beginning of incubation and then they were rapidly increased to maximal levels after 6 h. This may be due to the precipitation of Mg^{2+} at alkaline pH as $Mg_3(PO_4)_2$, suggesting that nitrate transport enzyme in these bacteria is Mg^{2+} -sensitive. The delayed increase in nitrate uptake may be explained by pH decrease in culture media during cultivation and thus solubilization of precipitate. When the medium was buffered with 20 mM phosphate, the nitrate uptake was completely inhibited at 0 mM Mg^{2+} and was maximal at 2 mM Mg^{2+} . In these bacteria, nitrate uptake is mediated by an enzyme sensitive to pH and Mg^{2+} . The enzyme is inhibited at pH 9 and requires 2 mM Mg^{2+} .



Methodology strategies for the purification and biophysical characterization of bacterial ATP-binding cassette transporters

M.P. Ween, V.G. Lewis, J.C. Paton and C.A. McDevitt, Research Centre for Infectious Diseases, School of Molecular Life Sciences, University of Adelaide, SA 5000, Australia.

Bacterial membrane proteins are essential for bacterial pathogenesis and survival. They have a range of functions including toxin release, drug resistance, cell adhesion, and nutrient acquisition. *Pseudomonas (P.) aeruginosa* is a clinically important bacterial pathogen which predominantly infects the immuno-compromised (e.g. AIDS, cancer) and burns patients. It also remains the leading cause of morbidity and mortality in cystic fibrosis patients. ATP binding cassette (ABC) transporters in *P. aeruginosa* have essential roles in drug resistance and nutrient uptake and, consequently, are ideal antimicrobial targets.

We have developed a strategy for the isolation of *P. aeruginosa* ABC transporters, with the objective of further studying their biochemical, biophysical and structural properties. To this end, we have developed a ligation independent cloning system to enable rapid screening of His-tag polarity and signal sequence modification in *Escherichia (E.) coli*. Once the optimal protein expression construct has been identified, expression can be optimised by screening various *E. coli* strains under different induction parameters. The remaining bottlenecks of membrane protein solubilization and purification are addressed by screening non-ionic and zwitterionic detergents for their membrane protein extraction, assessed by western blot. The His-tag protein is then purified by immobilized metal affinity chromatography and analysed by gel permeation chromatography for monodispersity.

One example of this methodology's success is in isolating an integral membrane transporter from *P. aeruginosa*. The manganese ABC permease from *P. aeruginosa* has important roles in growth and surviving oxidative stress, under iron restriction. We have shown that the Mn ABC permease is successfully solubilized by lysophospholipid analog detergents preferentially to non-ionic maltoside or glucoside detergents. This protein has been successfully purified to greater than 95% homogeneity and is amenable to future biophysical and structural investigations.

Re-examining the role of the voltage sensor in hERG channel inactivation

S.C.E. Wong,^{1,2} M.D. Perry¹ and J.I. Vandenberg,^{1,2} ¹Molecular Cardiology and Biophysics Division, Victor Chang Cardiac Research Institute, Darlinghurst, NSW 2010, Australia and ²St. Vincent's Clinical School, University of NSW, Darlinghurst, NSW 2010, Australia.

The human ether-a-go-go related gene (hERG) potassium channel plays an important role in repolarization of the cardiac ventricular action potential. A reduction in the current passed through hERG channels (I_{Kr}) prolongs the action potential duration resulting in a disorder known as Long QT syndrome (LQTS). This disorder can, in turn, lead to life-threatening arrhythmias. HERG channels are part of a family of voltage gated potassium channels (K_v) which have six transmembrane spanning segments in the protein. The fourth segment (S4) is highly conserved among all family members and has been identified as the voltage sensing region for activation. However, hERG channels have gating properties that are unique from other K_v family members. In particular transition from the open to inactivated states occurs much more rapidly and is intrinsically voltage dependent. We have used the technique of ϕ -value analysis to investigate whether the S4 segment also plays a role in hERG channel inactivation.

ϕ -value analysis allows us to determine the temporal order of conformational changes at given sites within the channel protein in response to a single transition step (*i.e.* from open to inactivated). Point mutations were introduced into the channel protein and the kinetic rates for the onset and recovery from inactivation were determined. The ϕ -value was then calculated by comparing perturbations to the energetics of the transition state (derived from $\Delta\log(k_f)$ for mutant relative to WT where k_f is the forward rate constant at 0mV) to that of the stable end states (derived from $\Delta\log(K_{eq})$ for mutant relative to WT where K_{eq} is the equilibrium between open and inactivated states at 0mV). ϕ -values are calculated from the ratio of $\Delta\log(k_f)$ to $\Delta\log(K_{eq})$. As $\Delta\log(K_{eq})$ is the denominator for calculating a ϕ -value, small values for $\Delta\log(K_{eq})$ can give inaccurate results (Cymes, Grosman & Auerbach, 2002). Previous analysis have shown that $\Delta\log(K_{eq})$ should be at least 0.5 in order for us to confidently accept the derived ϕ -value of a residue. ϕ -values in the range of 0 to 1 have been interpreted as indicating the extent to which the reaction has occurred, with the value of 0 indicating the last step in the pathway and a value of 1 indicating a change at the start of the reaction. We have previously used this technique to demonstrate the relative contribution of regions of the hERG channel protein to the inactivation process (Wang *et al.*, 2010). However, point mutations of charged residues within the S4 segment did not provide sufficient perturbations in the inactivation process for an accurate ϕ -value to be calculated.

In the present study, a tryptophan, alanine and serine mutagenesis scan was conducted for all non-charged residues within the S4 segment. Electrophysiological recordings were then carried out using the two-electrode voltage-clamp technique. The most dramatic effect of all the mutant channels studied was found at residue V535. The average shift in $\log(K_{eq})$ of V535 mutations to Trp or Ser were found to be 0.91 ± 0.10 (n=7) and 0.84 ± 0.11 (n=7) respectively. Derived mean ϕ -values for V535W and V535S were 0.49 ± 0.03 (n=7) and 0.57 ± 0.01 (n=7). The overall ϕ -value for all V535 mutants studied (W, S, I) is thus 0.53 ($R^2=0.98$). These results reveal that a conformational change in the S4 segment occurs midway through the inactivation process. Other residues showed only mild changes in $\log(K_{eq})$ and thus were not considered reliable enough to give an accurate ϕ -value.

For the first time we have identified a residue (V535) in the S4 segment of the hERG protein that when mutated enables an accurate ϕ -value determination. From this we can determine that a conformational change in the vicinity of V535 in the S4 segment occurs approximately halfway through the temporal sequence of events that mediates the interconversion of the open and inactivated states of the hERG K^+ channel. This result clearly indicates that the S4 segment plays an important role in the inactivation process. However, whether the S4 segment functions as the voltage sensor for inactivation, remains to be determined.

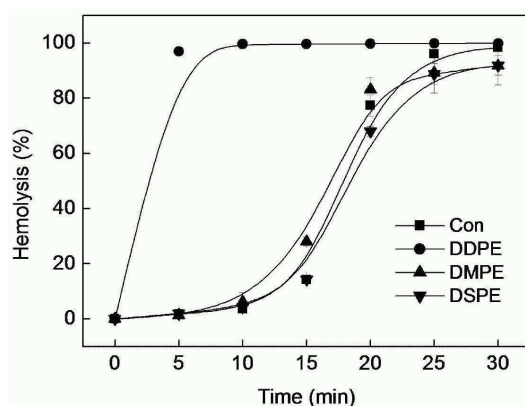
Cymes GD, Grosman C, Auerbach A. (2002) Structure of the transition state of gating in the acetylcholine receptor channel pore: a ϕ -value analysis. *Biochemistry* **41**: 5548-5555.

Wang D, Hill AP, Mann SA, Tan PS, Vandenberg JI. (2010) Mapping the sequence of conformational changes underlying selectivity filter gating in the hERG potassium channel. *Nature Structural and Molecular Biology* provisionally accepted 4 September 2010.

Facilitation of tolaasin-induced haemolysis by phospholipid composed of short length fatty acids

M.H. Kim and Y.K. Kim, Department of Environmental & Biological Chemistry, Chungbuk National University, Cheongju, Korea.

Tolaasin is a pore-forming antimicrobial peptide produced by *Pseudomonas tolaasii* and causes a brown blotch disease by disrupting membrane structures of cultivated mushrooms. It consists of 18 amino acids, its molecular mass is 1,985 Da and it has been demonstrated to form a left-handed α -helix. The mechanism of membrane-pore formation of tolaasin molecule has not known in detail. Since it forms enough for 4 turns of helix in solution, the length of tolaasin corresponds to near 20 Å, a little shorter than the thickness of membrane. Tolaasin channels are unstable in the artificial lipid bilayer and this may be explained by the comparison between the length of tolaasin channel and the thickness of lipid bilayer membrane. In control condition, bilayer was made with phosphatidyl ethanolamine (PE18:1/16:0) and phosphatidyl serine (PS18:1/18:0). The membrane is thicker than the estimated length of tolaasin channel and mismatch in thickness may make the channel unstable. Therefore, tolaasin may require phospholipids made with short length fatty acids to make the membrane thinner. In order to test this idea, the effects of various phospholipids composed of different length of fatty acids were investigated on haemolysis. When phosphatidyl ethanolamines made with decanoic acids (DDPE), myristic acids (DMPE), and stearic acids (DSPE) were added to the buffer containing RBCs and tolaasins, DDPE (200 nM) facilitates tolaasin-induced haemolysis. When the concentration of DDPE was adjusted from 0.2-200 nM, the haemolysis was stimulated at the concentrations above 2 nM, while fast, but not completed, hemolysis occurred only at 10 and 20 nM. The preincubated tolaasin and DDPE inhibited tolaasin-induced haemolysis. Binding of tolaasin and DDPE was completed within 5 minutes. Therefore, tolaasin molecules make more stable channels with phospholipids made with short length fatty acids.



Mapping the importance of 4 factors in creating monovalent ion selectivity in biological molecules

M. Thomas, D. Jayatilaka and B. Corry, University of Western Australia, 35 Stirling Hwy, Crawley, WA 6009, Australia.

The ability of macrocycles, enzymes, ion channels, transporters and DNA to differentiate between ion types is often crucial to their function. Using molecular dynamics simulations on both detailed systems and simple models we quantify the importance of four factors which affect the ion selectivity of such molecules, including the number of coordinating ligands (Thomas, Jayatilaka & Corry, 2007), their dipole moment (Noskov, Berneche & Roux, 2004), the cavity size (Doyle *et al.*, 1998) and their vibrational motion. The information resulting from our model systems is distilled into a series of 'selectivity maps' that can be used to 'read off' the relative free energy associated with binding of different ions, and to provide an estimate of the importance of the various factors. While our maps cannot capture all elements of real systems, it is remarkable that our simple model produces differential site binding energies in line with experiment and more detailed simulations for a variety of systems. This makes our maps a very useful tool for assisting in understanding the origins of selective binding and transport. Our studies show that the various suggested mechanisms of ion selectivity can be important in various situations. The chemical nature of the coordinating ligands is essential for creating thermodynamic ion selectivity in flexible molecules (such as 18-crown-6), but as the binding site becomes more rigid the number of ligands (as in ion channels) and the reduction of thermal fluctuations (as in amino acid transporters) can become important. In the future, our maps could aid in the determination of the local structure from binding energies and assist in the design of novel ion selective molecules.

- Doyle DA, Morais Cabral J, Pfuetzner RA, Kuo A, Gulbis JM, Cohen SL, Chait BT, MacKinnon R. (1998). The structure of the potassium channel: molecular basis of K⁺ conduction and selectivity. *Science* **280**, 67-77.
- Noskov S, Berneche S, Roux B (2004). Control of ion selectivity in potassium channels by electrostatic and dynamic properties of carbonyl ligands. *Nature* **431**, 830-834.
- Thomas M, Jayatilaka D, Corry B (2007). The predominant role of coordination number in potassium channel selectivity. *Biophysical Journal* **93**, 2635-2643.

GABA_B receptor gene knockdown impairs inhibition of N-type calcium channels in rat sensory neurons by α -conotoxin Vc1.1

H. Cuny, T. Yasuda, A. de Faoite and D.J. Adams, *Health Innovations Research Institute, RMIT University, Melbourne VIC 3083, Australia.*

G protein coupled GABA_B receptors are receptors for γ -aminobutyric acid (GABA) and are widely expressed in the central and peripheral nervous system. They regulate synaptic transmission and signal propagation by modulating the activity of voltage-gated calcium channels and inwardly rectifying potassium channels. Functional GABA_B receptors are heterodimers consisting of GABA_{B1} and GABA_{B2} subunits. The analgesic α -conotoxin Vc1.1, a peptide from the venom of the marine cone snail *Conus victoriae*, inhibits N-type calcium channels in sensory neurons *via* activation of G protein coupled GABA_B receptor (Callaghan *et al.*, 2008). Although there is unambiguous pharmacological evidence demonstrating that Vc1.1 does not interact directly with N-type calcium channels but inhibits them *via* a voltage-independent mechanism involving the GABA_B receptor, to date, there are no molecular studies confirming the interplay between Vc1.1 and the GABA_B receptor. The aim of the present study was to examine the effect of the GABA_B agonist baclofen and Vc1.1 on N-type calcium channel currents recorded in sensory neurons following transient knock-down of the GABA_B receptor using RNA interference (RNAi). Dorsal root ganglion (DRG) neurons isolated from 3-12 days old rats were transfected with small interfering RNAs (siRNAs) targeting both GABA_B subunits. One day after transfection a reduction of over 50% in mRNA levels for GABA_B subunits was observed compared to control cells (mock cells transfected without siRNA and scrambled non-targeting siRNA transfected cells), as demonstrated in quantitative real-time PCR analysis of a minimum of 4 independent experiments. Moreover, suppression of GABA_B protein expression was evaluated immunocytochemically using a high-content imaging system and confocal laser scanning microscopy 2-3 days after transfection. Quantitative analysis of immunofluorescence-labeled GABA_B proteins in DRG neurons revealed significantly reduced GABA_B expression in cells transfected with GABA_B-targeting siRNAs compared to control cells. Whole-cell patch-clamp studies conducted 1-3 days after transfection demonstrated that knock-down of functional GABA_B receptor expression significantly reduced the inhibition of N-type calcium channels in response to both baclofen (30 μ M) and Vc1.1 (100 nM) in isolated DRG neurons. This is in contrast to neurons transfected with a non-targeting siRNA which were not distinguishable from untransfected neurons. Taken together, these results confirm that α -conotoxin Vc1.1 modulates N-type calcium channels *via* activation of the GABA_B receptor in DRG neurons.

Callaghan, B., Haythornthwaite, A., Berecki, G., Clark, R.J., Craik, D.J., Adams, D.J. (2008), *Journal of Neuroscience*, **28**, 10943–10951.

Biological activity of α -conotoxins on N-type calcium channels in rat sensory neurons

B.P. Callaghan,¹ A. De Faoite,¹ N. Daly,² D.J. Craik² and D.J. Adams,¹ ¹Health Innovations Research Institute, RMIT University, Melbourne, VIC 3083, Australia and ²Institute for Molecular Biosciences, University of Queensland, Brisbane, QLD 4072, Australia.

Conotoxins are selective antagonists of a range of membrane receptors, ion channels and transporters associated with pain pathways. Previous studies have demonstrated the analgesic potential of several different α -conotoxins that competitively inhibit nAChRs with varying degrees of subtype selectivity. We have previously reported that the $\alpha 9\alpha 10$ nAChR-selective α -conotoxins Vc1.1 and RgIA inhibit N-type calcium channels in rat sensory neurons *via* a GABA_B receptor-dependent signalling mechanism, which may contribute to their pain relieving actions (Callaghan *et al.*, 2008). We have also recently shown that the synthetic cyclisation of Vc1.1 produced an orally active peptide by improving *in vivo* stability (Clark *et al.*, 2010). Here we report that α -conotoxin AuIB, a weak but selective $\alpha 3\beta 4$ nAChR antagonist, also inhibits high voltage-activated (HVA) Ca²⁺ channels in DRG neurons *via* a GABA_B receptor dependent pathway whereas MII, a potent $\alpha 3\beta 2$ nAChR antagonist does not. Native AuIB peptide found in the venom, has C1-C3, C2-C4 cystine globular connectivity whereas when AuIB is synthesized chemically, both the globular and ribbon (C1-C4, C2-C3 connectivity) isomers are formed. The ribbon isomer of AuIB was also examined on GABA_B receptor /N-type Ca²⁺ channel. α -Conotoxins were assessed on Ca²⁺ channel currents in rat DRG neurons using the whole-cell patch clamp recording technique. AuIB (100 nM) reduced peak Ca²⁺ channel current amplitude to $64.6 \pm 6.2\%$ of control with an IC₅₀ of 1.5 ± 0.3 nM (n = 17). Application of the ribbon isomer of AuIB (100 nM) did not affect Ca²⁺ channel current amplitude ($92.9 \pm 3\%$ of control, n = 5), whereas this isomer inhibits $\alpha 3\beta 4$ nAChRs (Grishan *et al.*, 2010). Application of the selective N-type Ca²⁺ channel inhibitor, ω -conotoxin CVID, confirmed that AuIB targets the N-type component of the HVA Ca²⁺ channel currents. Preincubation with the receptor antagonist CGP 55845, blocked the effect of AuIB on HVA Ca²⁺ channel currents. MII at concentrations up to 1 μ M did not inhibit depolarization-activated Ca²⁺ channel currents. The linker length of cyclised AuIB on Ca²⁺ channel current inhibition was also examined. Cyclised AuIB (100 nM) with 4 linking residues (GGAA) reduced Ca²⁺ channel current amplitude to $49.3 \pm 8.3\%$ of control with an IC₅₀ of 5.9 ± 0.5 nM (n = 4) and cyclised AuIB (100 nM) with 5 linking residues (AGAGA) reduced Ca²⁺ channel current amplitude to $69.1 \pm 8.8\%$ of control with an IC₅₀ of 21.3 ± 0.8 nM (n = 4). These findings demonstrate that α -conotoxins other than $\alpha 9\alpha 10$ nAChR-selective conotoxins inhibit N-type calcium channel currents *via* the GABA_B-mediated pathway and cyclisation of the peptide retains this inhibitory activity.

Callaghan B, Haythornthwaite A, Berecki G, Clark RJ, Craik DJ, Adams DJ. (2008) *Journal of Neuroscience* **28(43)**: 10943-51.

Clark RJ, Jensen J, Nevin S, Callaghan B, Adams D, Craik, D. (2010) *Angewandte Chemie (International ed. in English)* **49(37)**: 6545-8.

Grishin AA, Wang CI, Muttenthaler M, Alewood PF, Lewis RJ, Adams DJ. (2010) *Journal of Biological Chemistry* **285(29)**: 22254-63.

Illuminating the mechanism of hERG channel activators using voltage clamp fluorometry

P.S.P. Tan, A.P. Hill and J.I. Vandenberg, The Victor Chang Cardiac Research Institute, Lowy Packer Building, 405 Liverpool Street, Darlinghurst, NSW 2010, Australia.

hERG (human ether-á-go-go related gene) encoded channels are voltage-sensitive potassium ion channels that mediate cardiac repolarisations due to their unusual gating kinetics. In particular the mechanism of slow activation is not well understood. There are many drugs and compounds which cause block of hERG channels but recently a novel class of compounds which activate hERG channels has been discovered. Here we use voltage clamp fluorometry as a measure of voltage sensor movement to unravel the mechanism of hERG channel activators.

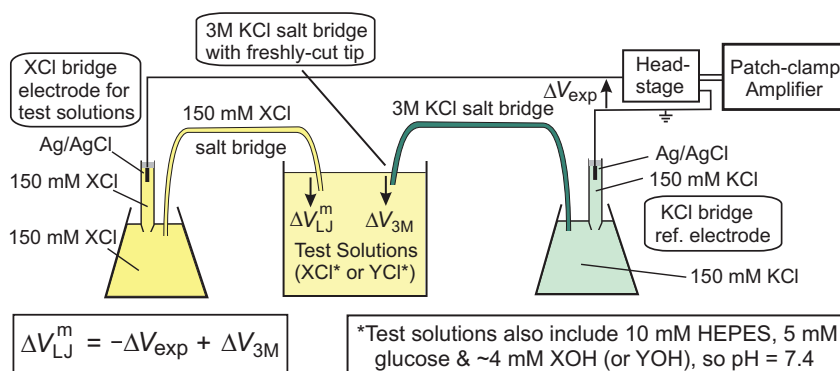
Methanthsulfonate-rhodamine (MTSR) fluorescence at position E518C of hERG channels was used to track voltage sensor movement. Depolarisation of E518C channels caused an increase in the fluorescent signal fit with a Boltzmann function with a $V_{0.5} = -6.3 \pm 1.1$. Application of hERG channel activator NS1643 (50 μ mol/L) caused a shift of the fluorescence response to $V_{0.5} = -22.6 \pm 2.9$. In addition NS1643 increased the rate of increase of the fluorescent signal. Previous studies have shown that NS1643 causes both a shift in the voltage dependence of current activation as well as an increase in the rate of action.

The results indicate that NS1643 causes a shift in the voltage dependence of current which is related to a shift in the voltage dependence of voltage sensor movement. In addition, NS1643 causes an increase in the rate of activation which is related to an increased rate of voltage sensor movement.

A new simple method for the experimental measurement of liquid junction potentials

P.H. Barry, T.M. Lewis and A.J. Moorhouse, Dept of Physiology, School of Medical Sciences, University of New South Wales, NSW 2052, Australia.

In electrophysiological experiments, particularly with patch clamp recordings, accurate potential measurements require corrections for liquid junction potentials (LJPs). Changes in LJPs can be fairly large especially under the dilution conditions used to determine relative ion permeabilities. In most cases, where the ion mobilities are known, these corrections can be calculated. To validate such calculated corrections, or to determine them if the ion mobilities are not known accurately, it is necessary to measure LJPs experimentally. 3M KCl electrodes have been widely used in the past with sharp microelectrodes to minimise LJPs, because K^+ and Cl^- ions have very similar, but not equal, mobilities and at such a concentration tend to overwhelm the LJP contribution of other ions, so that the LJPs tend to be somewhat independent of solution composition. Unfortunately, 3M KCl also produces major history-dependent problems in agar salt bridges or in the absence of a free-flowing junction (see Barry & Diamond, 1970; Neher, 1992), because the tip of the salt bridge or electrode takes up the composition of the previous solution in which it has been placed and no longer behaves as a 3M KCl junction. However, we have now shown that this problem with 3M KCl agar salt bridges can be overcome if the last 5 mm (at least) of the salt bridge (encased in polyethylene tubing) are cut off just before the salt bridge is placed into a test solution of different composition (or concentration), to thus ensure a fresh 3M KCl agar-solution in contact with the test solution. The measurements still need to be corrected for the small, but non-trivial, well-defined calculable shifts in reference potentials at the fresh 3M KCl agar-solution interface (ΔV_{3M}). The experimental setup is shown in the adjacent figure (modified from Fig. 3 of Barry *et al.*, 2010). X and Y represent different cations, for example, for LiCl dilution potentials, X would represent Li and there would be no Y needed. In this situation, the test solutions would represent ~1.0, ~0.5 and ~0.25 dilutions of the XCl salt, whereas in biionic measurements for two different salts at the same concentration, for example, X may represent K and Y represent Na, for a change from KCl to NaCl.



Using this technique, we have recently measured LJPs in diluted solutions of LiCl and NaCl (with and without 4 mM $CaCl_2$) and found them to agree within the experimental error (0.1 to 0.2 mV) to those LJPs calculated with the Henderson equation (using ion activities, rather than ion concentrations, and using the Windows version of the liquid junction potential program JPCalc;

Barry, 1994), reported in Sugiharto *et al.* (2010) and Barry *et al.* (2010). We have also now measured dilution potentials for KCl salts and biionic potentials for KCl:NaCl, with excellent agreement between the corrected experimental measurements of the biionic LJP [4.5 ± 0.1 mV ($n=14$), after a ΔV_{3M} correction of 0.7 mV] and the theoretically predicted LJP value of 4.4 mV (using ion activities). Excellent agreement was also true for measured and predicted KCl dilution potentials, though here the LJP correction was small, equal and opposite to the ΔV_{3M} value (0.3 mV and 0.7 ± 0.1 mV for the 0.5 and 0.25 dilutions respectively), so that the uncorrected ΔV_{LJ}^m value was ~0.0 mV in each case ($n=5$). This is due to the test and 3M KCl solutions being primarily KCl solutions, unlike the case where the 3M KCl overwhelms the LJP contributions of salts with very different anion and cation mobilities.

We have thus developed a straight-forward and reliable method to measure LJPs, which we have now validated with a number of salt solutions with well documented ionic properties.

Barry PH. (1994) *Journal of Neuroscience Methods*, **51**: 107-116

Barry PH & Diamond JM. (1970) *Journal of Membrane Biology*, **3**: 93-122.

Barry PH, Sugiharto S, Lewis TM, Moorhouse AJ. (2010) *Channels* **4(3)**: 142-149.

Neher E. (1992). *Methods in Enzymology* **207**: 123-131.

Sugiharto S, Carland JE, Lewis TM, Moorhouse AJ, Barry PH. (2010) *Pflügers Archiv* **460**: 131-152.

Identification of Nav1.8 channel domains responsible for μ O-conotoxin MrVIB binding and channel biophysical properties

O. Knapp,¹ T. Yasuda,¹ N. Lawrence,² R. J. Lewis² and D.J. Adams,¹ ¹Health Innovations Research Institute, RMIT University, Melbourne, VIC 3083, Australia and ²Institute for Molecular Bioscience, University of Queensland, Brisbane, QLD 4072, Australia.

Voltage-gated sodium channels (VGSCs) are expressed primarily in excitable cells, such as central and peripheral neurons and muscle, and play a pivotal role in the initiation and propagation of action potentials. To date, nine subtypes of the pore-forming α subunit have been identified, each with a distinct tissue distribution, biophysical property and sensitivity to the neurotoxin tetrodotoxin (TTX). The 260 kDa α -subunits exhibit intracellular N- and C-termini and consist of four domains, each containing six membrane-spanning segments. Na_v1.8, a TTX-resistant subtype, is predominantly expressed in sensory neurons and plays a pathophysiological role in neuropathic pain. In contrast to TTX-sensitive α -subtypes, Na_v1.8 exhibits slower activation and inactivation kinetics and is inhibited by μ O-conotoxin MrVIB from *Conus marmoreus* (Ekberg *et al.*, 2006). To determine which domain confers Na_v1.8 α -subunit its biophysical properties and MrVIB binding, we constructed various chimeric channels between Na_v1.8 and a TTX-sensitive Na_v1.2 that is expressed in the central nervous system. Wild type and chimeric channels were expressed in *Xenopus* oocytes and depolarization-induced Na⁺ currents were recorded using the two-electrode voltage clamp technique. Slow inactivation kinetics of Na_v1.8 was changed to fast kinetics when domain 1 and 2 was replaced by the corresponding domains of Na_v1.2; slow activation kinetics remained unaltered. MrVIB (1 μ M) inhibits Na_v1.8 currents by 80% whereas no significant effect was observed on Na_v1.2 currents. A similar sensitivity to MrVIB was observed for Na_v1.2 /1.8 chimeras containing Na_v1.8 domain 2. In contrast, Na_v1.2 /1.8 chimeras containing Na_v1.2 domain 2 were insensitive to MrVIB. Taken together, these results suggest that domain 2 of Nav1.8 is critical for MrVIB binding and activity. A previous study on Na_v1.4 reported that MrVIB hinders the voltage sensor in domain 2 from activating and, hence, the channel from opening (Leipold *et al.*, 2007). The binding of TTX may rely on a comparative mechanism since the presence of one or two binding sites within VGSCs Na_v1.8/1.2 chimeras had no effect compared to the wild type VGSC subtype Na_v1.8. All results were confirmed by a set of at least 10 cells/experiments.

Ekberg J, Jayamanne A, Vaughan CW, Aslan S, Thomas L, Mould J, Drinkwater R, Baker MD, Abrahamsen B, Wood JN, Adams DJ, Christie MJ, Lewis RJ. (2006) *Proceedings of the National Academy of Sciences USA* **103**: 17030-5.

Leipold E, DeBie H, Zorn S, Borges A, Olivera BM, Terlau H, Heinemann SH. (2007) *Channels (Austin)* **1(4)**: 253-262.

Lipid and lyso-lipid effects on the behavior of liposome co-reconstituted MscS and MscL

T. Nomura,¹ A.R. Battle² and B. Martinac,^{1,3} ¹Victor Chang Cardiac Research Institute, Darlinghurst, Sydney, NSW 2010, Australia, ²Department of Physiology and Pharmacology, School of Biomedical Sciences, The University of Queensland, St Lucia, QLD 4072, Australia and ³St. Vincent's Clinical School, The University of New South Wales, NSW 2052, Australia.

Bacterial mechanosensitive channels of small (MscS) and large (MscL) conductance have been proposed to play a major role in the protection of bacterial cells against hypo-osmotic shock. Although the genes of both channels have been cloned (Levina *et al.*, 1999; Sukharev *et al.*, 1994) and X-ray crystallographic analysis has revealed their 3D structure (Bass *et al.*, 2002; Chang *et al.*, 1998), much less is known about how lipids surrounding the channels in the bacterial cell membrane may influence mechanosensitivity of both channels. In this study, we examined the effects of various lipids and lyso-lipids on mechanosensitivity of MscS and MscL channels co-reconstituted into liposomes by the patch-clamp technique. Reconstitution into liposomes of different lipid composition such as phosphatidylethanolamine (PE), phosphatidylcholine (PC), phosphatidylglycerol (PG), and cardiolipin (CL) did not affect the pressure-threshold activation ratio of the channels. Addition of 5-30% cholesterol, which is known to affect the bilayer thickness (Mitra *et al.*, 2004), led to a decrease of the threshold activation ratio. In contrast, application of micromolar concentrations of lysophosphatidylcholine (LPC), which has been known as a mechanosensitive channel activator (Perozo *et al.*, 2002), led to an increase of the threshold activation ratio. These findings suggest that the cholesterol-induced difference in membrane thickness (hydrophobic mismatch) and the change in intrinsic lipid bilayer curvature induced by LPC affect mechanosensitivity of both channels to a different extent and by a different mechanism.

Bass, R.B., Strop, P., Barclay, M. & Rees, D.C. (2002) *Science* **298**, 1582-1587.

Chang, G., Spencer, R.H., Lee, A.T., Barclay, M.T. & Rees, D.C. (1998) *Science* **282**, 2220-2226.

Levina, N., Totemeyer, S., Stokes, N.R., Louis, P., Jones, M.A. & Booth, I.R. (1999) *EMBO Journal* **18**, 1730-1737.

Mitra, K., Ubarretxena-Belandia, I., Taguchi, T., Warren, G., & Engelman, D.M. (2004) *Proceedings of the National Academy of Science USA* **101**, 4083-4088.

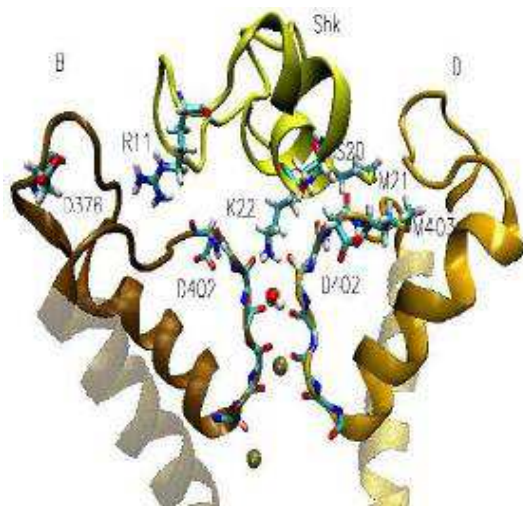
Perozo, E., Cortes, D.M., Sompornpisut, P., Kloda, A., & Martinac, B. (2002) *Nature* **418**, 942-948.

Sukharev, S.I., Blount, P., Martinac, B., Blattner, F.R. & Kung, C. (1994) *Nature* **368**, 265-268.

Binding of sea anemone toxin Shk to the potassium channel Kv1.3 from molecular dynamics simulations

M.H. Rashid and S. Kuyucak, School of Physics, University of Sydney, NSW 2006, Australia.

Potent blockers of Kv1.3 potassium channel are crucial in the activation of human effector memory T cells (*TEM*); selective blockers constitute valuable therapeutic leads for the treatment of autoimmune diseases mediated by *TEM* cells. Computational simulation at the molecular level is a powerful tool in understanding electrophysiological experiments performed on wild type and mutant channel. Here we go for molecular dynamics (MD) simulation on complex Kv1.3-Shk (sea anemone toxin) to measure the potency of Shk to channel Kv1.3.



Side view of Shk in complex with Kv1.3 potassium channel. Shk backbone is shown in yellow and the side chains of R11, M21, K22 and S20 residues involve in binding are explicitly shown. Two of the four monomers in Kv1.3 (B and D) are shown clearly.

Based on crystal structure of voltage-gated potassium channel Kv1.2 we have constructed a homology model of Kv1.3. Haddock has been used for the exploration of the conformational space and the determination of ligand /protein contacts. The potassium ion channel axis provides a natural reaction coordinate for unbinding of a sea anemone toxin (Shk). Along this coordinate we measure the binding energy of toxin with the channel. The computational results have an excellent platform due to a comprehensive collection of physiological data available to test the outcomes. We have run the MD simulation up to 10 ns for the channel-toxin complex in a solvated lipid bilayer environment. This confirmed that the toxin and the pore region of the channel are flexible in the binding. The last 5 ns is considered as the production time. Recognition residues and interaction contacts for the binding were identified during this time of simulation. Lys-22 goes far inside the channel. Among Kv1 family Kv1.3 has His-404 above the selectivity filter. His404 makes a hydrogen bond with Asp402 of the next monomer in a pattern of His(A)-Asp(B), His(B)-Asp(C), His(C)-Asp(D) and His(D)-Asp(A). This His(404)/Asp(402) pair does not allow Asp402 side chain to make any interaction with toxin. Arg11 comes closer to residues Asp376(B), His404(B), Ser379(B) and Asp402(B). Met21/Met403(D), His19/Asp402(D), Tyr23/Gly401(C) are the interacting residue pairs in the Shk-Kv1.3 complex. This is an agreement with the experimental (mutant cycle analysis) result (Lanigan *et al.*, 2002). To measure the potency of Shk we calculate the potential of mean force (PMF) of its unbinding from the channel. Weighted histogram analysis method (WHAM) is used to calculate PMF from Umbrella sampling data. The outcome PMF from the umbrella sampling simulation differ 1 kcal/mol from the experimental measurement. The consistency between the result of the simulations and the experimental data indicate that our three-dimensional models of the toxin-channel complex are reasonable. So our model can be used as a guide for future biological studies, such as the rational design of selective blocking agents of the Kv1.3 channel and mutation cycle analysis in toxins to increase selectivity and potency towards the channel. Thereby we are in search for more potent mutants of Shk.

Lanigan MD, Kalman K, Lefevre Y, Pennington MW, Chandy KG, Norton RS. (2002) *Biochemistry*, **41**: 11963-11971.

Stabilisation of quasi stable states by flash turnover of photosystem II core complexes from higher plants. Back reaction kinetics

P.J. Smith, B. Bataituti, Lu. Jin, E. Krausz and R.J. Pace, Research School of Chemistry, College of Science, Building 33 Science Rd, Australian National University, ACT 2601, Australia.

The smallest functionally active, stable photosystem II (PSII) complexes are termed core complexes, where the inner components of the multi-peptide PSII complexes are isolated by detergent solubilization from the thylakoid membrane and outer light harvesting systems. Functional membrane bound PSII from higher plant and PSII core complexes from oxygenic thermophilic cyanobacteria appear to retain dimer functionality (Kern *et al.*, 2005; Guskov *et al.*, 2009). The isolation of PSII core complexes from higher plants follows a different isolation procedure to that of thermophilic cyanobacteria (Smith *et al.*, 2002). The isolation of higher plant PSII cores leads to fully active complexes that may be mostly monomer in functional unit morphology. Although fully active, collaborations to generate flash turnover of higher plant cores had resulted in capture of only 10% of centres in the S2 state (Thapper *et al.*, 2009). We have examined single laser flash illumination turnover of higher plant PSII core complexes and measured the kinetics of the presence of S2 multiline signal after flash - delay, then rapid freeze to liquid nitrogen (77K). The temperature dependence of the S2 Multiline signal decay kinetics were measured for temperatures between 6°C and 20°C (280K and 293K). Conditions for full multiline signal intensity were recorded for a number of added quinone (artificial acceptor) : PSII core complex ratios (0 to 90 quinones per core complex on mole : mole basis).

The activation energy for the S2 multiline / S1 back reaction measured from an Arrhenius plot of the decay was 55kJ.mol⁻¹ (0.6eV). The magnitude of this activation energy is of the same order as that reported for the S2 multiline / S1 back reaction kinetics for PSII membrane samples (Seeliger, Kurreck & Renger, 1997). The time course for the loss of S2 multiline signal in higher plant PSII core complexes was observed to be two orders of magnitude faster than for the loss of multiline signal in PSII membrane samples. This very rapid back reaction is hypothesized to arise from the solution status of PSII core complexes as compared to the large membrane fragments associated with sub thylakoid PSII preparations. Such solution properties of the core complexes allow collisional dismutation of acquired and stabilized charge separation during the S1 to S2 turnover.

Kern J, Loll B, Zouni A, Saenger W, Irrgang KD, Biesiadka J. (2005) *Photosynthesis Research* **84**: 153–159.

Guskov A, Kern J, Gabdulkhakov A, Broser M, Zouni A, Saenger W. (2009) *Nature Structural & Molecular Biology* **16**:334-342.

Smith PJ, Peterson S, Masters VM, Wydrzynski T, Styring S, Krausz E, Pace RJ. (2002) *Biochemistry* **41**: 1981–1989.

Thapper A, Mamedov F, Mokvist F, Hammarström L, Styring S. (2009) *The Plant Cell* **21**: 2391-401.

Seeliger AG, Kurreck J, Renger G. (1997) *Biochemistry* **36**: 2459–2464.

Rapid characterization of bacterial motility using Dynamic Light Scattering (DLS)

R. Nixon-Luke, G. Bryant and J.N. D Goder, School of Applied Sciences, Royal Melbourne Institute of Technology, Melbourne, VIC 3000, Australia.

Cell motility is an important characteristic of many biological processes, and is ubiquitous in unicellular organisms such as bacteria. The bacterium *Escherichia coli* is a well studied model system for understanding cell motility. These cells execute random walks by alternating between swimming (or running) at speeds of tens of microns per second (for ~1 second), and then tumbling (changing direction) for 0.1 s.

Dynamic light scattering (DLS) has long been used for the measurement of Brownian motion in colloids, proteins and macromolecules, and is a routine technique for the determination of particle size in such Brownian systems. Dynamic light scattering can make accurate measurements over a very short timescale, is non-invasive, requires very little sample, and has a high sensitivity, making it a perfect tool to investigate living biological cells. Early in the development of DLS, its potential for studying bacterial motility was investigated (*e.g.* Nossal, Chen & Lai, 1971), however these investigations were complicated by a lack of understanding of the details of cell motility, as well as equipment limitations, and were never seriously pursued.

In this abstract we report on preliminary investigations of the motility of *E. Coli* using modern dynamic light scattering techniques. We have observed that the correlation functions measured at small scattering angles exhibit two distinct decays: the faster decay being due to the self propelled velocity (motility), and the second, slower decay being due to the normal diffusive motion. These functions were analysed using the model proposed by Nossal, Chen & Lai, and revised by Stock (1978), which was found to provide good agreement under most conditions. This analysis yields the velocity distributions, the average velocities and the fraction of non-motile cells. The diffusion coefficients of the cells can be either an input into the model, or a free parameter. Measurements of non-swimming (dead) cells are also used to obtain independent measures of the diffusion coefficient. We have investigated how the correlation function varies with time, and observed a decrease of average swimming speed as time progresses. The effect of scattering angle for living cells reveals much better theoretical fits at smaller angles, illustrating the effect that the bacteria's tumbling motion has on the correlation function as scattering angle increases.

Finally, we measured the average velocity as a function of temperature over the range 24-37°C. We found that cell motility increases with temperature up to a maximum value at 32°C, where the effect plateaus. The use of DLS for the study of cell motility is an area of research that is ripe for further study.

Nossal, R., Chen, S-H. & Lai, C.C. (1971). Use of laser scattering for quantitative determinations of bacterial motility. *Optics Communications* **4**: 35-39.

Stock, G.B. (1978). The measurement of bacterial translation by photon correlation spectroscopy. *Biophysical Journal* **22**: 79-96.

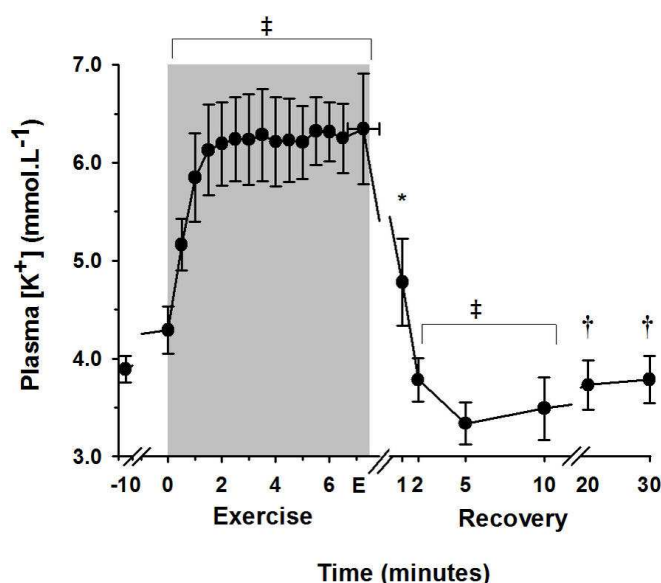
Arterial potassium regulation during a 2000 metre rowing trial

T. Atanasovska,^{1,2} F. Billaut,^{1,2} A.C. Petersen,^{1,2} D. Rouffet,¹ C. Steward,^{1,2} A. Trewin,^{1,2} B. Gatt,^{1,2} M. Altarawneh,^{1,2} I. Ng^{1,3} and M.J. McKenna,¹ ¹Institute of Sport, Exercise and Active Living (ISEAL), Victoria University, Melbourne, VIC 8001, Australia, ²School of Sport and Exercise Science, Victoria University, Melbourne, VIC 8001, Australia and ³Department of Anaesthesia & Pain Management, Royal Melbourne Hospital, Melbourne, VIC 3000, Australia.

Exercise induces myocytic potassium (K^+) efflux, resulting in a large rise in circulating K^+ concentration ($[K^+]$), that is largely dependent upon both exercise intensity and the contracting muscle mass. K^+ accumulation in muscle interstitial fluid has been linked to fatigue and performance decrements during exercise. Rowing involves intense contractions utilising a large proportion of the body's musculature. It was hypothesised that rowing at high intensity would cause a pronounced increase in circulating $[K^+]$ and muscle fatigue.

Eleven healthy, young adults (8 Male, 3 Female; age 24.73 ± 5.3 years, height 1.79 ± 0.09 m, mass 81.36 ± 12.2 kg, mean \pm SD) performed a maximal 2000 m trial on a rowing ergometer. All participants were recreationally active, had rowing experience (on-water or gymnasium) and included four well trained rowers. Radial arterial blood samples were drawn at -10 min, on the rowing ergometer immediately pre-exercise (0 min), every 30 s during exercise and at 1, 2, 5, 10, 20 and 30 min post-exercise and analysed for fluid shifts, plasma electrolytes and acid-base status. Instantaneous rowing power output was recorded every 30 s and cardiorespiratory data were collected continuously during the trial.

The time to complete 2000 m was 7.26 ± 0.59 min. Power output was 326 ± 81 W in the first 30 s, tended to decline slightly until 4 min and remained unchanged until the end of exercise. At end-exercise, pulmonary oxygen uptake increased to 4.27 ± 0.76 L.min⁻¹, ventilation to 121.2 ± 26.7 L.min⁻¹ and heart rate to 177.0 ± 9.8 beats.min⁻¹. Arterial $[K^+]$ (Figure) was 3.89 ± 0.13 mM at rest, rose slightly at pre-exercise ($p < 0.005$), increased to 6.13 ± 0.46 mmol.L⁻¹ after only 90 s exercise ($p < 0.001$) and remained unchanged thereafter for the rest of exercise ($p < 0.001$). Following exercise, plasma $[K^+]$ decreased abruptly to reach a nadir of 3.33 ± 0.22 mM at 5 min post-exercise ($p < 0.001$) and remained below pre-exercise levels at 30 min post-exercise ($p < 0.005$). Arterial $[K^+]$ was inversely correlated with power output ($r = -0.50$, $p < 0.05$). Plasma volume decreased from pre-exercise by 9.67 ± 2.29 % at end-exercise.



Blood [glucose] was unchanged during exercise but rose to a peak at 2 min post-exercise of 7.75 ± 1.18 mM ($p < 0.05$). Blood [lactate] increased progressively during exercise to peak at 10.87 ± 1.33 mM at end-exercise. Arterial pH decreased from 7.42 ± 0.02 units at pre-exercise to nadir of 7.07 ± 0.07 units ($p < 0.001$) at 5 min post-exercise.

A high arterial $[K^+]$ was reached and sustained throughout the high intensity rowing trial. This elevation was not as great as anticipated, given the high intensity and large contracting muscle mass. These suggest that after 90 s of exercise, muscular Na^+K^+ -ATPase activity was sufficient to match muscle K^+ release, thus minimizing an even more pronounced rise in extracellular $[K^+]$, in blood and most likely also in muscle.

Interaction of muscle glycogen status and nutrient supplementation on skeletal muscle adaptation following resistance exercise

D.M. Camera, A. Garnham, J.A. Hawley and V.G. Coffey, Health Innovations Research Institute, School of Medical Science, RMIT University, Bundoora, VIC 3083, Australia.

Background: The insulin/insulin-like growth factor (IGF) signalling pathway has been implicated in regulating exercise- and nutrient-induced adaptation in skeletal muscle given its putative capacity to direct diverse cell processes such as glucose transport, glycogen resynthesis, and protein synthesis (Coffey & Hawley, 2007). A downstream target within this pathway proximal to translation initiation is the ribosomal protein S6 (rpS6) which, when phosphorylated and activated, can enhance the translation of mRNAs that encode for ribosomal proteins and elongation factors that may represent a rate limiting step for protein synthesis (Ruvinsky & Meyuhas, 2006). The energy status of skeletal muscle has been shown to alter signal transduction networks that would be expected to effect translation and protein turnover (Atherton *et al.*, 2005). Muscle glycogen is the primary substrate for high intensity exercise and changes in metabolism with low muscle glycogen concentration may have detrimental effects on anabolic responses in skeletal muscle (Coffey *et al.*, 2009). Interestingly, while low glycogen may augment the adaptation response to a bout of endurance exercise the effect of decreased glycogen concentration on anabolic signalling and protein synthesis in muscle following resistance exercise is unknown.

Purpose: The aim of this study was to determine the effect of muscle glycogen content and nutrient supplementation on anabolic signalling in skeletal muscle during the early recovery period following resistance training (RT).

Methods: The evening before an experimental trial, eight male subjects (22.9 ± 0.9 years; BMI = 24.0 ± 0.8 kg/m²) performed a depletion protocol where one-leg undertook cycling exercise to exhaustion to lower muscle glycogen levels (Low) while the other leg rested and therefore maintained normal muscle glycogen (Norm). The following day subjects completed a unilateral bout of resistance exercise during which each leg performed 8 sets of 5 repetitions of leg press at 80% of the previously determined one repetition maximum. Following the completion of exercise subjects consumed a 500ml bolus protein/carbohydrate beverage (20 g whey protein + 40 g maltodextrin). Muscle biopsies were obtained from the *vastus lateralis* in both legs at rest and 1h after RT.

Results: The depletion protocol was effective in generating divergent muscle glycogen content that was higher in the control leg (Norm) than in the Low leg at rest (383 ± 43 vs. 184 ± 14 mmol/kg dry wt; $p < 0.05$) and remained different 1 h post-exercise (309 ± 41 vs. 135 ± 11 mmol/kg dry wt; $p < 0.05$). Nutrient ingestion resulted in significant increases in blood glucose and insulin ($p < 0.05$) during the early recovery period compared to resting levels. Ribosomal protein S6^{Ser235/6} phosphorylation increased significantly 1 h post exercise compared to rest ($p < 0.05$), however there were no differences between the Norm and Low legs at 1 h.

Conclusion: We show that despite significant disparity in muscle glycogen levels at rest and 1 h after resistance exercise, there were no differences in rpS6^{Ser235/6} phosphorylation between the Norm and Low glycogen legs. These results indicate that low muscle glycogen levels fail to suppress phosphorylation of a key component in skeletal muscle translation initiation following high-intensity resistance exercise when protein/carbohydrate supplementation is provided during recovery.

Atherton PJ, Babraj JA, Smith K, Singh J, Rennie MJ, Wackerhage H (2005) Selective activation of AMPK-PGC-1 α or PKB-TSC2-mTOR signaling can explain specific adaptive responses to endurance or resistance training-like electrical muscle stimulation. *FASEB Journal* **19(7)**: 786-8.

Coffey VG, Pilegaard H, Garnham AP, O'Brien BJ, Hawley JA (2009) Consecutive bouts of diverse contractile activity alter acute responses in human skeletal muscle. *Journal of Applied Physiology* **106(4)**: 1187-97.

Coffey VG, Hawley JA (2007) The molecular bases of training adaptation. *Sports Medicine* **37**: 737-763.

Ruvinsky I, Meyuhas O (2006) Ribosomal protein S6 phosphorylation: from protein synthesis to cell size. *Trends in Biochemical Sciences* **31**: 342-348.

The local dynamics of thermal sweat suppression following a systemic cholinergic blockade

C.A. Machado-Moreira,¹ P.L. McLennan,² S. Lillioja,¹ W. van Dijk,¹ J.N. Caldwell¹ and N.A.S. Taylor,¹ ¹School of Health Sciences, University of Wollongong, Wollongong, NSW 2522, Australia. and ²Graduate School of Medicine, University of Wollongong, Wollongong, NSW 2522, Australia..

Human eccrine sweat secretion can be fully inhibited by atropine, systemically administered in the correct dose. However, the dynamics of this suppression have not been thoroughly described. Therefore, using very sensitive methods, local sweat rates were measured simultaneously across several body segments, before and after a cholinergic blockade. Herein are described the temporal characteristics of thermal sweat suppression following atropine infusion. Eight males were passively heated (feet immersion (42-43°C), water-perfusion suit (48°C)). After core temperature increased ~0.5°C, and steady-state thermal sweating was established, the core temperature was clamped and atropine sulphate was gradually (over ~1 min) and intravenously infused (dorsal hand: 0.04 mg.kg⁻¹). Sweat rates were measured at 1s intervals using ventilated capsules positioned at the forehead, the dorsal surfaces of the forearm and hand, the palm and calf. Three variables were estimated: the phase delay between the start of the infusion and the first evidence of sweat reduction; the time required for full suppression of sweating; and the time constant for this decay. The blockade completely inhibited thermal sweating from all regions ($p < 0.05$), and this occurred, on average, within 5 min (Table: data are means with standard deviations). Indeed, the first evidence of suppression appeared within 60s, and the mean decay time constant was 144s. The rapidity of this action was remarkable, given that the infusion was delivered intravenously at the hand, and had to diffuse from the periglandular capillary and through the interstitial fluid before it could block receptors on the sweat gland. This was facilitated by an almost immediate cardiac acceleration (40±4 beats.min⁻¹) and presumably by the rapid reduction in peripheral vasoconstrictor tone to support pressure regulation. It took longer for the full suppression to become established at the forehead ($p < 0.05$), and this delay may be explained by its higher initial sweat rate. Indeed, a larger atropine dose is required to produce inhibition when sweating is more profuse (Cummings & Craig, 1967). Furthermore, it was only the total suppression time that was delayed, while neither the phase delays nor the time constants differed significantly among sites ($p > 0.05$).

Skin site	Phase delay (min)	Time constant (min)	Full suppression (min)
Forehead (N=6)	0.8 ±0.4	2.6 ±1.3	7.8 ±2.4 [†]
Dorsal forearm (N=6)	0.9 ±0.4	2.1 ±0.7	3.9 ±0.2
Dorsal hand	1.2 ±0.5	2.7 ±0.5	4.4 ±0.6
Palm	0.9 ±0.4	2.1 ±0.4	3.7 ±0.7
Upper calf	1.0 ±0.2	2.4 ±0.4	5.1 ±1.6
All sites (mean)	1.0 ±0.3	2.4 ±0.3	4.9 ±0.5

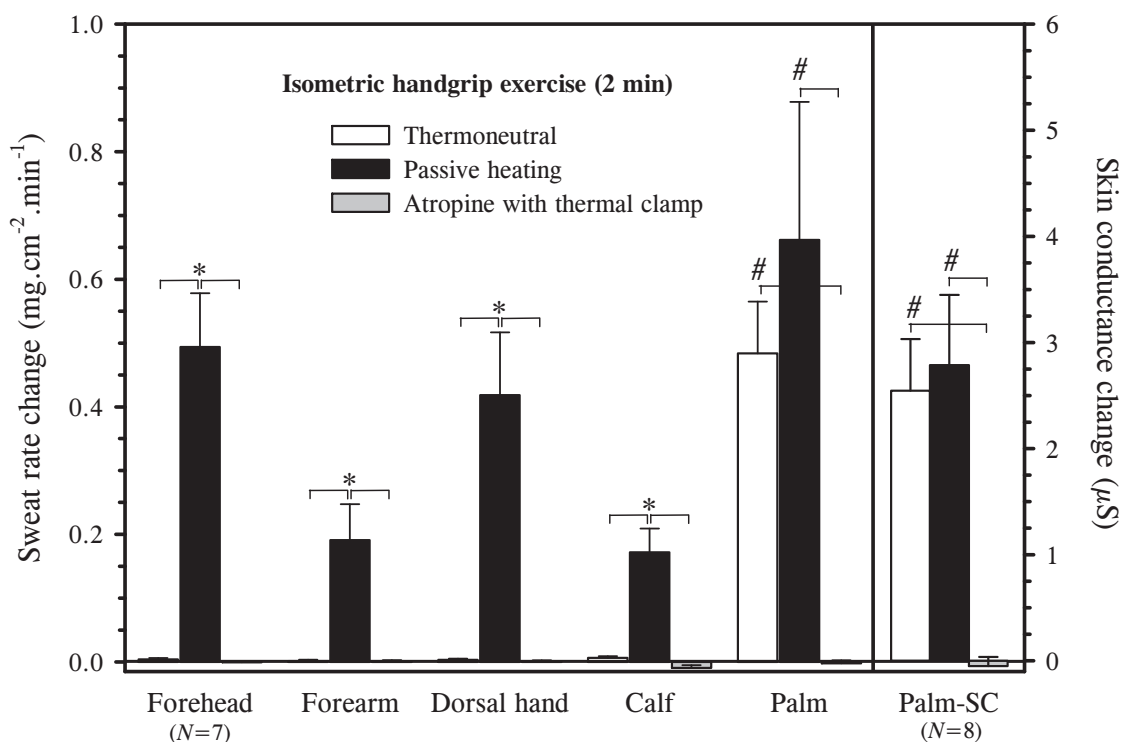
[†] significantly different from all other sites.

Cummings, E.G. & Craig, F.N. (1967). Influence of the rate of sweating on the inhibitory dose of atropine. *Journal of Applied Physiology*. **22**: 648-654.

Do non-cholinergic efferent pathways have a functional relevance during the thermal and non-thermal stimulation of human eccrine sweat glands?

C.A. Machado-Moreira,¹ P.L. McLennan,² S. Lillioja,¹ W. van Dijk,¹ J.N. Caldwell¹ and N.A.S. Taylor,¹ ¹School of Health Sciences, University of Wollongong, Wollongong, NSW 2522, Australia. and ²Graduate School of Medicine, University of Wollongong, Wollongong, NSW 2522, Australia..

Whilst the cholinergic modulation of thermally induced eccrine sweating has been extensively demonstrated, evidence concerning the neuropharmacological control of non-thermally mediated sweating is equivocal. However, a sparse distribution of noradrenergic nerve terminals surrounds the sweat gland, sweating can be induced by noradrenergic agonists, and it is also possible these glands receive dual innervation. Therefore, the long-held dogma is that non-thermally induced sudomotor responses are, at least in part, noradrenergically driven. Accordingly, this experiment was designed to test the hypothesis that sweating could not occur following a systemic cholinergic blockade. Sudomotor responses from nine healthy males were investigated when psychological (mental arithmetic), local pain and static exercise stimulations were applied under thermoneutral conditions (27.5-28°C), and also following passive heating (feet immersed 42-43°C, water-perfusion suit 33-48°C). Mean body temperature was then clamped (36.9±0.1°C), and atropine sulphate was administered (intravenous: 0.04 mg.kg⁻¹). Following complete sweat suppression, these stimuli were repeated. The isothermal clamp prevented the body temperature elevation that would normally accompany the cessation of sweating. Ventilated sweat capsules and skin conductance methods were used to measure sweat secretion from both glabrous and non-glabrous (hairy) skin surfaces. When thermoneutral, significant sweat secretion was evident only from glabrous skin following these non-thermal stimulations ($p < 0.05$; Figure). Passive heating induced sweating at all sites, and when these stimuli were superimposed upon this thermal load, significant sudomotor responses were evident from each site tested ($p < 0.05$). During the blockade, none of these stimuli elicited sweating, either as discharged or primary (skin conductance) sweat ($p < 0.05$). Therefore, these data demonstrate that sweating during these thermal, psychological and exercise stimulations was exclusively cholinergically mediated. Therefore, whilst eccrine sweat glands may indeed respond to catecholamines, the current results refute the proposition that functionally relevant noradrenergic, sudomotor pathways may exist.



The role of F-actin in vesicular secretion

Y. Jang and P. Thorn, School of Biomedical Sciences, The University of Queensland, QLD 4072, Australia.

Acute pancreatitis is an inflammatory process that leads to auto-digestion of pancreatic tissue by premature activation of digestive enzymes within pancreatic acinar cells. One of the prominent cellular events in acute pancreatitis is formation of vacuoles and rapid disruption of the actin cytoskeleton surrounding the lumen of pancreatic ducts (Nemoto *et al.*, 2004). The mechanisms behind reorganization of F-actin during vesicular secretion are still unclear, however it is generally accepted that secretory granules are coated with F-actin in response to secretagogue stimulation. F-actin coating of secretory vesicles may be a key process which regulates vesicle content release in exocytosis. Therefore, this study investigates the role of F-actin in vesicular secretion in pancreatic acinar cells.

Experiments were performed using clusters of acini, isolated from the pancreas of 2-5 week-old male CD-1 mice by digestion with collagenase. The effects of inhibiting F-actin polymerization were examined with 10 μM of Latrunculin B treatment prior to cell stimulation. Latrunculin is an actin perturbing drug which reduces F-actin and may have effects on fusion pore dynamics (Larina *et al.*, 2007). Firstly, the effects of increasing treatment time (0 to 35 min) of Latrunculin B on the F-actin coating of secretory vesicles were examined in confocal microscopy. After various treatment times, the cells were incubated with fluorescein for 5 minutes then stimulated with acetylcholine for 2 min. For the visualization of F-actin, acini were fixed with 4% paraformaldehyde and stained with Alexa 633-phalloidin. Latrunculin B inhibited F-actin coating of secretory granules at all time points. The longer exposure to the drug strongly decreased the F-actin. 5 minutes of exposure to the drug did not significantly change the structure and the size of the secretory vesicles. After 15 minutes of Latrunculin B treatment, the average size of the secretory granules increased three fold in comparison to the size of granules in control cells. The measured size of control vesicles was $1.05 \pm 0.19 \mu\text{m}$ (mean diameter \pm SEM, $n=100$) while the size of vesicles in Latrunculin B treated cells was $3.14 \pm 0.09 \mu\text{m}$. Latrunculin B did not affect the total number of exocytic events suggesting that F-actin plays a role in secretory vesicle maintenance. Therefore we hypothesize that the increased size of the secretory vesicles of Latrunculin B treated cells may be due to the vesicle swelling during exocytosis. To examine the appearance of zymogen granules in real time, two-photon excitation imaging of pancreatic acinar cells was performed. Time course Latrunculin B treatment and acetylcholine stimulation was processed in the acini for real time experimentation in equivalent conditions to those described above as an extracellular tracer. Vesicle fusion was visualized using sulforhodamine B over 10 minutes after stimulation under two-photon microscopy. Real time analysis revealed that secretory vesicles appeared as same size as the vesicles in control cells then swell with sequential exocytosis after stimulation resulted in Latrunculin B treatment for 15 minutes. Corresponding to the fixed cells imaging result, 5 minutes treatment of Latrunculin B did not cause the secretory vesicle extension.

In conclusion, the results of this study suggest that loss of F-actin during secretion weakens the secretory vesicle membrane and destabilizes granules. This supports the idea that impaired F-actin polymerization leads to retention of enzymes in the cytosol which may contribute to auto-digestion of the vacuolar membrane in acute pancreatitis. We are currently working on the mechanisms of granule swelling after Latrunculin treatment and its potential relationship to acute pancreatitis.

Nemoto, T., Kojima, T., Oshima, A., Bito, H., and Kasai, H. (2004). Stabilization of exocytosis by dynamic F-actin coating of zymogen granules in pancreatic acini. *Journal of Biological Chemistry* **279**, 37544-37550.

Larina, O., Bhat, P., Pickett, J.A., Launikonis, B.S., Shah, A., Kruger, W.A., Edwardson, J.M., and Thorn, P. (2007). Dynamic regulation of the large exocytotic fusion pore in pancreatic acinar cells. *Molecular Biology of Cell* **18**, 3502-3511.

The role of dynamin in fusion pore closure and endocytosis in pancreatic acinar cells

A. Banerjee and P. Thorn, School of Biomedical Sciences University of Queensland, Brisbane, QLD 4067, Australia.

Introduction: In previous work on mouse pancreatic acinar cells that secrete precursor digestive enzymes, we have shown that the end of exocytosis and beginning of endocytosis is marked by the closure of the fusion pore (Larina *et al.*, 2007). Here we show that the mechanism that closes the fusion pore is regulated by dynamin, a GTPase implicated in vesicle dynamics in other cells. We suggest that the closure of fusion pore is the limiting step in secretion that differentiates the two distinct irreversible processes - exocytosis and endocytosis - and following fusion pore closure the vesicle is committed to be internalized.

Methods: CD-1 mice were killed according to the approved ethical procedures of The University of Queensland. The pancreas was excised and collagenase-digested to produce fragments of pancreatic tissue. The tissue was suspended in extracellular buffer at 37°C and bathed in 800 µM extracellular dye Sulforhodamine B (SRB). The cells were stimulated with 600 nM Acetylcholine (ACh) which was limited at 2 min by applying the cholinergic antagonist, atropine (6 µM). Cells were then incubated in the extracellular buffer with or without the dynamin inhibitor Dyngo* (50 µM) for between 0 to 50 minutes. The cells were then centrifuged and resuspended in an extracellular buffer with the extracellular dye HPTS in place of SRB (800 µM). Endocytic objects were therefore labelled with SRB only and granules still undergoing exocytosis at the time of centrifugation were labelled with HPTS. The cells were then imaged using 2-photon microscopy with an excitation of 800 nm.

Results: Control cells (absence of Dyngo) had vesicles that still contained the first dye, SRB as the dye was unable to escape when the cells were resuspended due to the closure of the fusion pore. Control cells also showed vesicles with the second dye, HPTS indicating these vesicles are still exocytotic and in continuity with the extracellular environment. Using MetaMorph® imaging software, 2D surface area of vesicles in a particular cell was quantified as those which contain SRB (red) and that contain HPTS (blue) and expressed as a percentage of internalisation: endocytosis = red surface area/ (red + blue) surface area. The area of SRB-positive vesicles significantly increased over time 0 min - 18.9%, 5 min - 30.7%, 10 min - 35.9%, 20 min - 47.1%, 30 min - 53.2%, 50 min - 63%. In Dyngo-treated cells significantly fewer vesicles contained SRB, indicating the fusion pore had not closed and the dye was able to leave the vesicle upon resuspension in the HPTS. At 30 minutes there was a significant decrease in the area of SRB-positive vesicles ($53.2 \pm 2.1\%$, compared with $7 \pm 1.5\%$, $N=3$ (number of mice) *student t-test*: $p < 0.0001$).

Conclusion: The rate of endocytosis in pancreatic acinar cells appears to be quite slow, with internalisation continuing over the entire 50 minute time frame of our experiments. This is in contrast to other tissues such as frog neuromuscular junction, in which fast endocytosis occurs over 20 seconds and slow endocytosis occurs in 5 minutes (Royle & Lagnado, 2003). Application of a dynamin inhibitor significantly reduced the surface area of SRB-positive vesicles indicating the importance of dynamin in fusion pore closure. Our results support the idea that dynamin plays a critical role at the transition from exocytosis to endocytosis.

Larina O, Bhat P, Pickett JA, Launikonis BS, Shah A, Kruger WA, Edwardson JM, Thorn P. (2007) Dynamic regulation of the large exocytotic fusion pore in pancreatic acinar cells. *Molecular Biology of the Cell* **18**: 3502-11.

Royle S, Lagnado L. (2003) Endocytosis at the synaptic terminal. *Journal of Physiology* **553**: 345-355.

*Dyngo acts on a dynamin GTPase domain allosteric site. It was developed through a joint venture between the Children's Medical Research Institute (CMRI) and the University of Newcastle. It is marketed by Biolink (www.bio-link.com).

Multiple effects of anthracyclines on cardiac ryanodine receptors

A.D. Hanna, A.F. Dulhunty and N.A. Beard, Muscle Research Group, John Curtin School of Medical Research, The Australian National University, Canberra City, ACT 0200, Australia.

The anthracyclines doxorubicin and daunorubicin are powerful chemotherapeutics, used effectively in the treatment of various malignancies. The use of anthracyclines is limited however, due to dose-dependent cardiotoxic side effects developing in some patients. These effects present as both acute and chronic impairment of cardiac function and preclude anthracycline use in patients with a pre-existing heart condition. Current theories concerning acute mechanisms of anthracycline-induced cardiotoxicity suggest the drugs and their metabolites, doxorubicinol and daunorubicinol, accumulate in the sarcoplasmic reticulum (SR) of cardiomyocytes where they target SR proteins and cause changes in Ca^{2+} homeostasis. The cardiac ryanodine receptor (RyR2) has been implicated as a target, because the drugs have been shown to dramatically alter SR Ca^{2+} release. However the mechanism of the protein-drug interaction remains unknown and is thought to also involve anthracycline-induced oxidation of critical sulfhydryl groups and generation of free radicals.

Sheep hearts were excised from anaesthetised ewes (5% pentobarbitone (IV) followed by oxygen/hatthane). RyR2-enriched cardiac SR vesicles were obtained from sheep heart by centrifugation as described in Laver *et al.* (1995). SR vesicles (containing RyR2 channels) were reconstituted into artificial planar lipid bilayers formed across an aperture separating two solutions, equivalent to the cardiomyocyte cytoplasm (*cis*) and SR lumen (*trans*). The *trans* solution was held at virtual ground and voltage (+40mV or -40mV) was applied to the *cis* solution. Control RyR2 activity was recorded, before drugs were added to the *trans* solution.

Addition of low micromolar concentrations (0.5 μM to 10 μM) of anthracyclines to the *trans* (luminal) side of single RyR2 channels caused significant increase in channel activity in a concentration dependent manner. With higher concentrations of each drug, the increase in channel activity was followed by an inhibitory phase where there was a strong reduction in channel activity, which continued for the lifetime of the experiment (up to 30 min). Further investigation of the effects of daunorubicin showed that the activation effect was reversed by washout, but not the inhibitory effect, indicating that the two effects are mediated by separate mechanisms. This was confirmed using the reducing agent dithiothreitol (DTT) and the thiol modifying reagent *N*-ethylmaleimide (NEM), which were able to prevent or reduce the extent of the inhibitory effect but not the activation effect. These data suggest that inhibition of RyR2 activity was caused by oxidation of free thiol groups, likely on the RyR2 itself. Conversely, the reversal of activation following washout and the failure of DTT and NEM to prevent activation, suggests a ligand binding mechanism, either to the RyR2, or an associated regulatory protein.

The results provide novel evidence that anthracycline-induced biphasic modulation of RyR2 channels is mediated by two distinct mechanisms. Firstly, that the activation effect is mediated by a redox-independent mechanism, most likely ligand-binding to either the RyR2 itself or to an associated regulatory protein. Secondly, anthracycline-induced inhibition is caused by drug-induced thiol oxidation. Since this anthracycline-induced inhibition was not reversed by DTT we believe that, once formed, the disulfide bond/s become buried in the protein complex, thus inaccessible to DTT. In summary, we provide novel evidence that multiple effects on RyR2 channel activity may contribute to anthracycline-induced disruption of Ca^{2+} homeostasis and subsequent cardiotoxicity. This important new information may help in the eventual design of anthracyclines that do not detrimentally alter Ca^{2+} signalling in the heart.

Laver DR, Roden LD, Ahern GP, Eager KR, Junankar PR and Dulhunty AF (1995) Cytoplasmic Ca^{2+} inhibits the ryanodine receptor from cardiac muscle. *Journal of Membrane Biology* **147**: 7-22.

Ryanodine receptor phosphorylation in human heart failure

N.A. Beard,¹ M. Janczura,¹ A.F. Dulhunty,¹ P. Molenaar^{2,3} and D.R. Laver,⁴ ¹The John Curtin School of Medical Research, The Australian National University, Acton, ACT 2612, Australia, ²Department of Medicine, University of Queensland, Brisbane, QLD 4072, Australia, ³Faculty of Science and Technology, Queensland University of Technology, Brisbane, QLD 4000, Australia and ⁴School of Biomedical Sciences, University of Newcastle and Hunter Medical Research, Callaghan, NSW 2308, Australia.

Heart failure is a complex disorder, characterized by activation of the sympathetic nervous system, leading to dysregulated Ca²⁺ homeostasis in cardiac myocytes and tissue remodeling. In a variety of diseases, cardiac malfunction is associated with aberrant fluxes of Ca²⁺ across both the surface membrane and the internal Ca²⁺ store, the sarcoplasmic reticulum (SR). One prominent hypothesis residues is that in heart failure, the activity of the ryanodine receptor (RyR2) Ca²⁺ release channel in the SR is increased due to excess phosphorylation and that this contributes to excess SR Ca²⁺ leak in diastole, reduced SR Ca²⁺ load and decreased contractility (Huke & Bers, 2008). There is controversy over which serine residues in RyR2 are hyperphosphorylated in animal models of heart failure and whether this is *via* the CaMKII or the PKA-linked signaling pathway. S2808, S2814 and S2030 in RyR2 have been variously claimed to be hyperphosphorylated. Our aim was to examine the degree of phosphorylation of these residues in RyR2 from failing human hearts.

The use of human tissue was approved by the Human Research Ethics Committee, The Prince Charles Hospital, EC28114. Left ventricular tissue samples were obtained from an explanted heart of a patient with end-stage heart failure (Emery Dreifuss Muscular Dystrophy with cardiomyopathy) and non-failing tissue was from a patient with cystic fibrosis undergoing heart-lung transplantation with no history of heart disease. SR vesicles were prepared as described by Laver *et al.* (1995) and examined with SDS-Page and Western Blot. Transferred proteins were probed with antibodies to detect total protein phosphorylation, phosphorylation of RyR2 serine residues S2808, S2814, S2030 and for the key proteins calsequestrin, triadin, junctin and FKBP12.6. To avoid membrane stripping artifact, each membrane was exposed to one phosphorylation-specific antibody and signal densities quantified using Bio-Rad Quantity One software.

We found no distinguishable difference between failing and healthy hearts in the protein expression levels of RyR2, triadin, junctin or calsequestrin. We found an expected upregulation of total RyR2 phosphorylation in the failing heart sample, compared to a matched amount of RyR2 (quantified using densitometry) in healthy heart. Probing with antibodies detecting only the phosphorylated form of the specific RyR2 residues showed that the increase in total RyR2 phosphorylation in the failing heart was due to hyperphosphorylation of S2808 and S2814. We found that S2030 phosphorylation levels were unchanged in human heart failure. Interestingly, we found that S2030 has a basal level of phosphorylation in the healthy human heart, different from the absence of basal phosphorylation recently reported in rodent heart (Huke & Bers, 2008). Finally, preliminary results indicate that less FKBP 12.6 is associated with RyR2 in the failing heart, possibly as a consequence of PKA activation.

In conclusion, residues S2808 and S2814 are hyperphosphorylated in human heart failure, presumably due to upregulation of the CaMKII and/or PKA signaling pathway as a result of chronic activation of the sympathetic nervous system. Such changes in RyR2 phosphorylation are believed to contribute to the leaky RyR2 phenotype associated with heart failure, which increases the incidence of arrhythmia and contributes to the severely impaired contractile performance of the failing heart.

Huke S & Bers DM. (2008). Ryanodine receptor phosphorylation at serine 2030, 2808 and 2814 in rat cardiomyocytes. *Biochemical and Biophysical Research Communications* **376**, 80-85.

Laver DR, Roden LD, Ahern GP, Eager KR, Junankar PR & Dulhunty AF. (1995). Cytoplasmic Ca²⁺ inhibits the ryanodine receptor from cardiac muscle. *Journal of Membrane Biology* **147**, 7-22.

Inhibition of cardiac Ca²⁺ release channels as therapy for arrhythmia

D. Mehra,¹ D.F. van Helden,¹ H.S. Hwang,² B.C. Knollmann² and D.R. Laver,¹ ¹Department of Biomedical Sciences and Pharmacy, University of Newcastle and HMRI, Callaghan, NSW 2308, Australia and ²Department of Medicine, Division of Clinical Pharmacology, Vanderbilt University, Nashville, TN 37240, USA.

The ryanodine receptors (RyR2) are the calcium release channels in sarcoplasmic reticulum (SR) which is the main Ca²⁺ store in the heart. Mutations in RyR2 or calsequestrin cause arrhythmias as a result of increased diastolic Ca²⁺ release *via* RyR2. Such an abnormality manifests in Catecholaminergic Polymorphic Ventricular Tachycardia (CPVT), a form of cardiac arrhythmia which is the focus of our research.

Flecainide, a sodium channel blocker of the Class I anti arrhythmic group was found to prevent arrhythmia in CPVT by inhibiting RyR2 (Watanabe *et al.*, 2009). However, it is not clear how inhibition *per se* has an anti arrhythmic action because another inhibitor, tetracaine, has a pro-arrhythmic action (Watanabe *et al.*, 2009). It was noted that flecainide decreased channel mean open time whereas tetracaine increased channel closed times (Hilliard *et al.*, 2010). Therefore, we test the hypothesis that the therapeutic inhibition of RyR2 relies on reducing channel open times without affecting its closed times. Our approach is to measure the actions of a range of class 1 drugs on RyR2 open times in single channel recording and correlate this with their therapeutic action determined in isolated cardiomyocytes and in a CPVT mouse model.

RyR2 was isolated from sheep and human hearts as described previously (Laver *et al.*, 1995). RyRs were incorporated into artificial lipid bilayers and channel gating was measured by single channel recording. RyR2 open and closed times were measured in the presence of diastolic [Ca²⁺] (100 nmol/l cytoplasmic and 0.1 mmol/l luminal). SR Ca²⁺ release was measured using confocal microscopy on intact ventricular cardiomyocytes isolated from hearts of calsequestrin knockout mice (CPVT mouse model). Fura2-AM was used to measure the effect of Class I anti arrhythmic drugs on isoproterenol-induced calcium waves.

RyR2 open time was decreased by the Class Ic anti-arrhythmic drugs whereas Classes Ia and Ib had no significant effect at concentrations up to 50 µmol/l (see Table). None of the Class Ic drugs had any significant effect on RyR2 closed durations. The ability of the drugs to reduce RyR2 open times correlated with their ability to prevent the Ca²⁺ waves in cardiomyocytes; an indicator for their anti-arrhythmic efficacy. Both flecainide and propafenone suppressed ventricular tachycardia in calsequestrin knockout mice.

The data suggest that potency of RyR2 open time reduction rather than just a reduction in open probability determines efficacy of class I agents for the prevention of CPVT. This may lead to a paradigm shift in drug development process by directing strategies away from discovering high affinity compounds to searching for low affinity compounds with short residence time in the channel.

Comparison of the potency (IC₅₀) of class I drugs on the mean open time of cardiac RyRs and their IC₅₀s for reduction in frequency of Ca²⁺ waves in intact cardiomyocytes. n.d. = not done. n in parentheses.

	compound	IC ₅₀ (µmol/l) in RyR2 open time	IC ₅₀ (µmol/l) Ca ²⁺ waves
Class Ia	quinidine	>50 (5)	>6 (28)
	procainamide	>50 (5)	>15 (28)
	disopyramide	>50 (7)	>6 (28)
Class Ib	lidocaine	>50 (5)	>50 (28)
	mexilitine	>50 (6)	>6 (28)
Class Ic	flecainide	16.7 ± 4.0 (14)	2.0 ± 0.2 (36)
	R-propafenone	8.7 ± 0.6 (13)	1.1 ± 0.5 (36)
	S-propafenone	17.3 ± 1.6 (14)	5 ± 1 (36)
	encainide	22.5 ± 1.2 (9)	n.d.

Hilliard FA, Steele DS, Laver D, Yang Z, Le Marchand SJ, Chopra N, Piston DW, Huke S, Knollmann BC. (2010) *Journal of Molecular and Cellular Cardiology*, **48**: 293-301.

Laver DR, Roden LD, Ahern GP, Eager KR, Junankar PR & Dulhunty AF. (1995). *Journal of Membrane Biology* **147**: 7-22.

Watanabe H, Chopra N, Laver D, Hwang HS, Davies SS, Roach DE, Duff HJ, Roden DM, Wilde AA, Knollmann BC. (2009) *Nature Medicine* **15**: 380-383.

How additive effects of small changes in repolarising currents can increase the risk for atrial fibrillation – a modelling study

S.A. Mann,¹ J.I. Vandenberg¹ and D. Fatkin,² ¹Mark Cowley Lidwill Cardiac Electrophysiology Research Program, Victor Chang Cardiac Research Institute, 405 Liverpool St, NSW 2010, Australia and ²SR Bernice Research Program in Inherited Disease, Victor Chang Cardiac Research Institute, 405 Liverpool St, NSW 2010, Australia.

Atrial fibrillation (AF) is the most common cardiac arrhythmia and a frequent complication of cardiac and systemic disorders. Community-based studies have demonstrated familial aggregation of AF (Fox *et al.*, 2004; Arnar *et al.*, 2006) with the heritability of AF estimated to be 60% in one twin cohort (Christophersen *et al.*, 2009).

While these studies indicate that genetic factors have an important role in AF pathogenesis, the genes involved and mechanistic links with atrial arrhythmogenesis are incompletely understood. AF is predicted to be a complex trait in which one or more genetic variants, together with acquired “environmental” factors that alter atrial size and/or function, are involved in most cases (Fatkin, Otway & Vandenberg, 2007). Genome-wide association studies have been used to define common variants that modify susceptibility to AF in the general population (Milan *et al.*, 2010). Because of their frequency, common variants have a significant population impact but the effect size of individual variants is generally only small. Combinations of variants with small effect size may have additive, opposing, or synergistic actions, and the net effects of multiple variants are difficult to predict or demonstrate experimentally.

We performed *in silico* modelling using the Courtemanche human atrial action potential model (Courtemanche, Ramirez & Nattel, 1998) to assess the effects of combinations of multiple potassium variants on atrial action potential properties. For this we simultaneously altered the conductances of each of the five potassium channel components of the Courtemanche model by +10 or –10 percent of their original values. For each of the resulting 243 combinations we performed 1000 simulation runs - with additional random noise added to the potassium conductances - and measured the resulting action potential duration variabilities.

Our data demonstrate that multiple K⁺ variants of small effect size can have collective effects that are functionally equivalent to those attributable to single-gene mutations.

Arnar DO, Thorvaldsson S, Manolio TA, Thorgeirsson G, Kristjansson K, Hakonarson H, Stefansson K. (2006) Familial aggregation of atrial fibrillation in Iceland. *European Heart Journal* **27**: 708-12.

Christophersen IE, Ravn LS, Budtz-Joergensen E, Skytthe A, Haunsoe S, Svendsen JH, Christensen K. (2009) Familial aggregation of atrial fibrillation: a study in Danish twins. *Circulation, Arrhythmia and Electrophysiology* **2**: 378-83.

Courtemanche, M, Ramirez, R J, Nattel, S. (1998) Ionic mechanisms underlying human atrial action potential properties: insights from a mathematical model. *American Journal of Physiology* **275**: 301-21.

Fatkin D, Otway R, Vandenberg JI. (2007) Genes and atrial fibrillation: a new look at an old problem. *Circulation* **116**: 782-92.

Fox CS, Parise H, D’Agostino RB Sr, Lloyd-Jones DM, Vasan RS, Wang TJ, Levy D, Wolf PA, Benjamin EJ (2004) Parental atrial fibrillation as a risk factor for atrial fibrillation in offspring. *JAMA: The Journal of the American Medical Association* **291**: 2851-5.

Milan DJ, Lubitz SA, Kaab S, Ellinor PT. (2010) Genome-wide association studies in cardiac electrophysiology; recent discoveries and implications for clinical practice. *Heart Rhythm* **7**: 1141-8.

Measuring receptor motility and filopodia dynamics

K. Hendy,¹ Y. DeGraaf,¹ J. Clarke,¹ W.G. Thomas² and I.L. Gibbins,¹ ¹Anatomy & Histology, and Centre for Neuroscience, Flinders University, GPO Box 2100, Adelaide, SA 5001, Australia and ²School of BioMedical Sciences, University of Queensland, QLD 4072, Australia.

Signaling through G protein-coupled receptors (GPCRs) involves the orchestrated interactions of the receptor complex itself with elements of a dynamic actin cytoskeleton. Important components of the motile cell membrane include actin rich protrusions, termed filopodia, which can mediate interactions between the cell and its environment. However, the dynamics of GPCRs in a highly motile cell membrane are not well understood. Therefore, we have developed an experimental approach to measure membrane motility and GPCR motility in tandem, in live cells, during application of receptor agonists and modifiers of actin dynamics. We have utilised a Chinese Hamster Ovary (CHO) cell line expressing functional angiotensin II type 1a receptor (AT1AR) tagged with enhanced green fluorescent protein (eGFP) as a GPCR model system. Taking advantage of the imaging capabilities of our Leica SP5 laser scanning confocal microscope equipped with the unique combination of a high-speed resonant scanner and avalanche photo diode detectors, we are able to image receptor and membrane dynamics at very high speed and single photon sensitivity with minimal photodamage. Series of 50 images of live CHO-AT1AR-eGFP cells were captured at a rate of 20-25 frames per second, t=0, 10, and 20 min after addition of fluorescently labelled AT1AR agonist, angiotensin II-AlexaFluor647 (AngII-A647) (100nM). Effects of the actin polymerisation inhibitor, cytochalasin B (CB) (0.5 μ M, 2.5 μ M, 5 μ M), and the dynamin GTPase inhibitor dynasore (80 μ M) were also tested. Images were collated, processed and analysed primarily with ImageJ software. In the absence of agonist, high resolution imaging revealed a surprising amount of motility in the cell membrane and constitutive internalisation of the receptor was observed. In the presence of agonist, the high level of membrane motility remained in the presence of internalisation of ligand-bound receptors. In 4 of 5 cells, application of 0.5 μ M CB led to collapse and aggregation of filopodia 10 min after application. By 20 min post application, significant recovery of filopodial motion was observed. Immunocytochemistry labelling with antibodies for β -actin demonstrated a classic text-book distribution of actin including the appearance of stress fibres at the basolateral surface of control cells. Treatment with CB (0.5 μ M, 2.5 μ M, 5 μ M) revealed a reorganisation of the actin cytoskeleton, including the appearance of actin rich aggregations along the membrane and the disappearance of actin stress fibres. CB treated cells also showed a change to the overall cell morphology. In all 7 cells treated with 80 μ M dynasore, no obvious effect on filopodia motility was observed. This model system enables the measurement of filopodia movement in different states of receptor activation. Our results to date suggest that the analysis of agonist-receptor interactions, at least in cell lines, will be significantly confounded by the consequences of membrane motility. By coupling this model with advanced image analysis to extract and quantify different aspects of membrane and receptor motility (*e.g.* particle tracking, Raster Image Correlation Spectroscopy), we will enhance our understanding of GPCR signalling in a dynamic membrane environment.

Pulmonary surfactant membranes of hibernating ground squirrels possess increased fluidity but are capable of maintaining an ordered membrane structure at low temperatures

S. Orgeig,¹ L. Suri,¹ L. McCaig,² V. Picardi,³ R. Veldhuizen,² J. Staples,⁴ F. Possmayer⁵ and J. Perez-Gil,³

¹School of Pharmacy & Medical Sciences, Sansom Institute for Health Research, University of South Australia, Frome Rd, Adelaide 5001, Australia, ²Lawson Research Institute, University of Western Ontario, London, Ontario N6A 3K7, Canada, ³Department of Biochemistry, Faculty of Biology, Complutense University, Madrid, Spain, ⁴Department of Biology, University of Western Ontario, London, Ontario N6A 3K7, Canada and ⁵Departments of Obstetrics & Gynaecology and Biochemistry, University of Western Ontario, London, Ontario N6A 3K7, Canada.

Pulmonary surfactant, a mixture of lipids and proteins, regulates the surface tension at the air-liquid interface of the lung. Reduced body temperature during hibernation is accompanied in 13-lined ground squirrels (*Ictidomys tridecemlineatus*) by an increase in fluid monounsaturated phosphatidylcholine (PC) species (e.g. PC 16:0/16:1, PC 16:0/18:1) and phosphatidylglycerol (PG) species (e.g. PG 16:0/18:1, PG 18:0/18:2), but fewer disaturated PC and PG species (Possmayer *et al.*, 2010). Previously we speculated that altered surfactant lipid composition during metabolic depression states such as torpor or hibernation will reduce the phase transition temperature (T_m) of the mixture, enabling pulmonary surfactant to remain fluid over a broader range of temperatures and thereby maintaining respiratory function (Lang *et al.*, 2005). Here we analyze thermodynamic properties and behavior of surfactant from hibernating and summer-active 13-lined ground squirrels in relation to natural porcine surfactant, using differential scanning calorimetry and LAURDAN fluorescence spectroscopy. In addition we conducted epifluorescence studies to visualize changes in phase coexistence of surfactant films of hibernating and summer-active animals. Surfactant membranes of hibernators showed gel-to-fluid transitions at lower T_m with reduced enthalpy relative to membranes from summer-active squirrels. Both exhibited lower enthalpy than porcine surfactant. LAURDAN fluorescence and epifluorescence suggested possible structural rearrangements of surfactant membrane lipids and films, respectively, in hibernators. These exhibited a similarly dehydrated and condensed highly packed ordered phase as for summer active squirrels, despite differences in composition and T_m . In conclusion, pulmonary surfactant composition changes in hibernating squirrels to increase overall fluidity, but to maintain an ordered membrane structure at low temperature.

Possmayer F, McCaig L, Yao L, Zhao L, Staples J, Orgeig S, Veldhuizen RA. (2010). Coping with the cold: effect of hibernation on pulmonary surfactant in the thirteen-lined ground squirrel. *Biophysical Journal* **98**, 76a.

Lang CJ, Postle AD, Orgeig S, Possmayer F, Bernhard W, Panda AK, Jürgens KD, Milsom WK, Nag K & Daniels CB. (2005). Dipalmitoylphosphatidylcholine is not the major surfactant phospholipid species in all mammals. *American Journal of Physiology. Regulatory, Integrative and Comparative Physiology* **289**, R1426-R1439.

Aggregation state of A β peptides in model membranes

M.A. Sani, J.D. Gehman and F. Separovic, School of Chemistry, Bio21 Institute, University of Melbourne, VIC 3010, Australia.

Amyloid-beta (A β) peptides are postulated to cause loss of nerve cell function in individuals suffering from Alzheimer's disease (AD), where evidence suggests that interaction with the cell membrane correlates strongly with cytotoxicity. However, the molecular mechanism is still unclear and further evidence is required to identify the culprit promoting neuron loss. The peptides aggregate readily and form amyloid fibrils. We have been studying the interaction of A β 42 peptide with phospholipid membranes using solid-state NMR spectroscopy. However, the aggregation state of the peptide during the NMR experiment is not clear, nor is it obvious that it remains the same throughout the experiment.

The sample preparation is a very crucial aspect in studying the kinetics of A β aggregation: use of NaOH, trifluoroacetic acid (TFA) removal, peptide stock solution concentration and temperature are factors promoting completely different aggregation patterns, as observed with either Congo red or thioflavin T fluorescence. When TFA was removed from the peptide, using 5 mM HCl pre-treatment and freeze-drying as a routine procedure, aggregation was not observed, most likely due to the passage from low pH below the PI to a buffered aqueous phase (pH 7.4). Unfortunately, TFA is a strong counter ion that can lead to membrane degradation and dramatic errors in peptide weight estimation. When the TFA was not removed, a monomeric peptide stock solution was prepared in NaOH, and hexafluoroisopropanol was used to dissolve the peptide. Again, little fluorescence was observed from thioflavin T and no difference was observed when experiments were conducted at 28°C or 37°C.

The role of membrane lipids is another factor in A β aggregation and kinetic experiments using thioflavin T are being used to reveal if membranes play a critical role in accelerating amyloid formation. Large unilamellar vesicles (LUV) composed of palmitoylcholine (POPC), palmitoylserine (POPS) and cholesterol (Chol) in a molar ratio 1:1:1 were used as a mimic of the neuron cell membranes. A small concentrated volume of peptide in NaOH was externally added to a large buffered solution of LUV in a lipid/peptide molar ratio 30:1 and kept at 37°C with moderate shaking and peptide aggregation was monitored.

Amyloid plaques in the brain are rich in copper, zinc and iron, which bind to A β peptides. A β and metals have been proposed to promote lipid peroxidation and some evidence suggests that A β could drive the metals close to the membrane surface where membrane-oxidizing radicals could be generated. Solid-state NMR is being used to obtain some insights of A β -metal interactions with model membranes. Mutation of Tyr 10 replaced by an alanine or oxidation of Met 35, as encountered in AD patients brain, have shown different interactions with POPC/POPS/Chol (1:1:1) at the membrane surface as monitored by changes in the ³¹P chemical shift anisotropy and in the hydrophobic core of the phospholipid bilayers as revealed by the quadrupolar splittings in the deuterium NMR spectra.

Boltzmann statistics maximum entropy of solid-state NMR dipolar recoupling and magic angle spinning data

J.D. Gehman,¹ M.-A. Sani¹ and A.K. Mehta,² ¹School of Chemistry & Bio21 Institute, University of Melbourne, Melbourne, VIC 3010, Australia and ²Chemistry Department, Emory University, Atlanta, Georgia 30322, USA.

We have engineered algorithms to employ maximum entropy as commonly used to derive Boltzmann's distribution for application in solid state NMR data analysis. The approach is used to characterise distributions of chemical shift tensor parameters from magic angle spinning sideband peak intensities, as well as distances from rotational-echo double-resonance (REDOR) data, in heterogenous samples. In the case of REDOR data, the method can reveal multiple distances with relatively few data points, which is of particular benefit in application to biological systems. This reverses the common practice of comparing REDOR data to dephasing curves simulated for several preconceived structural models, by providing the information necessary to construct models based on unbiased data analysis. In the case of chemical shift tensor analysis, it allows arbitrarily complex phospholipid mixtures to be analyzed for subtle perturbations, for example by association with antimicrobial peptides.

The method provides for a model-free approach to data analysis, in the sense that one need not assume the presence of any specific number of different chemical shift tensors or distances that contribute to observed signal. The strategy differs from the more common practice of including a single weighted term in a fitting procedure, as each datum constitutes additional "information" and independently adds to or subtracts from the entropy of the distribution. A constrained optimisation problem with 100s of unknowns (the number of points used to approximate a continuous probability distribution of the desired parameter(s)) is thereby turned into an unconstrained optimisation problem with one coefficient for each data point.

The Boltzmann Statistics method also offers intriguing philosophical implications — it gives the broadest, and perhaps most probability distribution consistent with the data, but also helps to determine which data points hold the greatest information content, such that experimental time can be focussed on gaining the best signal-to-noise where it is likely to benefit most.

Measuring the incorporation of fluorescently labelled lipid analogues into the membrane of giant unilamellar vesicles

I.L. Salvemini,¹ J. Reid² and P.D.J. Moens,¹ ¹Centre for Bioactive Discovery in Health and Ageing, School of Science & Technology, University of New England, Armidale, NSW 2351, Australia and ²School of Science & Technology, University of New England, Armidale, NSW 2351, Australia.

The use of Giant Unilamellar Vesicles (GUVs) composed of fluorescently labelled lipid analogues has become an increasingly popular model to study both structural and complex biophysical properties of bilayers. However, there is a common assumption that the number of probes incorporated into the membrane of the GUVs is proportional to the mole fraction (%) of these lipid molecules in the original solvent solution.

A commercial confocal laser scanning microscope (Nikon C1) was used to obtain single point fluorescence correlation spectroscopy (FCS) data. The time dependence of the spontaneous fluctuations and the number of molecules in the detection volume (point spread function) was calculated using the autocorrelation function of the fluorescent signals. From these data, the diffusion coefficient (D_1) and the number of fluorescent molecules (N) incorporated into the membrane was obtained.

We successfully measured the diffusion coefficient of two different labelled lipid analogues (1,1-dioctadecyl-3,3,3,3-tetramethylindocarbocyanine perchlorate [DiIC₁₈] and BODIPY TMR-phosphatidylinositol (4,5) biphosphate [TMR-PI(4,5)P₂]) incorporated into the membrane of GUVs (Moens, Gratton & Salvemini, 2010). The results obtained for these lipid analogs are in good agreement with previously published data (Golebiewska *et al.* 2006; Golebiewska *et al.* 2008; Gielen *et al.* 2009).

We also show that the number of DiIC₁₈ molecules incorporated into the membrane of the GUVs (formed by the electroformation method) is in agreement with the expected number of molecules calculated from the mole fraction of the organic stock solution. However, we find that the actual proportion of β -BODIPY-HPC, TR-PI(4,5)P₂, and TMR-PI(4,5)P₂ incorporated into the bilayer is significantly less than the proportion of these lipids in the organic solvent stock solution.

These findings draw attention to the need to quantitatively measure the incorporation of these probes for experiments in which the concentration is of importance to the parameter being investigated.

Gielen E, Smisdom N, vandeVen am, De Clercq B, Gratton E, Digman M, Rigo J-M, Hofkens J, Engelborghs Y, Ameloot M. (2009) *Langmuir*. **25(9)**: 5209-18.

Golebiewska U, Gambhir A, Hangyás-Mihályiné G, Zaitseva I, Rädler J, McLaughlin S. (2006) *Biophysical Journal* **91(2)**: 588-99.

Golebiewska U, Nyako M, Woturski W, Zaitseva I, McLaughlin S. (2008) *Molecular Biology of the Cell* **19(4)**: 1663-9.

Moens PD, Gratton E, Salvemini IL. (2010) *Microscopy Research and Technique* Aug 23. [Epub ahead of print] <http://dx.doi.org/10.1002/jemt.20919>

Which residues are important within the N-terminal helix of hERG PAS domain to maintain a functional channel?

C.A. Ng,^{1,2} M. Hunter,¹ M.D. Perry,¹ M. Mobli,³ Y. Ke,¹ D. Stock,⁴ P.W. Kuchel,² G.F. King³ and J.I. Vandenberg,^{1,2} ¹Molecular Cardiology & Biophysics Division, Victor Chang Cardiac Research Institute, Lowy Packer Building, 405 Liverpool St, Darlinghurst, NSW 2015, Australia, ²School of Molecular Bioscience (G08), The University of Sydney, NSW 2006, Australia, ³Division of Chemistry & Structural Biology, Institute for Molecular Bioscience, The University of Queensland, St. Lucia, QLD 4072, Australia and ⁴Structural and Computational Biology Division, Victor Chang Cardiac Research Institute, Lowy Packer Building 405 Liverpool St, Darlinghurst, NSW 2015, Australia.

The hERG K⁺ channel plays an important role in maintaining proper repolarisation in the heart. Dysfunctional hERG, caused either by drug block or genetic mutation, results in long QT syndrome characterised by a prolonged QT interval on the surface electrocardiogram and an increased risk of cardiac arrhythmias and sudden death.

The cytoplasmic N-terminal domain of hERG contains a 110 residues Per-Arnt-Sim (PAS) domain (S26 to K135). Deletion of the N-terminal 135 residues of hERG results in a significantly faster rate of deactivation. Further, the WT rate of deactivation can be restored by external application of a recombinant protein corresponding to the N-terminal 135 residues. Subsequent studies showed that the deletion of just the N-terminal tail (Δ 2-26) had the same effect as deletion of M1 to K135 suggesting that it is the N-terminal tail rather than the PAS domain that is critical for the slow deactivation in hERG. In the previously solved crystal structure of the hERG PAS domain, the N-terminal tail (M1 to Q25) was disordered.

In this study, we have determined the structure of the PAS domain including the N-terminal tail using NMR spectroscopy. The NMR ensemble is very similar to the crystal structure except it exhibits an additional flexible N-terminal helix (T13 to E23). The functional role of this N-terminal helix is being explored through site-directed mutagenesis and two-electrode voltage clamp of *Xenopus* oocytes, which express the mutant hERG channels. Preliminary results show that this N-terminal helix is functionally important, in particular, T13A and D16A slow deactivation while F14A and R20A exhibit a faster deactivation compare to WT. Further investigation using a GGGS linkers displacement of the N-terminal helix shows a fast deactivation resembling the Δ 2-26 hERG, indicating this N-terminal helix plays a role of positioning the first 9 residues in a correct orientation to regulate deactivation of the channels.

Kinetics of glucose transport across the surface membranes of single fast- and slow-twitch muscle fibres of the rat

H.A. Rudayni, G. S. Posterino and D.G. Stephenson, Department of Zoology, School of Life Sciences, Faculty of Science and Technology, La Trobe University, VIC 3086, Australia.

Glucose is an essential substrate for muscle metabolism. It is transported across the surface membranes by members of a family of specialized proteins, known as glucose transporters (GLUTs). Currently there is no simple technique for directly measuring the kinetics of glucose transport across the surface membranes of muscle fibres, because intracellular glucose can neither be directly measured nor realistically calculated with sufficient accuracy in whole body or whole muscle experiments. The aim of this study was to develop a technique for directly measuring the uptake of a fluorescent glucose analog (2-(N-(7-nitrobenz-2-oxa-1,3-diazol-4-yl) amino)-2-deoxyglucose, 2-NBDG (Yoshioka *et al.*, 1996)) across the surface membrane of single muscle fibres.

All experiments were approved by the La Trobe University Animal Ethics committee. Adult male rats (Long-Evans hooded) were killed by deep anesthesia with isoflurane (4% v:v) and the *extensor digitorum longus* (EDL, predominantly fast-twitch) and *soleus* muscles (predominantly slow-twitch) were rapidly dissected, blotted dry on filter paper and then were pinned in a Petri dish under paraffin oil at resting length. Segments of single muscle fibres with intact surface membranes were isolated under a dissecting microscope. The ends of the fibre segments were carefully tied with fine surgical thread (Decknatel 10.0) while still immersed in paraffin oil and the preparation was transferred to a well made out of Bipax epoxy resin on a glass cover slip filled with paraffin oil which was placed on the stage of a fluorescence microscope. A droplet of modified physiological saline (MPS; mM: NaCl, 145 when no glucose was present and 135 with glucose; KCl, 3; MgCl₂, 3.5; HEPES, 10; EGTA, 2 and glucose, 0 or 20) containing 50 μM 2-NBDG, was also placed under oil on the cover slip and the preparation was incubated for known periods of time in this droplet, followed by a brief wash in a MPS droplet without 2-NBDG. The preparation was then carefully placed on the bottom of the cover slip and the fluorescence signal (450-480nm excitation/ 500nm dichroic mirror/ 510-530nm emission) was measured from a 70μm region in the middle of the preparation. The fibre segment was then returned to the 2-NBDG containing droplet and the cycle was repeated. The integrity of the surface membrane in the preparations was checked by blocking the GLUTs with cytochalasin B and the concentration of the 2-NBDG in the preparation was calibrated by measuring the 2-NBDG signal from Triton X-100 treated single fibre segments exposed to droplets of relaxing solution (mM: K⁺, 126; Na⁺, 36; EGTA, 50; total ATP, 8; creatine phosphate (CP), 10; free Mg²⁺, 1; HEPES, 90; pH 7.10; pCa (-log₁₀ [Ca²⁺]), <9.0) containing 2-NBDG. The 2-NBDG uptake curves could be well fitted by the expression $A(1-\exp(-kt))$, where A is the final [2-NBDG] in the fibre, k is the rate constant and t is time and the rate of 2-NBDG uptake was calculated assuming a cylindrical shape of the fibre segment. Equilibrium was effectively reached in less than 2 min in both EDL and *soleus* fibres.

In the presence of 50 μM 2-NBDG and in the absence of glucose, the basal rate of 2-NBDG uptake was 8.7 ± 2.5 pmol/cm²/s (n = 4) in the *soleus* and 5.3 ± 1.3 pmol/cm²/s (n=3) in the EDL fibres. Addition of 20 mM glucose to the 50 μM 2-NBDG MPS reduced the uptake rates of 2-NBDG by a factor of 3.5 in *soleus* fibres (2.5 ± 0.6 pmol/cm²/s, n=3) and by half in EDL fibres (2.6 ± 1.0 pmol/cm²/s, n=3). This corresponds to an average GLUTs dissociation constant for glucose of about 7.9 and 12.6 mM for the *soleus* and EDL fibres, respectively. Using these values, the projected maximum rates of basal glucose transport in the *soleus* and EDL fibres is similar (69.2 vs 66.8 pmol/cm²/s).

Yoshioka, K., Takahashi, H., Homma, T., Saito, M., Oh, K-B., Nemoto, Y., and Matsuoka., H. (1996). *Biochimica et Biophysica Acta* **1289**, 5-9.

Myotoxin induced regeneration of fast-twitch EDL skeletal muscles from aged mice results in fibre branching and increased susceptibility to dystrophic type eccentric damage

S.I. Head, A.S.J. Lee, A.J. Kee, P.W. Gunning and E.C. Hardeman, School of Medical Sciences, University of New South Wales, NSW 2052, Australia.

Duchenne muscular dystrophy is an X-linked recessive disorder characterized by progressive wasting of skeletal muscle. It is caused by the absence of dystrophin, a protein that, in normal muscle fibres, is located in close proximity to the internal face of the sarcolemma. Recent work from my laboratory carried out using aged mdx mice, which also lack dystrophin, has led to the proposal that it is the branched fibres, formed during the repeated bouts of regeneration, which are responsible for the terminal phase of muscle damage (Head, 2010; Chan, Head & Morley, 2007). In this hypothesis, damage results from the structural weakening of the muscle fibres at multiple branch points, and hence is not a primary consequence of the absence of dystrophin. In order to further test this hypothesis myotoxin (notexin) was used to induce injury in EDL muscles from aged (28 months old female C57BL6) WT mice. The resulting regenerated muscles contained “dystrophin positive” branched fibres. Mice were anaesthetised with a mixture of Ketamine (0.1 mg/g) and Xylazine (20 µg/g), a 1 cm incision on the lateral side of both hindlimbs was made to expose EDL. Notexin (0.2 µg) was injected intramuscularly into one EDL muscle, the contralateral EDL served as a control. Animals were allowed to recover for 21 days with daily monitoring and analgesic care. Post recovery the animals were killed with halothane and the EDL removed and attached to a force transducer (approved UNSW ethics). After the contractile analysis the muscle was detached from the force transducer, weighed and processed for histology. Single EDL muscle fibres were enzymatically isolated using 3mg/ml collagenase Type I (Sigma), and suspended in a relaxing solution containing 50mM EGTA in order to view individual fibres. 38% (n=3) of the regenerated fibres had branches while only 2% (n=3) of the control fibres had a small degree of branching. The regenerated muscles were significantly heavier than the contralateral muscle, 11.9mg ± 0.8 vs 9.8mg ± 0.2, absolute force was significantly larger in the regenerated muscle, 169mN ± 8 vs 145mN ± 8 while there was no significant difference in specific force 230mN/mm² ± 15 vs 231mN/mm² ± 14, (all case n=10 with means ± SEM & t-test). A lengthening/eccentric contraction was performed three times, at intervals of 5 min with a strain of 33% of fibre length. Regenerated muscles has a significant force deficit of 11% ± 3 (n=3), the force from control muscles was not affected (n=3). This study shows that notexin induced regeneration produces muscles that contain a population of branched fibres, the regenerated muscles have normal contractile properties and an increased susceptibility to eccentric damage. I propose that this increase in susceptibility to mild eccentric damage is the result off the presence of regenerated branched fibres within the muscle.

Head SI (2010). Branched fibres in old dystrophic mdx muscle are associated with mechanical weakening of the sarcolemma abnormal Ca²⁺ transients and a breakdown of Ca²⁺ homeostasis during fatigue. *Experimental Physiology* **95**, 641-56.

Chan S, Head SI, Morley JW (2007). Branched fibers in dystrophic mdx muscle are associated with a loss of force following lengthening contractions. *American Journal of Physiology. Cell Physiology* **293**, C985-92.

Identifying the skeletal muscle ryanodine receptor activation domain of triadin

E. Wium, A.F. Dulhunty and N.A. Beard, John Curtin School of Medical Research, Australian National University, ACT 0200, Australia.

Muscle function is influenced by Ca²⁺ handling proteins in the sarcoplasmic reticulum (SR) of muscle fibres. One such protein is the skeletal muscle ryanodine receptor type 1 (RyR1), a ligand gated Ca²⁺ release channel. This channel is regulated by a variety of SR luminal proteins including the Ca²⁺ binding protein calsequestrin (CSQ1) and two associated transmembrane proteins, triadin and junctin. While triadin was initially believed to be an anchoring protein which tethered CSQ1 to the RyR1, it has recently become apparent that it plays a larger role in RyR1 regulation. Triadin's luminal interaction with the RyR1 leads to an enhancement of channel activity, and three discrete regions of its luminal tail have been found to bind to RyR1 (Caswell *et al.*, 1999; Lee *et al.*, 2004). To identify whether one of these regions alone can regulate RyR1, we synthesized a peptide containing amino acids 200-232 of rabbit skeletal muscle triadin. We then determined its physical and functional interactions with purified RyR1s isolated from the skeletal muscle of euthanized rabbits (Wei *et al.*, 2009).

Using affinity chromatography, we confirmed that the 200-232 triadin peptide bound to RyR1s in solution. Functional studies confirmed that the peptide had more than just a physical interaction with RyR1. This was shown through [³H]ryanodine binding assays, where the amount of [³H]ryanodine binding to RyR1 is directly proportional to channel activity. Incubation of RyR1 with the peptide increased [³H]ryanodine binding ~1.7-fold, indicating that RyR1 activity is increased in the presence of the peptide. A similar effect was observed in lipid bilayer experiments where the current passing across a single channel is monitored in real-time. Purified RyR1s reconstituted in artificial lipid bilayers showed a significant ~1.8-fold increase in open probability when their luminal sides were exposed to peptide, relative to before peptide addition. As the effect of the peptide mimics the increased RyR1 activity induced by full-length triadin (Goonasekera *et al.*, 2007; Wei *et al.*, 2009), it appears that residues 200-232 of triadin are sufficient to replicate RyR1 regulation by full-length triadin.

The triadin sequence of this peptide was postulated to align as a β -strand *in vivo* to facilitate the RyR1-triadin interaction (Kobayashi *et al.*, 2000). To discover whether this structural element was important for RyR1 regulation and whether all residues in the peptide were necessary for RyR1 regulation, the experiments were repeated with a series of mutant peptides. When eight residues predicted to line up along one side of the putative β -strand were mutated to alanines, the peptide did not bind to or activate the RyR1. The mutations caused little change to the already disordered structure of the WT peptide, suggesting the residues themselves, not their structure, were essential for RyR1 regulation. As the RyR1 residues critical for Trisk95 binding are acidic (Lee *et al.*, 2004; Goonasekera *et al.*, 2007), it seemed likely that the basic residues on triadin would form charged-pair interactions with the RyR1. When only five basic residues in this region were mutated, the peptide similarly did not bind to RyR1 or regulate the channel. Therefore all or several of these five basic residues are critical for allowing Trisk95 to modulate RyR1 activity.

Caswell AH, Motoike HK, Fan H & Brandt NR. (1999). *Biochemistry* **38**, 90-97.

Goonasekera SA, Beard NA, Groom L, Kimura T, Lyfenko AD, Rosenfeld A, Marty I, Dulhunty AF & Dirksen RT. (2007). *Journal of General Physiology* **130**, 365-378.

Kobayashi YM, Alseikhan BA & Jones LR. (2000). *Journal of Biological Chemistry* **275**, 17639-17646.

Lee JM, Rho SH, Shin DW, Cho C, Park WJ, Eom SH, Ma J & Kim DH. (2004). *Journal of Biological Chemistry* **279**, 6994-7000.

Wei L, Gallant EM, Dulhunty AF & Beard NA. (2009). *International Journal of Biochemistry and Cell Biology* **41**, 2214-2224.

Possible contribution of SPRY2 and ASI regions of RyR1 to interdomain interaction

H. Willemse, S. Mirza, E.M. Gallant, H.S. Tae, L. Wei, M.G. Casarotto, R.T. Dirksen and A.F. Dulhunty, John Curtin School of Medical Research, Australian National University, ACT, 0200, Australia.

Excitation-contraction (EC) coupling is the process that links an action potential to muscle contraction. A physical interaction between the surface membrane Ca^{2+} channel, the dihydropyridine receptor (DHPR), and the sarcoplasmic reticulum (SR) ryanodine receptor (RyR1) Ca^{2+} release channel facilitates skeletal muscle EC coupling. However, the mechanism and sites of interaction between the DHPR and RyR1 are not understood. RyR1 contains 3 SPRY domains in the N-terminal one third of each of its four subunits. Generally, SPRY domains function as protein-protein interaction domains and were identified in *Dictyostelium discoideum* tyrosine kinase spore lysis A (SplA) and the mammalian RyR. The 2nd of the 3 domains (SPRY2, S¹⁰⁸⁵-V¹²⁰⁸) overlaps with the part of the RyR1 that support skeletal EC coupling and is a binding partner for the N-terminal residues in the II-III loop of the α_{1s} subunit of the DHPR as well as Imperatoxin A (IpTxA). As IpTxA and the II-III loop peptide increase the activity of RyR1 channels isolated from rabbit skeletal muscle, SPRY2 may contribute to an inhibitory regulatory module within the RyR1.

The SPRY2 domain may bind to a region within RyR1 which contains residues that exhibit close structural and functional similarity to the DHPR II-III loop N-terminal residues. This region (T³⁴⁷¹-G³⁵⁰⁰) contains the alternatively spliced (ASI) residues (D³⁴⁸³-G³⁴⁸⁷), present in the adult RyR1 (ASI(+)-RyR1) but excluded from the juvenile ASI(-)-RyR, and a neighbouring basic sequence. ASI(-)-RyR1 is upregulated in adults with myotonic dystrophy (Kimura *et al.* 2005). The ASI residues contribute to a regulatory module in the RyR1 and mutations of these residues or the adjacent basic residues affect skeletal EC coupling (Kimura *et al.* 2007; Kimura *et al.* 2009; Cheng *et al.* 2005). The positively charged residues in the ASI/basic region are aligned along one surface of an α -helix (Kimura *et al.* 2009). As a negatively charged F loop of the SPRY2 domain between residues P¹¹⁷⁰-A¹¹²¹ bind to the ASI/basic region (unpublished), these regions may interact to form the inhibitory module that is disrupted by IpTxA DHPR II-III loop N-terminal residue binding to the ASI/basic region. (Kimura *et al.* 2009). We predict that there may be different interactions between the F loop and ASI(-)-RyR1 and that mutation of residues in the F-loop that bind to the ASI/basic region would prevent endogenous F-loop binding to the ASI region. To test this hypothesis, we have first established that the characteristics of the interaction between the F-loop peptide and the recombinant RyR1.

Rabbit ASI(-)-RyR1 was expressed in HEK293 cells. Cells were harvested 48h after transfection, homogenised, ASI(-)-RyR1 partially purified and incorporated into an artificial lipid bilayer (phosphatidylethanolamine: phosphatidylserine: phosphatidylcholine; 5:3:2) with symmetrical 250mM cesium methanesulphonate solutions with 100nM cytoplasmic Ca^{2+} and 1mM luminal Ca^{2+} .

ASI(-)-RyR1 expressed well and was visualised on Western Blots at the expected 500kDa. When incorporated into bilayers it had a single channel conductance of 364 ± 20 pS. The relative open probability after adding $1 \mu\text{M}$ F-loop peptide was 2.8 ± 0.3 times greater than control, or after adding $100 \mu\text{M}$ F-loop peptide fell to 0.56 ± 0.07 . These changes in P_o are similar to changes recorded in RyR1 from rabbit skeletal muscle. The action of the F loop peptide on a mutant ASI(-)-RyR1 in which three residues in the F loop of the SPRY2 domain that bind to the isolated ASI region have been mutated will be examined next to test the prediction that the F loop peptide will either not affect the mutant RyR1, or will inhibit rather than activate the channel.

Cheng W, Altafaj X, Ronjat M, Coronado R (2005). *Proceedings of the National Academy of Sciences of the United States of America* **102**, 19225-19230.

Kimura T, Nakamori M, Lueck JD, Pouliquin P, Aoike F, Fujimura H, Dirksen RT, Takahashi MP, Dulhunty AF (2005). *Human Molecular Genetics* **14**, 2189-2200.

Kimura T, Pace SM, Wei L, Beard NA, Dirksen RT, Dulhunty AF (2007). *Biochemical Journal* **401**, 317-324.

Kimura T, Lueck JD, Harvey PJ, Pace SM, Ikemoto N, Casarotto MG, Dirksen RT, Dulhunty AF (2009). *Cell Calcium* **45**, 264-274.

***In vitro* interactions between C-terminal residues of the β_{1a} subunit of DHPR and RyR1 from skeletal muscle**

R.T. Rebeck, Y. Karunasekara, E. M Gallant, N.A. Beard, M.G. Casarotto and A.F. Dulhunty, Department of Structural Biology, John Curtin School of Medical Research, Australian National University, P.O. Box 334, Canberra, ACT 2601, Australia.

Excitation-contraction (EC) coupling is the process which links the excitatory action potential to contraction of the muscle. Essential to this process in skeletal muscle is the interaction between two calcium channels: the L-type voltage gated dihydropyridine receptor (DHPR) located in the transverse tubule and the ryanodine receptor (RyR1) located in the sarcoplasmic reticulum (SR). This interaction between the two channels triggers SR Ca^{2+} release through the RyR1, which raises cytosolic $[\text{Ca}^{2+}]$ from ~100 nM to 1-10 μM and enables contraction. The physical components of this channel-to-channel interaction are yet to be elucidated.

The last 35 C-terminal residues (V490-M524) and a hydrophobic heptad repeat motif (L478, V485 and V492) of the β_{1a} subunit of the DHPR have been shown to play an important role in EC coupling (Beurg *et al.* 1999; Sheridan *et al.*, 2004). However, the importance of the heptad repeat in EC coupling is controversial as Dayal *et al.* (2010) has recently shown that expression of a heptad repeat mutant (L478A, V485A, V492A) only slightly hinders EC coupling in a β_{1a} -null zebrafish model. Our aim was to investigate the functional and physical interaction between RyR1 and two 35 residue peptides: β_{1a} C-tail peptide, corresponding to the last 35 C-terminal residues of the β_{1a} subunit, (V490-M524; which contains only one of the hydrophobic residues in the heptad repeat) and β_{1a} A474-A508 peptide, which contains the full heptad repeat.

New Zealand rabbits were euthanized by captive bolt. Fractions of SR membrane, containing native RyR1, were collected from rabbit back and leg muscle by gradient centrifugation. RyR1 was purified by solubilising the SR and further gradient centrifugation. The physical interaction between RyR1 and the biotinylated β_{1a} peptides was investigated using streptavidin-agarose affinity chromatography. The functional action of β_{1a} peptides on RyR1 were measured by reconstituting RyR1 into artificial lipid bilayers and assessing channel response to peptide addition, and with [^3H]ryanodine binding.

We show that native and purified RyR1 bound to both β_{1a} peptides. As a functional consequence of the physical interaction between RyR1 and β_{1a} C-tail peptide, RyR1 activity increased 2 to 3-fold in the presence of the β_{1a} C-tail peptide (100 pM to 500 nM). Consistently, the β_{1a} peptide significantly increased [^3H]ryanodine binding to native RyR1 at Ca^{2+} concentrations between 1 and 10 μM . Significantly, there was also a 2-fold increase in native RyR1 activity in the presence of 10 and 100 nM β_{1a} A474-A508 peptide. These results demonstrate that the C-terminus of the β_{1a} subunit can modulate RyR1 activity by directly binding to the RyR1 and that the heptad repeat is not crucial for the functional interaction between the DHPR and RyR1. Preliminary data however indicate that three hydrophobic residues located along one surface of an α -helix between L496 and W503 are essential for the action of the C-tail peptide on RyR1 channel activity. Overall, the results suggest that through its C-terminus, the β_{1a} subunit modulates RyR1 activity under Ca^{2+} concentrations that occur in skeletal muscle fibres during EC coupling, but that the heptad repeat is not essential for this regulation.

Beurg M, Ahern CA, Vallejo P, Conklin MW, Powers PA, Gregg RG and Coronado R. (1999) *Biophysical Journal* **77**: 2953-2967.

Dayal A, Schredelseker J, Franzini-Armstrong C and Grabner M. (2010) *Cell Calcium* **47**: 500-506.

Sheridan DC, Cheng W, Carbonneau L, Ahern CA and Coronado R. (2004) *Biophysical Journal* **87**: 929-942.

GSTM2-2 C terminus modulates the contractility of cultured rat ventricular cardiomyocytes

R.P. Hewawasam, M.G. Casarotto, P.G. Board and A.F. Dulhunty, Department of Structural Biology, John Curtin School of Medical Research, Australian National University, GPO Box 334, Canberra, ACT 2601, Australia.

The ryanodine receptor (RyR) functions as an ion channel that releases Ca^{2+} from the sarcoplasmic reticulum and is essential for excitation-contraction coupling and contraction in striated muscle. In previous studies we have shown that the human muscle specific glutathione transferase M2-2 (GSTM2-2) is a high affinity inhibitor of cardiac muscle ryanodine receptors (RyR2) and a weak activator of skeletal muscle ryanodine receptors (RyR1) (Abdellatif *et al.*, 2007). Excessively active RyR channels are partly responsible for low store Ca^{2+} levels and defective release in heart failure. Therefore, inhibition of RyR2 is a potential strategy for the treatment of heart failure. GSTM2-2 is one of the few selective inhibitors of RyR2 that does not influence skeletal muscle RyR activity. Single channel lipid bilayer experiments and Ca^{2+} release assays conducted on the C-terminal half of GSTM2-2(GSTM2C) and the mutants, F157A and Y160A in the C terminal domain confirmed the importance of the helix 6 in the C-terminal fold for the inhibition of RyR2 (Hewawasam *et al.*, 2010). It has been reported in a qualitative study that a glutathione transferase from *Schistosoma japonicum* (Sj.GST26) can be internalised from the medium into a variety of mammalian cell types (Namiki *et al.*, 2003). Morris *et al.* (2008) also reported that proteins including GSTM2-2 containing a GST fold structure are efficiently internalized by L-929 cells. Therefore, the objective of this study was to confirm the fact that GSTM2C is capable of internalising into cultured cardiomyocytes and to determine the effect of GSTM2C on the cardiac function.

The study was performed on primary cardiomyocyte cultures from neonatal rats. Cells were seeded at a density of 1×10^5 cells per 35mm dish and used 2-3 days after plating. $1 \mu\text{M}$ GSTM2C tagged with oregon green dye was incubated with cultured cardiomyocytes for 24h and immunostained with anti α -actinin, which specifically stains α cardiac/skeletal actinin. Optical fields were randomly chosen and observed to ascertain the occurrence of spontaneous beats. Beating frequency and number of beating cells were counted from the control and $1 \mu\text{M}$ GSTM2C treated cells. Cell beating was recorded in both control and GSTM2C treated cells using a JVC video camera KY/F550 attached to Nikon TE2000-U microscope. Images were analysed using Image Pro plus 6.2 software and percentage cell shortening measured.

Confocal images of the cardiomyocytes stained with Oregon green-GSTM2C and anti α -actinin confirmed the uptake of GSTM2C into the cultured cardiomyocytes. A preliminary study showed that the beating frequency (contractions per min) in the control group was reduced significantly from 42.5/min to 6.9/min in the GSTM2C treated cells ($p < 0.001$). The number of spontaneously beating cells observed in the control group, 6.6%, was also significantly reduced to 1.9% ($p < 0.001$) in the drug treated group. In order to determine whether the above result is due to action potential failure or GSTM2 C terminus affecting the contraction mechanism, the degree of shortening in each beat was measured. The percentage shortening was significantly reduced from $7.5 \pm 1.0\%$ in the control group of cardiomyocytes to $2.9 \pm 0.6\%$ after GSTM2C treatment ($p < 0.001$), consistent with GSTM2C reducing Ca^{2+} release from the SR.

In conclusion, our results indicate that GSTM2 C terminus enters cardiomyocytes and alters the cardiac function by reducing Ca^{2+} release through RyR2 in ventricular cardiomyocytes.

Abdellatif Y, Liu D, Gallant EM, Gage PW, Board PG & Dulhunty AF. (2007) *Cell Calcium* **41**: 429-40.

Hewawasam R P, Liu D, Casarotto M G, Dulhunty AF, Board PG. (2010) *Biochemical Pharmacology* **80(3)**: 381-88.

Morris MJ, Craig SJ, Sutherland TM, Board PG, Casarotto MG (2009) *Biochimica et Biophysica Acta* **1788(3)**:676-85.

Namiki S, Tomida T, Tanabe M, Lino M, Hirose K (2003) *Biochemical and Biophysical research communications* **305**: 592-97.

Effects of membrane cholesterol depletion on excitation-contraction coupling in mammalian skeletal muscle

A.J.H. Hewson and B.S. Launikonis, School of Biomedical Sciences, The University of Queensland, Brisbane, QLD 4072, Australia.

Cholesterol in the lipid bilayer of plasma membranes is present in relatively large proportions compared to the internal membranes of eukaryotic cells. Its presence affects the biophysical properties of the membrane-embedded proteins. An excellent membrane signaling system to study the effects of membrane cholesterol is excitation-contraction coupling (EC coupling). This involves transduction of electrical signals throughout the sarcolemma and its invagination into the cell, the tubular (t-) system and the transduction of this signal to internal sarcoplasmic reticulum (SR) membrane for initiation of Ca^{2+} release. Therefore for functional EC coupling in skeletal muscle, Cl^- , K^+ , Na^+ and the voltage sensor must work at the level of surface membrane/t-system and Ca^{2+} release channels and Ca^{2+} pumps must work at the SR, two membranes with significantly different cholesterol contents. We aimed to assess the role of membrane cholesterol in these membranes by assessing the functionality of EC coupling after manipulating membrane cholesterol with methyl- β -cyclodextrin (M β CD) and saponin, agents that deplete membrane cholesterol and bind with membrane cholesterol and aggregate to form pores, respectively (Launikonis & Stephenson, 2001).

The Animal Ethics Committee at The University of Queensland approved the use of animals in this study. 2-3 mo old C57 mice and 2-3 mo old Wistar rats were killed by asphyxiation and the interossei and *extensor digitorum longus* (EDL) muscles were removed, respectively. Interossei fibres were transferred to a chamber with Na^+ -based physiological solution (with or without Cl^-) and either impaled with a glass microelectrode to measure resting membrane potential (V_m) with a GeneClamp 500 amplifier, or enzymatically dissociated and loaded with fura-2AM for imaging cytoplasmic Ca^{2+} on a Nikon wide-field fluorescence microscope equipped with a camera during field stimulation at 10 Hz with a pulse strength of ~ 30 V/cm for 0.5 ms. Intact EDL fibre bundles were exposed to a Na^+ -based physiological solution containing fluo-4 salt or fluorescein dextran. Fibres were mechanically skinned, trapping the dye in the t-system, and transferred to a chamber containing a K^+ -based internal solution. In some experiments, skinned fibres were bathed in an internal solution with 20 μM fluo-4 and release of SR Ca^{2+} was evoked by exposure to 30 mM caffeine. Fluo-4 or fluorescein dextran fluorescence signals were imaged on an Olympus FV1000 confocal microscope.

Treatment of skinned fibres with 10 mM M β CD for up to 10 min did not result in significant loss of fluorescence signal from the t-system ($n = 5$). Treatment of skinned fibres with 1 mg/ml saponin caused a rapid decline in fluorescence from the t-system due to creating cholesterol-dependent pores in the t-system ($n = 3$). The saponin-induced loss of t-system trapped dye was progressively reduced after 2 and 10 min pretreatment of the fibre with 10 mM M β CD ($n = 4$ each), indicating significant cholesterol is removed from the t-system by M β CD, without affecting t-system membrane integrity. Exposure of 10 mM M β CD to isolated intact fibres caused the formation of pores at the myotendon junction but not elsewhere in the preparation, as assessed by the loss of cytoplasmic fura-2. This may be a consequence of membrane weakening following collagenase treatment or a non-fluid nature of this section of membrane in these fibres. Assaying SR Ca^{2+} content with caffeine showed that 2 min treatment of the skinned fibre with 10 mM M β CD for 2 min reduced SR Ca^{2+} loading ability by about $60 \pm 6\%$ ($n = 10$). In a normal physiological solution, resting V_m initially hyperpolarized and then slowly depolarized in the presence of 30 mM M β CD over an hour ($n = 3$). In a Cl^- -free physiological solution, 30 mM M β CD caused a slow depolarization of the resting V_m over an hour ($n = 3$). Resting V_m remained relatively stable for more than an hour in the absence of M β CD ($n = 6$). Electrical stimulation of isolated intact fibres loaded with fura-2 induced partially fused Ca^{2+} transients that initially were potentiated by 2 or 3 mM M β CD and then declined within 1.5 and 4 min, respectively. These results suggest that depleting membrane cholesterol affects the function of t-system Cl^- and K^+ channels. An effect of membrane cholesterol manipulation on the t-system Na^+ channel and voltage-sensor cannot be excluded.

Launikonis BS, Stephenson DG (2001). Effects of membrane cholesterol manipulation on excitation-contraction coupling in skeletal muscle of the toad. *Journal of Physiology* **534**: 71-85.

The response of healthy and dystrophic mdx mouse muscle to prolonged elevations of cytoplasmic Ca²⁺

K.A. Burlinson and B.S. Launikonis, School of Biomedical Sciences, The University of Queensland, Brisbane, QLD 4072, Australia.

Duchenne Muscular Dystrophy (DMD) is the most common form of muscular dystrophy. It is caused by a mutation in the dystrophin gene resulting in the lack of the structural protein dystrophin. This results in numerous abnormalities in the dystrophic muscle, including the response of the membrane to stretch, calcium handling and the turnover of fibres within the skeletal muscle. A number of membrane proteins are responsible for shaping the Ca²⁺ transient in the cytoplasm. Therefore, with Ca²⁺ handling affected in dystrophic fibres, this signal can be different from that in healthy muscle fibres. This could lead to different downstream outcomes. We aimed to trigger a prolonged elevation of cytoplasmic Ca²⁺ in healthy and dystrophic muscle fibres, under different conditions, to observe the effect on the activation of signalling pathways by measuring cytoplasmic Ca²⁺ and observing membrane integrity and fibre status.

All experiments were approved by The Animal Ethics Committee at The University of Queensland. C57BL/10 (WT) and C57BL/10-mdx (mdx) mice were killed by asphyxiation following inhalation of CO₂. *Interossei* muscle from these mice were dissected out and individual fibres were enzymatically isolated. Selected isolated fibres were loaded with 10 μM Fura-2AM in a physiological solution and placed above a 20x objective of a Nikon inverted microscope in a customised experimental chamber with a glass coverslip as a base. The physiological solution used in experiments was either Na⁺ or K⁺-based, to polarise and depolarise the fibre, respectively, and had either 2 mM Ca²⁺ or was nominally Ca²⁺-free. Ca²⁺-free solution contained 1 mM EGTA and had raised Mg²⁺ from 1 to 3 mM. Cytoplasmic Fura-2 signals were collected from isolated fibres following excitation of the trapped dye with light at wavelengths of 340, 360 and 380 nm. Excitation wavelengths were generated in a Sutter DG4 monochromator that rapidly changed the pathway of light through the excitation filters. Light was passed through each excitation filter for <10 ms. Emitted light was collected by QuanTEM CCD digital camera and displayed on a computer monitor using MetaMorph software. Fura-2 was excited and fluorescence subsequently collected every 2 or 30 s during experiments. The ratio of the 340/380nm wavelengths was used to monitor cytoplasmic [Ca²⁺] and the 360nm wavelength (isosbestic point) was used to monitor [Fura-2] in the fibre. Calcium was leaked from the sarcoplasmic reticulum using the sarcoplasmic reticulum Ca²⁺-ATPase (SERCA) blocker cyclopiazonic acid (CPA).

In 0 Ca²⁺, K⁺-based solution, a 100 μM CPA treatment induced cell death observed as a hypercontracture or loss of cytoplasmic Fura-2 through a lysed surface membrane in 18 of 33 WT and 1 of 18 mdx fibres. In addition, all 5 mdx fibres survived exposure to 250 μM CPA. The cytoplasmic Ca²⁺ transient induced by the introduction of CPA did not appear to be different between the fibre types. In a Na⁺-based, 2 mM Ca²⁺ solution, the introduction of 50 μM CPA was sufficient to deplete the SR passed the activation threshold for store-operated Ca²⁺ entry (SOCE) in all 3 WT but not in all 3 mdx fibres. Store-operated Ca²⁺ entry was observed in all 4 mdx fibres when [CPA] was raised to 250 μM.

KAB was the Leonie Stanley Memorial Scholar of Muscular Dystrophy, Qld.

Muscle membrane permeability, damage and atrophy in Zucker obese rats

N. Capitanio,¹ E. Rybalka,¹ R. Murphy,² H. Latchman,² K. Croft³ and A. Hayes,¹ ¹Metabolism Exercise and Nutrition Unit, School of Biomedical and Health Sciences and Institute of Sport, Exercise science and Active Living (ISEAL), Victoria University, PO Box 14428, Melbourne City MC, VIC 8001, Australia, ²Department of Zoology, La Trobe University, La Trobe University, Melbourne, VIC 3086, Australia and ³Department of Medicine and the WA Heart Research Institute, University of Western Australia, Crawley, WA 6009, Australia.

Type 2 Diabetes (T2D) has a heterogeneous pathophysiology. Development of the disease is often related to the effects of an increase in fatty acid (FA) content. These include: 1) increased production of reactive oxygen species (ROS), and reduced antioxidant defences available (Johansen *et al.* 2005); 2) increase in inflammatory mediators leading to insulin resistance (Dandona, Aljada & Bandyopadhyay (2004) and apoptosis/necrosis (Shoelson, Herrero & Naaz, 2004); 3) reduced membrane fluidity which inhibits mitochondrial function (Lamson & Plaza, 2002); and 4) altered sarcoplasmic reticulum function (Eibschutz *et al.*, 1984; Ganguly *et al.*, 1986). These defects can be damaging to muscle thereby reducing muscle mass, function and morphology. The amount of muscle damage is examined with the use of a fluorescent dye known as Evans Blue Dye (EBD), which permeates any damaged or leaky tissue, thus exhibiting higher fluorescence. As such, the aim of this study was to determine if there is more skeletal and cardiac muscle damage and atrophy in T2D muscles at rest compared to normal muscles, and whether this damage is associated with increased lipase and protease activity.

Twenty eight male Zucker rats (a widely-used model of T2D) at 14 weeks of age, comprising of 14 Zucker Obese rats (OBESE) and 14 Zucker Lean (LEAN) rats, were injected with 1% EBD 24 hours prior to sampling to allow absorption into muscle tissue. On the following day, animals were anaesthetised (Nembutal, 60 mg.kg⁻¹) and a portion of EDL (fast-twitch), *soleus* (slow-twitch), and cardiac muscles were removed, covered in O.C.T. compound and frozen in isopentane cooled with liquid nitrogen, for later histological analysis of muscle damage and atrophy. The remainder of the muscles were immediately snap frozen in liquid nitrogen and stored at -80°C for later isoprostane (marker lipase-induced membrane breakdown) and calpain (marker of proteolysis) analyses.

Overall, OBESE rats had a significantly higher amount of muscle exhibiting EBD fluorescence than LEAN littermates in EDL and *soleus* ($p < 0.01$), and cardiac ($p < 0.05$) muscles. In addition, the fluorescent intensity was also shown to be significantly higher in EDL and cardiac muscle of OBESE rats ($p < 0.05$), with a trend in *soleus* muscle of OBESE rats ($p = 0.06$). Absolute and relative (per body weight) muscle masses were significantly lower in EDL and *soleus* ($p < 0.05$) of OBESE animals, concomitant with lower fibre area ($p < 0.05$). Cardiac muscle mass was significantly higher in OBESE rats ($p < 0.05$), but when taken as a percentage of total body weight, it was significantly lower than the LEAN group ($p < 0.01$). Despite the lower mass and higher muscle damage and/or membrane leakiness as shown by EBD fluorescence, no differences were observed in markers of necrosis as indicated by the presence of non-membrane bound nuclei, isoprostane production, or in μ -calpain, and calpain-3. Interestingly, total arachidonic acid content (a key component of plasma membranes) was found to be significantly lower in the EDL and *soleus* muscles of the OBESE animals ($p < 0.05$), but not in cardiac muscle.

In conclusion, this study showed that resting muscles from T2D rats exhibit higher skeletal and cardiac muscle damage and atrophy, which cannot be attributed to isoprostane production, inflammation or calpain activation.

Johansen JS, Harris AK, Rychly DJ, Ergul A. (2005). *Cardiovascular Diabetology* **4**(1), 5-16.

Dandona P, Aljada A, Bandyopadhyay A. (2004). *Trends in Immunology* **25**(1), 4-11.

Shoelson SE, Herrero L, Naaz A. (2007). *Gastroenterology* **132**(6), 2169-2180.

Lamson DW, Plaza SM. (2002). *Alternative Medicine Review*, **7**(2), 94-111.

Eibschutz B, Lopaschuk GD, McNeill JH, Katz S. (1984). *Research Communications in Chemical Pathology and Pharmacology*, **45**(2), 301-304.

Ganguly PK, Mathur S, Gupta MP, Beamish RE, Dhalla NS. (1986). *American Journal of Physiology*, **251**(14), E515-E523.

Stimulating the Notch signalling pathway does not improve muscle regeneration after myotoxic injury in dystrophic mice

J.E. Church,¹ J. Trieu,¹ A.P. Russell² and G.S. Lynch,¹ ¹Basic and Clinical Myology Laboratory, Department of Physiology, The University of Melbourne, VIC 3010, Australia and ²School of Exercise and Nutrition Sciences, Deakin University, 221 Burwood Highway, Burwood, VIC 3125, Australia.

Duchenne muscular dystrophy (DMD) is the most severe of the muscular dystrophies, affecting 1 in 3,500 live male births, and characterised by chronic muscle fibre degeneration and increasingly ineffective regeneration which results in fibrotic tissue infiltration and leads to major functional impairments. The Notch signalling pathway is a central regulator of development, and participates in regulation of myogenesis both in the embryo and postnatally following injury (Conboy *et al.*, 2002). Stimulation of the Notch signalling pathway has previously been shown to improve muscle regeneration in aged animals (Conboy & Rando, 2003). The present study sought to test the hypothesis that stimulation of the Notch signalling pathway would have a similarly beneficial effect on muscle regeneration in dystrophic mice.

Male C57BL/10 or *mdx* dystrophic mice (8-9 weeks) were used in these experiments. Briefly, mice were anaesthetised (ketamine 80 mg/kg and xylazine 10 mg/kg; *i.p.*) and the *tibialis anterior* (TA) muscle of the right hindlimb was injected with Notexin (1 µg/ml, *i.m.*) to cause complete muscle fibre degeneration. After 3 days, the mice were given a single intramuscular injection of either saline, a Notch antibody (to activate Notch signalling), a Jagged-Fc fusion protein (to inhibit Notch signalling), or their respective controls (Hamster IgG as a control for the Notch antibody and human Fc protein as a control for Jagged-Fc). Mice were then allowed to recover for a further 4 or 11 days (corresponding to 7 and 14 days post-injury). At these times, mice were anaesthetised (60 mg/kg, sodium pentobarbital, *i.p.*) and TA muscle function was assessed *in situ* using methods described previously (Gehrig *et al.*, 2010). Mice were killed at the end of the experiment by cardiac excision while still anaesthetized deeply.

We found that neither activation nor inhibition of Notch signalling at 3 days post-injury had any significant effect on force production by the regenerating muscles of either BL/10 or *mdx* mice when measured at 7 or 14 days post-injury. We then examined the effect of a single intramuscular injection of the Notch antibody (an activator of the signalling pathway) on muscle function in the *dko* mouse (a mouse model of muscular dystrophy with a more severe phenotype matching that of DMD patients). When muscle function was assessed 3 days after injection, force production was reduced significantly in the antibody-treated mouse compared with control ($p < 0.05$).

These results suggest that, contrary to our hypothesis, activating the Notch signalling pathway in injured muscles of C57BL/10 or *mdx* mice does not improve muscle regeneration, and that activating the pathway in a severely dystrophic but otherwise uninjured *dko* mouse actually reduces muscle function. These findings reflect the complex and progressive nature of the muscle wasting in muscular dystrophy, and indicate that the continuous cycles and heterogeneous nature of the degeneration and regeneration of muscle fibres in DMD will be a significant barrier for therapeutic modulation of developmental signalling pathways.

Conboy IM, Conboy MJ, Smythe GM & Rando TA. (2003) *Science* **302**: 1575-1577.

Conboy IM & Rando TA. (2002) *Developmental Cell* **3**: 397-409.

Gehrig SM, Koopman R, Naim T, Tjoakarfa C & Lynch GS. (2010). *American Journal of Pathology* **176**: 29-33.

Supported by the NHMRC (project grant #566818)

Influence of *myo*-inositol on protein turnover in C₂C₁₂ myotubes

E. Zacharewicz and A.P. Russell, Deakin University, 221 Burwood Hwy, Burwood, VIC 3125, Australia.

Introduction: Muscle atrophy is a devastating condition present in numerous neuromuscular and chronic diseases (Skipworth *et al.*, 2006). Loss of muscle tissue leads to weakness, loss of independence, reduced response to chemotherapies and is used as a negative prognostic factor (Al-Majid & McCarthy, 2001; Andreyev *et al.*, 1998; Tisdale, 2002). Identifying therapeutic targets which reverse muscular atrophy and maintain muscle mass remain key research priorities. Recently *d*-*myo*-inositol-1,2,6-trisphosphate (α -trinositol, AT) has been shown to attenuate the loss of body mass in a MAC-16 tumour murine cachexia model, attenuate protein degradation in C₂C₁₂ myotubes and increase protein synthesis *via* upregulating the phosphorylation of mTOR and attenuating the autophosphorylation of eukaryotic initiation factor 2 α (eIF-2 α) (Russell *et al.*, 2009, Russell *et al.*, 2010). However, AT is not naturally present in mammalian tissue and furthermore its association with target molecules in the body has not yet been fully characterised. Naturally occurring *myo*-inositol (MI) is present in all mammalian and plant cells, is obtained from the diet and synthesised *de novo* by kidney cells (Clements & Darnell, 1980; Clements & Reynertson, 1977; Holub, 1986). To date, no study has looked at the role of natural MI on the regulation of protein turnover. Therefore the aims of the study were to investigate the role of MI on protein synthesis and degradation and Akt and eIF2 α phosphorylation under catabolic conditions in C₂C₁₂ myotubes. A secondary aim was to investigate the role of MI in C₂C₁₂ myoblast cell proliferation.

Methods: C₂C₁₂ myotubes were treated with the catabolic stimuli dexamethasone (DEX, 1 μ M) for 24 h and TNF α (50 ng/ml) for 2 and 24 h, in the presence and absence of MI (100 μ M). Protein synthesis was determined by the incorporation of ³H-tyrosine into myotubes. Protein degradation was determined by the release of ³H-tyrosine into the medium as a fraction of total ³H-tyrosine. The expression of the muscle specific atrophy genes, muscle atrophy F box (MAFbx/atrogen-1) and muscle RING finger 1 (MuRF-1) was determined by PCR. The expression of phosphorylated Akt and eIF2 α proteins, as well as atrogen-1 and MuRF-1 proteins was determined by western blot analysis. Myoblast proliferation was determined by the incorporation of 5-bromo-2-deoxyuridine (BrDU) into newly synthesised DNA during serum starvation, with and without MI (0-1000 μ M), and in the presence of TNF α (0-250 ng/ml).

Results: DEX decreased protein synthesis by 15% ($p < 0.001$) and increased protein degradation by 34% ($p < 0.001$). MI, either alone, or when combined with DEX, did not influence protein synthesis or protein degradation. MI decreased MuRF1 mRNA by 18%, when compared to basal conditions ($p < 0.05$). DEX increased atrogen-1 mRNA expression by 47%, when compared to basal levels; an effect attenuated by 44% ($p = 0.05$) with MI. TNF α treatment did not influence protein synthesis or degradation. However, TNF α treatment for 2 h decreased MuRF-1 mRNA by 30% ($p = 0.04$) and increased atrogen-1 mRNA expression by 90% ($p = 0.09$). MI, either alone, or when combined with TNF α , had no effect on MuRF-1 or atrogen-1 mRNA levels. TNF α and serum starvation decreased myoblast proliferation by 18% ($p < 0.01$) and 16% ($p < 0.001$), respectively. MI blocked the serum starvation ($p < 0.008$), but not the TNF α , reduction in proliferation.

Conclusion: These results show that natural MI does not influence protein synthesis or degradation. However, MI attenuates the DEX-induced up regulation of atrophy-gene expression in C₂C₁₂ myotubes. The measurement of atrogen-1, MuRF1, Akt and eIF2 α protein levels is currently being performed. MI may play a protective role in maintaining C₂C₁₂ myoblast proliferation during serum starvation.

Al-Majid, S & McCarthy, DO. (2001) *Biological Research for Nursing*, **2**: 155-166.

Andreyev, HJ, Norman, AR, Oates, J & Cunningham, D 1998. *European Journal of Cancer (Oxford, England: 1990)* **34**: 503-509.

Clements, RS, Jr. & Darnell, B (1980) *American Journal of Clinical Nutrition*, **33**: 1954-1967.

Clements, RS, Jr. & Reynertson, R (1977) *Diabetes*, **26**: 215-221.

Holub, BJ (1986) *Annual Review of Nutrition*, **6**: 563-597.

Russell, ST, Siren, PMA, Siren, MJ & Tisdale, MJ (2009) *Cancer Chemotherapy And Pharmacology*, **64**: 517-527.

Russell, ST, Siren, PMA, Siren, MJ & Tisdale, MJ (2010) *Experimental Cell Research*, **316**: 286-295.

Skipworth, RJE, Stewart, GD, Ross, JA, Guttridge, DC & Fearon, KCH (2006) *Surgeon*, **4**: 273-283.

Tisdale, MJ (2002) *Nature Reviews Cancer*, **2**: 862.

Does folic acid supplementation during pregnancy reduce skeletal muscle mitochondrial biogenesis and insulin signalling in adult offspring?

D.S. Hiam,¹ G.D. Wadley¹ and J.A. Owens,² ¹Centre for Physical Activity and Nutrition, School of Exercise and Nutrition Sciences, Deakin University, Burwood, VIC 3125, Australia and ²School of Paediatrics and Reproductive Health, University of Adelaide, SA 5001, Australia.

Background: Folic acid plays a significant role in the health of a foetus and is often supplemented to women during pregnancy to prevent neural tube defects such as *Spina Bifida* (Lucock & Yates, 2009). However, recent evidence suggests that high doses of folic acid supplementation (FAS) during pregnancy might permanently alter the skeletal muscle metabolism in adult offspring. Indeed, Owens *et al.* (2009) have found that high FAS during pregnancy increases insulin sensitivity in adult males but decreases insulin sensitivity in adult female offspring (Owens *et al.*, 2009). Mitochondria are crucial to skeletal muscle metabolism and impaired mitochondrial biogenesis (synthesis) is implicated in the aetiology of insulin resistance and type 2 diabetes (Liu *et al.*, 2009). Interestingly, Owens *et al.* also found decreased expression of genes involved in mitochondrial biogenesis, such as PGC-1 α , and genes involved in insulin signalling, such as Akt in the skeletal muscle of these FAS animals (Owens *et al.*, 2009). Therefore, it is possible that high dose folic acid supplementation during pregnancy could also down-regulate the protein expression of skeletal muscle mitochondrial biogenesis markers and insulin signalling proteins in the offspring.

Aims: To examine the long-term effects of high folic acid supplementation during pregnancy on the markers of mitochondrial biogenesis and insulin signalling proteins in the skeletal muscle of the adult offspring.

Methods: Pregnant rats received either a control diet containing a normal amount of folic acid (2mg/kg) or a FAS diet containing a high dose of folic acid (6mg/kg). At 90 days of age, the young adult offspring were given intraperitoneal injection of sodium pentobarbital (180 mg/kg body weight) and the skeletal muscle was dissected out and quickly frozen in LN₂ and stored at -80°C. Skeletal muscle was collected and markers of mitochondrial biogenesis, the levels of mitochondrial proteins and insulin signalling proteins were measured by western blotting.

Results: IRS-1 protein expression was 42% higher in male FAS offspring compared to the male Control offspring ($p < 0.05$). The protein abundance of other insulin signalling proteins, such as Akt was not altered in either sex following FAS. Furthermore, there were no other significant differences between FAS offspring and Control offspring in either sex for markers of mitochondrial biogenesis (PGC-1 α and Tfam) and the levels of mitochondrial proteins (COX IV and Cytochrome C).

Conclusions: The results indicate that young adult males whose mothers were exposed to high folate levels during pregnancy had increased expression of the insulin signalling protein IRS-1 in association with improved insulin sensitivity that has been previously reported (Owens *et al.*, 2009). However, exposure to high levels of folate during pregnancy does not appear to alter markers of mitochondrial biogenesis or mitochondrial proteins in the adult offspring of either male or female rats.

Liu, J, Shen, W, Zhao, B, Wang, Y, Wertz, K, Weber, P & Zhang, P (2009) Targeting mitochondrial biogenesis for preventing and treating insulin resistance in diabetes and obesity: Hope from natural mitochondrial nutrients. *Advanced Drug Delivery Reviews*, **61**, 1343-52.

Lucock, M & Yates, Z (2009) Folic acid fortification: a double-edged sword. *Current Opinion in Clinical Nutrition and Metabolic Care*, **12**, 555-64.

Owens, J, Kong, W, Grant, P, Moretta, S, De Blasio, M, Harland, M, Gatford, K, Robinson, J & Dziadek, M (2009) Maternal folic acid supplementation in the rat improves insulin sensitivity in adult male offspring but impairs that of female offspring. *Proceedings of the Perinatal Society of Australia and New Zealand meeting in Darwin, April 2009* 45.

The effect of taurine and β -alanine supplementation on taurine content and contractile properties of skeletal muscle in the mdx mouse

D.M. Horvath,¹ A. Hayes¹ and C.A. Goodman,² ¹School of Biomedical and Health Sciences, Victoria University, Melbourne, VIC 8001, Australia and ²Department of Comparative Bioscience, University of Wisconsin, Madison, WI 53706, USA.

The amino acid taurine (Tau) has been suggested as a possible beneficial compound in the treatment of Duchenne muscular dystrophy (DMD) due to its effects on multiple targets associated with DMD pathology. There is evidence that the mdx mouse (a model of DMD) has lower Tau levels compared to controls during degeneration and that increased Tau levels in skeletal muscle correlates with tissue repair and restoration of function (McIntosh *et al.*, 1998). β -alanine competitively inhibits Tau uptake and has been previously reported to decrease Tau in skeletal muscle by up to 50% in rats (Dawson *et al.*, 2002). This decrease was associated with impaired exercise tolerance and an increase in fatigue.

This study examined skeletal muscle taurine levels (*plantaris* and diaphragm) and contractile function (*extensor digitorum longus* (EDL)) of six month old male control (C57BL10) and mdx mice after 4 weeks of 3% taurine or 3% β -alanine supplementation *via* drinking water. Muscles tested were dissected out under anaesthesia (40-50mg/kg of Nembutal i.p.) in accordance with the approval granted from the Victoria University Animal Ethics Experimentation Committee. Contractile function including a fatigue protocol was assessed (30°C, 70Hz, 250ms for 1 min) as previously described (Hamilton *et al.*, 2006). Recovery post-fatigue was then followed for 1 hour and tetanic force measurements recorded at 1, 2, 5, 10, 20, 30, 45 and 60 minutes.

Four weeks of Tau or β -alanine supplementation significantly ($p < 0.05$) increased and decreased skeletal muscle Tau levels, respectively. β -alanine supplementation reduced fatigue ($p < 0.05$) in both control and mdx mice, however Tau showed a similar effect in the mdx muscles only. After 10 minutes of recovery mdx Tau supplemented muscles produced significantly more force ($p < 0.05$) than both the β -alanine and non-supplemented mdx groups. Taurine supplementation had no effect on the recovery of the control group. β -alanine supplementation improved recovery in the control mice up to 10 minutes with no significant difference between supplement groups observed after this time.

The findings suggest that taurine may be able to decrease fatigue and improve recovery in the mdx mouse.

Dawson Jr R, Biasseti M, Messina S, Dominy J. (2002) *Amino Acids* **22(4)**: 309-24.

Hamilton EJ, Berg HM, Easton CJ, Bakker AJ. (2006) *Amino Acids* **31(3)**: 273-8.

McIntosh LM, Garrett KL, Megeney L, Rudnicki MA, Anderson JE. (1998) *Anatomical Record* **252(2)**: 311-24.

The molecular architecture of the heart's conduction system in health and disease

M.R. Boyett and H. Dobrzynski, *Cardiovascular Medicine*, University of Manchester, 46 Grafton Street, Manchester, M13 9NT, UK. (Introduced by Yue-kun Ju)

The cardiac conduction system (CCS) acts as the heart's wiring system and is vital for the initiation and coordination of the heart beat (Boyett, 2009). The main tissues comprising the CCS are the sinoatrial node (the pacemaker of the heart), atrioventricular node (responsible for slow action potential conduction from the atria to the ventricles and, thereby, a delay between atrial and ventricular systole) and the His-Purkinje system (responsible for fast action potential conduction throughout the ventricles and, thereby, the synchronised contraction of the ventricles) - they were discovered in the late 19th and early 20th centuries. The electrical activity of the CCS is ultimately dependent on the expression of ion channels and, using quantitative PCR and immunohistochemistry, we are mapping the expression of ~80 ion channel subunits in the CCS (*e.g.* Chandler *et al.*, 2009). Unsurprisingly, the expression pattern is very different from that in the working myocardium, but appropriate to explain the electrical activity of the CCS. For example, pacemaking in the sinoatrial node can be explained by the poor expression of the background K⁺ channel, K_{ir}2.1, the expression of the pacemaker ion channel, HCN4, and perhaps the high expression of the low voltage-activated Ca²⁺ channels, Ca_v1.3 and Ca_v3.1; slow conduction through the atrioventricular node can be explained by the poor expression of the major Na⁺ channel, Na_v1.5, and the major gap junction channel, Cx43; fast conduction through the His-Purkinje system can be explained by the high expression of Na_v1.5 and expression of the large conductance gap junction channel, Cx40. The heart rate of the mouse is about 100× faster than that of the human and this can be explained by differences in ion channel expression: analysis suggests that channels carrying outward current are generally more highly expressed in the mouse sinoatrial node and this is expected to result in a shorter action potential (essential in the case of a higher heart rate) and channels carrying inward current are also generally more highly expressed in the mouse sinoatrial node and this may be responsible for the faster heart rate of the mouse.

There is dysfunction of the CCS in the aged heart, in heart failure (HF), atrial fibrillation and possibly diabetes (Boyett, 2009). For example, a substantial proportion (~16%) of HF patients die of bradyarrhythmias and there is dysfunction of all parts of the CCS in HF: there can be sinus bradycardia and prolongation of atrioventricular nodal conduction and heart block, and ~26% of HF patients have left bundle branch block. We and others are showing a widespread remodelling of ion channels in the CCS in heart failure – for example, in a rat model of heart failure (following pulmonary hypertension), 14 out of 21 transcripts for ion channels and related proteins were altered in the sinoatrial node (the CCS appears peculiarly sensitive to HF – for example, in this model only 4/21 transcripts were altered in the atrial muscle. The dysfunction of the CCS in disease is likely to be the result of the remodelling of ion channels - for example, the sinus bradycardia in HF and atrial fibrillation has been attributed to a downregulation of HCN4 in the sinoatrial node (Boyett, 2009). There is even evidence of 'dysfunction' in trained athletes: sinus bradycardia, prolongation of atrioventricular nodal conduction and heart block and incomplete right bundle branch block. The effects of athletic training have been attributed to 'high vagal tone', but there is no evidence for this and instead it is more likely to be the result of a remodelling of ion channels (Boyett, 2009). The CCS is more extensive than originally thought and specialised nodal-like tissue encircles the tricuspid and mitral valves, pulmonary artery and aorta and is potentially responsible for atrial tachycardias and ventricular outflow tract tachycardias (Boyett, 2009).

M.R. Boyett. (2009). 'And the Beat Goes On'. The cardiac conduction system: the wiring system of the heart. *Experimental Physiology* **94**, 1035-1049.

Chandler NJ, Greener ID, Tellez JO, Inada S, Musa H, Molenaar P, Difrancesco D, Baruscotti M, Longhi R, Anderson RH, Billeter R, Sharma V, Sigg DC, Boyett MR, Dobrzynski H. (2009). Molecular architecture of the human sinus node - insights into the function of the cardiac pacemaker. *Circulation* **119**, 1562-1575.

Distribution and functional role of IP₃R receptors in mouse sino-atrial node

Y.K. Ju, Department of Physiology (F13), University of Sydney, NSW 2006, Australia.

Inositol 1,4,5-trisphosphate receptors (IP₃Rs) have been implicated in the generation of cardiac arrhythmias, although the mechanism involved is unclear. In mammalian sinoatrial node (SAN), where the heart beat originates, the expression and functional role of IP₃Rs have not been investigated.

In order to determine whether SAN cells express IP₃Rs and their functional role in cardiac pacemaking, we used a range of techniques to study mRNA and protein expression and distribution. We first examined mRNA expression of *Ip₃rs*, *Hcn4*, *Ryr2* and *Stim1* genes across different regions of the mouse heart, including central SAN, peripheral SAN, AV node, atria and ventricle. We found that all three *Ip₃r* isoforms were expressed in the SAN and other regions of the heart. In contrast, *Hcn4* expression was highest in the central SAN and showed progressive reduction in peripheral SAN, AV node, atria and ventricle.

Whole mount SANs were co-labelled with Cx43 antibody and either IP₃R1 or IP₃R2 antibody. Cx43 antibody was used to distinguish central SAN from peripheral SAN. We found very weak labelling of IP₃R1 in the central SAN, identified by absence of Cx43. IP₃R1 labelling appeared in the peripheral SAN, especially in the interatrial septum, which also showed strong expression of Cx43. In contrast, the entire SAN, including the central and peripheral SAN and the surrounding atrial tissue, was uniformly labelled with IP₃R2 antibody. The results suggested that while the SAN expressed three IP₃Rs isoforms, IP₃R2 was the only protein isoform detected in the central SAN and isolated single pacemaker cells. We also found that Ca²⁺ sparks induced by membrane-permeable IP₃ (IP₃-BM) were predominately located near the sarcolemma (within 1.5 μm). The IP₃R agonist endothelin-1 (ET-1) induced sinoatrial arrhythmias as revealed by SAN electrical mapping. ET-1 and IP₃-BM increased intracellular Ca²⁺ and pacemaker firing rate whereas the IP₃R antagonist, 2-aminoethoxydiphenyl borate (2-APB), decreased Ca²⁺ and firing rate. Both of these effects were absent in SANs from IP₃R2 knockout mice. We estimate that the contribution of Ca²⁺ release from IP₃Rs to normal heart rate could be up to 14 % based on the spontaneous firing rate of isolated SANs from WT v. IP₃R2 KO mice. The results provided clear evidence that the heart rate modulated by ET-1 and 2-APB was *via* their interaction with IP₃Rs.

All animal experiments were approved by animal ethics committees of all listed research institutes. IP₃R2 knock out mice are gift from Dr. Ju Chen. The details of gene targeting and generation of IP₃R2-deficient mice were published previously (Li *et al.*, 2005).

Li X, Zima AV, Sheikh F, Blatter LA, Chen J. 2005) Endothelin-1-induced arrhythmogenic Ca²⁺ signaling is abolished in atrial myocytes of inositol-1,4,5-trisphosphate(IP3)-receptor type 2-deficient mice. *Circulation Research* **96(12)**: 1274-81.

This study was supported National Health and Medical Research Council of Australia (program grant 354400 and project grant 570926) and the Health Research Council of New Zealand.

Proteins in the lumen of the sarcoplasmic reticulum determine cardiac RyR channel activity, cardiac function and the structure of Ca²⁺ release units

A.F. Dulhunty and N.A. Beard, John Curtin School of Medical Research, Australian National University, PO Box 334, ACT 2601, Australia.

The activity of ryanodine receptor (RyR2) Ca²⁺ release channels in the intracellular sarcoplasmic reticulum (SR) Ca²⁺ store of cardiac myocytes must be low during diastole for efficient Ca²⁺ accumulation by the SR for release during systole and for appropriate lowering of cytoplasmic Ca²⁺. RyR2 channels become “leaky” in inherited and acquired disorders in which high cytosolic [Ca²⁺] during diastole leads to delayed after depolarisations (DADs) and arrhythmias (catecholaminergic polymorphic ventricular tachycardia (CPVT)). The “leaky” RyR can also deplete the SR Ca²⁺ store, reducing systolic Ca²⁺ release and cardiac output.

Low RyR2 activity during diastole in healthy myocytes is maintained by the integrated actions of ligands and associated proteins. Cytoplasmic proteins that depress RyR2 activity include members of the glutathione transferase family and the chloride intracellular channel protein, CLIC-2 (Hewawasam *et al.*, 2010). RyR2 channels are exquisitely sensitive to luminal [Ca²⁺]. However luminal proteins that influence the response of RyR2 to luminal Ca²⁺ and their binding sites on the minute luminal domain of RyR2 are only just being defined. The luminal proteins include the Ca²⁺ binding proteins calsequestrin (CSQ2) and the histidine rich protein (HRP) as well as the membrane spanning triadin and junctin, which bind to RyR2 and to CSQ2. Mutations in CSQ2 as well as RyR2 lead to DADs and CPVT. To understand how luminal factors regulate cardiac output, numerous transgenic models have been developed in which the luminal proteins have been knocked out, under expressed or over expressed (Knollman, 2009; Fan *et al.*, 2008). The general consensus is that none of the proteins is essential, *i.e.* animals survive with altered expression, but are often unable to cope with stress and develop CPVT. A major change with CSQ2 knockout is proliferation of the SR to maintain the Ca²⁺ store. The structure of the SR is also influenced by triadin and junctin expression. However the transgenic studies do not reveal the role of the targeted protein, how it interacts with RyR2 or the mechanisms that allow it to regulate RyR2 and Ca²⁺ release, because of the compensatory changes in SR structure and in expression of other proteins.

In contrast to the explosion in transgenic models, basic studies of the role of luminal proteins in cardiac SR function are few. This is also in contrast to extensive studies of interactions between the luminal proteins in skeletal muscle, albeit from only a handful of laboratories. A long held assumption, that we now believe is incorrect, is that the luminal proteins interact with RyR2 in the heart in the same way as they interact with RyR1 in fast-twitch skeletal muscle. As a consequence interactions between fast-twitch skeletal proteins have been extrapolated to the cardiac system, despite the fact that there are different isoforms of the RyR, CSQ and triadin in the two tissues and the demands on the Ca²⁺ store are vastly different. This is particularly true for CSQ, where the polymerization of the skeletal isoform dictates both Ca²⁺ binding capacity and its ability to influence RyR1 activity in response to changes in luminal [Ca²⁺]. Cardiac CSQ2 does not polymerize when exposed to physiological free [Ca²⁺] of ~1 mM and an ionic strength of ~150 mM, in contrast to CSQ1 which is mostly polymerized under these conditions (Wei *et al.*, 2009). In hindsight it was not surprising that we find that CSQ2 activates RyR2, while CSQ1 inhibits RyR1 (Wei *et al.*, 2009). Our preliminary evidence suggests that the interaction between junctin and RyR2 may also be isoform-specific. Our hypothesis is that CSQ2 acts to ensure strong Ca²⁺ release from cardiac SR with each heart beat, in contrast to its role in conserving the SR Ca²⁺ store in skeletal muscle for occasional maximal exertions.

Knollmann BC. (2009) *Journal of Physiology* **587**: 3081-3087.

Fan GC, Yuan Q, Kranias EG. (2008) *Trends in Cardiovascular Medicine* **18**: 1-5.

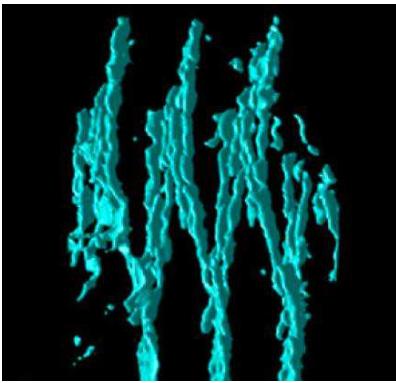
Wei L, Hanna AD, Beard NA, Dulhunty AF. (2009) *Cell Calcium* **45**: 474-484.

Hewawasam R, Liu D, Casarotto MG, Dulhunty AF, Board PG. (2010) *Biochemical Pharmacology* **80**: 381-388.

A new twist in cardiac muscle: dislocated and helicoid arrangements of myofibrillar z-disks in mammalian ventricular myocytes

M.B. Cannell, I.D. Jayasinghe, D.J. Crossman, D. Baddeley and C. Soeller, Department of Physiology University of Auckland New Zealand. (Introduced by Yue-Kun Ju)

The general structure of cardiac muscle cells has been established by light and electron microscopy for some time, but detailed information on 3D organization is less common as is the organization of proteins that enable high speed signal transduction to take place. To provide information for detailed modeling of cardiac cell function we have been examining the organization of myofibrils, sarcoplasmic reticulum, t-tubules and associated proteins by confocal fluorescence microscopy. These studies show that the basic 3D organization of the myofilaments is complex, with dislocations and helicoidal structures evident (see figure). Such a complex structure may arise during normal growth but it also has important implications for arrhythmogenesis *via* calcium wave propagation. While the sarcoplasmic reticulum calcium release channel (RyR) is generally close to z-lines and separated laterally by $\sim 0.6 \mu\text{m}$, the longitudinal separation should be set by the sarcomere length which is considerably longer $1.9\text{-}2.2 \mu\text{m}$. Therefore one would expect that a Ca wave would be able to propagate more easily in the transverse direction than longitudinally. However, it is well known that calcium waves propagate throughout the cell rather uniformly (*e.g.* Berlin, Cannell & Lederer, 1989). Our observation (Jayasinghe *et al.*, 2010) of dislocated z-lines that have RyRs associated with them helps explain this paradox; the dislocations coupled with the jitter in longitudinal RyR spacing will assist longitudinal calcium wave propagation.



For normal excitation-contraction coupling, calcium influx *via* l-type calcium channels (DHPRs) triggers the release of calcium from RyRs and 2D analysis of the colocalization of DHPRs and RyR in rat suggested that most ($\sim 60\%$) of the DHPRs were grouped opposite the RyRs (Scriven, Dan & Moore, 2000). However, when analysis is performed in 3D, the colocalization is significantly lower ($\sim 45\%$) (Fletcher *et al.*, 2010). This recent finding underscores the importance of studying structure in 3D especially when the underlying resolution of the microscope is insufficient at the spatial scale of interest. In human, we find an even lower level of colocalization which suggests that normal EC coupling may arise from a combination of tightly coupled release triggered by DHPR activation plus a component due to local calcium diffusion from nearby DHPRs and Ryrs.

At the near molecular scale, we find that RyRs are not packed into junctional regions as a single cluster but rather as smaller groups of RyRs forming super clusters. This again suggests that local diffusion between release sites plays an important role in normal excitation-contraction coupling. It is possible that this partial uncoupling of RyRs from DHPRs serves to protect excitation contraction coupling during the normal trafficking of proteins and sub-cellular remodeling which would be important as the heart never has a chance to rest and rebuild. On the other hand, this looser coupling makes arrhythmogenesis *via* calcium waves more likely and may help explain the propensity of the remodeled, diseased heart to develop arrhythmias.

1. Berlin, J.R., Cannell, M.B. & Lederer, W.J. (1989) ITI in single rat cardiac ventricular cells: Relationship to fluctuations in intracellular calcium. *Circulation Research* **65**, 115-126.
2. Jayasinghe, I.D., Crossman, D.J., Soeller, C., Cannell, M.B. (2010) A new twist in cardiac muscle: dislocated and helicoid arrangements of myofibrillar Z-Disks in mammalian ventricular myocytes. *Journal of Molecular and Cellular Cardiology* **48(5)**, 964-971.
3. Scriven, D.L., Dan, P., Moore, E.D.W. (2000) Distribution of proteins implicated in excitation-contraction coupling in rat ventricular myocytes. *Biophysical Journal* **79**, 2682-2691.
4. Fletcher, P.A., Scriven, D.L., Schulson, M.N., Moore, E.D.W. (2010) Multi-image colocalization and its statistical significance. *Biophysical Journal* **99**, 1996-2005.

Mechanisms of contractile dysfunction in lamin A/C-deficient hearts

D. Fatkin, Sr Bernice Research Program in Inherited Heart Diseases, Molecular Cardiology Division, Victor Chang Cardiac Research Institute, Darlinghurst, NSW 2010, Australia.

Mutations in the *LMNA* gene that encodes the nuclear lamina proteins, lamin A and lamin C, have been associated with diverse human disorders and are the most common cause of familial dilated cardiomyopathy (DCM). The mechanisms by which nuclear protein defects result in cardiac contractile dysfunction are incompletely understood. Mice with a targeted deletion of the *Lmna* gene develop DCM and are a useful model to study disease pathogenesis. Homozygous *Lmna* knockout (*Lmna*^{-/-}) have severe DCM and die by 6-8 weeks of age, while heterozygous (*Lmna*^{+/-}) mice develop a milder phenotype in adult life with reduced survival after 40 weeks. Previous studies have established that lamin A/C-deficient nuclei have increased deformability and reduced survival when subjected to biaxial strain. On the basis of these findings, it has been proposed that mechanical stress-induced apoptosis contributes significantly to the development of DCM in patients with *LMNA* mutations. The aim of our study was to test this “structural hypothesis” by determining the effects of interventions to modify mechanical stress in *Lmna*^{+/-} mice. Serial echocardiography and tissue studies were performed in wildtype (WT) and *Lmna*^{+/-} mice before and after exercise training, thoracic aortic constriction (TAC), and administration of a β -adrenergic receptor-blocking drug, carvedilol. Echocardiography was performed in anaesthetized mice (avertin 2.5%). Mice were ventilated and anaesthetized for surgical procedures with ketamine (75 mg/kg), xylazine (20 mg/kg) and atropine (0.6 mg/kg). Tissue analyses were performed post-mortem in excised hearts. We first evaluated the biophysical properties of isolated cardiomyocytes from mice aged 12 weeks (prior to DCM) and found changes in nuclear size and shape in *Lmna*^{+/-} mice, as well as altered distribution of perinuclear desmin and enhanced swelling responses to hypo-osmotic stress. Groups of 12 week-old WT and *Lmna*^{+/-} mice underwent a 6-week exercise training program. Contrary to our predictions, neither moderate nor severe intensity exercise training induced cardiomyocyte apoptosis (assessed by TUNEL assay and caspase-3 activation) or DCM. Sustained left ventricular pressure overload generated by TAC resulted in apoptosis and contractile dysfunction in WT and in *Lmna*^{+/-} mice, with no differences in severity between the genotype groups. We found however, that regular moderate exercise training attenuated DCM development in male *Lmna*^{+/-} mice. Oral administration of carvedilol from 6 weeks to 40 weeks also had a protective effect against DCM in male *Lmna*^{+/-} mice.

These data indicate that lamin A/C-deficient cardiomyocytes have intrinsic structural defects but that mechanical stress-induced apoptosis is not a major determinant of DCM. We propose that altered cytoskeletal stability due to loss of normal nuclear anchoring may impair force transmission and promote DCM in *Lmna*^{+/-} hearts. Exercise training and carvedilol administration from an early age are promising strategies for DCM prevention and warrant further clinical evaluation.

Hot and cold running ion pumps

S.L. Myers,¹ F. Cornelius,² H.-J. Apell³ and R.J. Clarke,¹ ¹School of Chemistry, University of Sydney, NSW 2006, Australia, ²Department of Physiology and Biophysics, University of Aarhus, DK-8000 Aarhus C, Denmark and ³Faculty of Biology, University of Constance, D-78435 Constance, Germany.

Crystal structures of the Na⁺,K⁺-ATPase from both a warm-blooded animal (pig) (Morth *et al.*, 2007) and a cold-blooded animal (shark) (Shinoda *et al.*, 2009) have recently been published. Although the structures of the enzyme from these two species appear very similar, we have discovered major differences in their kinetics,

From investigations of K⁺ occlusion by the phosphoenzyme intermediate of the Na⁺,K⁺-ATPase and its K⁺-stimulated dephosphorylation *via* stopped-flow fluorimetry we have found that, whereas both enzymes appear to have similar rate constants of K⁺-occlusion of 370-380 s⁻¹, the two enzymes have very different rate constants of dephosphorylation. For the shark enzyme, dephosphorylation proceeds with a rate constant of only 48 (±2) s⁻¹ at 24°C and pH 7.4, whereas for the pig enzyme the rate constant is >365 s⁻¹. The dephosphorylation is, thus, the major rate-determining step of the shark enzyme under saturating concentrations of all substrates. For the pig enzyme, on the other hand, the major rate-determining step under the same conditions is the conformational E2-E1 transition of unphosphorylated enzyme and its associated K⁺ release to the cytoplasm. The differences in rate constant of the dephosphorylation reaction of the two enzymes are paralleled by compensating changes to the rate constant for the E2-E1 transition (Kahlid *et al.*, 2010), which explains why the differences in the enzymes' kinetic behaviour have not previously been identified in steady-state kinetic studies of the enzyme's entire reaction cycle.

In mammals, heat generation by the Na⁺,K⁺-ATPase as a by-product of ion pumping is thought to make approximately a 12% contribution towards the maintenance of body temperature. Therefore, the possibility should be investigated whether under physiological conditions the differences in Na⁺,K⁺-ATPase kinetics, which we have identified between a warm- and a cold-blooded animal, could in part be responsible for the higher body temperature of warm-blooded animals.

Khalid M, Cornelius F, Clarke RJ. (2010) *Biophysical Journal* **98**: 2290.

Morth JP, Pedersen BP, Toustrup-Jensen MS, Sørensen TL, Petersen J, Andersen JP, Vilsen B, Nissen P. (2007) *Nature* **450**: 1043-9.

Shinoda T, Ogawa H, Cornelius F, Toyoshima C (2009) *Nature* **459**: 446-50.

Mapping the ion translocation pathway in the glutamine transporter SNAT3

S. Bröer,¹ S. Balkrishna,¹ H.-P. Schneider² and J.W. Deitmer,² ¹Research School of Biology, Australian National University, Canberra, ACT 0200, Australia and ²Allgemeine Zoologie, Fachbereich Biology, Technical University of Kaiserslautern, Kaiserslautern, D-67653 Germany.

The glutamine transporter SNAT3 plays a pivotal role in the release of glutamine from brain astrocytes, the uptake and release of glutamine from hepatocytes and the uptake of glutamine in epithelial cells of the kidney. SNAT3 has a complex mechanism involving the cotransport of Na⁺ and the antiport of protons. In addition substrate-dependent and independent ion-conductances are observed. In order to understand the mechanism of the transporter in more detail, we explored the ion translocation pathway by experimental and theoretical approaches.

Until recently, database searches have not revealed homology to any known transporter structure. Comparison of hydropathy plots of the hydantoin permease Mhp1 with the hydropathy plot of SNAT3, however, revealed a significant similarity allowing us to generate a homology model of the transporter. The SNAT3 model suggests an overall topology that is similar to the Mhp1 structure. In this model helix 1 and 6 are lining the translocation pore and a putative Na⁺-binding site was identified involving residues asparagine 76, methionine 79 in helix 1 and valine 377 and threonine 380 in helix 8.

In line with this model we previously found that mutation of threonine 380 and of asparagine 76 changed the permeability properties of the transporter. Mutation of valine 377 to larger hydrophobic residues resulted in transporters with little activity. Mutation of valine 377 to leucine, however resulted in an active transporter molecule. This conservative exchange abolished the substrate-dependent conductance at pH 8.4, but not at pH 7.4. This is opposite to the change observed in a threonine 380 to alanine substitution, where the conductance at pH 7.4 is abolished. This confirms previous observations that the transporter has different conductance properties at different pH-values. As shown previously mutation of asparagine 76 to aspartate introduces a chloride-conductance that is tightly controlled by pH. We combined this mutation with a truncation of the C-terminal histidine in order to explore whether this residue changes the pH-dependence of the conductance. In this double mutant the anion conductance was still pH-gated, but showed little rectification compared to the N76D mutant.

The results suggest that asparagine 76, valine 377 and threonine 380 line the translocation pore of the glutamine transporter SNAT3. All three residues significantly alter the conductance of the transporter which is consistent with their suggested position close to the substrate and ion binding site of the transporter.

Glutamate transporter loss-of-function mutations cause human dicarboxylic aminoaciduria

R.M. Ryan,¹ C.G. Bailey,² A.D. Thoeng,² C. Ng,² K. King,² J.M. Vanslambrouck,² C. Auray-Blias,³ R.J. Vandenberg,¹ S. Bröer⁴ and J.E.J. Rasko,⁵ ¹Department of Pharmacology, University of Sydney, NSW 2006, Australia, ²Gene & Stem Cell Therapy Program, Centenary Institute, Camperdown, NSW 2050, Australia, ³Service of Genetics, Dept. of Pediatrics, Université de Sherbrooke, Sherbrooke, Québec, Canada, ⁴Research School of Biology, Australian National University, ACT 0200, Australia and ⁵Cell and Molecular Therapies, Sydney Cancer Centre, Royal Prince Alfred Hospital, Camperdown, NSW 2050, Australia.

Excitatory amino acid transporter 3 (EAAT3) has been shown to be the major epithelial transporter of glutamate and aspartate in the kidney and intestine in rodents. EAAT3 is also found in the brain where it is responsible for clearing the major excitatory neurotransmitter glutamate from the extracellular space. In this study we describe two mutations in EAAT3 that cause human dicarboxylic aminoaciduria, an autosomal recessive disorder of urinary glutamate and aspartate transport that has been associated with mental retardation. The single point mutation R445W causes an increase in substrate affinity and a significant reduction in transport and cell-surface expression. The non-functional deletion mutation, I395del, exhibits negligible cell surface expression. Our study provides definitive evidence that EAAT3 is the major renal transporter of glutamate and aspartate in humans and implicates EAAT3 in the pathogenesis of neurological disorders.

Determining the physiological state of a membrane protein: investigating the P-glycoprotein crystal structure

M.L. O'Mara and A.E. Mark, School of Chemistry and Molecular Biosciences, University of Queensland, St Lucia, QLD 4072, Australia .

P-glycoprotein is one of the major multi-drug transporters in humans. Expressed primarily in barrier tissues, P-glycoprotein (P-gp) exports a wide range of substrates and is a cellular first defence mechanism against xenotoxins. P-gp is a member of the ABC transporter superfamily, utilising the energy released from Mg^{2+} catalysed ATP binding and hydrolysis between the two nucleotide binding domains (NBDs) to induce a conformational change across the two transmembrane domains (TMDs). This conformational change drives the translocation of substrate across the membrane. Recent studies have crystallized homologues of P-gp in an ATP bound conformation (Dawson & Locher, 2006). Here the two TMDs are in an outwardly splayed conformation and are connected to the tightly coupled NBDs which form a characteristic nucleotide sandwich dimer, with nucleotide analogues sandwiched between them. In 2009 a medium resolution crystal structure of murine P-gp was solved in an alternate conformation, with inwardly facing TMDs and a wide gap separating the two NBDs (Aller *et al.*, 2009). The large conformational differences between the structures gave rise to questions as to whether this nucleotide-free structure represents an alternative conformation in the transport cycle, or whether this structure arose as a crystallization artefact. Here we address these questions *via* two sets of molecular dynamics (MD) simulations: one of P-gp in a cholesterol enriched POPC bilayer, and the second in the crystallographic mother liquor.

Simulations of the crystallographic mother liquor demonstrate that the nucleotide-free structure of P-gp is stabilized primarily by protein-protein contacts in the unit cell crystal lattice. Removal of these contacts is sufficient to destabilize the P-gp crystal structure. The instability arises from an attractive potential between the NBDs, resulting in a salt bridge between D558 and H1228. Experimentally, cholesterol is necessary for the functional activity of P-gp, however MD simulations demonstrate that the presence of cholesterol alone in a POPC membrane is not sufficient to stabilize the P-glycoprotein crystal structure. We are identifying the underlying factors producing the instability of the P-gp crystal structure and examining the effects of different ionic solutions on structural stability of P-gp.

Dawson RJ, Locher KP. (2006) Structure of a bacterial multidrug ABC transporter. *Nature* **443**: 180-5.

Aller SG, Yu J, Ward A, Weng Y, Chittaboina S, Zhuo R, Harrell PM, Trinh YT, Zhang Q, Urbatsch IL, Chang G. (2009) Structure of P-Glycoprotein reveals a molecular basis for poly-specific drug binding. *Science* **323**: 1718-1722.

Acquisition and dissemination of multidrug resistance in cancer via microparticles

R. Jaiswal,¹ S. Sambasivam,¹ J. Gong,¹ J.M. Mathys,² V. Combes,³ G.E. Graw³ and M. Bebawy,¹ ¹Faculty of Pharmacy, The University of Sydney, NSW 2006, Australia, ²Department of Molecular and Clinical Genetics, Royal Prince Alfred Hospital, Camperdown, NSW 2050, Australia and ³Vascular Immunology Unit, Discipline of Pathology, Sydney Medical School, The University of Sydney, NSW 2006, Australia.

Background: A major obstacle to the successful treatment of cancer is the acquisition of multi-drug resistance (MDR), a unique drug resistance in which tumors display cross-resistance to a wide range of unrelated drugs. MDR in cancer cells is typically caused by overexpression of efflux transporters constituting the ATP Binding Cassette Superfamily, of which P-glycoprotein (P-gp) and the Multidrug Resistance Associated protein (MRP1) are the most prominent. These transporters with their remarkable efflux capacity maintain sublethal intracellular drug concentrations, effectively rendering cancer cells treatment unresponsive.

The cellular regulation of these transporters was initially known to occur either pre- or post-transcriptionally. However, we recently discovered a novel non-genetic pathway of MDR acquisition in which microparticles (MPs) provide the vehicle for intercellular transfer of functional P-gp from multidrug resistant donor cells to drug sensitive recipient cancer cells.

Objective: The current study investigated the role of regulatory nucleic acids contained within the MP cargo in the acquisition and regulation of traits in recipient cells.

Methods and Results: MPs isolated from donor MDR cells, VLB₁₀₀ (MDR⁺) were co-cultured with drug-sensitive CCRF-CEM (MDR⁻) cells for 4 h to allow for MP binding and P-gp transfer. The MP localisation on the cell surface and internalisation in recipient cells was visualised using confocal imaging. The acquisition of fully functional P-gp following MP transfer was established by flow cytometry following direct immunolabeling and by assessing Rhodamine 123 dye exclusion.

Using quantitative RT-PCR the MPs were observed to incorporate and transfer transporter transcripts including those for *ABCB1* and *ABCC1*. We observed a significant 218 fold increase and 30% decrease in *ABCB1* and *ABCC1* mRNA respectively in recipient cells following MP coculture, the resulting phenotype being reflective of that observed in the donor cell population. In examining a potential contribution by regulatory nucleic acids towards this differential profile in recipient cells, we identified *micro-RNAs* as key mediators in this pathway.

Conclusions: These findings serve to further our understanding of the intercellular pathway regulating trait acquisition in cancer cell populations and provide a basis for the development of alternative treatment strategies targeting the emergence of MDR in cancer.

This work is funded by the NSW Cancer Council.

Microparticles confer multidrug resistance in breast cancer

J. Gong,¹ R. Jaiswal,¹ S. Sambasivam,¹ J-M. Mathys,² V. Combes,³ G.E. Grau³ and M. Bebawy,¹ ¹Faculty of Pharmacy, The University of Sydney, NSW 2006, Australia, ²Department of Molecular and Clinical Genetics, Royal Prince Alfred Hospital, Camperdown, NSW 2050, Australia and ³Vascular Immunology Unit, Discipline of Pathology, Sydney Medical School, The University of Sydney, NSW 2006, Australia.

Rationale: Despite decades of using cytotoxic drugs, the incidence of cancer relapse is still prevalent. One mechanism contributing to this is multidrug resistance (MDR). MDR occurs when a tumour cell becomes resistant to a number of structurally and functionally unrelated cytotoxic drugs following exposure to a single agent, resulting in a tumour cell that no longer responds to therapy even if drugs of different classes are used. One mechanism contributing to the emergence of MDR is the over-expression of efflux transporters, in particular, P-glycoprotein (P-gp). This transporter maintains a sublethal intracellular drug concentration, effectively rendering cancer cells treatment unresponsive.

Microparticles (MP) are plasma membrane-derived vesicles 0.1-1µm in diameter released by blebbing from various cell types. As such, MP are made up of fragments of the parent cell's plasma membrane and contain its cell surface proteins and cytoplasmic material (Mack *et al.*, 2000). We have previously shown in human acute lymphoblastic leukaemia cells that MP are shed spontaneously from drug-resistant cells, are capable of binding to drug-sensitive cells, and in doing so, transfer functional P-gp to drug-sensitive cells, conferring MDR (Bebawy *et al.*, 2009). Here we demonstrate that this also occurs in solid tumour cells such as the MCF-7 breast cancer cell line. Specifically, we demonstrate that the multidrug resistant MCF-7/Dx cell line spontaneously sheds MP and that these MP carry the multidrug transporter. Furthermore, we demonstrate that MP derived from these cells also transfer transporter transcript and regulatory nucleic acids (microRNAs).

Methods: To determine if MP are shed from drug-resistant cells, the isolated MP population was labelled with FITC-annexin V and analysed by flow cytometry. To determine if MP transferred P-gp to drug-sensitive cells, a co-cultured population of drug-sensitive cells with MP were labelled with FITC-anti-P-gp and analysed by flow cytometry. Transferred P-gp was deemed functional by the daunorubicin dye exclusion assay. Quantitative real time PCR was used to determine the levels of expression of transcripts and microRNAs in donor cells, MP and recipient cells following MP coculture.

Results: Our results show that the multidrug resistant MCF-7/Dx cell line spontaneously sheds MP and that these MP are capable of carrying functional P-gp to the drug-sensitive cell line, rendering recipient cells MDR. We have also determined that MP are capable of incorporating and transferring transporter transcripts and microRNAs, leading to changes in the recipient cells which are reflective of the donor cell phenotype.

Conclusion: The significance of this study is in the elucidation of a non-genetic pathway for the acquisition of P-gp mediated MDR in cancer. This has the potential for translation into clinical outcomes as it provides another avenue by which resistance to chemotherapy can be addressed.

Bebawy, M, Combes, V, Lee, E, Jaiswal, R, Gong, J, Bonhoure, A & Grau, G.E. (2009) Membrane microparticles mediate transfer of P-glycoprotein to drug sensitive cancer cells, *Leukemia* **23**, 1643-9.

Mack, M, Kleinschmidt, A, Bruhl, H, Klier, C, Nelson, P.J, Cihak, J, Plachy, J, Stangassinger, M, Erfle, V & Schlondorff, D. (2000) Transfer of the chemokine receptor CCR5 between cells by membrane-derived microparticles: a mechanism for cellular human immunodeficiency virus 1 infection, *Nature Medicine* **6**, 769-75.

This work was supported by a research grant from the NSW Cancer Council.

Cadherin dynamics and the cytoskeleton

*M. Smutny, S. Mangold, S. Wu, G. Gomez, E. Kovacs, N.A. Hamilton and A.S. Yap, Division of Molecular Cell Biology, Institute for Molecular Bioscience, The University of Queensland, St. Lucia, QLD 4072, Australia.
(Introduced by Pierre Moens)*

Classical cadherin adhesion receptors are major determinants of tissue organization both in health and disease. They have long been thought to function in close cooperation with the actin cytoskeleton. Despite this, the molecular mechanisms responsible for cadherin-actin cooperation are poorly understood and lack, indeed, a clear over-arching conceptual framework. A major analytic challenge is to develop approaches to encompass both the dynamics of adhesion receptor organization and the intrinsic dynamics of actin polymer assembly/disassembly and organization. We are tackling this problem by using lentiviral shRNA systems to “replace” endogenous proteins with XFP-tagged transgenes; and then combining live cell imaging (including FRAP and photactivation) with mathematical modelling in order to quantitatively characterize cadherin and cytoskeletal dynamics. This multimodal approach is yielding a picture of functional cytoskeletal modules that cooperate, in a context-dependent fashion, to regulate the stability and turnover of cell-cell junctions.

Detecting stem cell differentiation using fluorescence lifetime microscopy (FLIM) by the phasor approach

E. Gratton, Laboratory For Fluorescence Dynamics, 3210 Natural Sciences II, University of California, Irvine, CA 92679, USA.

In fluorescence lifetime microscopy (FLIM) of live tissues a major issue is the assignment of auto-fluorescence to specific molecular components and their interactions within the physiological context. Analyzing the intensity decays with a multi-exponential fit is often not sufficient to properly describe this complexity. Here we use the phasor approach to FLIM to analyze complex decays in a live tissue. Each chemical species was identified and categorized by its specific location in the phasor plot. This phasor fingerprint reduces the importance of knowing the exact lifetime distribution of fluorophores and allows interpreting the FLIM images directly in molecular terms. The phasor signatures of different species have been used to separate many tissue components inside the testes of an Oct4-GFP transgenic mouse and to map the relative concentration of auto-fluorescence, GFP, collagen, retinol, retinoic acid, FAD and NADH. Furthermore the analysis of the fluorescence decay with higher harmonics of the phasor plot can separate different tissue components that have the same location in the phasor plot at one harmonic, but arise from different lifetime distributions. The phasor approach to lifetime imaging in live tissue provides a unique fit-free and straightforward method for interpreting complex decays in terms of molecular features the relative concentration of fluorophores. This method has the potential to become a non-invasive tool to characterize the local microenvironment and monitor differentiation and diseases in label-free live tissues.

Light, x-rays or electrons for imaging malaria parasites?

L. Tilley,¹ E. Hanssen,² N. Klonis,¹ M. Dixon,¹ P. McMillan,¹ N. Abu-Bakar¹ and C. Whitchurch,³ ¹La Trobe Institute for Molecular Science, and Centre of Excellence for Coherent X-ray Science, La Trobe University, Melbourne 3086, VIC, Australia, ²Electron Microscopy Unit, Bio21 Molecular Science and Biotechnology Institute, University of Melbourne, Parkville, VIC 3010, Australia and ³Institute for the Biotechnology of Infectious Diseases, University of Technology Sydney, NSW, 2007, Australia.

Imaging technologies have provided us with phenomenal insight into the micro- and nano-scopic domains and efforts to answer the major medical and biotechnology questions of the 21st century will be heavily reliant on the use of advanced imaging techniques. However there are limitations. Conventional light microscopy can be used with hydrated (in some cases, live) cells but has limited resolution, particularly for full-field imaging. Conventional electron microscopy offers very high resolution however the strong absorption of electrons by air and by the sample means that it can only be used with very thin, fixed, dehydrated samples. Imaging technologies that overcome some of the disadvantages of optical and electron microscopies are keenly sought.

We have used two “bridging” imaging modalities to explore sub-cellular topography. Three-dimensional structured illumination microscopy (3D-SIM) permits super-resolution fluorescence imaging of cells that are specifically labelled with fluorescent probes. Immunoelectron tomography offers high resolution imaging of individual ultrastructural features in a cellular context. Combined with serial sectioning and immunogold labeling it permits precise mapping of whole cell architecture.

The malaria parasite, *Plasmodium falciparum*, develops within human erythrocytes. As it grows the parasite establishes a membrane network outside its own limiting membrane in the cytoplasm of its host cell. These membrane structures play an important role in the trafficking of virulence proteins to the host cell surface, however their ultrastructure is only partly defined and there is on-going debate regarding their origin, organization and connectivity. Parasite endocytic processes are also poorly understood. The parasite consumes host haemoglobin in order to support its own growth. Small packets of haemoglobin are transferred from the host cell cytoplasm to a parasite digestive vacuole for haemoglobin digestion and heme detoxification however the precise mechanism for uptake is debated. Advanced imaging methods have provided novel insights into parasite cell architecture and functional cell biology.

Molecular transport in cells by the pair correlation fluctuation method

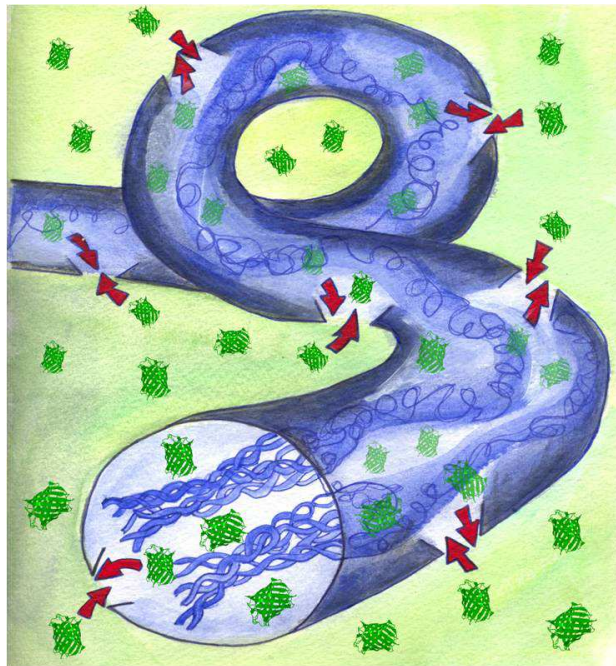
M.A. Digman, 3210 Natural Sciences 2, Laboratory For Fluorescence Dynamics, University of California Irvine, Irvine, CA 92679, USA.

Traditional fluctuation spectroscopy methods are employed to determine molecular diffusion in cells. While these methods provide information about a local dynamics in a specific point in the cell, they do not respond to the question of the path taken by a molecule to travel from one point to another. This kind of question is generally addressed by techniques such as single particle tracking. However, in single particle tracking the same molecule must be observed for an extended period of time and the molecule must be isolated from others. Also, many single particle trajectories must be recorded before we have sufficient statistics to delineate the path following by the particles. These conditions are difficult to achieve and the collection of many trajectories takes some time, especially if the volume to be interrogated is small. As a consequence, single particle tracking is used with large and bright particles. We developed a method in which we can follow relatively dim molecules in the presence of many other molecules, and statistically follow the flow of many molecules at a time. We have applied this method to the traffic of molecules inside the nucleus of cells and among the cytoplasm and the nucleus.

***In vivo* pair correlation analysis of enhanced green fluorescent protein (EGFP) intra nuclear diffusion**

E. Hinde, F. Cardarelli, M.A. Digman and E. Gratton, Laboratory for Fluorescence Dynamics, Department of Biomedical Engineering, University of California, Irvine, CA 92697, USA.

Intra nuclear diffusion is fundamental to enabling crucial cellular processes like gene transcription, DNA replication, DNA repair and epigenetic regulation to take place. The diffusion of molecules within the nucleus is obstructed by the steric constraints imposed by the nuclear environment. The extent to which nuclear architecture directs the diffusive route taken by these molecules is of significant interest. No methods proposed thus far have the capability to measure overall molecular flow in the nucleus of living cells. Here we apply the pair correlation function analysis (pCF) to measure molecular anisotropic diffusion in the interphase nucleus of live cells. In the pCF method we cross correlate fluctuations at several distances and locations within the nucleus, enabling us to define migration paths and barriers to diffusion. We use monomeric EGFP as a prototypical inert molecule and measure its flow in and between the different nuclear environments, marked by Hoechst 33342 as a reference of DNA density.



As schematically shown in the figure above our results suggest that there are two disconnected molecular flows throughout the nucleus, associated with high and low DNA density regions. We observe that the different density regions of DNA form a networked channel that allow EGFP to diffuse freely throughout, however with restricted ability to traverse the channel barriers. Upon more detailed analysis in time, rare bursts of EGFP molecules were detected entering and exiting the channel, with a characteristic time of approximately 300ms. The intermittent nature of this transit suggests an intrinsic localized change in chromatin structure which periodically turns on and off. Preliminary results obtained during mitosis, suggest the chromosomes to impart a markedly different mechanism toward regulating the equivalent transit. This is the first *in vivo* demonstration of the intricate chromatin network showing channel directed diffusion of an inert molecule with high spatial and temporal resolution.

SPontaneous Oscillatory Contraction (SPOC): Quantifying contractile performance in isolated human cardiomyocytes under partial activation

J.E. Robinson,¹ R. Whan,² F. Braet,² Y. Su,² S. Ishiwata,³ M. Yamane,³ T. Kagemoto,³ N. Fukuda,⁴ J. Hughes,¹ T. Kraft,⁵ J. van der Velden,⁶ S.B. Marston,⁷ M. Steenman,⁸ P.S. Macdonald⁹ and C.G. dos Remedios,¹ ¹Muscle Research Unit, Bosch Institute, Department of Anatomy and Histology, University of Sydney, NSW 2006, Australia, ²Australian Centre for Microscopy and Microanalysis, University of Sydney, NSW 2006, Australia, ³Department of Physics, Faculty of Science and Engineering, Waseda University, Tokyo, Japan, ⁴Department of Cell Physiology, School of Medicine, Jikei University, Tokyo, Japan, ⁵Molecular and Cellular Physiology, Medical School Hanover, Hanover, Germany, ⁶Laboratory for Physiology, Institute for Cardiovascular Research, VU University Medical Centre, Amsterdam, The Netherlands, ⁷National Heart and Lung Institute, Imperial College London, London, United Kingdom, ⁸Institut du Thorax, Université de Nantes, Nantes, France and ⁹Heart and Lung Transplant Unit, St Vincent's Hospital, Darlinghurst, Australia.

Under conditions of partial activation, striated muscle fibres exhibit repetitive, cyclic auto-oscillation between rapid-lengthening (relaxation) and slow-shortening (contraction) phases. This phenomenon is termed SPontaneous Oscillatory Contraction (SPOC), and represents a third state of muscle that exists intermediate to contraction and relaxation. The cardiac SPOC period and shortening velocity have been correlated with heart rate in various animals. Thus, SPOC is likely to reflect the physiology of the heart as it functioned in life. Small bundles of skinned, immobilised human cardiomyocytes suspended by adhesive tape were exposed to precise ionic conditions to induce SPOC, and recorded at high spatial and temporal resolution using live cell microscopy. Quantitative analysis allows us to draw conclusions about how the SPOC parameters, including total SPOC period and rates of shortening and lengthening, change with age in non-failing human heart samples, from 3 weeks to 65 years. Further, we look at SPOC as a technique for demonstrating and quantifying a functional defect in cardiomyectomy samples from patients diagnosed with hypertrophic cardiomyopathy (HCM), where a causal genetic mutation has been identified. SPOC might be applied in future as a tool to assist with the diagnosis and risk stratification of HCM patients.

The effects of membrane potential and cytoplasmic calcium concentration on calcium extrusion across the tubular system in mammalian skeletal muscle

J.N. Edwards and B.S. Launikonis, School of Biomedical Sciences, The University of Queensland, Brisbane, QLD 4072, Australia.

The regulation of cytoplasmic Ca^{2+} is essential in the maintenance of skeletal muscle function and survival. This is achieved by the combined activities of ion transporters such as SERCA, NCX, PMCA, found embedded within the sarcoplasmic reticulum (SR) and plasma membranes. Upon Ca^{2+} release from the SR, $[\text{Ca}^{2+}]_{\text{cyto}}$ can globally reach $\sim 2\mu\text{M}$ and it is during such an event that highlights Ca^{2+} extrusion is an essential regulatory mechanism, as this is ~ 20 times the resting $[\text{Ca}^{2+}]_{\text{cyto}}$. We have shown that during cell wide Ca^{2+} release events, there is an initial increase in t-system (extracellular) Ca^{2+} , followed by a net decline due to the activation of a store-operated calcium entry (SOCE) current. Although the SOCE current has recently generated significant levels of interest, information on the rates of t-system Ca^{2+} uptake (cytoplasmic Ca^{2+} extrusion) remains limited. Therefore, we aimed to characterise the effects of membrane potential and $[\text{Ca}^{2+}]_{\text{cyto}}$ on the rate of cytoplasmic Ca^{2+} extrusion in mammalian skeletal muscle.

Wistar rats were killed by asphyxiation in accordance to the guidelines set by the Animal Ethics Committee of the University of Queensland. *Extensor digitorum longus* and *soleus* muscles were rapidly excised, pinned out and fully immersed in paraffin oil. Small bundles of intact fibres were isolated and exposed to a Na^+ -based physiological solution containing the fluorescent dye, fluo-5N salt. Single fibres were then isolated and mechanically skinned (resulting in the trapping the dye in the t-system) and transferred to a chamber containing a K^+ or Na^+ -based internal solution to set the membrane potential. A 'release solution' with low Mg^{2+} , 5mM BAPTA and 5mM caffeine was used to chronically deplete sarcoplasmic reticulum Ca^{2+} stores and activate SOCE. T-system fluo-5N fluorescence was imaged on an Olympus FV1000 confocal microscope in either xy or xyt mode in polarized and depolarized fibres with known cytoplasmic Ca^{2+} concentrations, at rest or during SR Ca^{2+} release. The net change in t-system fluo-5N signal was used as an indicator of Ca^{2+} movements across the t-system.

Fluo 5N trapped in the sealed t-system was calibrated (*in situ*) and in the presence of different concentrations of bovine serum albumin. Following low $[\text{Ca}^{2+}]_{\text{t-system}}$ (achieved by chronic activation of SOCE with 'release solution') the t-system could be reloaded with internal solutions containing 1 mM EGTA (either 100, 200 or 800 nM free Ca^{2+}). This rate of uptake was markedly greater in depolarized cells (Na^+ based solutions) compared to polarized cells (K^+ based solutions), most likely due to an increased driving force for Ca^{2+} to exit the cell. Interestingly, vacuoles were seen in some fibres. Vacuoles retained fluo 5N for > 20 mins in the presence of a 'release solution' whereas a fluorescence signal from transverse tubules was rapidly lost. We have also measured for the first time, a SOCE flux and t-system uptake in slow-twitch fibres from the *soleus* muscle which are currently being explored.

The effect of suramin (a calmodulin antagonist) on caffeine-induced Ca^{2+} -release in mechanically skinned fast-twitch skeletal muscle fibres of the rat

D.W. Williams, G.S. Posterino and D.G. Stephenson, Department of Zoology, Latrobe University, VIC 3086, Australia.

Calmodulin (CaM) is a ubiquitous, multifunctional calcium binding protein, which binds to the ryanodine receptor (RyR1) in skeletal muscle (Tripathy *et al.*, 1995). Ca^{2+} -free CaM binds to RYR1 and increases RYR1s affinity for calcium, while Ca^{2+} -bound CaM inhibits RYR1s affinity for calcium (Rodney *et al.*, 2000). The precise role of CaM in the regulation of calcium release in physiological preparations remains unknown. Suramin is a broad acting CaM antagonist known to displace bound CaM from RyRs (Sigalas *et al.*, 2009). In this study we investigated the effects of suramin on Ca^{2+} release from the sarcoplasmic reticulum (SR) in freshly mechanically skinned muscle fibres where the SR is intact under conditions where the suramin treatment did not affect the ability of the contractile apparatus to develop force.

All experiments conducted were approved by the La Trobe University Animal Ethics committee. Rats were killed by an overdose of isoflurane (4% volume: volume) and whole EDL muscles were removed and pinned out on a bed of Sylgard at resting length under paraffin oil. Single fibres were then isolated under a dissecting microscope, mechanically skinned, and mounted between a pair of forceps and a sensitive force transducer. After mounting to the force recording apparatus, fibres were bathed in a K-based solution that mimics the normal intracellular environment with respect to pH (7.10); monovalent ions (137 mM); Mg^{2+} (1 mM); divalent cations (60 mM); total ATP (8 mM); osmolality (295 mOsm/L); $[\text{Ca}^{2+}] \sim 100$ nM. The relative SR Ca-content and ease of Ca^{2+} moving through the RyR1s can be estimated from the force response following the transfer of the fibre to a SR- Ca^{2+} -depleting solution containing caffeine (30 mM) and low $[\text{Mg}^{2+}]$ (50 μM) (Lamb & Stephenson, 1991). A similar area under the caffeine-induced force response is indicative of similar SR Ca-content and a faster rate of rise of the caffeine-induced force and/or a greater force peak (for same SR Ca-content) indicate a greater SR Ca^{2+} -efflux through the RyR1. Fibres were repeatedly bathed in a SR Ca-loading solution ($[\text{Ca}^{2+}] \sim 300$ nM) for increasing amounts of time (10-120 s) to reload the SR Ca to various levels and then the SR Ca^{2+} was fully released in the SR-Ca-depleting solution. Fibres were randomly divided into two groups (control and test) then exposed for 2 min to 100 μM suramin (test) or exposed to a like solution *sans* suramin (control). After the suramin/*sans* suramin treatment, the fibres were washed for 10 min and the SR Ca-loading/caffeine release protocol was repeated for both groups. Suramin treatment resulted in a marked reduction in the caffeine induced rate of rise (time between 20 and 80% of peak caffeine response decreased by $25.9 \pm 7.1\%$ (S.E.M.) of control ($p < 0.01$) at 30 s load without changing the area under the caffeine-induced force responses ($p > 0.1$). Suramin also increased the peak force of submaximal caffeine responses by $20.70 \pm 5.99\%$ of maximum force for a 30 s load ($n=4$). Thus, the results show that treatment with 100 μM suramin for 30 s increases the SR Ca^{2+} -efflux through the RyR1, which is consistent with suramin removing the CaM from RyRs on the intact SR.

Lamb GD, Stephenson DG. (1991) *Journal of Physiology*, **434**: 507-528.

Rodney GG, Williams BY, Strasburg GM, Beckingham K, Hamilton SL. (2000) *Biochemistry*, **39**: 7807-7812.

Sigalas C, Bent S, Kitmitto A, O'Neill S, Sitsapesan R. (2009) *British Journal of Pharmacology* **156**: 794-806.

Tripathy A, Xu L, Mann G, Meissner G. (1995) *Biophysical Journal* **64**: 106-119.

Calcium regulation of apoptosis in pancreatic acinar cells

J.V. Gerasimenko,¹ P. Ferdek,¹ A.V. Tepikin,² O.H. Petersen¹ and O.V. Gerasimenko,¹ ¹Cardiff School of Biosciences, Cardiff University, Museum Avenue, Cardiff CF10 3AX, UK and ²The Physiological Laboratory, The University of Liverpool, Crown Street, Liverpool L69 3BX, UK. (Introduced by Grigori Rychkov)

We have studied calcium regulation of induction of apoptosis in pancreas. In pancreatic acinar cells, the earliest events were found to be cytosolic calcium elevations due to release of calcium from intracellular stores. As a result of that calcium levels also increased in mitochondria aiding mitochondrial depolarization and mPTP. High mitochondrial calcium at the time of oxidant stress was found to be the crucial factor in the cell fate. When mitochondrial calcium was low, then apoptosis did not occur regardless of other stores' content. We also studied Bcl-2 family members, well known regulators of apoptosis involved in regulation of intracellular calcium homeostasis. Most interesting was a potential link between Bcl-2 family proteins and a passive calcium release from the intracellular stores. We found that BH3 mimetics induce calcium release from the ER that leads to the formation of calcium plateau. Inhibition of either IP3Rs or RyRs reduced but did not abolish BH3-elicited calcium release. Further, we have shown that loss of Bcl-2 protein decreases calcium release from the ER and increases cytosolic calcium clearance in pancreatic acinar cells.

Gerasimenko J, Ferdek P, Fischer L, Gukovskaya AS, Pandol SJ. (2010) *Pflügers Archiv European Journal of Physiology* **460(5)**: 891-900

Gerasimenko O, Gerasimenko J. (2010) *Methods in Molecular Biology* **591**: 201-10.

Baumgartner HK, Gerasimenko JV, Thorne C, Ferdek P, Pozzan T, Tepikin AV, Petersen OH, Sutton R, Watson AJ, Gerasimenko OV. (2009) *Journal of Biological Chemistry* **284(31)**: 20796-803.

The application of complementary luminescent and fluorescent imaging techniques to visualize nuclear and cytoplasmic Ca²⁺ signaling during *in vivo* differentiation of slow muscle cells in zebrafish embryos

C.Y. Cheung,¹ S.E. Webb,² D.R. Love³ and A.L. Miller,² ¹Department of Anatomical and Cellular Pathology, Prince of Wales Hospital, CUHK, Hong Kong, China, ²Section of Biochemistry and Cell Biology, Division of Life Science, HKUST, Hong Kong, China, and ³School of Biological Sciences, University of Auckland, Auckland, New Zealand. (Introduced by Grigori Rychkov)

Intact zebrafish embryos were used as an *in vivo* animal model to investigate the role of Ca²⁺ signaling during the differentiation of slow muscle cells (SMCs) within forming skeletal muscle. Transgenic zebrafish were generated using an α -actin promoter that targeted apoaequorin expression specifically to muscle cells. Two distinct Ca²⁺ signaling periods (CSPs) were visualized in the developing SMCs: between ~17.5-19.5 hours post-fertilization (hpf) and after ~23 hpf, separated by a ~3.5 hour Ca²⁺ signaling quiet period. Further spatial characterization of these Ca²⁺ signals using confocal fluorescent microscopy and calcium green-1 dextran as a reporter, indicated that the earlier CSP displayed distinct nuclear and cytoplasmic components, whereas the later CSP was predominantly cytoplasmic. Both CSPs consisted of a series of oscillating Ca²⁺ waves generated at distinct frequencies, while the earlier CSP also displayed a slow rise then fall in the Ca²⁺ baseline-level. Imaging of cyclopamine- and forskolin-treated wild-type, or *smo*^{-/-} mutant embryos, where SMCs do not form, confirmed the specific cell population generating the signals. Treating embryos with antagonists indicated that both IP₃Rs and RyRs are responsible for generating the temporal characteristics of the Ca²⁺ signaling signature, and that the latter plays a necessary role in SMC differentiation and subsequent myotome patterning (Cheung, *et al.*, 2010). Together, these data support and extend the proposition that specific spatiotemporal patterns of spontaneous Ca²⁺ signals might be used for different as well as combinatorial regulation of both nuclear and cytosolic signal transduction cascades, resulting in myofibrillogenesis in SMCs as well as myotome patterning (Webb & Miller, 2010).

Cheung, C.Y., Webb, S.E., Love, D.R., and Miller A.L. (2010) *International Journal of Developmental Biology*, *In Press*. DOI 10.1387/ijdb.103160cc

Webb, S.E., and Miller, A.L. (2010) *In: Calcium Signaling*, CHS Press (Eds. Berridge, M.J., Putney, J., Roderick, L., Bootman, M.D). *In Press*.

STIM:Orai stoichiometry and the trapping and activation of store-operated calcium channels

P.J. Hoover and R.S. Lewis, Department of Molecular and Cellular Physiology, Stanford University School of Medicine, Stanford, CA 94305, USA. (Introduced by Grigori Rychkov)

The activation of store-operated Ca^{2+} entry (SOCE) by depletion of Ca^{2+} stores results from the redistribution of the ER Ca^{2+} sensor STIM1 and the CRAC channel protein Orai1 to ER-plasma membrane (PM) junctions where they form closely apposed clusters. Recent studies support a two-part diffusion-trap model for this process, in which the C-terminal polybasic domain of STIM1 binds to phosphoinositides in the junctional plasma membrane and the STIM1 CRAC activation domain (CAD) binds to Orai1, effectively trapping and activating mobile CRAC channels. Store depletion-induced oligomerization of STIM1 has emerged as the essential trigger for this sequence of events, as shown by the ability of artificial STIM1 crosslinking to elicit clustering at junctions and activate CRAC channels in the absence of store depletion. STIM1 traps and activates CRAC channels through the binding of the CRAC activation domain (CAD, aa 342-448) to the N- and C-termini of Orai1.

Crosslinking of individual CRAC channels by the isolated CAD protein fragment suggests that each channel probably contains four STIM binding sites. To determine the minimum number of binding events required to trap a CRAC channel at the ER-PM junction, we measured the junctional ratio of STIM1 to Orai1 as the expression level of Orai1 was increased relative to that of STIM1 in HEK 293 cells. At high Orai1 expression, the STIM:Orai ratio reached a minimum value of ~0.3, or 1.2 STIM/tetrameric CRAC channel, suggesting that a single STIM1 is capable of arresting a CRAC channel at the junction. To determine how CRAC channel activity varies with the number of binding sites occupied by STIM1, we measured I_{CRAC} density in HEK cells expressing a constant amount of STIM1 and increasing levels of Orai1. We found that CRAC channel activation is a highly nonlinear bell-shaped function of Orai1 expression, and that the minimum stoichiometry sufficient for trapping the channels at junctions fails to evoke significant activation. A simple cooperative gating model fitted to the data suggests that only CRAC channels with 4 sites occupied contribute significant current. This highly nonlinear activation of CRAC channels supports earlier conclusions based on current noise analysis (Prakriya & Lewis, 2006) that the slow development of whole-cell CRAC current after store depletion reflects the stepwise recruitment of individual channels from a silent to a high open-probability state as they enter ER-PM junctional sites.

Prakriya M, Lewis RS. (2006) *Journal of General Physiology* **128**: 373-86.

Peroxiredoxin 4 is confined to the endoplasmic reticulum in human brain and associated with Lewy body formation in Parkinson's disease and dementia with Lewy bodies

L.J. Turnbull and J.H.T. Power, Department of Human Physiology, School of Medicine, Flinders University, Bedford Park, Bedford Park, SA 4042, Adelaide.

Parkinson disease (PD) is a progressive neurodegenerative disorder characterised by formation of Lewy bodies within the dopaminergic neurons within the *substantia nigra* and depending on the staging of the disease, marked loss of these neurons. Similarly, dementia with Lewy bodies (DLB) involves the formation of Lewy bodies within the cortical neurons resulting in marked synaptic loss and eventually neuronal loss and dementia.

Lewy bodies contain a range of cellular proteins including a high proportion of α -synuclein, a small protein whose suspected role is in synaptic vesicle recycling. There is still debate as to whether Lewy bodies are protective or destructive to neurons. Yeast models expressing alpha synuclein suggest that α -synuclein blocks trafficking from the endoplasmic reticulum to the Golgi apparatus and results in endoplasmic reticulum stress.

Peroxiredoxin IV is the least characterized of the peroxiredoxin family of antioxidant enzymes and is different from other 2-Cys members in that it contains a hydrophobic leader which suggests that peroxiredoxin IV is a secreted protein. Recent pulse chase experiments have indicated that peroxiredoxin IV is in fact confined to the endoplasmic reticulum and possibly involved in protection against endoplasmic reticulum oxidative stress and as a molecular chaperone. This study was conducted to determine the cellular localization of this enzyme in the human brain and whether peroxiredoxin IV is present in the endoplasmic reticulum and associated with the formation of Lewy bodies in PD and DLB.

Human brain proteins from control, PD and DLB tissue were separated using PAGE, transferred to a Polyvinylidene difluoride membrane (PVDF) and then probed with a peroxiredoxin IV antibody to determine the specificity of the antibody and the molecular forms. Light immunohistochemistry using the same antibody was performed using paraffin embedded sections from the same tissue to determine the general distribution of peroxiredoxin IV. Confocal immunofluorescence using the peroxiredoxin IV antibody and specific cellular and organelle markers was used to determine the specific cellular and sub-cellular distribution. In addition, colocalization with α -synuclein was used to determine if peroxiredoxin IV and the endoplasmic reticulum was associated with Lewy body pathology in PD and DLB.

On Western blotting, peroxiredoxin IV stained as two prominent proteins at approximately 27kd and 65kd under reducing conditions. Peroxiredoxin IV is predicted to be 31kd with a 4kd leader sequence indicating the monomer in human brain is the cleaved mature form. This protein functions as a committed dimer and the 65kd form is probably the dimer although it is slightly larger than predicted. Peroxiredoxin IV was abundant in neurones, both light and confocal immunohistochemistry showed prominent granular staining in the neurones with low level staining in oligodendrocytes. Astrocytes did not appear to be labelled and low level staining microglia appeared to be from ingested material. Peroxiredoxin IV co-localised with the ER/Golgi marker SAR1 indicated that peroxiredoxin IV is confined to the ER in human brain supporting cellular pulse chase studies. SAR1 had a slightly larger area of distribution suggesting that peroxiredoxin IV does not translocate to the Golgi. However, peroxiredoxin IV did not co-localise with the lysosomal marker Lamp2 indicating it is not associated cellular degradation *via* lysosomes.

Co-localization of peroxiredoxin IV with the Lewy body marker α -synuclein showed that there is a close association between Lewy body formation and the ER. In pre-Lewy body neurones, α -synuclein and peroxiredoxin IV positive vesicular aggregations were observed to be coalescing between the ER and Golgi supporting recent findings in yeast models that α -synuclein blocks docking of ER vesicles with the Golgi apparatus. A variety of Lewy body forms were observed and all forms were closely associated with the ER as determined by the peroxiredoxin IV staining.

In conclusion these results show for the first time that peroxiredoxin IV is present in human neurones and that it is confined to the ER. These results also suggest that Lewy bodies are seeded from α -synuclein vesicular aggregations unable to dock with the Golgi apparatus giving new insights into the formation of this pathologic structure.

ProBDNF inhibits neurites outgrowth in neurons of mice by activating RhoA

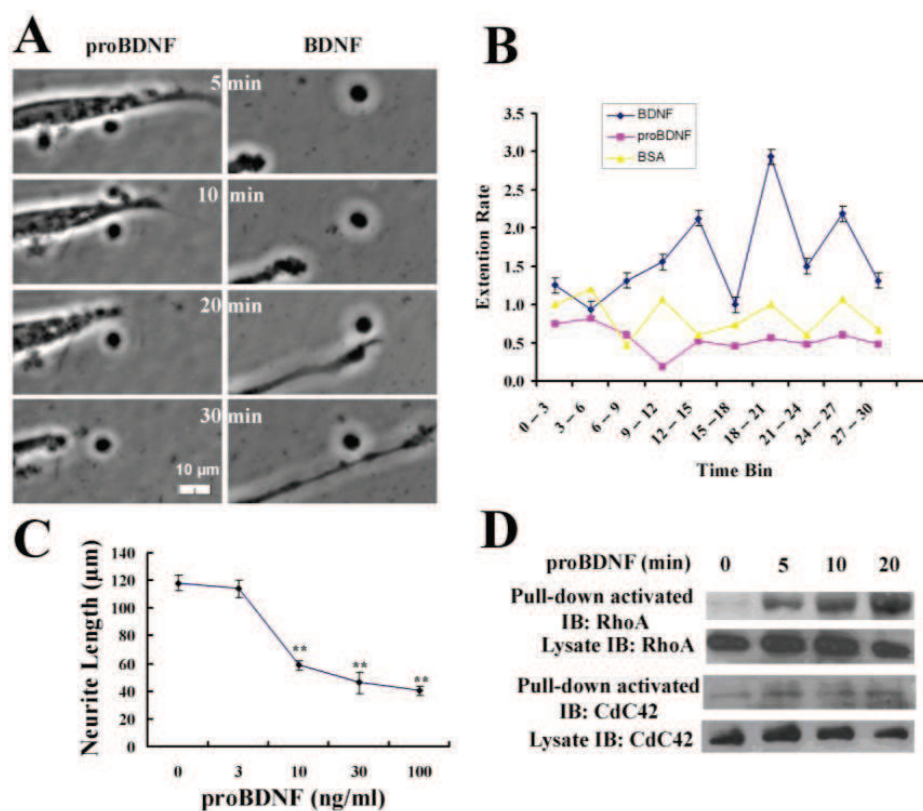
Y. Sun, Y. Lim, J.H. Zhong, M. Yang and X.F. Zhou, Department of Human Physiology and Centre for Neuroscience, Flinders University, GPO Box 2100, Adelaide, SA 5042, Australia.

Background: Brain-derived neurotrophic factor (BDNF) is a potent molecule regulating dendritic trees and synaptic plasticity, however, whether the BDNF precursor (proBDNF) plays any role in the neurite growth is unknown. This study investigated whether proBDNF has a physiological role in the neurite growth of neonatal cortex neuron *in vitro*. We focus on the following the aspects, the dose effect of proBDNF on neurite outgrowth, ELISA assay to test proBDNF and BDNF after stimulated neurons by 45 mM KCl for 30 min, distribution of RhoA, cdc42, F-actin *via* immunohistochemistry after gradient or uniform of proBDNF added, and examined the down streaming signals of RhoA and cdc42.

Methods: The cortex from neonatal C57BL/6 (n=12) mice were rapidly removed and cultured. Live images were collected every 6 s for 30 min by using Nikon BioStation and analyzed *via* the advanced software. Primary neurons were incubated in proBDNF at various concentrations for 24 h and the lengths were measured. 8×10^6 cells were dissociated for 24 h, treated with 50 ng/ml proBDNF for 0, 5, 10, 20 min, the neuron cell lysates of 100 μ g protein in 0.5 ml RIPA buffer were incubated in 10 μ g Rho binding domain (RBD) agarose gel for RhoA and cdc42 activity assays. The pull-down and total proteins were evaluated by western blotting. Data are mean \pm SEM from 3 independent experiments.

Results: Live imaging showed the clear collapse of growth cones in response to proBDNF (50 ng/ml) and the elongation to BDNF (50 ng/ml) at the indicated point (Figure A). proBDNF caused a 34% decrease in the extension rate after 6 min and maintained throughout a 30 min treatment. Meanwhile, neurons treated with BDNF spent 63% of the time extending (Figure B). proBDNF (10, 30, 100 ng/ml) resulted in a 50% decrease in length (58.6 μ m vs 118.1 μ m) compared with 0 ng/ml proBDNF group (Figure C) but proBDNF 3 ng/ml had no significant effects on the length. 5 min after proBDNF treatment, RhoA activity was increased by 5 fold 20 min after proBDNF incubation (Figure D). Interestingly, no difference in activated cdc42 level was seen during the proBDNF incubation.

Conclusion: Live imaging demonstrated that proBDNF repulsed growth cones and induced the neurite collapse of cortical neurons in neonatal mice. Statistical analysis showed the dose-dependent effect of proBDNF on neurite collapse. proBDNF rapidly activated RhoA without affecting the cdc42 level. Thus, proBDNF inhibits neurite growth *via* activating RhoA in neonatal cortical neurons of mice.



** $p < 0.001$, two-sample t test.

Postsynaptic GABA_A receptor number and enhanced gaboxadol induced change in holding currents in Purkinje cells of the dystrophin-deficient mdx mouse

S.I. Head,¹ S.L. Kueh,² J. Dempster³ and J.W. Morley,^{1,2} ¹School of Medical Science, University of New South Wales, NSW 2052, Australia, ²School of Medicine, University of Western Sydney, NSW 2560, Australia and ³Strathclyde Institute of Pharmacy and Biomedical Sciences, University of Strathclyde, Glasgow, Scotland, UK.

Duchenne muscular dystrophy (DMD) results from an absence of the protein dystrophin. It is characterized by severe wasting of skeletal muscle. In about a third of these patients, there is evidence of an accompanying cognitive and behavioral deficit. In the cerebellum dystrophin is normally localized at the postsynaptic membrane of GABAergic synapses on Purkinje cells. Here, we investigate the effect of an absence of dystrophin on the number of GABA_A channels located at the synapse in cerebellar Purkinje cells of the dystrophin-deficient mdx mouse. Whole-cell patch-clamp recordings of spontaneous miniature inhibitory postsynaptic currents (mIPSCs) were performed in cerebellar slices from mdx and littermate control mice, which had been killed by an halothane according to UNSW ethics guidelines. Using non stationary noise analysis, we found a significant difference in the number of receptors at GABAergic synapses in mdx mice (38.38 ± 2.95 ; n=14) compared to littermate controls (53.03 ± 4.11 ; n=12) ($p = 0.01$). In response to the application of the GABA agonist gaboxadol we found a significant difference in the gaboxadol induced change in holding current in mdx mice (65.01 ± 5.89 pA; n=9) compared to littermate controls (37.36 ± 3.82 pA; n=8). The results show that in cerebellar Purkinje cells of dystrophin-deficient mdx mice there is a reduction in the number of receptors localised at GABAergic synapses, and an increase in extrasynaptic GABA_A receptors, indicating that dystrophin plays an important role in ion channel localization and stabilization at the postsynaptic membrane. If similar changes occur in the CNS in boys with DMD, it may impact on the function of neural networks and contribute to motor, behavioral and cognitive impairment apparent in many boys with DMD.

Huntingtin associated protein 1 associates with amyloid precursor protein and regulates its trafficking and A β levels

X.F. Zhou, G.Z. Yang, J.J. Lu, Y. Lim, J.H. Zhong and M. Yang, Department of Human Physiology and Centre of Neuroscience, Flinders University, Adelaide, SA 5001, Australia.

Amyloid precursor protein (APP) is a type I transmembrane receptor-like molecule involved in the pathogenesis of Alzheimers disease. Following endocytosis, APP is delivered to endosomes, where β - and γ -secretases are localized and A β neurotoxic peptide is produced. Huntingtin associated protein 1(HAP1) is a brain-enriched protein and participates in intracellular trafficking in neurons. HAP1 interacts with kinesin light chain and dynactin p150Glued, regulates the anterograde and retrograde transport of a number of proteins including proBDNF and APP (McGuire *et al.*, 2006). However, how HAP1 regulates APP trafficking and the significance of this regulation remain unknown.

Using HEK 293 cells transfected with HAP1-CFP and APP-YFP plasmids, we showed that these two proteins were highly colocalized. Immunohistochemical data showed that these two proteins are present in a number of brain regions such as cortex, hippocampus and hypothalamus with a similar distribution patterns in the mouse and human brains. Confocal microscopy showed that they also co-exist in a number of subcellular structures. FRET analysis showed that the FRET efficiency between HAP-CFP and APP-YFP was over 20%, much higher than negative and positive controls, indicating these two molecules were close to each other *in vivo*. Immunoprecipitation experiments on over-expressed HEK293 cell lysates or on human brain homogenates showed that HAP1 and APP were present in the immunoprecipitated samples forming a complex. To see whether HAP1 regulates APP subcellular trafficking, we cultured cortical neurons from HAP1^{+/+} and HAP1^{-/-} neonatal mice and analyzed the co-localization of APP with organelles marker proteins. The results showed that APP has a high co-localization ratio with giantin GM130 (cis-Golgi marker), Golgi97 (trans-Golgi complex marker), EEA1 (early endosome marker) and SEC22b (ER-Golgi intermediate compartment marker) in HAP1^{-/-} cortical neurons, but has no significant difference with GRP78 (endoplasmic reticulum marker), CD71 (recycling endosome marker), Lamp1 (lysosome marker) and VPS35 (retromer marker) in neurons between HAP1^{+/+} and HAP1^{-/-} mice. However, there was a lower co-localization ratio between APP and the autophagy marker beclin1 in HAP1^{-/-} neurons, compared with wt neurons. These results suggest that APP is retained in cis-Golgi, trans-Golgi complex, early endosome and ER-Golgi intermediate compartment when HAP1 is deleted, and HAP1 may increase the APP trafficking to autophagy vesicles. Sucrose gradient fractionations on wt and HAP^{-/-} brain homogenates showed that the APP distribution is altered. In the normal wt brain there was only one peak of APP, corresponding to membranous organelles such as Golgi and ER, whereas in the HAP1^{-/-} mice, there were two peaks of APP distribution: one is near to the bottom of the gradient and the other was in the cytosol fractions. Interestingly, GM130, EEA1 and GRP78 had a similar distribution pattern to APP in HAP1^{-/-} mice. APP internalization assay using antibody imaging and biotinylation techniques on HAP1^{-/-} neurons showed that significant alteration in APP endocytosis in HAP1^{-/-} neurons and abnormal re-insertion of APP into the cytoplasmic membrane. Live imaging analysis and FRAP assay on APP-YFP vesicles in HAP1^{-/-} neurons showed that the trafficking speed was reduced and the number of motionless particles were increased. To see whether HAP1 regulates A β production, we cultured cortical neurons from Alzheimers disease mice and knocked down HAP1 protein with interference RNA. We found that the down-regulation of HAP1 increases A β levels.

Taken together, our data suggest that HAP1 associates with APP and regulates APP subcellular trafficking to the non-amyloidogenic pathway. Up-regulation of HAP1 may increase APP re-insertion into cytoplasmic membrane and reduce A β production.

McGuire JR, Rong J, Li SH, Li XJ. (2006) Interaction of Huntingtin-associated protein-1 with kinesin light chain: implications in intracellular trafficking in neurons. *Journal of Biological Chemistry* **281**: 3552-3559.

Huntingtin-associated protein 1 (HAP1) regulates exocytosis via multiple mechanisms

K. Mackenzie, X.F. Zhou and D.J. Keating, Discipline of Human Physiology, Centre of Neuroscience, Flinders University, Sturt Rd, Adelaide, 5042, Australia.

Subcellular localisation and protein interaction data indicate that HAP-1 may be important in vesicle trafficking and microtubule transport. However, no physiological evidence exists to verify this possibility. Our study reports a novel role of HAP-1 as a regulator of exocytosis by influencing the rate of exocytosis, fusion pore dynamics and the size of the readily releasable pool (RRP) which consists of vesicles released immediately upon stimulation. Chromaffin cells from the adrenal gland were used for our exocytosis assays. Cells were cultured from adrenal glands taken from dead 8 week old mice using collagenase (Type A, Roche). Carbon-fibre amperometry was used to investigate exocytosis in single chromaffin cells. We applied +800 mV to a carbon fibre electrode placed on the surface of a single chromaffin cell. We simultaneously measured current caused by the oxidation of released catecholamines and analysed the number of current spikes, representing single exocytotic events, occurring in this time. Chromaffin cells were cultured from HAP-1^{-/-} (KO), HAP-1^{+/-} (Het) and HAP-1^{+/+} (WT) mice. Similar levels of exocytosis triggers by a 70mM K⁺ solution were found in WT (102.2 ± 10.2 exocytotic events, n= 29) and Het (90.8 ± 11.5, n=20) cells while exocytosis in KO cells was significantly reduced (60.4 ± 7.1, n=35) compared to WT ($p<0.01$) or Het ($p<0.05$) cells. The duration of the pre-spike "foot signal", an indicator of fusion pore opening, was found to be prolonged in KO cells (3.0 ± 0.1 ms) compared to WT (2.3 ± 0.1 ms, $p<0.05$) and Het (2.9 ± 0.1 ms, $p<0.05$) cells indicating that HAP-1 may function in stabilizing the formation of the fusion pore. The size of the RRP is also regulated by HAP-1 as the number of vesicles undergoing exocytosis following treatment with a hyperosmotic solution in KO cells (19 ± 5.3, n=7) is less than in WT (54.4 ± 8.9, n=7, $p<0.01$) or Het (46 ± 9.2, n=8, $p<0.05$) cells. Real-time PCR also indicates the downregulation of exocytosis-related genes in KO cells. Our findings implicate, for the first time, the involvement of HAP1 in the regulation of exocytosis at multiple levels including vesicle localisation, membrane fusion and gene transcription.

Circulating ceramide, inflammation and insulin resistance

M.J. Watt,¹ J. Boon,¹ D.C. Henstridge,² J.S. Oakhill,³ B.A. Kingwell² and A.J. Hoy,¹ ¹Biology of Lipid Metabolism Laboratory, Department of Physiology, Monash University, Clayton, VIC 3800, Australia., ²Baker IDI Heart and Diabetes Institute, Melbourne, VIC 3004, Australia and ³St. Vincent's Institute of Medical Research, Fitzroy, VIC 3065, Australia.

Obesity is associated with an increased risk of developing insulin resistance, a condition that precedes the development of type 2 diabetes. Although this relationship is well recognised, the mechanisms linking obesity to insulin resistance remain unresolved. One explanation is that obesity is associated with an 'oversupply' of lipids, which leads to the storage of lipids in tissues such as the liver and skeletal muscle that in turn cause insulin resistance. Another is that obesity is accompanied by low-grade inflammation that negatively impacts on insulin signal transduction. Ceramide accumulation in skeletal muscle is associated with the development of insulin resistance and pharmacological blockade of ceramide ameliorates lipid-induced insulin resistance in obesity (Holland *et al.*, 2007). Ceramides are also known to circulate in plasma, even though they are insoluble in aqueous environments. While plasma ceramides are increased in type 2 diabetes patients (Haus *et al.*, 2009), the mode of ceramide transport *in vivo* and the role of circulating ceramide in the development of insulin resistance and inflammation remains unresolved.

We first assessed ceramide levels in human plasma which was fractionated by fast performance liquid chromatography. The eluted fractions containing lipoproteins were identified by analysis of the ultraviolet absorption spectrum and confirmed by measuring cholesterol in each fraction. Ceramide was transported exclusively by very low density lipoproteins (VLDL, ~10%), low density lipoproteins (LDL, ~50%) and high density lipoproteins (HDL, ~40%). Total plasma ceramide content was increased in obese, type 2 diabetes (T2DM) patients compared with lean, insulin sensitive aged-matched individuals (Lean: 13.8 ± 1.1 vs T2DM: 17.4 ± 1.3 μ M). Ceramides were higher in LDL (55%, $P = 0.006$) of T2DM, but not in VLDL ($P = 0.76$) or HDL ($P = 0.16$). LDL-ceramide was positively associated with insulin resistance (HOMA-IR), fasting insulin and glucose but not body mass index (a marker of adiposity), triglyceride or cholesterol. Thus, LDL-ceramide is associated with insulin resistance in humans.

To assess circulating ceramide function in cell culture, a novel approach was used to replicate the *in vivo* environment by creating LDL containing ceramides. This method depletes the LDL core of neutral lipids which allows for the introduction of ceramide into an intact LDL. LDL-ceramide (either C16:0 or C24:0 ceramide) mildly decreased insulin-stimulated glucose uptake in L6-GLUT4myc myotubes after 24 h treatment (~30%), whereas no effect was observed at 6 h. The reduction in insulin responsiveness was not associated with an impairment in Akt phosphorylation, suggesting no direct effect on distal insulin signalling. Interestingly, intracellular ceramide was increased with LDL-ceramide, although we are unable to provide definitive evidence for receptor-mediated uptake. LDL-ceramide activated pro-inflammatory signalling in RAW 264.7 macrophages, resulting in c-Jun terminal kinase activation and increased TNF- α secretion, but surprisingly, not IL-6 secretion. The conditioned media from LDL-ceramide treated macrophages decreased insulin-stimulated glucose uptake in L6-GLUT4myc myotubes, whereas no effect was observed with LDL conditioned media.

Overall, these results show that ceramides are elevated in the plasma of obese, type 2 diabetes patients and that this is related to insulin resistance, and not adiposity or generalised dyslipidemia. Furthermore, LDL-ceramide can cause insulin resistance in skeletal myotubes, albeit mildly, and activate pro-inflammatory signalling in macrophages, that in turn creates a milieu that decreases insulin sensitivity.

Haus JM, Kashyap SR, Kasumov T, Zhang R, Kelly KR, Defronzo RA & Kirwan JP. (2009). Plasma ceramides are elevated in obese subjects with type 2 diabetes and correlate with the severity of insulin resistance. *Diabetes* **58**, 337-343.

Holland WL, Brozinick JT, Wang LP, Hawkins ED, Sargent KM, Liu Y, Narra K, Hoehn KL, Knotts TA, Siesky A, Nelson DH, Karathanasis SK, Fontenot GK, Birnbaum MJ & Summers SA. (2007). Inhibition of ceramide synthesis ameliorates glucocorticoid-, saturated-fat-, and obesity-induced insulin resistance. *Cell Metabolism* **5**, 167-179.

This study was supported by the NHMRC.

Dual, but opposing, roles for the double stranded RNA-dependent protein kinase in metabolic homeostasis

G.I. Lancaster, Baker IDI Heart and Diabetes Research Institute, 75 Commercial Road, Melbourne, VIC 3004, Australia.

Chronic inflammation is a hallmark of obesity and contributes to the development of numerous diseases, including insulin resistance, Type 2 diabetes, atherosclerosis and cancer. Metabolic and immune signalling pathways are intimately linked and understanding how nutrient excess promotes cellular inflammation is of considerable importance in understanding the pathogenesis of many chronic metabolic diseases. A recent study in *Cell* identified double stranded RNA-dependent protein kinase (PKR) as a core component of a “metabolic inflammasome” linking stress signalling to metabolic disease (Nakamura *et al.*, 2010). Using murine embryonic fibroblasts and macrophages from PKR-deficient mice on an inbred C57BL/6 background our results confirm that PKR is required for the induction of pro-inflammatory responses triggered by nutrient excess. However, and remarkably, PKR-deficient cells had 2 to 3-fold increases in the levels of numerous intracellular lipid types, including diacylglycerol and ceramide, lipid species linked to inflammation and insulin resistance, following treatment with fatty acids.

To examine the *in vivo* consequences of PKR deletion, we placed PKR-deficient and wild type (WT) mice on a high fat diet. PKR knockout (KO) mice had increased total body fat mass, higher leptin levels and increased lipid accumulation in skeletal muscle and liver. Furthermore, high fat fed PKR KO mice were hyperinsulinaemic, glucose intolerant and insulin resistant, compared to WT mice. Gene expression analysis of PKR-deficient and wild type macrophages, skeletal muscle and liver identified marked increases in the levels of the fatty acid transporter (FAT) CD36 and several fatty acid binding proteins (FABP). While we observed significantly greater recruitment of macrophages into the white adipose tissue of PKR KO mice, this was associated with similar levels of the pro-inflammatory genes Tnf and Il6 but higher levels of the anti-inflammatory gene Il10. We conclude that while PKR deletion may confer protection from nutrient excess-driven inflammation, it also promotes lipid accumulation, most likely *via* an increase in the expression of FAT/CD36 and specific FABP. Importantly, *in vivo* excess lipid accumulation appears to be the predominating effect of PKR deletion, leading to exacerbated glucose intolerance and insulin resistance.

Nakamura, T., Furuhashi, M., Li, P., Cao, H., Tuncman, G., Sonenberg, N., Gorgun, C.Z., and Hotamisligil, G.S. (2010). Double-stranded RNA-dependent protein kinase links pathogen sensing with stress and metabolic homeostasis. *Cell* **140**: 338-348.

The emerging role of HDL in glucose metabolism

B.A. Kingwell, A.K. Natoli, M. Reddy-Luthmoodoo, A.L. Carey, A.L. Siebel, D. Sviridov and B.G. Drew, Baker IDI Heart and Diabetes Institute, Melbourne, VIC 3004, Australia. (Introduced by M.J. Watt)

The association of low plasma levels of high-density lipoprotein (HDL) with states of impaired glucose metabolism and type 2 diabetes mellitus is well established, but the mechanistic links remain to be fully elucidated. Recent data from our laboratory (Drew *et al.*, 2009) and others suggests that HDL directly influences glucose metabolism through multiple mechanisms. This presentation will discuss the emerging evidence and mechanisms by which HDL modulates glucose metabolism in the context of the well established actions of HDL.

Low HDL has been traditionally considered an atherosclerotic risk factor on the basis of convincing epidemiology, demonstrating an association with negative cardiovascular outcomes, even at very low levels of LDL. The process of cholesterol removal from peripheral cells such as macrophages, for transport to the liver and subsequent excretion is termed reverse cholesterol transport, and is generally viewed as the most important anti-atherosclerotic action of HDL. However, in addition to reverse cholesterol transport, HDL is now known to convey an impressive spectrum of protective properties including inhibition of inflammation, oxidation and thrombosis, as well as vasodilatation *via* nitric oxide.

Recent experimental and clinical developments linking HDL to glucose metabolism suggest yet another beneficial action of HDL that may have relevance to diabetes. We have shown that HDL elicits reductions in blood glucose in patients with type 2 diabetes (Drew *et al.*, 2009) which likely occurs through multiple actions including stimulation of pancreatic β -cell insulin secretion (Drew *et al.*, 2009; Fryirs *et al.*, 2010) and increased glucose uptake into skeletal muscle *via* activation of the AMP-activated protein kinase (AMPK) signaling pathway (Drew *et al.*, 2009). In addition, given the established role of lipid accumulation and inflammation in the pathogenesis of type 2 diabetes, it is highly likely that the reverse cholesterol transport and anti-inflammatory actions of HDL in metabolic tissues contribute to improved insulin sensitivity and thus glucose homeostasis. We therefore hypothesized that HDL may improve insulin sensitivity *via* lipid removal and anti-inflammatory actions in macrophages associated with excess adiposity/ectopic lipid deposition. A variety of macrophage cell models including RAW 264.7 (mouse), THP-1 (human) and primary human macrophages from healthy participants were incubated separately with an acetylated LDL lipid challenge and then co-treated with either HDL (50 μ g/mL) or vehicle for 18 hours. Fresh conditioned media from macrophage cultures was applied (1:10) to primary human skeletal muscle cell cultures derived from 5 unmedicated patients with type 2 diabetes for 24 hours and insulin-mediated glucose uptake (2-deoxyglucose) measured. In all models, acetylated LDL treatment reduced insulin-mediated glucose uptake to basal levels and co-treatment with HDL restored insulin mediated glucose uptake to control levels. These data suggest that macrophage inflammation associated with excess/ectopic adiposity is reduced by HDL and these effects may contribute to improved insulin sensitivity and glucose homeostasis.

Research in this area is in a preliminary phase, with the potential for HDL elevation to provide metabolic protection yet to be proven in a chronic context. However, findings to date provide fertile ground for mechanistic speculation regarding links between HDL and glucose metabolism in the context of diabetes (where HDL is low and fasting plasma glucose is poorly controlled) and aerobic conditioning (where HDL is high and fasting plasma glucose is tightly controlled). These findings highlight the possibility that HDL-raising therapies already in advanced clinical development for vascular disease may also have efficacy in the prevention and management of type 2 diabetes.

Drew BG, Duffy SJ, Formosa MF, Natoli AK, Henstridge DC, Penfold SA, Thomas WG, Mukhamedova N, de Courten B, Forbes JM, Yap FY, Kaye DM, van Hall G, Febbraio MA, Kemp BE, Sviridov D, Steinberg GR & Kingwell BA. (2009). High-density lipoprotein modulates glucose metabolism in patients with type 2 diabetes mellitus. *Circulation* **119**, 2103-2111.

Fryirs MA, Barter PJ, Appavaroo M, Tuch BE, Tabet F, Heather AK & Rye KA. (2010). Effects of high-density lipoproteins on pancreatic β -cell insulin secretion. *Arteriosclerosis, Thrombosis and Vascular Biology* **30**: 1497 - 1499.

Calorie restriction versus exercise: which produces the best health outcomes?

L.K. Heilbronn,¹ D. Samocha-Bonet,² E. Larsen-Meyer,³ L. Redman,³ A. Civitarese,³ S. Smith³ and E. Ravussin,³
¹Level 6 Eleanor Harrald Building, Discipline of Medicine, The University of Adelaide, Adelaide, SA 5005, Australia, ²Garvan Institute, Darlinghurst, NSW 2010, Australia and ³Pennington Biomedical Research Centre, Baton Rouge, LA 70808-4124, USA. (Introduced by Matt Watt)

The prevalence of obesity is rapidly escalating worldwide and obesity is closely linked to the development of insulin resistance, metabolic syndrome and type 2 diabetes. Negative energy balance is key in reversing the metabolic defects associated with obesity and produces an array of health benefits that cannot be matched by any one drug that is currently on the market. These include improved lipid profiles and insulin sensitivity, reduced ectopic lipid deposition, blood pressure and reduced inflammatory cytokine production. However, the optimal method to achieve negative energy balance is debated. Here I compare studies of reduced energy intake to increased energy expenditure, and in particular focus on the differential effects of these interventions on lean mass preservation, energy metabolism and insulin action.

In free living studies, moderate calorie restriction (CR) nearly always produces greater weight loss, but there is evidence to suggest that aerobic exercise may provide equal or greater health benefits and is better to maintain weight loss following CR. Here, I report findings from the CALERIE studies, where we compared 25% CR versus 12.5% CR plus 12.5% increase in energy expenditure by aerobic exercise training under stringent laboratory conditions for 6-months in healthy overweight individuals. In this study, energy requirements were carefully assessed, all foods were provided for 3.5 months whilst individuals attended weekly training sessions to learn how to accurately count calories, and all of the exercise sessions were conducted under supervision. Under these conditions, CR and CR+EX produced equal energy deficits; and thus equal losses in body weight, subcutaneous fat cell size and subcutaneous, visceral and liver fat stores by MRI. No changes were observed in intramyocellular lipid, but CR+EX led to slightly greater preservation of lean body mass at 3-months, and greater improvements in fitness and insulin sensitivity at 3- and 6-months. Similar results were produced from the CALERIE study conducted at Washington University where participants were randomised to either 20% CR or a 20% increase in physical activity alone.

We also observed that energy expenditure in the 24-hour chamber was reduced more than predicted based on the loss of mass in both CR and CR+EX indicating metabolic adaptation, but there was no change in spontaneous physical activity. Total daily energy expenditure was reduced only in CR, and was greater than was accounted for based on the decrease in sedentary energy expenditure. This suggests that the CR group also reduced daily activity. This result is found following prolonged CR in monkeys, although CR rodents that are given access to a running wheel exercise more than *ad-libitum* fed animals. We also observed that CR and CR+EX produced similar increases in mitochondrial biogenesis and SIRT1 expression in muscle and equivalent reductions in DNA damage, although functional changes in mitochondria were not observed. Interestingly, a recently completed study that we have conducted of high fat overfeeding also produced an increase in mitochondrial biogenesis, despite induction of insulin resistance, lending support to the growing body of evidence that suggests that mitochondrial dysfunction may be a consequence rather than a cause of insulin resistance.

So, should we promote dieting or exercise? This probably depends on whether the goal is weight loss or maximal improvement in health. Without close dietary and exercise support, exercise alone is unlikely to produce much weight loss. However, dieting alone reduces sedentary energy expenditure and physical activity which will promote weight regain over time. We have shown that the combination of CR+EX prevents reductions in total energy expenditure, and may also provide slightly greater health benefits than dieting alone.

Probing the interaction between psalmotoxin 1 and acid sensing ion channel 1a, an analgesic drug target

N.J. Saez,¹ M. Mobli,¹ M. Bieri,³ A.K. Malde,² A.E. Mark,^{1,2} P.R. Gooley,³ L.D. Rash¹ and G.F. King,^{1,2}

¹Institute for Molecular Bioscience, University of Queensland, St Lucia, QLD 4072, Australia, ²School of Chemistry and Molecular Biosciences, University of Queensland, St Lucia, QLD 4072, Australia and

³Department of Biochemistry and Molecular Biology, Bio21 Molecular Science and Biotechnology Institute, University of Melbourne, Parkville, VIC 3010, Australia.

Acid sensing ion channel 1a (ASIC1a) is one of the primary acid sensors in the peripheral and central nervous system, and it has emerged as a novel target for the development of drugs to treat chronic pain, neurodegeneration, and possibly depression (Sluka *et al.*, 2009). The only known selective inhibitor of ASIC1a is psalmotoxin-1 (PcTx1), a 40-residue disulfide-rich peptide isolated from the venom of the Trinidad chevron tarantula *Psalmopoeus cambridgei*. PcTx1 is a potent blocker of ASIC1a (IC₅₀ ~0.5nM) but it does not inhibit other ASIC subtypes (Escoubas *et al.*, 2000). Remarkably, PcTx1 has analgesic activity comparable to morphine in rat models of acute pain (Mazzuca *et al.*, 2007). With a view to using PcTx1 as a lead for development of novel analgesics, we developed an efficient bacterial expression system for production of recombinant toxin and determined a high-precision structure using 3D/4D triple resonance NMR spectroscopy. Site-directed mutagenesis revealed a highly cationic pharmacophore located within one of the intercystine loops. Molecular dynamics simulations in combination with NMR spin relaxation and relaxation dispersion measurements revealed significant motion in this loop over a wide range of timescales (ps to ms), thus precluding the use of rigid body docking protocols for modelling the toxin:channel complex. Instead, we used HADDOCK (Dominguez *et al.*, 2003) to dock the toxin onto a homology model of rat ASIC1a (rASIC1a). Key interacting residues identified from mutagenesis of the toxin and the channel were used as ambiguous interaction restraints and the sidechains of residues at the interaction interface were allowed to move during simulated annealing and refinement. The resulting model of the PcTx1:rASIC1a complex reveals a novel mode of interaction dominated by ion pair interactions involving arginine residues in the β -hairpin loop containing the toxin pharmacophore. The toxin:channel model is currently being used for *in silico* screening of chemical libraries to find nonpeptide mimetics of PcTx1.

Dominguez C, Boelens R & Bonvin AM (2003) *Journal of the American Chemical Society* **125**: 1731-1737.

Escoubas P, De Weille JR, Lecoq A, Diochot S, Waldmann R, Champigny G, Moinier D, Ménez A, Lazdunski M. (2000) *Journal of Biological Chemistry* **275**: 25116-25121.

Mazzuca M, Heurteaux C, Alloui A, Diochot S, Baron A, Voilley N, Blondeau N, Escoubas P, Gélot A, Cupo A, Zimmer A, Zimmer AM, Eschalier A, Lazdunski M. (2007) *Nature Neuroscience* **10**: 943-945.

Sluka KA, Winter OC & Wemmie JA (2009) *Current Opinion in Drug Discovery & Development* **12**: 693-704.

Conotoxins targeting voltage-gated sodium channels: Designing new analgesics

R.S. Norton,^{1,2} K.K. Khoo,^{1,2,3} Z. Kuang,² B.J. Smith,² M.J. Wilson,⁴ M-M. Zhang,⁴ J.E.F. Rivier,⁵ D. Yoshikami,⁴ B.M. Olivera⁴ and G. Bulaj,^{4,6} ¹Monash Institute of Pharmaceutical Sciences, Monash University, Parkville, VIC 3052, Australia, ²The Walter & Eliza Hall Institute of Medical Research, 1G Royal Parade, Parkville, VIC 3052, Australia, ³The Department of Medical Biology, University of Melbourne, Parkville, VIC 3010, Australia, ⁴Department of Biology, University of Utah, Salt Lake City, Utah 84112, USA, ⁵Salk Institute for Biological Studies, La Jolla, CA 92037, USA and ⁶Department of Medicinal Chemistry, College of Pharmacy, University of Utah, Salt Lake City, Utah 84108, USA.

μ -Conotoxins are a group of toxins from predatory marine cone snails that target voltage-gated sodium channels (VGSCs), blocking the passage of sodium ions through the channel. Several neuronal VGSC subtypes have been implicated in the perception of pain; as such, modulators of these subtypes of VGSCs could have potential therapeutic use as analgesics. μ -conotoxin KIIIA (μ -KIIIA) shows potent analgesic activity following its systemic administration in mice (Zhang *et al.*, 2007). Structure-activity studies indicated that the key residues important for VGSC-blocking activity (K7, W8, R10, D11, H12, R14) mostly resided on an alpha-helical motif and that the first disulfide bond could be removed without significant loss of activity (Khoo *et al.*, 2009). These findings suggested a route for minimization of μ -KIIIA by retaining the key residues on an α -helical scaffold.

In stabilizing α -helices, the use of (*i, i+4*) lactam bridges has proven to be a successful approach. For a mimetic of μ -KIIIA, the result that Cys9 can be replaced with no significant loss in activity generates a position in the helix that can be substituted to form a helix stabilizing (*i, i+4*) lactam bridge to either residue 5 or 13, both of which are non-essential residues and are replaceable. We have designed and synthesized several analogues of μ -KIIIA; all of them are truncated at both N- and C-terminal ends, and the remaining sequence is stabilized by a lactam bridge at strategic locations. The helicity of the six lactam analogues has been analysed using NMR spectroscopy and molecular modelling, and their activities have been tested against a range of VGSC subtypes. Our findings highlight important structure-activity relationships and provide a basis for the design of new minimized peptides and helical mimetics as novel analgesics.

Zhang MM, Green BR, Catlin P, Fiedler B, Azam L, Chadwick A, Terlau H, McArthur JR, French RJ, Gulyas J, Rivier JE, Smith BJ, Norton RS, Olivera BM, Yoshikami D, Bulaj G. (2007) *J Biol Chem* **282**, 30699-30706.

Khoo KK, Feng ZP, Smith BJ, Zhang MM, Yoshikami D, Olivera BM, Bulaj G, Norton RS. (2009) *Biochemistry* **48**, 1210-1219.

Subverting the biological actions of *Conus* peptides to modulate physiological responses

R.J. French, Department of Physiology & Pharmacology and Hotchkiss Brain Institute, University of Calgary, Calgary, Alberta T2N 4N1, Canada. (Introduced by David J. Adams)

The peptides from various *Conus* venoms have been grouped by Olivera (1997) into cabals, whose members have synergistic actions even though members of a single cabal may have different targets. For example, members of the motor cabal may inhibit muscle contraction and induce flaccid paralysis by blocking either neuromuscular transmission, or by targeting muscle sodium channels to block the generation of muscle action potentials. On the other hand, different members of the lightning strike cabal appear to induce excitotoxic shock, with rapid-onset rigid paralysis, by inhibition of sodium channel inactivation and by block of voltage-gated potassium channels. Actions of *Conus* peptides, studied in species other than the natural prey, have revealed cases of unexpected and specific targeting which open possibilities for pharmacological modulation of a variety of processes. Examples include certain μ -conotoxins, nominally considered to be members of the motor cabal, which inhibit particular neuronal sodium channel isoforms more strongly than their canonical target from skeletal muscle. Thus, in a mouse model, μ -conotoxin KIIIA has performed more effectively as an analgesic than lidocaine (Zhang *et al.*, 2007). Conkunitzin-S1, a member of the Kunitz inhibitor family of peptides, blocks certain voltage-gated potassium channels (Bayrhuber *et al.*, 2005) and thereby has the potential to enhance electrical bursting activity. The molecular correlates and physiological consequences of these surprising and striking actions are becoming evident.

Bayrhuber M, Vijayan V, Ferber M, Graf R, Korukottu J, Imperial J, Garrett JE, Olivera BM, Terlau H, Zweckstetter M, Becker S. (2005) *Journal of Biology Chemistry* **280**: 23766-70.

Olivera BM (1997) *Molecular Biology of the Cell* **8**: 2101-8.

Zhang MM, Green BR, Catlin P, Fiedler B, Azam L, Chadwick A, Terlau H, McArthur JR, French RJ, Gulyas J, Rivier JE, Smith BJ, Norton RS, Olivera BM, Yoshikami D, Bulaj G (2007) *Journal of Biology Chemistry* **282**: 30699-706.

Calcium, Vc1.1 and $\alpha 9\alpha 10$ nicotinic acetylcholine receptors

M. Chebib, N. Absalom, G. Liang, E. Pera, C. Chu and H-L. Kim, Faculty of Pharmacy A15, The University of Sydney, NSW 2006, Australia.

Nicotinic acetylcholine receptors (nAChRs) are ligand-gated ion channels involved in fast synaptic transmission. nAChRs are pentameric complexes formed from a combination of alpha and beta subunits to form heteromeric channels, or alpha subunits alone in the case of homomeric channels. Stoichiometric differences have been conclusively shown to exist with $\alpha 4\beta 2$ nAChR subtypes ($(\alpha 4)_3(\beta 2)_2$ and $(\alpha 4)_2(\beta 2)_3$) and that calcium permeability differs between the two receptor populations (Tapia *et al.*, 2007). The $\alpha 9\alpha 10$ heteromeric complex is found in inner hair cells, and is potently and selectively inhibited by the conotoxins Vc1.1 and RgIA (Vincler *et al.*, 2006; Halai *et al.*, 2009). It has been shown to exist as one stoichiometric population ($(\alpha 9)_2(\alpha 10)_3$) (Plazas *et al.*, 2005). We have investigated the roles of both stoichiometry of $\alpha 9\alpha 10$ receptors and calcium concentration on conotoxin inhibition of ACh-evoked currents heterologously expressed in *Xenopus* oocytes. We have altered intracellular and extracellular calcium concentrations, and the ratio of $\alpha 9$ and $\alpha 10$ subunit mRNA to change the relative abundance of the subunits to infer stoichiometry. Our data show that Vc1.1, but not RgIA or atropine, inhibits $\alpha 9\alpha 10$ receptors in a biphasic manner under the varying conditions and infer that these receptors exist in at least two stoichiometric forms.

Halai R, Clark RJ, Nevin ST, Jensen JE, Adams DJ, Craik DJ (2009) *Journal of Biological Chemistry* **284**: 20275-84.

Plazas PV, Katz E, Gomez-Casati ME, Bouzat C, Elgoyhen AB. (2005) *Journal of Neuroscience* **25**: 10905-12.

Tapia L, Kuryatov A, Lindstrom J (2007) *Molecular Pharmacology* **71**: 769-776.

Vincler M, Wittenauer S, Parker R, Ellison M, Olivera BM, McIntosh JM (2006) *Proceedings of the National Academy of Sciences USA* **103**: 17880-17884.

Analgesic conotoxins: modulation of voltage-gated calcium channels in pain pathways

D.J. Adams, Health Innovations Research Institute, RMIT University, Melbourne, VIC 3083, Australia.

The small and highly structured peptides found in the venom of marine cone snails target a wide variety of membrane receptors and ion channels in normal and diseased states. A number of these peptides (conotoxins) have shown efficacy *in vivo* including inhibitors of voltage-gated sodium (Na_v) and calcium (Ca_v) channels and nicotinic acetylcholine receptors (nAChRs) which are in preclinical development for the treatment of chronic and neuropathic pain. A number of structurally related ω -conotoxins bind directly to and selectively inhibit N-type calcium channels of nociceptive dorsal root ganglion (DRG) neurons. Among these, ω -conotoxin MVIIA (Prialt) still maintains its orphan drug status as a valuable alternative intrathecal analgesic for the management of chronic intractable pain, especially in patients refractory to opioids. Newly discovered ω -conotoxins from *Conus catus* are more potent and selective for N-type ($\text{Ca}_v2.2$) calcium channels over other Ca_v s (Berecki *et al.*, 2010). Furthermore, in spinal cord slices, these peptides reversibly inhibited excitatory monosynaptic transmission between primary afferents and dorsal horn superficial lamina neurons. In the rat partial sciatic nerve ligation model of neuropathic pain, ω -conotoxins CVIE and CVIF significantly reduced allodynic behaviour. Another family of conotoxins, the α -conotoxins, competitively inhibit nAChRs and bind at the interface between specific subunits allowing them to discriminate among different nAChR subtypes. α -Conotoxins Vc1.1 (ACV1) and RgIA are small disulfide bonded peptides currently in development as a treatment for neuropathic pain (Vincler *et al.*, 2006). It was proposed that the primary target of Vc1.1 and RgIA is the $\alpha 9\alpha 10$ neuronal nAChRs. Surprisingly, however, we found that Vc1.1 and RgIA more potently inhibit the N-type ($\text{Ca}_v2.2$) Ca^{2+} channel currents in rat sensory neurons *via* a voltage-independent mechanism involving the G protein-coupled GABA_B receptor (GABA_BR) (Callaghan *et al.*, 2008). This was the first demonstration of α -conotoxins acting *via* the G protein-coupled GABA_BR modulating native $\text{Ca}_v2.2$ channels. Recent molecular studies confirm that Vc1.1 and RgIA inhibit N-type Ca^{2+} channels *via* GABA_BR activation. Transient transfection of DRG neurons with small interfering RNAs (siRNAs) to knock-down the GABA_BR reduced mRNA levels for GABA_B subunits by >50% compared to control cells and suppressed GABA_BR protein expression. Whole-cell patch clamp recording of DRG neurons conducted 1-3 days after transfection demonstrated that knockdown of functional GABA_BR expression significantly reduced the inhibition of N-type Ca^{2+} channels in response to both baclofen and Vc1.1. This was in contrast to neurons transfected with a non-targeting siRNA which were indistinguishable from untransfected neurons, confirming that α -conotoxin Vc1.1 modulates N-type Ca^{2+} channels *via* activation of GABA_BR in DRG neurons. Our current findings have the potential to introduce a paradigm shift in thinking about the targets of α -conotoxins. GABA_BR may play a critical role in pain pathways and are a clear therapeutic target for these and modified conotoxins.

Berecki G, Motin L, Haythornthwaite A, Vink S, Bansal P, Drinkwater R, Wang CI, Moretta M, Lewis RJ, Alewood PF, Christie MJ, Adams DJ. (2010) *Molecular Pharmacology*, **77**: 139-148.

Callaghan B, Haythornthwaite A, Berecki G, Clark RJ, Craik DJ, Adams DJ. (2008) *Journal of Neuroscience*, **28**: 10943-10951.

Vincler M, Wittenauer S, Parker R, Ellison M, Olivera BM, McIntosh JM. (2006) *Proceedings of the National Academy of Sciences of the USA*, **103**: 17880-17884.

Temporal relationships between intraluminal manometry and actual gut movement in the isolated rabbit small intestine

P.G. Dinning,¹ M. Costa,² J.W. Arkwright,³ S.J. Brookes² and N.J. Spencer,² ¹Department of Gastroenterology, St. George Clinical School, University of New South Wales, Kogarah, NSW 2217, Australia, ²Department of Human Physiology, School of Medicine, Flinders University, PO Box 2100, Adelaide, SA 5001, Australia and ³Material Science and Engineering, CSIRO, West Lindfield, NSW 2070, Australia.

The content of the intestine is propelled by coordinated movements of the muscle layers involving both myogenic and neurogenic mechanisms. The relation between motions of the gut wall and the resulting intraluminal pressure has not been well established. We have investigated this relationship in isolated segments of rabbit small intestine taken from 4 animals killed by i.v. injection of lethobarbital (0.5ml/Kg). Segments of 40 cm were placed into an organ bath containing warm (36°C) oxygenated Krebs solution, constantly bubbled with carbogen gas. Krebs was infused *via* the cannulated oral end at 2-4ml/minute and the contents could be expelled and measured at the anal end *via* a non-return valve. Motions of the intestinal wall was recorded by a video camera placed above the bath. Spatio-temporal maps of changes in diameter (Dmaps) were constructed from the video recordings (Hennig *et al.*, 1999). Spatiotemporal maps of intraluminal pressure (Pmaps) were constructed from high-resolution fibre-optic manometry recordings (Arkwright *et al.*, 2009). The relation between movements and intraluminal pressure were compared during periods of motor activity that occurred spontaneously or elicited by slow distension or by erythromycin (10-6M). A total of 85 minutes of combined Dmaps and Pmaps were analysed. During this period 813 longitudinal muscle contractions, 288 circular muscle contractions in the diameter maps and 1049 pressure events were identified in the pressure maps. All antegrade propagating circular muscle contractions were associated with high pressure waves and with outflow at the anal end indicating propulsive motor activity. Incomplete propagating circular muscle contractions were also associated with pressure waves. In the segment of intestine not invaded by these contractions, peaks of pressure were recorded simultaneously indicating a common cavity. Pressure waves of a much lower amplitude were also associated with spontaneous pendular longitudinal muscle contractions. These results will enable a more appropriate interpretation of manometry *in vivo*.

Hennig GW, Costa M, Chen BN, Brookes SJ. (1999) *Journal of Physiology* **517**: 575-590.

Arkwright JW, Underhill ID, Maunder SA, Blenman N, Szczesniak MM, Wiklendt L, Cook IJ, Lubowski DZ, Dinning PG. (2009) *Optics Express* **17**: 22423-22431.

Gap junction coupling between smooth muscle cells modulates responses to inhibitory motorneurons and exogenous ATP

S.E. Carbone,¹ D.A. Wattchow,² N.J. Spencer¹ and S.J.H. Brookes,¹ ¹Human Physiology and Centre for Neuroscience, Flinders University, Sturt Rd, Bedford Park, SA 5042, Australia and ²Flinders Medical Centre Department of Surgery, Sturt Rd, Bedford Park, SA 5042, Australia.

We have previously reported that electrophysiological responses of gut smooth muscle cells, including inhibitory junction potentials, are absent during the first 30–60 minutes after setting up preparations *in vitro*. Here, we investigated the mechanisms that underlie this temporary unresponsiveness.

Methods: Segments of guinea pig ileum, with mucosa and submucosa removed, were used for intracellular recording under current clamp conditions. Circular smooth muscle cells were impaled with glass micropipettes filled with carboxyfluorescein (5%) and KCl (1M), in Krebs solution (34°C) containing 1 μ M hyoscine and 1 μ M nicardipine to inhibit smooth muscle contractions. We recorded resting membrane potential (RMP), inhibitory junction potentials (IJPs) evoked by single shot stimuli, and responses to ATP applied locally by pressure ejection (140kPa nitrogen pulses, 50–100ms duration, 10mM). Cells were dye-filled by 0.5nA hyperpolarising pulses (50% duty cycle for 2 minutes, followed by 1 minute diffusion). Dissections were carried out in cool Krebs solution (14°C). The start of the equilibration period was considered as being the moment when warmed Krebs solution (35°C) first reached the recording chamber.

Results: The recording chamber warmed to 34–35°C within the first 5 minutes of the equilibration period (n=3), however IJP amplitude was typically less than 1mV for the first 30 minutes (n=12). IJP amplitude then increased gradually so that by 90–120 minutes, IJP amplitude averaged $-11.5\text{mV} \pm 1.6\text{mV}$ (n=12). Cells with IJPs less than 1mV were classed as ‘unequilibrated’ and cells with IJPs greater than 10mV were classed as ‘equilibrated’. ‘Unequilibrated’ cells were significantly hyperpolarised compared to equilibrated cells where RMPs were $-58.8 \pm 1.4\text{mV}$ and $-47.2 \pm 0.4\text{mV}$ respectively (cells=23 and 64, n=12, $p < 0.0001$). Input resistance was significantly greater in ‘unequilibrated’ cells ($15.5 \pm 1.9\text{M}\Omega$) than ‘equilibrated’ cells ($8.7 \pm 0.7\text{M}\Omega$, n=12, $p < 0.0001$). ‘Unequilibrated’ cells showed significantly less dye coupling (mean= 2.1 ± 0.3 carboxyfluorescein-filled profiles) compared to ‘equilibrated’ cells (mean= 4.4 ± 0.3 , n=12, $p < 0.0001$). Addition of gap junction blockers carbenoxolone (100 μ M) and 18 β Glycyrrhetic acid (10 μ M) made “equilibrated” cells change their characteristics back to a state similar to “unequilibrated” cells. In the presence of carbenoxolone, circular smooth muscle cells had a more negative resting membrane potential, smaller IJP amplitude, increased input resistance and reduced dye coupling. Glycyrrhetic acid similarly reduced IJP amplitude, increased input resistance and reduced dye coupling between ‘equilibrated’ cells. These results suggests that gap junction coupling between smooth muscle cells may increase during the equilibration period and may underlie the changes in IJP amplitude. In other cell types, gap junction permeability is reduced by high cytosolic $[\text{Ca}^{2+}]$. We tested whether influx of calcium, during the set-up procedure, might cause uncoupling during the ‘equilibration’ period. Preparations were dissected in low $[\text{Ca}^{2+}]$, high $[\text{Mg}^{2+}]$ Krebs solution (mM: Ca^{2+} 0.25; Mg^{2+} 2.5 at 14°C), and transferred into normal Krebs solution at 35°C for recording. There was no significant reduction of the equilibration period in these preparations. Lastly we tested whether the loss of IJPs during the equilibration period was associated with a loss of sensitivity by smooth muscle cells to ATP; the transmitter of the fast IJP. Hyperpolarisations evoked by local application of 10mM ATP were significantly smaller in ‘unequilibrated’ cells ($0.3 \pm 0.3\text{mV}$) compared to ‘equilibrated’ cells ($-13.0 \pm 1.1\text{mV}$, n=6, $p < 0.0001$), paralleling the change in amplitude of the IJP. This suggests that the loss of neuronal input may be due to a change in electrophysiological properties of the postsynaptic cell during equilibration.

In conclusion, following set-up of dissected gut preparations *in vitro*, smooth muscle cells show significant changes in electrophysiological properties that recover during the “equilibration period”. Smooth muscle cells are hyperpolarised and have a reduced response to inhibitory stimulation either by inhibitory motorneurons or by exogenous application of ATP. During this period gap junction coupling is suppressed. Pharmacologically blocking gap junctions mimics the change in electrophysiological properties during the equilibration period. The change in gap junction coupling does not appear to be due to influx of calcium into smooth muscle cells during the set-up procedure.

KV4 and ANO1 / TMEN16A chloride channel expression profiles distinguish between atypical and typical smooth muscle cells in the mouse renal pelvis

R.J. Lang,¹ J. Iqbal,¹ M.A. Tonta,¹ H.C. Parkington¹ and H. Hashitani,² ¹Department of Physiology, School of Biomedical Sciences, Monash University, Clayton, VIC 3191, Australia and ²Department of Cell Physiology, Nagoya City University Graduate School of Medical Sciences, Nagoya 467-8601, Japan.

Previous intact preparation experiments and calcium imaging have suggested that atypical smooth muscle cells (SMCs) in the proximal renal pelvis are likely to be the pacemaker cells that drive pyeloureteric peristalsis (Lang *et al.*, 2007). However, their electrical characteristics, location and mechanisms of pacemaker generation remain obscure. Standard perforated-patch patch clamp, intracellular microelectrode recording and immunohistochemistry techniques were used. In some experiments a transgenic mouse with enhanced yellow fluorescent protein (eYFP) exclusively expressed in cells containing α -smooth muscle actin (α -SMA) were used.

Single atypical eYFP- α -SMA⁺ SMCs could be distinguished electrophysiologically from typical eYFP- α -SMA⁺ SMCs by the absence of a voltage-operated transient 4-aminopyridine-sensitive ('A-type' KV4) K⁺ current (I_{KA}) and the absence of spontaneous transient outward currents (STOCs) arising from the opening of large conductance Ca²⁺-activated K⁺ (BK) channels. Both typical and atypical SMCs displayed spontaneous transient inward currents (STICs) flowing through niflumic acid (NFA)-sensitive Cl⁻ channels. However, 25% of typical SMCs also displayed a large NFA-sensitive Cl⁻ current which displayed relatively slow kinetics of activation and deactivation, presumably reflecting a relatively high internal Ca²⁺ concentration. Atypical SMCs also fired prolonged large inward currents (LICs), which were cation-selective and blocked by La³⁺ or ryanodine. Immunostaining for ANO1/ TMEN16A Cl⁻ channel subunits was found predominately in the distal regions of the renal pelvis, co-localizing with intense immunostaining for α -SMA. In contrast, α -SMA⁻ interstitial cells (ICs) were distinguished by the presence of a Xe991-sensitive KV7 current, a small I_{KA} current, tetraethylammonium-sensitive BK channel STOCs and Cl⁻-selective STICs blocked by NFA. Intense TMEN16A immunostaining also located to a population of Kit⁻ α -SMA⁻ ICs in the proximal and mid regions of the renal pelvis.

We conclude that (i) KV4⁺, BK STOC⁺, α -SMA⁺ SMCs are the typical SMCs that facilitate muscle wall contraction, (ii) TMEM16A or KV7 immunoreactivity may be useful makers of Kit⁻ ICs in the urogenital tract, and (iii) KV4⁻ α -SMA⁺ atypical SMCs firing cation-selective LICs are likely to be the pelviureteric pacemakers.

Lang RJ, Hashitani H, Tonta, MA, Parkington, HC & Suzuki H. (2007) Spontaneous electrical activity and Ca²⁺ transients in typical and atypical smooth muscles and interstitial cells of Cajal-like cells of mouse renal pelvis. *Journal of Physiology* **583**, 1049-1068

Controlling uterine contractions: the role of interstitial cells

H.C. Parkington,¹ Q. Li,¹ M.A. Tonta,¹ J. Iqbal,¹ M.M. Davies,¹ K.W. Taylor,¹ S.P. Brennecke,² H.A. Coleman,¹ R.J. Lang¹ and P.J. Sheehan,² ¹Department of Physiology, Monash University, Clayton, VIC 3800, Australia. and ²Royal Women's Hospital, Corner Grattan Street and Flemington Road, Parkville, VIC 3052, Australia.

During labour, the smooth muscle cells (SMCs) in the wall of the uterus generate strong, rhythmic contractions that are necessary for vaginal delivery. Such contractions are kept in abeyance before the onset of labour and the transition into labour involves the activation of contraction associated processes. The processes recruited in this switch are incompletely understood. Rhythmic, controlled SM contractions are exquisitely exemplified in the functioning of the gastrointestinal tract. In this location "interstitial cells" (ICs), described initially over 100 years ago by Cajal, play a major role in organ rhythmicity. In the last decade, ICs have also been identified within the wall of the uterus, but their role remains elusive. Here we investigated the role of uterine ICs in late pregnant and labouring human and mouse uterus using a variety of approaches.

Tissues were obtained from women undergoing caesarean delivery. Mice were studied 24 hours before delivery and in labour. Either membrane potential or cytoplasmic Ca^{2+} was recorded simultaneously with tension. In single SMCs and ICs isolated with collagenase, ionic currents were recorded and molecular fingerprinting assessed using single-cell RT-PCR. Cellular localizations of proteins of interest were made using immunohistochemical techniques.

Uterine ICs stained with vimentin but since this can stain several cell types, in human uterine tissue distinction was made between ICs, fibroblasts and immune cells by a co-staining approach. Prolyl 4-hydroxylase, which identifies fibroblasts, co-localized with vimentin in cells that had a small volume around the nucleus, and 2 long slender projections. Unphosphorylated connexin 43 and c-Kit identify ICs, and cells co-staining with these had a large cell volume with 3-5 projections emanating from the nuclear region. CD45, which identifies macrophages, did not co-stain with vimentin. Vimentin staining, in cells located amongst the SMCs, doubled in human tissues obtained during labour ($2.4\pm 0.3\%$) compared with those in late pregnancy but not in labour ($1.3\pm 0.2\%$). Isolated SMCs had a robust large-conductance, Ca^{2+} -activated K^+ current, which was absent from ICs. This was verified in pairs of SMC and IC from 20 women using single-cell RT-PCR.

In mice, vimentin staining did not occur amongst the SMCs in the outer, longitudinal muscle layer, although vimentin staining was observed between SMC bundles in this layer. In contrast, strong vimentin and c-Kit staining occurred amongst the SMC of the inner circular muscle layer, and in the loose tissue between the two muscle layers. This segregation provided as close as might be possible to a natural "IC knock-out" preparation, which we exploited to further probe the role of ICs in uterine pacemaking. Isolated circular strips were always spontaneously contractile, and the SMC had "resting" potentials of -57 ± 3 mV. In contrast, longitudinal strips were always quiescent, with resting potentials of -71 ± 2 mV. In view of the high density of vimentin-staining cells in the loose intermediate region between the two muscle layers, we made circular and longitudinal strips that had: (1) as much intermediate material as possible removed; and (2) as much intermediate material as possible retained. Circular strips with intermediate material attached were spontaneously contractile, while removing this material led to the abolition of this activity. In contrast, longitudinal strips remained quiescent, whether or not intermediate material was present. However, longitudinal strips with intermediate *and* circular muscle remaining attached always contracted spontaneously. These spontaneous contractions in fully intact longitudinal strips were abolished by imatinib (2×10^{-4} M), which putatively blocks c-Kit.

In conclusion, ICs may well play a role in the generation of spontaneous uterine contractions. In mouse uterus, interaction between ICs and circular SMCs appears to be required for full development of pacemaking. In addition, vimentin/c-Kit staining cells appear critical for the spread of contractions between the two muscle layers. The longitudinal muscle is the more important for successful vaginal delivery, while the circular layer appears to play a greater role in generating contractions. In human uterus, the smooth muscle layers are more diffuse and a circular/longitudinal distinction is not evident. The tissue is arranged in thin layers throughout the wall, with the SMC within each layer in the same orientation but with a different orientation in adjacent layers. Here, cells that link the SMCs within this intricately layered network are likely to be critical for organized contraction of the organ, such as is necessary for timely vaginal delivery. ICs may fulfil this role.

Developmental programming following prenatal alcohol exposure: models and mechanisms of disease

K.M. Moritz, School of Biomedical Sciences The University of Queensland St Lucia 4067. (Introduced by Caroline McMillen)

Chronic prenatal exposure to high doses of alcohol can cause a range of developmental abnormalities but whether alcohol causes detrimental effects in the fetus following short term exposure or at low doses is somewhat controversial. Many women cease drinking upon pregnancy recognition but many continue to drink during pregnancy with the pattern of drinking varying from occasional drinking to routine consumption of a low amount of alcohol on a daily basis. In this study we hypothesized that the dose and timing of exposure may be critical in determining both the short and long term effects of alcohol on fetal development and outcomes in offspring.

Thus, we have used the following three rat models of alcohol exposure to explore the immediate and/or long term consequences for the fetus and offspring:

1. High dose binge (HD) in which rats are administered 1mg/kg alcohol (or saline as a control) by oral gavage on days 14 and 15 of pregnancy.
2. Chronic low dose exposure (CL) in which the dam has *ab lib* access to a liquid diet containing 6% alcohol (~15% calories derived from alcohol) or a control diet throughout pregnancy.
3. Periconceptional exposure (PC) where the dam has *ad lib* access to a liquid diet containing 12% alcohol (~30% calories derived from alcohol) from 4 days prior to mating and then for the first 4 days of pregnancy.

Maximal blood alcohol content (BAC) reached approximately 0.11%, 0.03-0.05% and 0.1% in the HD, CL, and PC models respectively. Offspring in the HD model were born growth restricted and remained small throughout lactation but experienced catch up growth after weaning and were of a similar weight to control animals in adulthood. Animals in the CL group were lighter at day 20 of pregnancy but were of similar weight to control animals throughout weaning and early adulthood. Animals in the PC were of a similar weight to controls at day 20 of pregnancy and have yet to be studied as offspring. As adults, both male and female offspring in the HD group had elevated blood pressure (BP, $p < 0.001$) whilst BP was normal in the CL group. Renal function was altered in the HD offspring with males showing an increase in GFR ($p < 0.001$) whilst females showed a decreased GFR ($p < 0.01$). There were alterations in the ability of the CL offspring to concentrate urine following dehydration. Offspring in both the HD and CL groups had a reduced number of nephrons in the kidney (~20-30% reduction compared to controls) when examined using unbiased stereology. In the HD group there were significant changes in genes regulating branching morphogenesis in the fetal kidney whilst apoptosis was elevated in the fetal kidneys of animals in the CL and PC groups. This suggests that kidney development is susceptible to alcohol and that multiple mechanisms may contribute to the impairment in renal development and the subsequent low nephron number. The dose and timing of alcohol exposure is likely to be important in determining the subsequent risk of adult onset disease.

Intrauterine inflammation: effects on fetal lung development

T.J.M. Moss, The Ritchie Centre, Monash Institute of Medical Research. P.O. Box 5418, Clayton, VIC 3168, Australia. (Introduced by Helena Parkington)

Intrauterine infection or inflammation is common in cases of preterm birth, especially those that occur at very early gestational ages. Exposure of the fetus to prenatal infection or inflammation is independently associated with alterations in the risk of several neonatal diseases associated with prematurity. For example, evidence of exposure to infection/inflammation before birth is associated with a reduction in the risk of neonatal respiratory distress syndrome (RDS). This life threatening disease, which accounts for many neonatal deaths, is believed to be due primarily to a lack of pulmonary surfactant. The association between intrauterine inflammation and reduced risk of RDS suggests that prenatal inflammation stimulates fetal pulmonary surfactant production. In studies using sheep we have shown that experimentally induced intrauterine inflammation or infection (induced by amniotic fluid injection of lipopolysaccharide or live ureaplasmas) causes a precocious increase in pulmonary surfactant in the preterm lungs (Moss *et al.*, 2002a; Moss *et al.*, 2008) that improves preterm lung function, consistent with observations of human preterm infants. The effects of intrauterine inflammation appear to result from direct action of proinflammatory stimuli on the fetal lungs (Moss *et al.*, 2002b) rather than by systemic signals, such as stimulation of the fetal hypothalamic-pituitary-adrenal axis and activation of the classical glucocorticoid-mediated lung maturation pathway (Notsos *et al.*, 2002). These initial experiments have focused investigation of responsible mechanisms on local pulmonary factors that might be induced by inflammation and stimulate surfactant production.

A prime candidate for mediating inflammation-induced surfactant production by the preterm lung is prostaglandin E₂ and/or other arachidonic acid metabolites. Prostaglandin E₂ is a fundamental mediator of inflammation; limited available evidence indicates it can induce surfactant production in preterm lungs. Our experiments demonstrate that intrauterine inflammation induces expression of enzymes responsible for prostaglandin production in fetal lung tissue. Lung tissue analyses from these same experiments have demonstrated also that paracrine/autocrine production and/or metabolism of glucocorticoids in fetal lung tissue may occur in response to inflammation, as a result of inflammation-induced changes in expression of 11 β hydroxysteroid dehydrogenase (types 1 and 2). This effect might account for at least some of the changes in fetal lung development induced by inflammation.

In order to address the role of glucocorticoid signaling in the response of the fetal lungs to inflammation, we are inducing intrauterine inflammation in transgenic pregnant mice carrying glucocorticoid receptor knockout fetuses. Consistent with our studies using sheep, intra-amniotic injection of lipopolysaccharide in wild-type mice induces large increases in surfactant protein gene expression in the preterm lungs. Demonstration of this same effect in the GR knockout mice would demonstrate this effect is independent of GR signaling.

The possibility exists that there are previously unknown mechanisms of stimulating surfactant production by the preterm lungs, which might be exploited as novel therapies for preventing respiratory distress syndrome in preterm infants. Elucidation of the effects of inflammation on the fetal lungs and other organs will allow more refined approaches to care of preterm infants exposed to inflammation *in utero*.

- Moss TJ, Knox CL, Kallapur SG, Nitsos I, Theodoropoulos C, Newnham JP, Ikegami M, Jobe AH. (2008) Experimental amniotic fluid infection in sheep: Effects of *Ureaplasma parvum* serovars 3 and 6 on preterm or term fetal sheep. *American Journal of Obstetrics and Gynecology*. **198(1)**: 122.e121-122.e128.
- Moss TJM, Newnham JP, Willett KE, Kramer BW, Jobe AH, Ikegami M. (2002a) Early gestational intra-amniotic endotoxin: Lung function, surfactant, and morphometry. *American Journal of Respiratory and Critical Care Medicine* **165(6)**: 805-811.
- Moss TJM, Nitsos I, Kramer BW, Ikegami M, Newnham JP, Jobe AH. (2002b) Intra-amniotic endotoxin induces lung maturation by direct effects on the developing respiratory tract in preterm sheep. *American Journal of Obstetrics and Gynecology* **187(4)**: 1059-1065.
- Nitsos I, Moss TJM, Cock ML, Harding R, Newnham JP. (2002) Fetal responses to intra-amniotic endotoxin in sheep. *Journal of the Society for Gynecologic Investigation*. **9(2)**: 80-85.

Early origins of cardiovascular disease: The heart of the matter

K. Wang,¹ K.J. Botting,^{1,2} D. A. Brooks,¹ L. Zhang,¹ L. Rattanaray,¹ S. Zhang,¹ J. Duffield,² C. Suter,³ I.C. McMillen¹ and J.L. Morrison,¹ ¹Early Origins of Adult Health Research Group, School of Pharmacy and Medical Sciences, Sansom Institute of Health Research, SA 5001, Australia, ²Discipline of Physiology, University of Adelaide, SA 5001, Australia and ³Victor Chang Cardiac Research Institute, Lowy Packer Building, Liverpool Street, Darlinghurst, NSW 2010, Australia.

Cardiovascular disease currently affects over 3 million Australians. Reduced growth in fetal life together with accelerated growth in childhood results in an increased risk of hypertension and ~50% greater risk of coronary heart disease in adult life. It is unclear why changes in growth patterns in early life lead to a vulnerability to cardiovascular disease. Left ventricular hypertrophy is the strongest predictor of progressive heart disease and poor cardiovascular outcomes in adult life. Pathological ventricular hypertrophy begins as an adaptive response to increase cardiac pump function. However, if this response is prolonged it can lead to dilated cardiomyopathy, heart failure and sudden death. We propose that the mechanisms that support the growth of the heart when substrate supply is restricted during fetal life are the same as those which are recruited to induce pathological hypertrophy in later life. This may explain the vulnerability of the heart to the development of cardiovascular disease as the heart ages and is required to undergo hypertrophy in response to ischemic heart disease or hypertension in order to maintain cardiac output. Insulin-like growth factor 1 (IGF1) has been implicated in the initiation of ventricular hypertrophy. In a range of experimental models, IGF1 acts *via* the IGF1 receptor (IGF1R) both *in vivo* and *in vitro* to increase the size of cardiomyocytes. Recently it has been shown *in vitro* that when the IGF1R signalling pathway is blocked, addition of IGF2 results in an increase in the size of cardiomyocytes. This suggests that IGF2 may act to stimulate heart cell growth through the IGF2 receptor (IGF2R), which is interesting as the IGF2R has traditionally been viewed as a receptor which acts to clear IGF2, rather than as a receptor which is part of a ligand mediated growth pathway.

The adaptation of the fetal heart to a period of reduced substrate supply and decreased body growth has critical consequences for heart health in later life because at birth, the human heart contains most of the cardiomyocytes it will have for life. The growth of the heart in early development initially occurs through the division and hence proliferation of mononucleated cardiomyocytes which then undergo differentiation to form binucleated cardiomyocytes. These cells are unable to divide and heart growth then predominantly occurs through an increase in the size of the binucleated cardiomyocytes (hypertrophy). In a sheep model of intrauterine growth restriction (IUGR), induced by restriction of placental growth, we have investigated the proliferation and growth of cardiomyocytes and the pattern of differentiation of mononucleated to binucleated cardiomyocytes in the fetal heart. We have found that heart mass was maintained relative to fetal body mass, but that there was a relative increase in the size of binucleated cardiomyocytes in the heart of the IUGR sheep fetus. In addition, the low birth weight lamb has increased relative left ventricular weight at 21d of age. We propose that in response to a poor substrate supply in the fetus, the IGF1R signalling pathway plays a protective role in the heart through its anti-apoptotic and angiogenic actions. We also suggest that once up-regulated, the IGF2R signalling pathway mediates cardiomyocyte hypertrophy. This is a novel and significant hypothesis as it places the IGF2R, rather than the IGF1R, signalling pathway as a key mechanism underlying the changes in heart cell growth *in utero* which may contribute to a later vulnerability of the heart to pathological hypertrophy.

Maternal diets rich in fat programme obesity, hypertension and altered sympathetic nervous system activity in adult offspring

J.A. Armitage,^{1,2} L.J. Prior,² S.L. Burke² and G.A. Head,² ¹Department of Anatomy and Developmental Biology, Building 76 Monash University, Wellington Road, Clayton, VIC 3800, Australia and ²Neuropharmacology Laboratory, Baker IDI Heart and Diabetes Institute, PO Box 6492 St Kilda Road Central, Melbourne, VIC 8008, Australia. (Introduced by Janna Morrison)

The prevalence of obesity and related disease are rising rapidly worldwide. The majority of Australian adults are overweight or obese and the cardiovascular and metabolic consequences are predicted to have high financial and social costs. Adult risk factors, genetic predisposition and socioeconomic factors all contribute to the development of obesity and obesity related hypertension however there is compelling evidence that the early life environment also contributes to disease progression. This process is termed “developmental programming” and it is hypothesized that maternal dietary imbalance in pregnancy results in fetal and neonatal adaptations including redistribution of blood flow, altered organogenesis and growth in response to altered nutritional availability later in life (Barker 2001; Armitage, Taylor & Poston, 2005). Maternal obesity, maternal essential fatty acid deprivation (Weisinger *et al.*, 2001), or high fat consumption in pregnancy can programme obesity and hypertension in the offspring (Khan *et al.*, 2003). This programmed obesity related hypertension has been associated with dysfunction of the peripheral vascular, metabolic and renal systems (Armitage *et al.*, 2004). We hypothesized that the hypertension and obesity seen in offspring of fat fed mothers was associated with elevated sympathetic nerve activity and altered hypothalamic responses to peripheral appetite controlling peptides and hormones including leptin and ghrelin, and developed an animal model to test the hypothesis.

Female New-Zealand White rabbits were fed either a control (3.5% fat) or high fat diet (HFD, 13.5% fat) for 3 weeks prior to mating and throughout gestation and lactation. After weaning, all offspring were fed a calorie controlled 3.5% fat diet. At 4 months of age all rabbits were instrumented with intracerebroventricular (icv) cannulae and renal nerve electrodes under isoflurane anaesthesia (Prior *et al.*, 2010). The central ear artery was catheterized and arterial pressure, heart rate and sympathetic nerve activity recorded under basal conditions and in response to a stressful stimulus; a jet of air blowing at 100 L/min was directed at the face for 10 minutes. The cardiovascular and renal sympathetic nerve responses to increasing doses of leptin (recombinant murine leptin Peprtech USA, 5-100ng delivered icv) and ghrelin (human ghrelin Auspep, Melbourne 1-5 nMol, icv) on separate days. Body weight was similar between groups, however HFD offspring (n = 9) had heavier visceral white adipose tissue compared with control offspring (n = 8, $p < 0.05$). Rabbits from fat fed mothers demonstrated greater mean arterial pressure (+7%, $p < 0.05$) tachycardia (+11%, $p < 0.05$) and elevated renal sympathetic activity (+17%, $p < 0.05$) compared with control offspring. The cardiovascular and sympathetic responses to acute stress were similar between groups. Interestingly, although icv administration of ghrelin reduced the pressor, tachycardic and RSNA response to stress in both groups, this reduction in stress responses was abrogated in offspring of fat fed rabbits, compared with controls ($p < 0.05$).

Maternal high fat feeding during pregnancy and suckling results in the development of obesity related hypertension in the offspring. Our results indicate that elevated renal sympathetic activity is associated with the hypertension and that perturbations of the leptin and ghrelin systems in the hypothalamus may underlie the phenotype. Further understanding of which hypothalamic nuclei are affected are the subject of ongoing work.

Armitage JA, Khan IY, Taylor PD, Nathanielsz PW, Poston L. (2004) *Journal of Physiology* **561(2)**: 355-377.

Armitage JA, Taylor PD, Poston L. (2005). *Journal of Physiology* **565(1)**: 3-8.

Barker DJ. (2001). *British Medical Bulletin* **60**: 69-88.

Khan IY, Taylor PD, Dekou V, Seed PT, Lakasing L, Graham D, Dominiczak AF, Hanson MA, Poston L. (2003). *Hypertension* **41(1)**: 168-175.

Prior LJ, Eikelis N, Armitage JA, Davern PJ, Burke SL, Montani JP, Barzel B, Head GA. (2010.) *Hypertension* **55(4)**: 862-868.

Weisinger HS, Armitage JA, Sinclair AJ, Vingrys AJ, Burns PL, Weisinger RS. (2001). *Nature Medicine* **7(3)**: 258-259.

Early life environments and programming of the vascular phenotype

M. Tare, Department of Physiology, Monash University, VIC 3800, Australia.

Disturbances in the early life environment can have life long repercussions on cardiovascular health. Perturbations during critical times in development including fetal and early postnatal life can influence arterial structure and function, predisposing to cardiovascular disease. We have studied the effects of a variety of early life challenges on vascular function. Challenges investigated include vitamin D deficiency, several different models of intrauterine growth restriction, prenatal glucocorticoid or alcohol exposure, and the lactational environment. The striking finding to emerge from this work is that the nature of vascular dysfunction exhibits regional heterogeneity. Vascular mechanisms that are targeted include endothelial function, neuromuscular transmission, smooth muscle reactivity and wall stiffness. Of these mechanisms, we have found that a change in wall stiffness is generally the most consistent indicator that there has been an exposure to an early life insult. Intrauterine growth restriction causes stiffening of the coronary arteries of the fetal sheep. Alcohol exposure in the fetal sheep causes stiffening of arteries across the body. Some insults can also give rise to functionally opposing responses in different vascular beds. For instance, maternal alcohol intake results in endothelial vasodilator dysfunction in coronary arteries and hyperfunction in the mesenteric arteries of fetal sheep. Changes in vascular function that persist into adulthood increase the risk of cardiovascular disease. Seven year old sheep exposed to two days of prenatal glucocorticoids early in pregnancy had significantly increased coronary artery stiffness. Aged rats exposed to vitamin D deficiency during early life had persistent alterations in renal artery function including altered wall stiffness and augmented neurovascular constriction. The early postnatal environment can also influence vascular function. Changes in the lactational environment can either rescue or aggravate disturbances in vascular function caused by prenatal insults. Although not tested in all models, there appears to be sexual dimorphism in the nature and extent of vascular dysfunction, with males tending to have worse outcomes than females. In conclusion, a variety of early life insults can induce adaptations in the developing vasculature that may cause lasting alterations in function. Persistence of vascular dysfunction into adulthood will increase the risk of cardiovascular disease.

Selective loss of visceral pain in the aganglionic rectum of lethal spotted mutant mice

V.P. Zagorodnyuk, M. Kylah, S. Nicholas, S.J.H. Brookes and N.J. Spencer, Department of Human Physiology, Flinders University, GPO Box 2100, Adelaide, SA 5001, Australia.

Aims. Mutations in the gene coding for endothelin 3 each account for approximately 5% of human cases of Hirschsprungs disease. Mice with deletions of endothelin 3, lethal spotted (ls/ls) mouse, show comparable defects - loss of both enteric neurons and ganglia (aganglionosis) in the distal bowel. We have previously established that many extrinsic sensory neurons have transduction sites in enteric ganglia, including low threshold, wide-dynamic range mechanoreceptors (Lynn *et al.*, 2003; Spencer *et al.*, 2008). Preliminary results showed that the visceromotor responses (VMRs) to noxious levels of rectal distension were reduced or absent in ls/ls mice. The aim of this study was to investigate in details extrinsic innervation of colorectum and VMRs in ls/ls mice.

Methods. In anaesthetized mice (200-300 µl of 6 mg/ml of pentobarbital sodium, s.c.), electromyogram recordings were made from the transverse oblique abdominal muscles during noxious rectal distensions (up to 120 mmHg) to activate VMRs. Extrinsic spinal innervation of the mouse colorectum in wild type and ls/ls mice was investigated by retrogradely labelling of DRG neurons with DiI tracer injected into the rectum, by immunohistochemistry to sensory neurons marker, calcitonin gene related peptide (CGRP) and by extracellular recordings from fine rectal nerve trunks *in vitro*.

Results. Intraluminal distension (15-20 s, increments of 20 mmHg), applied to the colorectum of anaesthetized wild type mice, consistently evoked VMRs with a threshold of approximately 20 mmHg, which increased linearly with pressure up to 120 mmHg (n=9). When the same incremental distensions were applied to the aganglionic colorectum of ls/ls mice, no detectable visceromotor responses were elicited (n=11). VMRs evoked by intraluminal distension (20-100 mmHg) of the bladder (n=6) or by somatic stimuli (calibrated pinch to the tail or hind limb, n=14) were not different between wild type and ls/ls mice. We tested whether there was a complete loss of functional pain pathways from the colorectal region of the gut in ls/ls mice. Electrical stimulation (1-20 Hz, 0.4 ms, 60 V, 10 s) applied to the exposed rectum consistently evoked VMRs in both wild type (n=14) and ls/ls mice (n=12). However, responses in mutant mice were significantly smaller ($p<0.001$) than controls. In control mice (n=4), the greatest number of DiI-labelled neurons were located in dorsal root ganglia of S1 and S2, with a small proportion of neurons labelled in L3. In ls/ls mice (n=6), significantly fewer neurons (60-80% loss) were labelled in S1 and S2 than in wild type controls ($p<0.001$). In ls/ls mice (n=4), the aganglionic rectum had a significant reduction in immunoreactivity to CGRP compared with controls (n=4). Stretch-induced firing of low threshold stretch-sensitive afferents in ls/ls mice (n=27) was approximately half that of control mice (n=25, $p<0.0001$) while stretch-induced firing of serosal high threshold afferents did not differ significantly between control (n=14) and mutant (n=17) mice.

Conclusions. The current study has identified that, in addition to colorectal aganglionosis, mice deficient in endothelin 3 also have a selective deficiency in nociception from the aganglionic colorectum. The results revealed a significant reduction in density of spinal sensory innervation of aganglionic rectum and impairment of mechanosensitivity of low threshold, wide-dynamic range mechanoreceptors which together may account for a loss of VMRs in ls/ls mice.

Lynn PA, Olsson C, Zagorodnyuk V, Costa M & Brookes SJ. (2003) Rectal intraganglionic laminar endings are transduction sites of extrinsic mechanoreceptors in the guinea pig rectum. *Gastroenterology* **125**, 786-794.
Spencer NJ, Kerrin A, Singer CA, Hennig GW, Gerthoffer WT & McDonnell O. (2008) Identification of capsaicin-sensitive rectal mechanoreceptors activated by rectal distension in mice. *Neuroscience* **153**, 518-534.

Supported by NH&MRC of Australia grant n 535033.

Purinergic signalling via ATP-gated ion channels mitigates noise-induced hearing loss

G.D. Housley,^{1,2} Y. Sivakumaran,¹ T.L. Loh,¹ S.F. Tadros,¹ A.C.Y. Wong,¹ P.R. Thorne,^{2,3} S.M. Vlajkovic² and A.F. Ryan,⁴ ¹Department of Physiology & Translational Neuroscience Facility, School of Medical Sciences, University of New South Wales, NSW 2052, Australia, ²Department of Physiology, Faculty of Medical and Health Sciences, The University of Auckland, New Zealand, ³Audiology Section, Faculty of Medical and Health Sciences, The University of Auckland, New Zealand and ⁴Departments of Surgery & Neuroscience & VA Medical Center, University of California, San Diego, La Jolla, CA 92093, USA.

We tested the hypothesis that activation of P2X₂ receptor-mediated signal transduction in the cochlea mitigates noise-induced hearing loss (NIHL). ATP-gated ion channels assembled from P2X₂ receptor subunits are expressed by the cochlear sensory hair cells, associated epithelial supporting and secretory cells, and by the spiral ganglion neurons. These sites of expression may be activated by noise-induced release of ATP to affect sound transduction, cochlear electrochemical homeostasis, and auditory neuron excitability (see Housley, Bringmann & Reichenbach, 2009, for a review). This P2X₂ receptor signalling is up-regulated by sustained exposure to high noise levels (Wang *et al.*, 2003), suggesting a potential relationship. Wildtype (WT) and P2X₂ receptor knockout (KO) mice (C57BL/6J background strain) were exposed to two noise conditions: acute - high level noise, and long-term - medium level (environmental) noise. In the case of the acute study (30 minutes, 95 dB SPL, 1 octave (8 – 16 kHz) white noise), hearing sensitivity was measured by auditory brainstem response (ABR) before, immediately after, and then two weeks after the noise exposure, to determine temporary (TTS) and permanent (PTS) threshold shifts.* The WT and KO mice groups had comparable TTS within the noise band, however, the KO mice sustained high frequency PTS. In the second study, WT and KO mice were born into either an acoustically attenuated “quiet” environmental chamber, or an environmental chamber providing exposure to moderate ambient noise (75 dB white noise). After four months, both WT and KO mice in the “noise chamber” had significantly worse hearing than the mice in the “quiet chamber”. However, as seen in the acute noise study, hearing loss in the KO mice extended to higher frequencies than in the WT mice.

Conclusion: In the absence of P2X₂ receptor signalling (KO mice), NIHL in the cochlea is exacerbated for both high-level, short-term noise exposure and long-term moderate noise levels. Thus P2X₂ receptor signalling is oto-protective, providing intrinsic reduction of high-frequency NIHL.

*The mice were anaesthetized using ketamine (40 mg/kg); xylazine (8 mg/kg); acepromazine (0.5 mg/kg) (i.p.) during the ABR measurements following a protocol approved by the UNSW Animal Care and Ethics Committee.

Housley GD, Bringmann A, Reichenbach A (2009) *Trends in Neurosciences* **32**: 128-141.

Wang J C-C, Raybould NP, Luo L, Ryan AF, Cannell MB, Thorne PR, Housley GD (2003) *NeuroReport* **14**: 817-823.

Supported by the National Health & Medical Research Council (Australia).

Extracellular recording of viscerofugal neurons in guinea-pig colon

T.J. Hibberd, N.J. Spencer and S.J.H. Brookes, *Human Physiology and Centre for Neuroscience. School of Medicine. Flinders University, Bedford Park, SA 5042, Australia.*

Viscerofugal neurons have cell bodies in the myenteric plexus of the gut wall and project out of the gut to synapse with postganglionic sympathetic neurons in the abdominal prevertebral ganglia. Noradrenergic sympathetic neurons in turn project back into the gut, where they inhibit transmitter release from enteric neurons. This reflex circuit, when activated by mechanical and chemical stimulation of the intestine, causes inhibition of gut motility and secretion. Much of our current understanding of viscerofugal neurons has been deduced from intracellular recordings of cholinergic synaptic input onto sympathetic nerve cell bodies, where many viscerofugal terminals synapse. Direct extracellular recordings from axons of viscerofugal neurons, from mesenteric nerves, would make possible more detailed investigation of their physiology. However, this has not been possible to date because of the presence of spinal sensory neurons within the same nerve trunks. Previously, we have reported that maintaining preparations of guinea pig distal colon in organotypic culture for a period of 3-5 days causes degeneration of extrinsic nerve fibres which have been severed from their cell bodies. In these preparations, viscerofugal neurons and their axons survive and we were able to make direct extracellular electrophysiological recordings from identified viscerofugal axons. Our current aim was to determine whether axons of viscerofugal neurons could be recorded in mesenteric nerves in acute preparations (that had not been organ-cultured).

Methods: Close extracellular recordings from colonic nerve trunks were made from flat sheet preparations of guinea pig distal colon freshly removed from humanely killed guinea pigs. Preparations were studied *in vitro*, after removal of the mucosa, sub-mucosa and circular muscle layers. The nicotinic receptor agonist, DMPP, was ejected onto myenteric ganglia through a micropipette (5-10 μ m tip) using nitrogen pulses (100kPa, 10-40ms). Putative viscerofugal nerve cell body locations were identified when DMPP-stimulation of a ganglion evoked a burst of action potentials in the recorded colonic nerve. Ganglia were classified as responsive or non-responsive (to DMPP) and the results were mapped onto a printed micrograph of the preparation. The recorded nerve trunk was then filled with biotinamide and locations of viscerofugal nerve cell bodies projecting into the recorded nerve trunk were mapped.

Results: DMPP-sensitive sites were significantly associated with the presence of viscerofugal nerve cell bodies. In ten mapped preparations, 16 of 24 ganglia containing viscerofugal nerve cell bodies were DMPP-sensitive. Conversely, 158 of 162 ganglia without viscerofugal nerve cell bodies were non-responsive to DMPP. This association was highly significant ($p < 0.001$). In responsive ganglia, spritzes of DMPP evoked bursts of action potentials from 100-1000ms in duration, typically of small amplitude (<200 μ V peak-to-peak). In many cases, single units could be discriminated with firing rates at up to 50Hz. None of the DMPP-responsive units were activated by capsaicin.

Conclusion: Single unit recordings of viscerofugal neurons can be made using standard intracellular recording techniques *in vitro*. Identified axons of viscerofugal neurons are abundant in colonic nerves and can be distinguished with high reliability by their responses to localised application of a nicotinic agonist. This result paves the way for detailed characterisation of viscerofugal neuron activity.

Cardiac SR Ca²⁺ release channels and adrenergic stimulation

D.R. Laver,¹ J. Li,¹ N.A. Beard,² A.F. Dulhunty² and D.F. van Helden,¹ ¹School of Biomedical Sciences and Pharmacy, University of Newcastle and HMRI, Callaghan, NSW 2308, Australia and ²John Curtin School of Medical Research, Australian National University, Canberra, ACT 0200, Australia.

Adrenergic stimulation of the heart involves phosphorylation of many intracellular Ca²⁺ handling proteins including the ryanodine receptor Ca²⁺ release channels (RyRs) in the SR. It is known that RyRs can be phosphorylated at three serine residues at 2808, 2814 and 2030 (Huke & Bers, 2008) and that phosphorylation of RyRs *via* PKA causes an increase in RyR activity cardiomyocytes. However, little is known about how phosphorylation of RyRs alters their regulation by intracellular Ca²⁺ and our aim was to explore this physiologically important question.

In our experiments, RyRs were isolated from rat hearts, which had been rapidly removed, perfused with Krebs buffer in a Langendorff apparatus. One group of hearts was perfused with 1 μmol/l isoproterenol (β1- and β2-adrenergic agonist) and the other group without (control) and immediately snap frozen in liquid N₂ in order to capture their state of phosphorylation. SR vesicles containing RyRs were isolated from the heart tissues as previously described for sheep heart (Laver *et al.*, 1995). The buffers used for RyR isolation also contained 20 mmol/l NaF to prevent dephosphorylation of RyRs by endogenous phosphatases. This approach allowed the RyRs to be phosphorylated by the physiological signalling processes resulting from adrenergic stimulation of cardiomyocytes. RyRs were incorporated into artificial planar lipid bilayers and their activity was measured using single channel recording in the presence of a range of luminal and cytoplasmic [Ca²⁺]. Western Blots were used to determine RyR phosphorylation state.

Adrenergic stimulation of rat hearts caused an increase in heart rate from 278±16 to 460±35 (n=6) which was sustained for 1 min prior to freezing. This stimulation caused an increase in phosphorylation at S2808 without any change at S2814 and S2030. The activity of RyRs from isoproterenol stimulated hearts (ISO RyRs, n=25) was 3-fold higher than control RyRs (n=24) at diastolic [Ca²⁺] (100 nmol/l) but was not significantly different at systolic [Ca²⁺] (>1 μmol/l). At diastolic [Ca²⁺], addition of Protein Phosphatase1 (PP1, 5 min) reduced the activity of ISO RyRs by 98 ± 2.6% (n=4) and control RyRs by 70 ± 20% (n=4) but this treatment had no effect at systolic [Ca²⁺]. ISO RyRs displayed a 100-fold channel-to-channel variation in activity which was larger than, and encompassed, the range of activity seen for control RyRs and PP1 treated RyRs. A subpopulation of ISO RyRs (13 of 25) were typical of control RyRs hearts and another, excited subpopulation (8 of 25), had 10-fold higher opening rates.

The effects of adrenergic stimulation on RyR2 regulation by cytoplasmic and luminal Ca²⁺ were accurately fitted by a model based on a tetrameric RyR structure with four Ca²⁺ sensing mechanisms on each subunit (Laver, 2007; Laver & Honen, 2008). Phosphorylation did not alter the ion binding affinities for these sites. Rather, it increased channel opening rate and decreased the channel closing rate associated with Ca²⁺ binding to the cytoplasmic and luminal activation sites.

The results indicate that: 1) Adrenergic stimulation causes a rapid increase in phosphorylation at S2808; 2) which increases RyR2 activity during diastole but not during systole; 3) RyRs show large channel-to-channel variations in activity most likely as a result of varying degrees of phosphorylation at S2808; and 4) adrenergic stimulation increases the proportion of phosphorylated RyRs in the SR. The increase in RyR2 activity will contribute to an increase in the frequency of the SR Ca²⁺ uptake-release cycle which in turn generates the increased heart rate seen during exercise and stress.

Huke S, Bers DM. (2008). Ryanodine receptor phosphorylation at Serine 2030, 2808 and 2814 in rat cardiomyocytes. *Biochemistry and Biophysical Research Communications* **376**: 80-85.

Laver DR, Roden LD, Ahern GP, Eager KR, Junankar PR, Dulhunty AF. (1995). Cytoplasmic Ca²⁺ inhibits the ryanodine receptor from cardiac muscle. *Journal of Membrane Biology* **147**:: 7-22.

Laver DR. Ca²⁺ (2007) Stores regulate ryanodine receptor Ca²⁺ release channels via luminal and cytosolic Ca²⁺ sites. *Biophysical Journal*, **92**: 3541-3555.

Laver DR, Honen BN. (2008) Luminal Mg²⁺, a key factor controlling RyR2-mediated Ca²⁺ release: Cytoplasmic and luminal regulation modelled in a tetrameric channel. *Journal of General Physiology*, **132**: 429-446.

Cardiac ischemic stress: Ca²⁺ and sex scenarios

J.R. Bell and L.M.D. Delbridge, Cardiac Phenomics, University of Melbourne, VIC 3010, Australia.

Important sex differences exist in cardiovascular heart disease, and much of this differential is cardiac specific. Pre-menopausal women are protected from ischemic heart disease compared with age-matched men, but prevalence increases steadily post-menopause. There is growing awareness of the extent to which cardiac function can be influenced by sex and sex hormones, however the fundamental mechanisms responsible for these sex differences are not well understood. Female and male cardiomyocytes exhibit markedly different calcium (Ca²⁺) handling characteristics which reflect the influences of endogenous levels of sex steroids on myocyte Ca²⁺ transport mechanisms. Experimental studies show that, compared with males, female myocytes operate on a relatively low Ca²⁺ cycling load, with Ca²⁺ entry through L-type channels reduced and sarcoplasmic reticulum Ca²⁺ cycling downregulated. Overall, diastolic and systolic Ca²⁺ operational levels are higher in male myocytes – with endogenous estrogen and testosterone playing reciprocal regulatory roles in maintaining this difference. Ca²⁺ is a major causative factor in many of the pathologies associated with ischemia/reperfusion, including arrhythmogenesis, contractile dysfunction and multiple forms of cardiomyocyte death. Ca²⁺ overload triggers hypercontracture and activates calpain, leading to sarcolemmal rupture and a loss of cell integrity. It also promotes mitochondrial Ca²⁺ loading, causing the mitochondrial permeability transition pore to open. Subsequent mitochondrial swelling leads to cytochrome c release and caspase-mediated apoptosis. With more severe ischemic insults, an uncoupling of the mitochondria depletes ATP levels and necrotic injury occurs. Evidence suggests Ca²⁺ also triggers autophagy, though whether this is responsible for ischemia-induced autophagy is yet to be resolved. Limiting Ca²⁺ loading in ischemia/reperfusion substantially improves post-ischemic outcomes. The extent of Ca²⁺ overload is partly mediated by the actions of Ca²⁺/calmodulin-dependent protein kinase (CaMKII). Responsive to fluctuations in Ca²⁺, CaMKII functionally modulates many ion channels and transporters within the cardiomyocyte. Hence, an initial rise in Ca²⁺ levels during ischemia activates CaMKII, augmenting Ca²⁺ entry and increasing intracellular Ca²⁺. Male only studies have shown that inhibiting CaMKII during ischemia/reperfusion reduces Ca²⁺ overload and attenuates apoptotic and necrotic cardiomyocyte death. We hypothesized that the lower operational levels of Ca²⁺ in female cardiomyocytes may limit the influence of CaMKII in ischemia/reperfusion injury and mediate the cardioprotection afforded to female hearts. We have recently shown CaMKII-mediated injury in simulated ischemia/reperfusion is attenuated in female myocytes. CaMKII inhibition (KN93) markedly enhanced male myocyte survival after a simulated ischemic event, but had only marginal effects on the more resilient female myocytes. Further studies will discern the fundamental mechanisms of this sex differential and how it may be modulated in complex disease settings (cardiac hypertrophy, diabetes).

Cardiomyopathies: When is Ca²⁺ the culprit?

M. Ward, Department of Physiology, FMHS, University of Auckland, Auckland 1142, New Zealand..

The coordinated contraction and relaxation of the heart that allows it to function as a pump arises from transient changes in the concentration of Ca²⁺ within the myocytes. Influx of Ca²⁺ during the cardiac action potential triggers release from the intracellular Ca²⁺ store (the sarcoplasmic reticulum, or SR), rapidly increasing the cytosolic [Ca²⁺] ~10-fold. Ca²⁺ then activates cross-bridge cycling, and force production, by binding to the regulatory sites on troponin C. Relaxation takes place when the [Ca²⁺] returns again to resting levels as it is removed from the cytosol by two principle transport mechanisms: re-uptake into the SR by the Ca²⁺-ATPase (SERCA2a); and transport across the sarcolemma (SL) by the Na⁺/Ca²⁺ exchanger (NCX). Given the key role of Ca²⁺ in the mechanical activity of the heart, it is not surprising that Ca²⁺ mis-handling is often implicated in cardiomyopathies where force production is compromised. However, many other changes also occur in hearts *en route* to failure, such as extracellular matrix remodelling and increased β -adrenergic stimulation. The impact of these changes on a beat-to-beat basis remains unclear, particularly since most studies only examine force and Ca²⁺ during steady-state, or single beat responses. In this study, we utilised an animal model of hypertensive failure to gain insights into Ca²⁺ homeostasis in the recovery from non-steady-state interventions in isolated left ventricular preparations.

Measurements of isometric force and [Ca²⁺]_i were made at 37°C in left ventricular trabeculae from failing spontaneously hypertensive rat (SHR) hearts, and their normotensive Wistar-Kyoto (WKY) controls. At 1Hz, peak stress was reduced in SHR (14.5 ± 2.4 mN mm⁻² versus 22.5 ± 6.7 mN mm⁻² for WKY), although the Ca²⁺ transients were bigger (peak [Ca²⁺]_i 0.60 ± 0.08 μ M versus 0.38 ± 0.03 μ M for WKY) with a slower decay of fluorescence (time constant 0.105 ± 0.005 s versus 0.093 ± 0.002 s for WKY). Two experimental protocols were used to potentiate force as a probe of dynamic Ca²⁺ cycling: (i) an interval of 30s rest, and (ii) a 30s train of paired-pulses, and the recirculation fraction (RF) calculated for recovery to steady-state. No difference was found between rat strains for RF calculated from either peak force or Ca²⁺, although the RF was dependent on potentiation protocol. Since SR uptake is slower in SHR, the lack of change in RF must be due to a parallel decrease in trans-sarcolemmal Ca²⁺ extrusion. This view was supported by a slower decay of caffeine-induced Ca²⁺ transients in SHR trabeculae. Confocal analysis of LV free wall showed t-tubules were distorted in SHR myocytes, with reduced intensity of SERCA2a and NCX labelling in comparison to WKY.

Defining the roles of Ca²⁺ entry in endothelin-1 and thromboxane A₂ receptor mediated vascular contractile responses

Y.Y. Chan, N. Scrimgeour, G.Y. Rychkov and D.P. Wilson, *Discipline of Physiology, School of Medical Sciences, University of Adelaide, SA 5000, Australia.*

Introduction: Ca²⁺ is an important mediator of vascular contractility, which can enter the cytosol through voltage-gated L- and T-channels and intracellular SR Ca²⁺ release. Upon depletion of the SR Ca²⁺ store, Ca²⁺-release activated Ca²⁺ (CRAC) channels, which are composed of plasma membrane bound Orai1 and SR-bound STIM1, form functional channels, allowing store refilling. Although endothelin-1 (ET-1) and thromboxane A₂ are both potent vasoconstrictors implicated in various vascular disease states, they mediate Ca²⁺ entry and vasoconstriction through uniquely different mechanisms.

Aim and Method: To identify the role of IP3 receptors, CRAC-, L- and T-channels in ET-1 and thromboxane A₂-mediated vasoconstriction. Using an *in vitro* rat artery model, functional vascular myography coupled with patch clamp analysis were used to identify the activation and inhibition of Ca²⁺ entry pathways mediated by agonists and pharmacological inhibitors of ion channels, respectively.

Results: Brief sequestration of extracellular Ca²⁺ using EGTA (5mM) revealed that approximately 20% ET-1-mediated vasoconstriction involved IP3-mediated SR Ca²⁺ ($p < 0.05$; $n = 4$). Following SR Ca²⁺ depletion using cyclopiazonic acid (10mM) (a SERCA pump inhibitor) and 2-aminoethyl diphenyl borate (100mM) (which is known to block IP3 receptors, CRAC channels and potentially non-selective cation channels), vascular contractility was abrogated ($P < 0.05$; $n = 4$), indicating a role for both IP3 receptors and CRAC channels. Blocking extracellular Ca²⁺ entry using combined L-/T-channel blockers, mibefradil (1mM) ($p < 0.05$; $n = 7$) and efonidipine (0.021mM) ($p < 0.05$; $n = 13$) attenuated approximately 65% ET-1-mediated vasoconstriction in the microvasculature (Ball *et al.*, 2009). Patch clamp analysis of I_{CRAC} has revealed that in addition to blocking L- and T-channels, both mibefradil and efonidipine also inhibited CRAC channels. In contrast, thromboxane A₂-mediated vasoconstriction only involved Ca²⁺ entry through L-channels and RhoA-Rho kinase Ca²⁺-independent sensitization and does not involve IP3 receptors, T or CRAC channels.

Conclusion: In the microvasculature, ET-1 mediates Ca²⁺ entry *via* L, T, IP3 receptors and CRAC channels. In contrast to the traditional L-type Ca²⁺ channel blockers, the more recently developed combined L-/T-channel blockers may provide additional benefit through blockade of CRAC channels, which may effectively enable clinical modulation of SR Ca²⁺ release.

Ball CJ, Wilson DP, Turner SP, Saint DA, Beltrame JF. (2009) Heterogeneity of L- and T-channels in the vasculature: Rationale for the efficacy of combined L- and T-blockade. *Hypertension* **53**: 654-660.

The role of G-CSF in the growth and development of skeletal muscle cells *in vitro*

C.R. Wright,¹ E.L. Brown,¹ A.C. Ward² and A.P. Russell,¹ ¹Centre for Physical Activity and Nutrition Research, School of Exercise and Nutrition Sciences, Deakin University, 221 Burwood Hwy, Burwood, VIC 3125, Australia and ²School of Medicine, Deakin University, Pigdons Road, Geelong, VIC 3217, Australia.

Background: Granulocyte-Colony Stimulating Factor (G-CSF) is a cytokine which stimulates the production of hematopoietic stem cells from bone marrow. Since its discovery and approval for clinical use, various roles for G-CSF outside the hematopoietic system have emerged. Recently, G-CSF treatment has been shown to increase skeletal muscle mass, strength and regeneration in rodent models of muscle disease and damage (Stratos *et al.*, 2007; Pitzer *et al.*, 2008). However, the molecular mechanisms underlining these responses are poorly understood. In cells expressing the G-CSF Receptor (G-CSFR), ligand binding activates several intracellular signalling cascades such as JAK/STAT, Akt, and ERK1/2 (Liongue *et al.*, 2009). These signalling pathways are of vital importance in the regulation of skeletal muscle during hypertrophy, atrophy and regeneration. However, it is unknown whether the G-CSFR is expressed in skeletal muscle, or if these signalling pathways are activated in response to G-CSF treatment.

Methods: *RT-PCR:* mRNA expression for the G-CSFR was determined by RT-PCR. The resulting PCR fragment was separated and purified from a 2% Agarose gel and sequenced. *Western Blotting:* Protein was separated on a polyacrylamide gel and transferred to PVDF membrane. The membrane was probed for the proteins of interest. *Proliferation:* C₂C₁₂ proliferation was measured by the BrdU Labelling and Detection Kit III (Roche), according the manufacturers instructions. *Protein Degradation / Synthesis:* Protein synthesis and degradation was determined by the amount of radio-labelled H³-tyrosine incorporated and released from the cells, respectively.

Results: The expression of the G-CSFR was detected in C₂C₁₂ cultures by RT-PCR and western blotting, as well as in mouse and human muscle by western blotting and immunofluorescence. 30 min G-CSF (4ng/ml, 40ng/ml) treatment in C₂C₁₂ myotubes increased the phosphorylation of STAT3. Preliminary data showed Akt and ERK1/2 phosphorylation was also increased. However, the rate of proliferation, protein synthesis and protein degradation remained unchanged under basal and catabolic conditions.

Summary/Conclusion: The expression of the G-CSFR in skeletal muscle suggests that G-CSF/G-CSFR may be of importance to muscle physiology. Activation of STAT3 signalling, and the potential activation of Akt and ERK1/2 in C₂C₁₂ myotubes, elicits potential signalling pathways for G-CSF/G-CSFR in skeletal muscle. However, a functional outcome remains elusive.

- Liongue C, Wright C, Russell AP & Ward AC. (2009). Granulocyte colony-stimulating factor receptor: stimulating granulopoiesis and much more. *International Journal of Biochemistry and Cell Biology* **41**, 2372-2375.
- Peterson JM & Pizza FX. (2009). Cytokines derived from cultured skeletal muscle cells after mechanical strain promote neutrophil chemotaxis in vitro. *Journal of Applied Physiology (Bethesda, Md. 1985)* **106**, 130-137.
- Pitzer C, Kruger C, Plaas C, Kirsch F, Dittgen T, Muller R, Laage R, Kastner S, Suess S, Spoelgen R, Henriques A, Ehrenreich H, Schabitz WR, Bach A & Schneider A. (2008). Granulocyte-colony stimulating factor improves outcome in a mouse model of amyotrophic lateral sclerosis. *Brain* **131**, 3335-3347.
- Stratos I, Rotter R, Eipel C, Mittlmeier T & Vollmar B. (2007). Granulocyte-colony stimulating factor enhances muscle proliferation and strength following skeletal muscle injury in rats. *Journal of Applied Physiology (Bethesda, Md. 1985)* **103**, 1857-1863.

β_2 -adrenoceptors are the dominant subtype involved in early muscle regeneration after injury

J.E. Church,¹ J. Trieu,¹ P. Moore,¹ P. Gregorevic² and G.S. Lynch,¹ ¹Basic and Clinical Myology Laboratory, Department of Physiology, The University of Melbourne, VIC 3010, Australia and ²Laboratory for Muscle Research & Therapeutics Development, Baker IDI, PO Box 6492, St Kilda Road Central, VIC 8008, Australia.

Skeletal muscles can be injured by a myriad of insults that can compromise their functional capacity. Regenerative processes are often slow and incomplete, and so developing novel therapeutic strategies to enhance muscle regeneration represents an important research area. We have shown previously that the β -adrenoceptor (AR) signalling pathway plays an important role in skeletal muscle regeneration after injury (Beitzel *et al.*, 2004, 2007), and that transgenic mice lacking both β_1 - and β_2 -ARs have delayed regeneration following myotoxic injury (Sheorey *et al.*, 2008). In the present study we investigated the contribution of β -AR signalling to early muscle regeneration, to determine the relative contribution of individual β -AR subtypes to muscle repair after injury.

Mice (8-9 weeks) lacking β_1 -adrenoceptors (β_1 -AR KO), β_2 -adrenoceptors (β_2 -AR KO), or both subtypes of β -adrenoceptors (β_1/β_2 -AR KO), were obtained from The Jackson Laboratory (Bar Harbour, ME, USA). Littermate wildtype mice were used as controls for the β_1 -AR KO and β_2 -AR KO mice, while control mice for the β_1/β_2 -AR KO mice were from a C57BL/6 background, as employed previously (Sheorey *et al.*, 2008). Muscle function was determined by assessing the contractile properties of the *tibialis anterior* (TA) muscle *in situ* (Gehrig *et al.*, 2010). Briefly, mice were anaesthetised (60 mg/kg, sodium pentobarbital, *i.p.*), the right TA muscle was surgically exposed, and the distal tendon was attached to the lever arm of a force transducer, with the knee and foot immobilised. At the conclusion of the experiment the mice were killed by cardiac excision while still anaesthetised deeply.

When muscle function was examined in uninjured TA muscles, both β_2 -AR KO mice and β_1/β_2 -AR KO mice produced significantly less force than their respective controls ($p < 0.05$), however, TA muscles from β_1 -AR KO mice showed no significant deficit in force production. To determine the relative contribution of the individual β -AR subtypes to early muscle regeneration, mice were anaesthetised (ketamine 80 mg/kg and xylazine 10 mg/kg; *i.p.*) and the TA muscle of the right hindlimb was injected with the myotoxin, Notexin (1 μ g/ml, *i.m.*) to cause complete muscle fibre degeneration. Mice were allowed to recover for 7, 10 or 14 days, after which TA function was assessed *in situ*. β_1/β_2 -AR KO mice produced significantly less force than their controls at 7 days post-injury ($p < 0.05$) but force production had increased to similar levels as control at 10 and 14 days post-injury. Muscles from β_2 -AR KO mice showed a similar pattern of force production during regeneration with significantly less force at 7 days but similar force production at 10 and 14 days post-injury, while muscles from β_1 -AR KO mice did not exhibit force deficits at any stage during regeneration.

These results suggest that the β_2 -adrenoceptor is the dominant β -AR subtype involved in early muscle fibre regeneration. Selective stimulation of β_2 -adrenoceptors may therefore be a therapeutic strategy to improve the rate, extent and efficacy of the regenerative process, and may have important implications for other conditions where muscle wasting and weakness are indicated.

Beitzel F, Gregorevic P, Ryall JG, Plant DR, Sillence MN & Lynch GS. (2004) *Journal of Applied Physiology* **96**: 1385-1392.

Beitzel F, Sillence MN & Lynch GS. (2007) *American Journal of Physiology, Endocrinology and Metabolism* **293**: E932-940.

Gehrig SM, Koopman R, Naim T, Tjoakarfa C, Lynch GS. (2010) *American Journal of Pathology* **176**: 29-33.

Sheorey R, Ryall JG, Church JE & Lynch GS. (2008) *Proceedings of the Australian Physiological and Pharmacological Society* **39**: 76P.

Supported by the NHMRC (project grant #509313)

Muscle-specific heat shock protein 72 (HSP72) overexpression improves muscle structure and function in dystrophic *mdx* mice

S.M. Gehrig,¹ T.A. Sayer,¹ C. van der Poel,¹ D. Henstridge,² J.D. Schertzer,¹ J.E. Church,¹ M.A. Febbraio² and G.S. Lynch,¹ ¹Basic and Clinical Myology Laboratory, Department of Physiology, The University of Melbourne, VIC 3010, Australia and ²Cellular and Molecular Metabolism Laboratory, Baker IDI, PO Box 6492, St Kilda Road Central, VIC 8008, Australia.

Duchenne muscular dystrophy (DMD) is the most severe of the muscular dystrophies, affecting 1 in 3,500 live male births. Affected patients generally die in their twenties, with respiratory and/or cardiac failure ultimately causing death in most cases (Finsterer, 2006). Absence of the dystrophin protein results in muscle fibre fragility, whereby contractions result in membrane tears and Ca²⁺ influx. Coupled with abnormalities in intracellular Ca²⁺ handling, this results in an elevated cytosolic [Ca²⁺], resulting in the subsequent activation of degenerative pathways. Chronic muscle fibre degeneration and increasingly ineffective regeneration results in fibrotic tissue infiltration leading to major functional impairments in DMD patients. Heat shock protein 72 (HSP72) has been shown to protect contractile function and improve calcium handling dynamics under conditions of stress in cardiac muscle (Kim *et al.*, 2006). We tested the hypothesis that HSP72 overexpression would ameliorate the dystrophic pathology and thus preserve muscle function in *mdx* dystrophic mice.

Female *mdx* mice were crossed with male mice expressing a rat inducible HSP72 transgene under the control of a chicken β -actin promoter, which limited transgene expression to skeletal and cardiac muscle (and brain) tissue (Marber *et al.*, 1995). F₁ generation males were mated with female *mdx* mice to yield an equal proportion of *mdx*^{HSP72} and *mdx* littermate controls. Mice (25-30 week old) were anaesthetised (60 mg/kg sodium pentobarbitone), and the functional properties of diaphragm muscle strips were measured *in vitro* as described previously (Lynch *et al.*, 1997). Mice were killed by diaphragm and cardiac excision while still anaesthetized deeply. Diaphragm muscle strips were also frozen for subsequent histological analysis. Blood was sampled to measure serum creatine kinase (CK) levels, a myoplasmic protein commonly used as a measure of whole body muscle breakdown. In a separate group of mice, Evans blue dye (EBD) was injected (1% w/v, 10 μ l/g BM, *i.p.*) for assessment of damaged and necrotic muscle fibres.

HSP72 protein expression was elevated significantly in the muscles of *mdx*^{HSP72} compared with *mdx* littermate control mice. HSP72 overexpression improved specific (normalised) force in isolated diaphragm muscle strips ($p < 0.05$), reduced collagen infiltration ($p < 0.05$) and reduced minimal Ferets variance coefficient (used as an index of the severity of the pathology; $p < 0.05$). Serum CK levels were significantly lower in *mdx*^{HSP72} compared with *mdx* littermate controls ($p < 0.05$), which was further supported by a reduction in EBD-positive fibres indicating fewer damaged and/or necrotic fibres ($p < 0.05$).

Overexpression of HSP72 improved the dystrophic skeletal muscle pathology in *mdx* mice, especially in the severely affected diaphragm muscle. Further research is required to determine the therapeutic potential of this novel approach for DMD and related conditions.

Emery AE. (2002) *Lancet* **359**: 687-695.

Finsterer J. (2006) *Lung* **184**: 205-215.

Kim Y-K, Suarez J, Hu Y, McDonough PM, Boer C, Dix DJ, Dillman WH. (2006) *Circulation* **113**: 2589-2597.

Lynch GS, Rafael JA., Hinkle RT, Cole NM, Chamberlain JS, & Faulkner JA. (1997) *American Journal of Physiology. Cell Physiology* **272**: 2063-2068.

Marber MS, Mestral R, Chi S-H, Sayen R, Yellon DM, Dillman WH (1995) *The Journal of Clinical Investigation* **95**: 1446-1456.

Properties and proteolytic activity of m-calpain in rat skeletal muscle

J.P. Mollica, R.M. Murphy and G.D. Lamb, Department of Zoology, La Trobe University, Melbourne, VIC, 3086, Australia.

m-Calpain is a ubiquitously expressed Ca^{2+} -dependent protease with diverse functionality in skeletal muscle including, but not limited to, roles in cell migration, fusion and membrane repair. It is believed to require $>100 \mu\text{M}$ free $[\text{Ca}^{2+}]$ for activation (Cong *et al.*, 1989; Elce *et al.*, 1997), although this requirement may be dependent on phosphorylation status and/or phospholipid binding (Goll *et al.*, 2003). Given the peak tetanic $[\text{Ca}^{2+}]$ within skeletal muscle fibres normally reaches only 2-20 μM (Baylor & Hollingworth, 2003), this raises the question of how m-calpain fulfills its role as a protease in skeletal muscle.

EDL and *soleus* muscles were dissected from male Long-Evans hooded rats sacrificed by anaesthetic overdose (4% v: v halothane) with approval of the La Trobe University Animal Ethics Committee. Western blotting was used to quantify the absolute amount of m-calpain by comparing known concentrations of pure rat recombinant m-calpain to whole skeletal muscle homogenates. The total amount of m-calpain was found to be $\sim 1.0 \mu\text{mol/kg}$ muscle mass in predominantly slow-twitch soleus muscle and $\sim 0.3 \mu\text{mol/kg}$ muscle mass in fast-twitch *extensor digitorum longus* muscle. Experiments in which mechanically skinned fibre segments were washed in aqueous solutions for set times showed that $\sim 75\%$ of the total m-calpain is freely diffusible within a quiescent fibre.

The proteolytic activity of m-calpain was also assessed using mechanically-skinned single fibres. Once skinned, the fibre segment was stretched to approximately twice its resting length so that no force-producing cross-bridges could be formed, with the resulting passive force being due to extension of titin, a large elastic sarcomeric protein that is a known substrate for m-calpain. Proteolysis of titin was gauged from the decline in passive force when a stretched fibre segment was exposed to $1 \mu\text{M}$ rat recombinant m-calpain over a range of elevated free $[\text{Ca}^{2+}]$. Proteolytic activity of m-calpain was observed even with free $[\text{Ca}^{2+}]$ as low as $4 \mu\text{M}$, and the rate of decline of passive force reached $\sim 17\%$ / min at $20 \mu\text{M}$ free Ca^{2+} . The rate of passive force decline was even greater at higher free $[\text{Ca}^{2+}]$, reaching $\sim 250\%$ / min at $500 \mu\text{M}$ Ca^{2+} . In the presence of $20 \mu\text{M}$ free $[\text{Ca}^{2+}]$, porcine-derived native m-calpain added exogenously at $1 \mu\text{M}$ resulted in proteolysis of titin at 9% / min, approximately half the rate observed with the rat recombinant m-calpain under the same conditions. Passive force decline over the physiological range of free $[\text{Ca}^{2+}]$ was also measured both with and without ATP present in the solution and proteolytic activity was found to be the same in both cases. With both native and recombinant m-calpain, proteolytic activity could always be rapidly stopped by lowering the free $[\text{Ca}^{2+}]$ to $<10 \text{ nM}$. Furthermore, the proteolytic activity of m-calpain at $2 \mu\text{M}$ free Ca^{2+} was unchanged irrespective of whether or not the m-calpain had been activated at higher $[\text{Ca}^{2+}]$ beforehand.

In conclusion, these findings demonstrate that m-calpain displays considerable proteolytic activity at physiological Ca^{2+} conditions occurring in muscle fibres. Furthermore, the findings distinguish its regulation from that of the other ubiquitous calpain, μ -calpain, which becomes more Ca^{2+} -sensitive following exposure to elevated $[\text{Ca}^{2+}]$, suggestive that the ubiquitous calpains likely have quite different roles in skeletal muscle.

Baylor SM & Hollingworth S. (2003). *The Journal of Physiology* **551**, 125-138.

Cong J, Goll DE, Peterson AM & Kapprell HP. (1989). *The Journal of Biological Chemistry* **264**, 10096-10103.

Elce JS, Hegadorn C & Arthur JS. (1997). *The Journal of Biological Chemistry* **272**, 11268-11275.

Goll DE, Thompson VF, Li H, Wei W & Cong J. (2003). *Physiological Reviews* **83**, 731-801.

Properties of AMP kinase (AMPK) β isoforms and glycogen related proteins in segments of single fibres from rat skeletal muscle

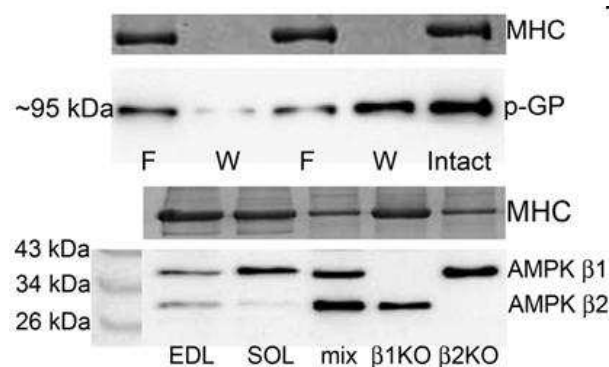
R.M. Murphy,¹ H. Latchman,¹ B. Kemp,² P. Gooley³ and D.I. Stapleton,³ ¹Department of Zoology, La Trobe University, Melbourne, VIC 3086, Australia, ²St Vincent's Institute of Medical Research, Fitzroy, VIC 3065, Australia and ³Bio21 Institute, The University of Melbourne, VIC 3010, Australia.

To understand function and regulation of proteins it is important to have knowledge about their properties in the physiological environment. In this study, we have used small segments of single skeletal muscle fibres dissected from rat skeletal muscle to examine diffusibility and fibre type expression of a number of glycogen related proteins as well as AMPK isoforms.

Male Long-Evans hooded rats (6-8 months old) were sacrificed using a lethal overdose of fluothane in accordance with the La Trobe University Animal Ethics Committee and the *extensor digitorum longus* (EDL) and *soleus* (SOL) muscles were excised. To compare fibre type differences EDL (exclusively type II) and SOL (predominantly type I) muscle fibres were analyzed for AMPK β 1 and β 2, glycogen branching enzyme (GBE), glycogen debranching enzyme (GDE), glycogen phosphorylase (GP), phospho-GP and glycogen synthase (GS). To measure protein diffusibility, individual fibres were dissected from muscles that had been immersed in paraffin oil and then mechanically-skinned and exposed to physiological K^+ -based solution (pCa < 10) for 1 and 10 min. The wash solution (W) and their matched fibres (F) were analyzed side by side using Western blotting (Murphy *et al.*, 2006). For fibre type comparisons, the amount of each protein was normalized to the amount of an abundant muscle protein (*i.e.* actin or myosin) and then expressed relative to the amount of the given protein present in the SOL fibres. Identity of AMPK β isoforms was confirmed by their absence in muscle homogenates from respective knock-out mice.

Proteins related to glycogen breakdown (GDE, GP, p-GP) were present in higher amounts in fast-compared with slow-twitch muscle (Table). Proteins related to glycogen synthesis were similar (GS) or lower (GBE) in slow- compared with fast-twitch muscle (Table). The AMPK β isoforms had the opposite abundances in fast- and slow-twitch muscle. Some proteins were freely diffusible (GBE, AMPK β 1 and β 2), some appeared to be weakly bound (GP, p-GP), whilst GDE was much more tightly associated with a muscle structure and likely bound with glycogen which reportedly washes out <40% in 10 min (Goodman *et al.*, 2005). Given that ~80% of the GP appeared in the wash, it is likely that there is considerable excess of this enzyme compared with the amount of glycogen present. These findings strongly suggest that when glycogen related proteins or AMPK are examined in skeletal muscle, the fibre type dependence must be taken into account. This is particularly important in human skeletal muscle which is typically heterogeneous with respect to fibre types present and so these proteins should be examined in individual fibres.

Protein / enzyme	Approx amount in EDL	Amount appearing in wash after 10 min	
	compared with SOL	EDL	SOL
AMPK β 1	0.4	70%	70%
AMPK β 2	4	70%	70%
GBE	0.2	80%	85%
GDE	5	20%	50%
GP	100	80%	40%
phospho-GP	10	60%	40%
GS	1	ND	ND



Goodman C, Blazev R & Stephenson G. (2005). *Clinical and Experimental Pharmacology and Physiology* **32**, 749-756.

Murphy RM, Verburg E & Lamb GD. (2006). *Journal of Physiology* **576**, 595-612.

Pre-, hemi- and postfusion stages of lamellar body (LB) exocytosis in the rat lung: mechanisms of regulation and implications for surfactant release

P. Diel, Institute of General Physiology, Albert-Einstein-Allee 11, 89081 Ulm, Germany. (Introduced by Peter Thorn)

Exocytotic systems in biology are highly variable with regard to vesicle size, content solubility, dynamics of release and modes of stimulation. The alveolar type II cell is a paradigm for a “slow secreter”, with vesicles (lamellar bodies = LBs) of about 100-fold diameter (i.e. \approx 1 million-fold volume) of a synaptic vesicle, and a poorly soluble, lipoprotein-like secretory product (surfactant). Due to their large size and sequential (rather than simultaneous) mode of release, LBs in type II cells are an ideal model system to elucidate single vesicle-related events in the course of exocytosis using live-cell imaging techniques. We have developed several fluorescence techniques that enable a “dissection” of the exocytotic process into various stages, based on quantum yield, solubility, diffusion and accumulation of dyes in different compartments according to biophysical properties and modes of application. In combination with other techniques, these methods allow to estimate with high spatial and temporal resolution the hemifusion lifetime, the instance of fusion pore formation, dynamics and physical forces of fusion pore expansion, and postfusion events in and around single fused LBs. We found that an elevation of the cytoplasmic Ca^{2+} concentration ($[\text{Ca}^{2+}]_c$) above \approx 300 nmol/l is a stimulus for LB fusion events, where the amount of fusion correlates with the integrated $[\text{Ca}^{2+}]_c$ over time. Each fusion event is initiated by a hemifusion phase, i.e. a period of lipid merger between plasma and LB membrane, which can be detected by a decay of light intensity (SLID = scattered light intensity decrease) of the limiting LB membrane in darkfield microscopy. After fusion pore formation, LB contents remain within the fused LB, because the fusion pore opens slowly and surfactant is a hydrophobic material that does not immediately disintegrate. Cells expressing actin-GFP form a dense “actin coat” around the fused and swollen LB, and this actin coat formation is necessary for surfactant release through the pore. When actin coat formation is prevented by removal of Ca^{2+} or by pharmacological treatment with Ca^{2+} channel blockers, surfactant release is inhibited. The dependence of actin coat formation and contraction on extracellular Ca^{2+} prompted to investigate localized $[\text{Ca}^{2+}]_c$ changes at the site of fusion. Fluo-4-fluorescence measurements revealed transient $[\text{Ca}^{2+}]_c$ elevations around single fused LBs subsequent to fusion pore formation (FACE = fusion-activated Ca^{2+} entry). Current experiments aim at elucidating the molecular components of Ca^{2+} entry in type II cells. We conclude that the postfusion phase plays an important active role and is rate-limiting for the release of surfactant. Ca^{2+} channels, which are selectively activated and/or accessible to the extracellular space during this phase account for a yet undetected postfusion Ca^{2+} signal, boosting release of vesicle contents. This type of Ca^{2+} -secretion-coupling may exist in all cell types, where vesicle content release by diffusion through a slowly expanding pore is not sufficient or fast enough.

Targeting membrane lipids to modulate amyloid precursor protein processing

B. Garner, Illawarra Health and Medical Research Institute, University of Wollongong, Wollongong, NSW 2522, Australia and School of Biological Sciences, University of Wollongong, Wollongong, NSW 2522, Australia.

(Introduced by Peter Thorn)

Inhibition of cerebral amyloid- β (A β) deposition represents a therapeutic target for Alzheimer's disease (AD). A β is derived from the amyloid precursor protein (APP) *via* two sequential cleavages that are mediated by β -secretase and the γ -secretase complex. Such amyloidogenic APP processing occurs in lipid raft microdomains of cell membranes (Vetrivel *et al.*, 2005) and it is known that modulating the distribution of cholesterol in lipid rafts can regulate APP processing and A β production (Simons *et al.*, 1998). Certain ATP-binding cassette (ABC) transporters regulate lipid transport across cell membranes and, as recent studies reveal, within membrane microdomains (Glaros *et al.*, 2005). We therefore examined the role that ABCA1, A2, A7 and G1 may play in regulating neuronal lipid homeostasis and APP processing. In addition, we directly modulated raft lipid composition using glycosphingolipid (GSL) synthesis inhibitors as another means to assess the impact membrane lipid composition has on APP processing. Our studies revealed that ABCA1, A2 and G1 were expressed in human neurons as was ABCA7, albeit at much lower levels. The same transporters were also expressed in human brain (Kim *et al.*, 2008). Cellular cholesterol efflux to apolipoprotein acceptors was accelerated by over-expressing ABCA1, A7 or G1 (but not A2) in HEK293 cells (Kim *et al.*, 2007, Chan *et al.*, 2008). Extracellular A β levels were reduced when CHO cells stably expressing human APP (CHO-APP) were transfected with ABCA1, A7 or G1 (but not A2); implying regulation of APP processing by ABC transporters was correlated with lipid efflux activity (Kim *et al.*, 2007). In very recent studies, we assessed the capacity of three ABCA1 mutants (that do not promote cholesterol efflux) to modulate APP processing and, unexpectedly, these also reduced A β production. Co-immunoprecipitation experiments indicated ABCA1 and APP physically interact which suggests a novel pathway by which ABCA1 may regulate APP processing. Using a different approach to modulate cellular lipid homeostasis, we reduced membrane GSL levels using synthetic ceramide analogues based on the D-1-phenyl-2-decanoylamino-3-morpholino-1-propanol (PDMP) structure that are established glucosylceramide synthase inhibitors. PDMP and related compounds PMP and EtDO-P4 inhibited A β secretion from CHO-APP cells with approximate IC₅₀ values of 15, 5 and 1 μ M, respectively (Li *et al.*, 2010). In addition, EtDO-P4 inhibited endogenous A β production by human neurons. In conclusion, ABC transporter mediated modulation of APP processing may involve lipid-dependent and -independent processes. Our studies also provide novel information regarding the regulation of APP processing by synthetic ceramide analogues that could offer a novel therapeutic avenue to explore as a treatment for AD.

- Chan SL, Kim WS, Kwok JB, Hill AF, Cappai R, Rye KA & Garner B (2008) *Journal of Neurochemistry* **106**: 793-804.
- Glaros EN, Kim WS, Quinn CM, Wong J, Gelissen I, Jessup W & Garner B (2005) *Journal of Biological Chemistry* **280**: 24515-23.
- Kim WS, Suryo Rahmanto A, Kamili A, Rye KA, Guillemin GJ, Gelissen IC, Jessup W, Hill AF & Garner B (2007) *Journal of Biological Chemistry* **282**: 2851-61.
- Kim WS, Weickert CS & Garner B (2008) *Journal of Neurochemistry* **104**: 1145-66.
- Li H, Kim WS, Guilemin GJ, Hill AF, Evin G & Garner B (2010) *Biochimica et Biophysica Acta*, **1801**: 887-895.
- Simons M, Keller P, De Strooper B, Beyreuther K, Dotti CG & Simons K (1998) *Proceedings of the National Academy of Sciences of the United States of America* **95**: 6460-4.
- Vetrivel KS, Cheng H, Kim SH, Chen Y, Barnes NY, Parent AT, Sisodia SS & Thinakaran G (2005) *Journal of Biological Chemistry* **280**: 25892-900.

The effect of membrane-active peptides on membrane dynamics and molecular order

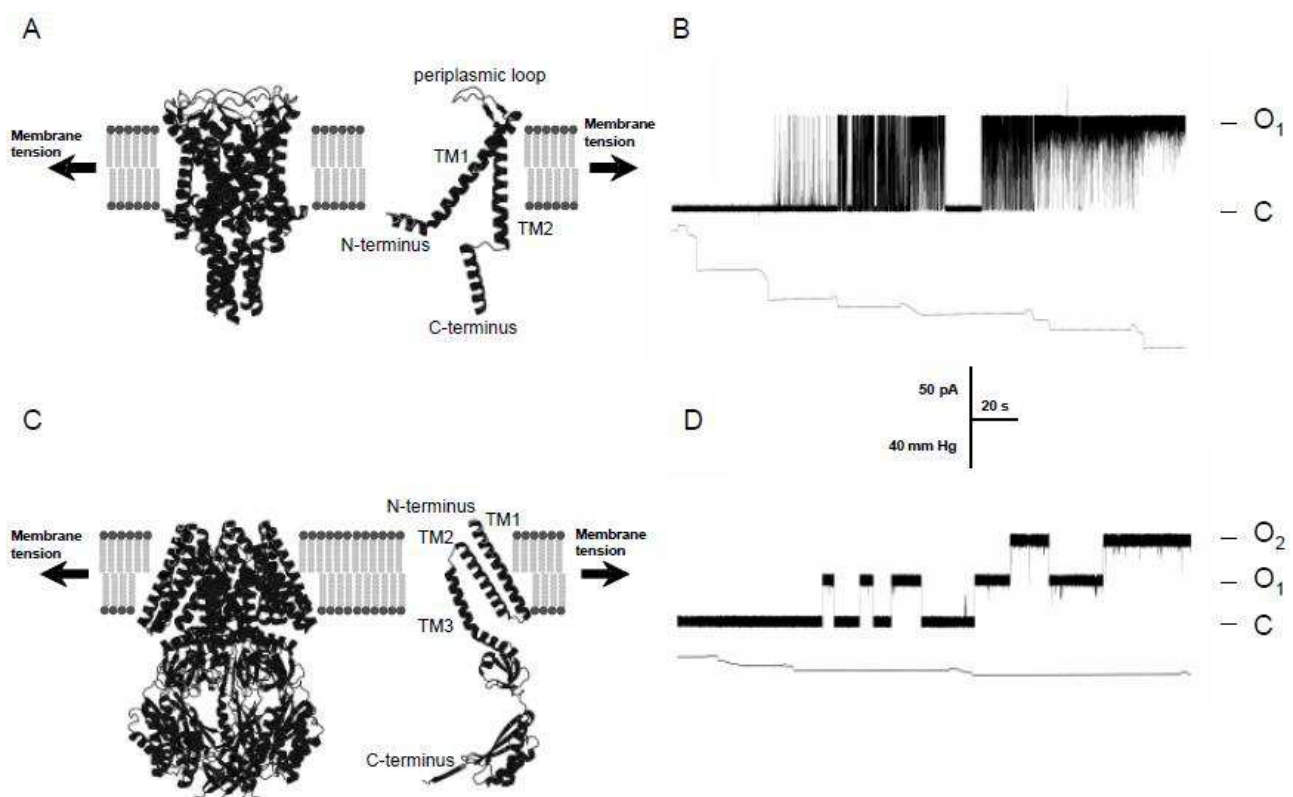
F. Separovic, School of Chemistry, Bio21 Institute, University of Melbourne, VIC 3010, Australia.

The results of solid-state NMR studies aimed at determining the orientation and location of antimicrobial peptides obtained from Australian tree frogs and amyloid peptides in phospholipid membranes will be discussed. The detailed structure of these peptides in membranes is difficult to determine as they disrupt the phospholipid bilayer. Solid-state NMR techniques are being used to determine the conformation and mobility of these pore-forming peptides in order to understand the mechanisms by which they exert their biological effect that leads to the disruption of biological membranes. Both static and magic angle spinning techniques have been applied to antimicrobial peptides in a range of model membranes, which reveal that the peptide activity is strongly dependent on the lipid composition of the bilayer and correlate with the selectivity for bacterial membranes. Similarly, the membrane interactions and structural changes of A β (1-42) and A β (1-40) from Alzheimer's disease are dependent on the presence of cholesterol and metal ions, which have been implicated in the disease. The data from both the amyloid and antimicrobial peptides reveal the importance of using appropriate membranes systems for studying membrane-active peptides.

Mechanisms of mechanosensation: Evolutionary origins of mechanosensitive ion channels

B. Martinac, Victor Chang Cardiac Research Institute, Lowy Packer Building, 405 Liverpool St, Darlinghurst, NSW 2010, Australia and St Vincent's Clinical School, University of New South Wales, NSW 2052, Australia.

Mechanosensitive (MS) ion channels are found in all types of living cells where they play an important role in mechanosensory transduction processes ranging from turgor control in bacteria and plant cells to hearing, touch, renal tubular function and blood pressure regulation in mammals. They convert mechanical stimuli acting upon membranes of biological cells into electrical or chemical signals (Hamill & Martinac, 2001). In the evolution of different life forms on Earth these ion channels may be among the oldest sensory transduction molecules that evolved as primary signalling elements in response to stimuli from the surrounding environment. The concept of ion channels gated by mechanical stimuli arose originally from studies of specialized mechanosensory neurons (Hamill & Martinac, 2001). Their discovery in embryonic chick skeletal muscle (Guharay & Sachs, 1984) and in frog muscle (Brehm *et al.*, 1984) over twenty five years ago demonstrated the existence of MS ion channels in many non-specialized types of cells. (Sachs, 1988) Instrumental for the discovery of MS channels was the invention of the patch clamp technique (Hamill *et al.*, 1981), which allowed the first direct measurements of single MS channel currents in a variety of non-specialized cells (Hamill & Martinac, 2001), including bacteria and archaea (Martinac, 2004). Studies of MS ion channels carried out over the last twenty five years have greatly contributed to our understanding of the molecular mechanisms underlying the physiology of mechanosensory transduction.



Bacterial MS channels. (A) The structure of the pentameric MscL channel (left) and a channel monomer (right) from *M. tuberculosis* according to the 3D structural model. (B) A current trace of a single MscL channel reconstituted into azolectin liposomes (w/w protein/lipid of 1:2000) recorded at +30 mV pipette potential. The channel gated more frequently and remained longer open with increase in negative pressure applied to the patch-clamp pipette (trace shown below the channel current trace). (C) 3D structure of the MscS homoheptamer (left) and a channel monomer (right) from *E. coli*. (D) Current traces of two MscS channels reconstituted into azolectin liposomes (w/w protein/lipid of 1:1000) recorded at +30 mV pipette voltage. Increase in pipette suction (trace shown below the channel current trace) caused an increase in the activity of both channels. C and O_n denote the closed and open state of the n number of channels. (Modified from Martinac *et al.*, 2008)

The cloning and structural determination of bacterial MscL and MscS channels (Figure), cloning and genetic analysis of the *mec* genes in *Cenorhabditis elegans*, genetic and functional studies of the TRP-type MS channels as well as functional and genetic studies of the TREK and TRAAK 2P-type K⁺ MS ion channels continue to promote our understanding of the role that MS channels play in the physiology of mechanosensory transduction in living organisms (Venkatachalam & Montell, 2007). In recent years the scientific and medical community has become increasingly aware of the importance of aberrant mechanosensitive channels

contributing to pathophysiology of various diseases including heart failure and dysfunction, muscular dystrophy and polycystic kidney disease, to name a few (Venkatachalam & Montell, 2007; Martinac *et al.*, 2008). At present, MS channel proteins are at the focus of structural, spectroscopic, computational and functional studies aiming to understand the molecular basis of mechanosensory transduction in living cells.

Brehm, P, Kullberg, R & Moody-Corbett, F. (1984) *Journal of Physiology* **350**: 631-648.

Guharay, F & Sachs, F. (1984) *Journal of Physiology* **352**: 685-701.

Hamill, OP & Martinac, B. (2001) *Physiological Reviews* **81**:685-740.

Hamill, OP, Marty, A, Neher, E, Sakmann, B & Sigworth, FJ. (1981) *Pflügers Archiv European Journal of Physiology* **391**: 85-100.

Martinac, B. (2004) *Journal of Cell Science* **117**: 2449-2460.

Martinac, B, Saimi, Y & Kung, C. (2008) *Physiological Reviews* **88**: 1449-1490.

Sachs, F. (1988) *Critical Reviews in Biomedical Engineering* **16**: 141-169.

Venkatachalam, K & Montell, C.(2007) *Annual Review of Biochemistry* **76**: 387-417.

Supported by grants from the Australian Research Council and National Health & Medical Research Council.

Molecules in motion: imaging peptides, their receptors and diffusion models

I.L. Gibbins, S. Goh, Y. DeGraaf, K. Hendy and J. Clarke, Anatomy & Histology and Centre for Neuroscience, Flinders University, GPO Box 2100, Adelaide, SA 5001, Australia. (Introduced by Peter Thorn)

Although neuropeptides and the G-protein coupled receptors (GPCRs) through which they operate have been well studied for more than 30 years now, many aspects of their function remain mysterious. When considering the roles of neuropeptides as transmitters in peripheral autonomic and sensory pathways, two questions remain largely unanswered: (1) can neuropeptides mediate non-synaptic neurotransmission? (2) how do neuropeptide signalling systems interact to modulate the excitability of neurons in a physiological milieu that includes a wide range of non-neural agents that also can affect neuronal excitability? For several years we have been examining these questions, focussing on interactions between substance P (SP) and angiotensin II (AngII) on prevertebral sympathetic neurons of guinea-pigs and on cell lines expressing NK1 receptors for SP or AT1A receptors for AngII. Intracellular electrophysiological recordings of guinea-pig coeliac ganglion neurons strongly suggest that receptors for SP and AngII converge on common intracellular signal transduction pathways to inhibit the same potassium channels to increase neuronal excitability. Based on combined electrophysiological and confocal microscopic analyses, most of SP released from collaterals of unmyelinated visceral nociceptive afferents probably acts non-synaptically. Mathematical modelling of SP diffusion using realistic morphological parameters derived from electron microscopy and direct measurements of SP diffusion coefficients with fluorescence correlation spectroscopy (FCS) or raster image correlation spectroscopy (RICS) show that physiological rates of afferent stimulation can generate concentrations of SP from non-synaptic release sites that are well within the range to affect the excitability of sympathetic neurons. Recently we have been using a confocal microscope with a high-speed resonant scanner and highly sensitive avalanche photodiodes to image the movement of EGFP-linked AngII receptors in CHO cells at rates of 20-25 frames/s. In addition to showing a considerable degree of constitutive internalisation of the receptors, these images have revealed the remarkably mobile nature of the cell membrane and the receptors it contains. Taken together, our data and models suggest that the environment within which peptides interact with their receptors is highly complex, such that they rarely occur under equilibrium conditions. In real life, it is most probable that sympathetic neurons are nearly always exposed to neuropeptides, peptide hormones and other agents at concentrations that increase their excitability significantly above a nominal resting levels. Somehow, the central nervous system must take this into account when regulating the degree of preganglionic drive to the peripheral neurons. Similarly, within the dorsal horn of the spinal cord, non-synaptic peptidergic transmission has the potential to greatly modify the processes underlying nociception.

Neuromuscular fatigue: interactions between central and peripheral factors

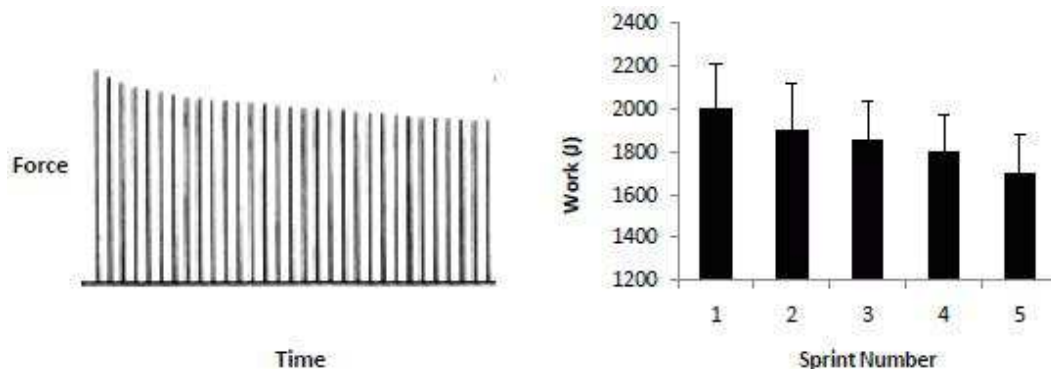
M. Amann, VA Medical Center, GRECC 182, 500 Foothill Drive, Salt Lake City, UT 84148, USA. (Introduced by Mark Hargreaves)

Over the past years evidence from us and others has accumulated indicating that the development of peripheral locomotor muscle fatigue is confined to a certain limit which varies between humans. Central motor drive to these muscles – and therefore exercise performance – during human athletic activities appears to be regulated to avoid the development of peripheral locomotor muscle fatigue beyond an “individual critical threshold”. The existence of a degree of peripheral fatigue that is never exceeded during high intensity endurance exercise prompted us to propose the role of peripheral locomotor muscle fatigue as a carefully regulated variable. In various experiments we have challenged this postulate from different perspectives and our results further verify its validity. Based on the knowledge gained from previous observations we outlined a model linking central motor drive with the metabolic milieu within the working locomotor muscles. Our model suggests that, during high intensity endurance exercise, somatosensory feedback from the working muscles imposes inhibitory influences on the magnitude of central motor drive with the purpose to regulate and restrict the level of exercise-induced peripheral locomotor muscle fatigue. As we also qualified, this proposed feedback mechanism is likely only one of several potential contributors to the modulation of central motor drive and that its relative contribution will change with varying conditions such as, for example, severe hypoxemia. In more recent work, we experimentally tested this model *via* pharmacologically modifying somatosensory pathways originating in the working limbs during whole body exercise. After initial difficulties with the lumbar epidural application of a local anesthetic and the associated loss of locomotor muscle strength we switched to an intrathecally applied opioid analgesic. These experiments were the first ever to selectively block lower limb afferent feedback during cycling exercise without affecting maximal locomotor muscle force output. In the absence of neural feedback from the working limbs, central motor drive was about 8% higher during the opioid trial and end-exercise peripheral locomotor muscle fatigue exceeded, for the first time, the critical threshold by nearly 50%. The outcome of these studies further confirms our hypothesis claiming that afferent feedback inhibits central motor drive and restricts the development of peripheral fatigue to an individual critical threshold.

Fatigue during intermittent exercise: novel insights and real-world applications

D.J. Bishop, Institute of Sport, Exercise and Active Living (ISEAL) and School of Sport and Exercise Science, Victoria University, Melbourne, Australia..

There is a reversible decline in the force production of muscles when they are used at near their maximum capacity. This has been classically demonstrated by stimulating repeated short tetani in an isolated fibre (e.g., left-hand panel of figure; Lannergren & Westerblad, 1991). Such experiments have provided valuable insights regarding potential determinants of fatigue (Allen, Lamb, & Westerblad, 2008). Nonetheless, the application of such findings to dynamic exercise has been questioned. However, a similar pattern for the decline in muscle performance can also be observed when athletes are asked to repeat short-duration sprints (< 10 s), interspersed with brief recoveries (< 30 s) (e.g. right-hand panel of figure; Bishop, Edge, Davis, & Goodman, 2004). An additional advantage of this approach is that it is possible to investigate the potential influence of neural/brain factors on the fatigue process.



We are interested in how fatigue manifests during intermittent sprint exercise, and the potential underpinning muscular and neural mechanisms. Such information is important as a better understanding of the factors contributing to fatigue is arguably the first step in order to design interventions (*i.e.* training programs, ergogenic aids) that could eventually improve intermittent-sprint ability.

At the muscle level, limitations in energy supply, which include phosphocreatine hydrolysis and the degree of reliance on anaerobic glycolysis and oxidative metabolism, and the intramuscular accumulation of metabolic by-products, such as hydrogen ions, emerge as key factors responsible for fatigue. Although not as extensively studied, the use of surface electromyography techniques have revealed that failure to fully activate the contracting musculature and/or changes in inter-muscle recruitment strategies (*i.e.* neural factors) are also associated with fatigue outcomes. Via the use of deception, it has recently been demonstrated that prior knowledge of the end-point of exercise (*i.e.* sprint number) is also able to influence the mechanical output profile (*i.e.* fatigue) during intermittent sprint exercise.

Allen, D.G., Lamb, G.D., & Westerblad, H. (2008). Skeletal muscle fatigue: cellular mechanisms. *Physiological Reviews* **88**(1), 287-332.

Bishop, D., Edge, J., Davis, C., & Goodman, C. (2004). Induced metabolic alkalosis affects muscle metabolism and repeated-sprint ability. *Medicine & Science in Sports & Exercise*, **36**(5), 807-813.

Lannergren, J., & Westerblad, H. (1991). Force decline due to fatigue and intracellular acidification in isolated fibres from mouse skeletal muscle. *Journal of Physiology*, **434**, 307-322.

Erythrocyte shape, metabolism and membrane transport – computations

*P.W. Kuchel, Singapore Bioimaging Consortium (SBIC) A*STAR, 11 Biopolis Way, #02-02 Helios Building, Singapore 138667.*

Our aim in modelling cellular responses to chemical and physical perturbations is to gain insights into underlying structural, transport, and metabolic mechanisms. Such models can enable predictions of cell behaviour under conditions that are not experimentally accessible; or the models can be added to others thus building up the complexity of the model to describe highly-nonlinear cellular phenomena such as metabolic and structural oscillations. The cellular system under study has been the human erythrocyte. Data on cell shape on the minute-to-hour time scale have been obtained with NMR-diffusion spectroscopy and differential interference contrast (DIC) light microscopy; on the sub-second time scale fast image capture of membrane ‘flickering’ has been carried out with DIC microscopy. Data processing and modelling of cell shape-changes and membrane flickering have been carried out by using Mathematica. A drive to understand the “link” between the rate of transmembrane pumping of Na^+ via the Na,K-ATPase, and the rate of glycolysis has used multinuclear NMR spectroscopy. Again modelling of the system has been set up in Mathematica. The next challenge is fitting multi-parameter models to real experimental data. For this we are using a Monte Carlo Markov chain (MCMC) approach.

Acknowledgements: Ron Clarke, Bob Chapman, Gemma Figtree, Stuart Grieve, Tim Larkin, Christoph Naumann, David Philp, Max Puckeridge, David Szekely, Jamie Vandenberg.

Fast acquisition of multidimensional NMR experiments by maximum entropy reconstruction of non-uniformly sampled data

M. Mobli, Institute for Molecular Bioscience, The University of Queensland, St. Lucia, QLD 4072, Australia.

(Introduced by John Gehman)

The discrete Fourier transform (DFT) played a seminal role in the development of modern nuclear magnetic resonance (NMR) spectroscopy. Nevertheless it has a number of well-known limitations. Chief among them is the difficulty of obtaining high-resolution spectral estimates from short time records, because the ability to resolve signals with closely-spaced frequencies is largely determined by the longest evolution time sampled.

The ability to obtain accurate, high-resolution spectral estimates from short data records is critical in many applications of NMR spectroscopy because the available sampling time is limited, for example due to sample instability or simply due to constraints on available instrument time. In practice the latter is mainly encountered in multidimensional NMR experiments where the data collection time is directly proportional to the number of data samples collected in the indirect time dimensions (indirect time dimensions correspond to time delays between RF pulses; real time is referred to as the acquisition dimension). Furthermore, at very high magnetic field, the competition between the goals of short data collection time and high resolution becomes more severe as the bandwidth spanned by the nuclear resonances increases linearly with field strength, necessitating a decrease in the time between samples in order to avoid aliasing.

Non-Fourier methods of spectrum analysis provide an avenue to high-resolution spectral estimates from short data records. Over the past three decades a host of non-Fourier methods of spectrum analysis have been developed, including maximum entropy, maximum likelihood and Bayesian methods, the filter diagonalization method, G-matrix Fourier transform, back projection reconstruction, and multidimensional decomposition. These methods span a continuum of assumptions about the nature of the signal, and restrictions (or lack thereof) on the characteristics of the data sampling. MaxEnt reconstruction lies at the extreme of making few assumptions about the signal, and furthermore can be applied to data collected in essentially arbitrary fashion (non-uniform sampling, NUS).

Extensive use of synthetic and experimental, non-uniformly sampled data in 2-4 dimensions, processed using MaxEnt has enabled us to both theoretically and practically evaluate the pros and cons of this method. The results suggest the method to be resilient to false positives and robust in situations of poor signal to noise, with the consequence of producing non-linear reconstructions.

Toward the virtual heart: graphics processor accelerated interactive simulations of cardiac function

D. Szekely, A.P. Hill and J.I. Vandenberg, The Mark Cowley Lidwill Program in Cardiac Electrophysiology, Victor Chang Cardiac Research Institute, Level 6, Lowy Packer Building, 405 Liverpool Street, Darlinghurst, NSW 2010, Australia.

Heart disease is the leading cause of death in the developed world. Despite this, our understanding of the mechanisms of cardiac dysfunction, particularly acute disorders related to the electrical system of the heart is limited. Our goal is to create a realistic virtual model of the heart to develop insight into this clinically important problem.

Using the multiscale modelling approach, we began at the molecular level with mathematical descriptions of the ion channels, pumps and buffers present in every heart cell. Integration of these subcellular components reproduces the cardiac action potential waveform the basic unit of cardiac electricity at the single cell level. From this building block we can extend our simulations to simple strings (1D), sheets (2D) and wedges (3D) of cells and even include descriptions of the overall architecture, anatomical detail and tissue heterogeneity necessary to simulate realistic hearts. At each level of complexity we have endeavored to gather appropriate experimental data to validate the model.

The computational complexity of the virtual heart has been prohibitive until very recently. However, the continued development of massive parallelisation using graphics processor technology has allowed us to compute the electrical activity of over several thousand cells concurrently. This has made the virtual heart a much more realistic and achievable goal.

Vesicle docking and delivery: Life in the TIRF zone

A.C.F. Coster, School of Mathematics & Statistics, University of New South Wales, NSW 2052, Australia and Garvan Institute of Medical Research, Darlinghurst, NSW 2010, Australia.

Cells traffic membrane-embedded proteins to the plasma membrane *via* a variety of mechanisms. One of these is the docking and fusing of vesicles with the plasma membrane. Even this mechanism, however can happen *via* several modalities.

Given the live-cell imaging techniques using total internal reflection (TIRF) microscopy (in which the first ~200nm of the cell surface is observed using fluorescent markers attached to the molecules), it is now becoming possible to view the dynamics of these processes, albeit that in some systems the vesicles are below the resolution of the system.

In order to systematically extract these delivery events from other background traffic, we need robust, quantitative descriptions of the dynamics. These can then be employed in automated detection systems to analyse the system under a variety of perturbations.

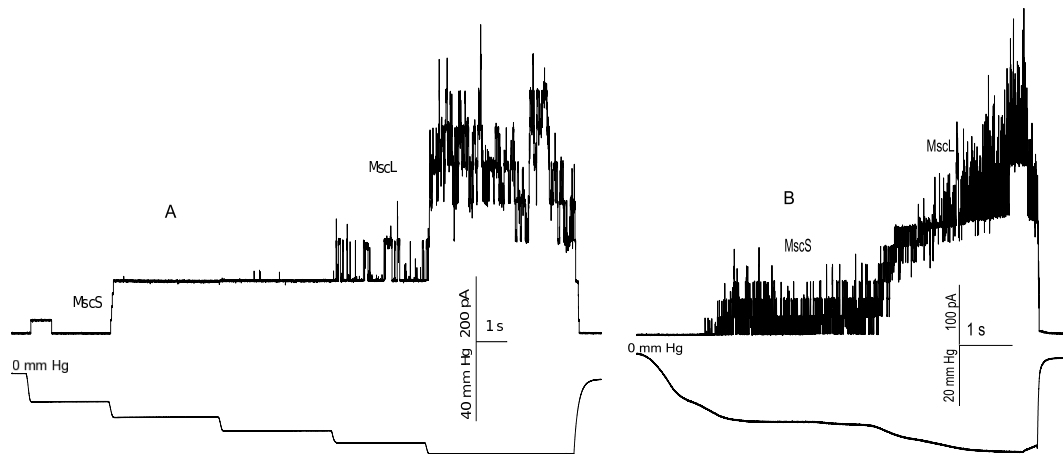
Such an automated detection system has been developed within the Diabetes & Obesity Group at the Garvan Institute of Medical Research. The proteins of interest in this case are the glucose transporters GLUT4, which are highly insulin-responsive. These may be brought to the plasma membrane *via* methods including the full fusion of the vesicles, and also *via* a process termed “Kiss-and-Run”, whereby a pore connection is made between the vesicle and plasma membrane allowing diffusion of the GLUT4 proteins across the boundary. The vesicle does not, however, become fully integrated, but, after a period, detaches from the plasma membrane. Thus, the amount of GLUT4 delivered depends on the amount of time the “Kiss” persists, and also on the physical dimensions of the vesicle and pore connection.

The model for this process can also be used to explore the possibilities of differential diffusion rates of the molecules in the vesicle and the plasma membrane. In the case of GLUT4 vesicles in adipocytes, the analysis of TIRF imagery is further exacerbated by the fact that the ~80nm diameter vesicles are well below the microscope resolution. Advances in the understanding of these processes are still, however, being made, with the use of mathematical modelling and sophisticated image analysis techniques. Current work is exploring the modelling and imaging of the “Kiss-and-Run” delivery process, and the insights this may additionally give us into the diffusion characteristics of the membranes.

Lipid effects on the gating behaviour and reconstitution of MscL and MscS

A.R. Battle,^{1,2} T. Nomura² and B. Martinac,^{2,3} ¹School of Biomedical Sciences, The University of Queensland, St Lucia, QLD 4072, Australia, ²The Victor Chang Cardiac Research Institute, Darlinghurst, NSW 2010, Australia and ³St Vincent's Clinical School, The University of New South Wales, NSW 2052, Australia.

The mechanosensitive channels of large (MscL) and small (MscS) conductance act as osmosensors in bacterial cells against hypo-osmotic shock (Martinac, 2007). MscL has been extensively studied by reconstitution into liposomes (Häse *et al.*, 1995; Moe & Blount, 2005), however MscS has proved more difficult to reconstitute, requiring high protein-lipid ratios (Sukharev, 2002; Vásquez *et al.*, 2007). We recently published an improved reconstitution method for both MscL and MscS in soy azolectin (Battle *et al.*, 2009), a mixture that contains lipids, sugars and sterols. We have expanded these results and show here the effect of both individual and mixtures of lipids on the reconstitution and channel gating behaviour of co-reconstituted MscL and MscS. Introduction of the highly charged lipid cardiolipin causes rapid gating of MscS (Figure, A) in comparison to soy azolectin (Figure, B), indicating that lipid charge may play a significant role on channel gating dynamics.



MscS/MscL co-reconstitution. **A:** in soy azolectin. **B:** in mixture of phosphatidyl ethanolamine/ phosphatidyl choline/cardiolipin at a wt/wt ratio of 7:2:1, both recordings at a pipette voltage of +30 mV.

Battle AR, Petrov E, Pal P, Martinac B. (2009) *FEBS Letters* **583**: 407-12.

Häse CC, Le Dain AC, Martinac B. (1995) *Journal of Biological Chemistry* **270**: 18329-34.

Martinac, B. (2007) *Current Topics in Membranes* **58**: 25-57.

Moe P & Blount P. (2005) *Biochemistry* **44**: 12239-44.

Sukharev S. (2002) *Biophysical Journal* **83**: 290-8.

Vásquez V, Cortes DM, Furukawa H, Perozo E. (2007) *Biochemistry* **46**: 6766-73.

Mapping the sequence of conformational changes underlying selectivity filter gating in a potassium channel

A.P. Hill,^{1,2} D. Wang,^{1,2} S. Mann,^{1,2} M. Perry,¹ P. Tan¹ and J.I. Vandenberg,^{1,2} ¹Mark Cowley Lidwill Research Program in Cardiac Electrophysiology, Victor Chang Cardiac Research Institute, 405 Liverpool Street, Darlinghurst, NSW 2010, Australia and ²St. Vincent's Clinical School, UNSW Faculty of Medicine, Victoria Street, Darlinghurst, NSW 2010, Australia.

The potassium channel selectivity filter both discriminates between K⁺ and sodium ions and contributes to gating of ion flow. Static structures of conducting (open) and non-conducting (inactivated) conformations of this filter are known, however the sequence of protein rearrangements that underlie interconversion between these two states is not. Using ϕ -value analysis we have studied the macromolecular rearrangements associated with selectivity filter gating in the human ether-a-go-go-related gene (hERG) K⁺ channel, a key regulator of the rhythm of the heartbeat. We have found that closure of the selectivity filter gate is initiated by K⁺ exit and then followed in sequence by conformational rearrangements of the pore domain outer helix, extracellular turret region, voltage sensor domain, intracellular domains and pore domain inner helix. In contrast to the simple linear models proposed for opening and closing of ligand-gated ion channels, a much more complex spatial and temporal sequence of widespread domain motions connects the open and inactivated states of the hERG K⁺ channel.

Rigid body Brownian dynamics simulations of ion channels and channel blockers

D. Gordon and S.H. Chung, Research School of Biology, The Australian National University, Canberra, ACT 0200, Australia.

Ion channels allow cells to regulate the flow of ions across cell membranes in a controlled manner. This ionic flow is responsible for a host of key functions in the organism, including nerve signaling, muscle contraction, chemical signaling, and the regulation of metabolism. The presence of various kinds of channel blocker molecules can impede the normal flow of ions through ion channels, leading to important physiological consequences, both beneficial (*e.g.* calcium channel blocker drugs for high blood pressure) and detrimental (*e.g.* various polypeptide toxins). Therefore, it is important to be able to computationally model the dynamics and energetics of various channel blockers interacting with channels. We report on the development of a system that uses rigid body Brownian dynamics to simulate the interaction between blockers, ion channels, and ions. This allows us to elucidate binding, unbinding and blocking mechanisms, and to directly simulate the effects that blocker molecules have on ionic currents. The use of Brownian dynamics, rigid body dynamics and macroscopic electrostatics means that our simulation can be run on long timescales, allowing the direct measurement of ionic currents.

Our model system contains an ion channel embedded in a lipid bilayer membrane as well as one or more channel blocker molecules, and is solvated by water and ions. The channel is represented as a fixed rigid body and the blocker molecules as mobile rigid bodies. The ions are explicitly represented as spherical charged particles, whereas the water is implicit. The force field for the system contains various terms for short range interactions between the ions, channel and blocker molecules, frictional and random forces that drive the Brownian motion of the ions and blockers, and long range electrostatic forces which are given by the solution to Poisson's equation. The latter are the most challenging to model, and we have developed new methods for efficiently solving Poisson's equation in our molecular system and applying these solutions to our simulation.

The other major component of our simulation is the motion algorithm. We have developed a new algorithm for simulating the rigid body Brownian motion of the blockers (Gordon, Hoyles & Chung, 2009). A rotational and translational Langevin equation is formulated, and a numerical solution algorithm is proposed, based on the velocity Verlet algorithm, with additional steps being needed to handle the more complicated rotational algebra and extra frictional terms.

We have tested our simulation in various applications involving voltage gated potassium channels. We have examined a number of candidate blockers, including small classical blocker molecules like 4-aminopyridine (4AP) and tetraethylammonium (TEA), polypeptide toxins such as charybdotoxin (CTX), and other small charged molecules. Our aim is to elucidate the binding, unbinding and blocking mechanisms for a range of different channels and blockers.

Gordon D, Hoyles M, Chung SH. (2009) An algorithm for rigid-body Brownian dynamics. *Physical Review. E, Statistical, Nonlinear, and Soft Matter Physics* **80**, 066703-1 - 066703-12.

Metamorphic chloride intracellular channel proteins: evidence for transmembrane extension and membrane induced oligomerisation of CLIC1

S.C. Goodchild,¹ S.N. Breit,² P.M. Curmi³ and L.J. Brown,¹ ¹Department of Chemistry and Biomolecular Sciences, Macquarie University, NSW 2109, Australia, ²St. Vincent's Centre for Applied Medical Research, St. Vincent Hospital and University of New South Wales, NSW 2010, Australia and ³School of Physics, University of New South Wales, NSW 2052, Australia.

Classically, the study of protein structure is based on the assumption that the native protein fold is unique, with at most small structural alterations to facilitate function. However, the existence of several proteins capable of independently interchanging between two or more vastly different but stable folds arising from the same amino acid sequence have been shown. These proteins have collectively been termed “metamorphic” (Murzin, 2008).

The highly conserved Chloride Intracellular Channel (CLIC) protein family is an example of the metamorphic protein class. While the function of the CLIC proteins is not well understood, the CLICs are expressed as soluble proteins but can also reversibly auto-insert into the membrane to form active ion channels. This conformational transition has previously been shown to involve a large-scale unfolding between the C- and N-domains for CLIC1 (Goodchild *et al.*, 2010). The CLIC1 homologue also displays the unique ability to undergo a dramatic structural metamorphosis from a monomeric state, displaying a classic glutathione-S-transferase fold, to a soluble all α -helical dimer solution upon oxidation (Littler *et al.*, 2009). Furthermore, in the presence of membranes, the effect of oxidation has been shown to increase the interaction of CLIC1 with the lipid bilayer (Goodchild *et al.*, 2009). However to date, experimental evidence characterising the dramatic structural rearrangements that must occur within CLIC1 to confer favourable interactions with the membrane and enable formation of an ion channel pore are lacking.

In the current study, site-directed fluorescence labeling of a series of single cysteine residues (T44C, T45C, K49C, C89) within the vicinity of the single putative transmembrane domain (aa24-46) of CLIC1 was performed using a novel labeling strategy described recently (Goodchild *et al.*, 2010). Fluorescence Resonance Energy Transfer (FRET) was used to monitor for changes in the distance from a single native Trp35, located within the transmembrane, to each of the 1,5-IAEDANS acceptor labeled cysteine residues. This was performed in both the soluble CLIC1 form and upon the addition of lipid bilayers. The FRET changes observed indicate that an extension of residues 24-46 occurs upon interaction with the membrane. This result is consistent with the current model of a single extended helical transmembrane region. To test the hypothesis that the CLIC1 forms an oligomeric channel structure in the presence of membranes, a population of CLIC1 labeled with a donor fluorescent label (1,5-IAEDANS) was mixed with a population of CLIC1 labeled with an acceptor fluorescent label (5-IAF). Appreciable FRET interaction and thus evidence for oligomerisation was only detected upon oxidation of the CLIC1 in the presence of the membrane. Together, these two FRET results reinforce the notion of the CLIC protein family as dynamic and metamorphic entities and challenge many accepted views of protein structure. Currently, our labeling scheme is being extended to further refine our model for the structural transitions and environmental triggers of CLIC1 membrane-induced metamorphosis.

Goodchild, SC, Howell, MW, Cordina, NM, Littler, DR, Breit, SN, Curmi, PM, Brown, LJ (2009), *European Biophysical Journal* **39**, 129-38.

Goodchild, SC, Howell, MW, Littler, DR, Mandyam, RA, Sale, KL, Mazzanti, M, Breit, SN, Curmi, PM, Brown, LJ (2010), *Biochemistry* **49**, 5278-89.

Littler, DR, Harrop, SJ, Fairlie, WD, Brown, LJ, Pankhurst, GJ, Pankhurst, S, DeMaere, MZ, Campbell, TJ, Bauskin, AR, Tonini, R, Mazzanti, M, Breit, SN, Curmi, PM (2004), *Journal of Biological Chemistry* **279**, 9298-305.

Murzin, AG (2008), *Science*. **320**, 1725-6.

pH dependence of the Ca²⁺ release activated Ca²⁺ (CRAC) channel

N.R. Scrimgeour, D.P. Wilson and G.Y. Rychkov, School of Medical Sciences, University of Adelaide, Adelaide, SA 5005, Australia.

CRAC channels activated by the depletion of intracellular Ca²⁺ stores provide a major pathway for Ca²⁺ entry in many cell types. Characteristic properties of CRAC channels include high selectivity for Ca²⁺ over monovalent cations, feedback inhibition by permeating Ca²⁺, known as fast Ca²⁺ dependent inactivation (FCDI), and block by low external pH (Malayev & Nelson, 1995). The functional CRAC channels are composed of a tetramer of the Orai1 proteins, which forms the channel pore, and a protein called stromal interaction molecule 1 (STIM1), a Ca²⁺ binding protein that plays the role of Ca²⁺ sensor in the endoplasmic reticulum (Soboloff *et al.*, 2006). The glutamate 106 residue (E106) in a predicted transmembrane domain of Orai1 has been reported to act as the selectivity filter and to play a role in FCDI of CRAC channels (Yamashita *et al.*, 2008). In this work we show that glutamate 106 is also a protonation site responsible for I_{CRAC} block at low pH.

STIM1 and Orai1 were previously subcloned into pCMV-Sport6 and the GFP co-expressing vector pAdTrack-CMV (Scrimgeour *et al.*, 2009). The Orai1 E106D mutation was generated using pCMV-Sport6-Orai1 as a template according to the protocol specified by the QuikChange II site-directed mutagenesis kit (Stratagene). Whole-cell patch clamping was performed at room temperature using a computer based patch-clamp amplifier (EPC-9, HEKA Elektronik) and PULSE software (HEKA Elektronik).

I_{CRAC} mediated by heterologously expressed Orai1 and STIM1 was inhibited by low pH reaching virtually complete block at pH 5.5. The apparent pKa of CRAC channel pH dependence was 7.8±0.1 (n=4). The E106D Orai1 mutant, which has higher selectivity for Na⁺ over Ca²⁺ and is blocked by Ca²⁺ in time and voltage dependent manner (Yamashita *et al.*, 2008), showed no such dependence on pH. In contrast, lowering pH from 7.4 to 6.3 or below increased the amplitude of the current and reduced the extent of inactivation at negative potentials suggesting that the Ca²⁺ block of Na⁺ current was reduced. The apparent pKa of the block of Na⁺ conductance through E106D mutant by Ca²⁺ was 6.1±0.1 (n=4). Investigation of Ca²⁺ currents mediated by this mutant in the absence of all permeable monovalent cations in the external solution revealed that FCDI of E106D is much faster than that of WT Orai1 and is progressively reduced at lower external pH.

Overall, these results suggest that ring of negative charges at position 106 in the Orai1 pore controls not only the selectivity of the channel, but also contributes to a complex mechanism of FCDI and accounts for the pH dependence of CRAC channel.

Malayev A & Nelson DJ (1995). *Journal of Membrane Biology* **146**, 101-111.

Scrimgeour N, Litjens T, Ma L, Barritt GJ & Rychkov GY (2009). *Journal of Physiology* **587**, 2903-2918.

Soboloff J, Spassova MA, Tang XD, Hewavitharana T, Xu W & Gill DL (2006). *Journal of Biological Chemistry* **281**, 20661-20665.

Yamashita M, Navarro-Borelly L, McNally BA & Prakriya M (2007). *Journal of General Physiology* **130**, 525-540.

The congenital Long QT Syndrome: broad lessons from a rare disease

R.S. Kass, Department of Pharmacology, Columbia University Medical Center, 630 168th Street, New York, NY 10032, USA.

The Long QT syndrome (LQTS), a rare (1:2500 to 1:10,000) inherited disorder associated with an increased propensity to arrhythmogenic syncope, polymorphous ventricular tachycardia, and sudden cardiac death, has provided a wealth of information about fundamental mechanisms underlying human cardiac electrophysiology that has come about because of true collaborative interactions between clinical and basic scientists. Our understanding of the mechanisms that determine the critical plateau and repolarization phases of the human ventricular action potential have been raised to new levels through these studies with impact on the manner in which potassium channels, sodium channels, and channel-associated proteins regulate this critical period of electrical activity. To date, more than 12 genes have been linked to LQTS, but the majority of disease causing mutations occur in genes coding for two potassium channels (KCNH2 (LQT-2) and KCNQ1 (LQT-1) and the principal heart sodium channel (Nav1.5 (LQT-3)). It is clear that there are distinct risk factors associated with the different LQTS genotypes, and building on collaboration between clinical and basic science teams mutation-specific therapeutic approaches have been developed in a gene-dependent manner. The greatest difference in risk factors becomes apparent when comparing LQT3 syndrome patients (*SCN5A* mutations) and patients with LQT1 syndrome (*KCNQ1* mutations). Some broad insights into the structure, function, and regulation of KCNQ1/KCNE1 (IKS potassium) and Nav1.5 (sodium) channels have emerged from specific studies of LQTS gene mutations. The potential for understanding a mechanistic basis for arrhythmia risk was realized soon after the first genetic information relating mutations in genes coding for distinct ion channels became available and is still the focus of extensive investigation and has bridged into investigations of mutant channel activity in cardiac myocytes derived from inducible pluripotent stems cells, cells that have unique and powerful potential to provide a personalized approach to management of this and other heritable rhythm disorders.

Molecular mechanism of store-operated calcium entry (SOCE) in skeletal muscle and potential role in fatigue resistance

R.T. Dirksen, A.D. Lyfenko and L. Wei, University of Rochester, Department of Pharmacology and Physiology, Rochester, NY 14642, USA.

In skeletal muscle, store-operated calcium entry (SOCE) is a trans-sarcolemmal calcium influx pathway activated when sarcoplasmic reticulum (SR) calcium stores are depleted. Recently, we demonstrated that SOCE activation in skeletal myotubes involves a functional coupling between STIM1 calcium sensor proteins in the sarcoplasmic reticulum (SR) and calcium-permeable Orai1 channels in the sarcolemma. However, the precise mechanism and physiological role of SOCE in adult skeletal muscle remains largely unknown. Here we investigated the mechanism and physiological role of SOCE in single *flexor digitorum brevis* (FDB) fibres from adult mice. Using a Mn^{2+} quench assay, we found that thapsigargin-induced SR calcium store depletion activates a calcium influx pathway in adult FDB fibres that is inhibited by: 1. multiple SOCE channel blockers (La^{3+} , BTP-2 and SKF96365); 2. prior expression of cherry-tagged dominant negative murine Orai1 (E108Q); or 3. STIM1 knockdown 12 days after *in vivo* electroporation of murine specific STIM1 siRNAs. To determine the potential role of SOCE in maintaining SR calcium stores during repetitive stimulation, we monitored myoplasmic calcium transients in mag-fluo-4 loaded mouse FDB fibres during repetitive high frequency tetanic stimulation (60 consecutive 500ms, 50Hz stimulation trains every 2.5s). Peak calcium transient amplitude was reduced dramatically with each tetanus by conditions that inhibit SOCE (*e.g.* addition of 0.5 mM Cd^{2+} /0.2 mM La^{3+} , 10 μ M BTP-2, 50 μ M SKF96365, and STIM1 knockdown).

To further assess the role of SOCE in skeletal muscle, we generated skeletal muscle-specific HA-tagged dominant negative murine Orai1 transgenic mice (HSAdnOrai) using a transgene containing the human skeletal muscle actin promoter (kindly provided by Dr. J. Molkenin). HSAdnOrai mice survive beyond weaning, grow and breed normally. Western blot analysis using an HA antibody confirmed dnOrai1 transgene expression in skeletal muscle, but not in heart, lung, brain, spleen kidney or liver. Primary skeletal myotubes derived from HSAdnOrai mice lack SOCE following SR calcium store depletion as assessed in Mn^{2+} quench, calcium influx, and whole cell patch clamp assays. In addition, compared to WT mice, the decline in peak calcium transient amplitude during repetitive tetanic stimulation was significantly increased in FDB fibres from HSAdnOrai mice. Together, these results demonstrate that STIM1-Orai1 coupling mediates SOCE in adult skeletal muscle and that this process limits SR calcium store depletion and the development fatigue during repetitive stimulation. In addition, muscle-specific HSAdnOrai transgenic mice are a powerful tool for future studies designed to assess the physiological role of SOCE in skeletal muscle.

Skeletal muscle ROS and glucose uptake during contraction

G.K. McConell¹ and T.L. Merry,² ¹*Institute of Sport, Exercise and Active Living and the School of Biomedical and Health Sciences, Victoria University, VIC 8001, Australia and* ²*Department of Sport and Exercise Science, University of Auckland, New Zealand.*

Exercise stimulates skeletal muscle glucose uptake by increasing GLUT-4 translocation from intracellular vesicles to the cell membrane through a mechanism(s) that differs from insulin stimulation. Although the pathway(s) through which contraction stimulates skeletal muscle glucose uptake is unclear, there is evidence for separate and collective contribution of several signalling intermediates including AMP-activated protein kinase (AMPK), nitric oxide (NO), calcium/calmodulin-dependent kinase (CaMK) and more recently, reactive oxygen species (ROS).

Exposure of isolated skeletal muscle to exogenous ROS increases glucose uptake (Toyoda *et al.*, 2004). In addition, intense contraction of isolated mouse EDL muscle increases ROS production and the antioxidant N-acetylcysteine (NAC) attenuates increases in skeletal muscle glucose uptake (Sandstrom *et al.*, 2006). Although Sandstrom *et al.* presented evidence to suggest that AMPK may play a role in ROS-mediated glucose uptake during contraction, we have recently shown that the increase in glucose uptake during *ex vivo* contraction is attenuated by NAC similarly in wild type and AMPK kinase dead mouse muscle (Merry *et al.*, 2010c). These results indicated that ROS regulate skeletal muscle glucose uptake during *ex vivo* contraction via AMPK-independent mechanisms. Interestingly, we have preliminary evidence suggesting that nitric oxide and ROS may interact during *ex vivo* contractions to regulate skeletal muscle glucose uptake, potentially via S-glutathionylation and/or peroxynitrite signalling.

Until recently the role of ROS in the regulation of contraction-stimulated skeletal muscle glucose uptake had only been examined using these isolated muscle models. In the absence of blood flow, such models depend on diffusion gradients for substrate delivery and clearance, and result in non-uniform delivery of oxygen to all muscle fibres. Furthermore, *ex vivo* muscle preparations generally involve supra-maximal highly fatiguing stimulation protocols. Therefore, we investigated the role of ROS signalling in the regulation of skeletal muscle glucose uptake during contraction/exercise in intact preparations by infusing NAC during moderate intensity *in situ* contractions in rats (Merry *et al.*, 2010a) and during exercise in humans (Merry *et al.*, 2010b). Unlike *ex vivo* contraction, we found that NAC did not affect skeletal muscle glucose uptake during contractions *in situ* and exercise *in vivo*. These results provide evidence that under physiological contraction/exercise conditions ROS may not be involved in the regulation of skeletal muscle glucose disposal and that previous results obtained using intense *ex vivo* contractions may not be relevant to normal exercise. However, more studies are required in this emerging area of interest before definitive conclusions can be drawn.

Merry TL, Dywer RM, Bradley EA, Rattigan S and McConell GK. (2010a) *Journal of Applied Physiology* **108**, 1275-1283.

Merry TL, Wadley GD, Stathis CG, Garnham AP, Rattigan S, Hargreaves M and McConell GK. (2010b) *Journal of Physiology* **588**, 1623-1634.

Merry TL, Steinberg GR, Lynch GS and McConell GK. (2010c) *American Journal of Physiology* **298**, E577-585.

Sandstrom ME, Zhang SJ, Bruton J, Silva JP, Reid MB, Westerblad H and Katz A. (2006) *Journal of Physiology* **575**, 251-262.

Toyoda T, Hayashi T, Miyamoto L, Yonemitsu S, Nakano M, Tanaka S, Ebihara K, Masuzaki H, Hosoda K, Inoue G, Otaka A, Sato K, Fushiki T and Nakao K. (2004) *American Journal of Physiology. Endocrinology and Metabolism* **287**, E166-173.

Effects of S-glutathionylation, S-nitrosylation and oxidation on Ca-sensitivity and force: a balancing act

G.D. Lamb, J.P. Mollica, T.L. Dutka, G.S. Posterino and R.M. Murphy, Department of Zoology, La Trobe University, Melbourne, VIC 3086, Australia.

Reactive oxygen species (ROS) and reactive nitrogen species (RNS) are important for skeletal muscle function both in physiological and pathological conditions. These agents are generated in active muscle and can induce both acute and long term effects on muscle function. Exposure of intact fast-twitch muscle fibres to the oxidant hydrogen peroxide (H_2O_2) affects force principally by altering myofibrillar Ca^{2+} sensitivity, initially producing increased sensitivity, followed by a decrease with more prolonged exposure (Andrade *et al.*, 1998). Experiments on skinned fibres show that these effects can be attributed to H_2O_2 interacting with glutathione and myoglobin, causing S-glutathionylation and oxidation of the contractile apparatus respectively (Lamb & Posterino, 2003; Murphy *et al.*, 2008). H_2O_2 can also oxidize the sarcoplasmic reticulum Ca^{2+} release channels, the ryanodine receptors, and studies on isolated channels show that this oxidation has a large stimulatory effect on Ca^{2+} -induced Ca^{2+} release. However, experiments on skinned and intact fibres show that acute H_2O_2 -induced oxidation has little or no effect on action potential-induced Ca^{2+} release, the normal physiological process governing Ca^{2+} release (Posterino *et al.*, 2003). Application of nitric oxide donors, on the other hand, produce a decrease in submaximal force in skinned muscle fibres, due primarily to a decrease in myofibrillar Ca^{2+} sensitivity (Spencer & Posterino, 2009), brought about by S-nitrosylation of the contractile apparatus. More extensive exposure of muscle to oxidants or nitrosylating agents can also lead to a decrease in both maximum force and Ca^{2+} -sensitivity of the contractile apparatus, likely due primarily to oxidation of reactive sulphhydryls in the myosin heads. The overall effect on muscle function of ROS and RNS generated in physiological and pathological conditions is determined by the balance of these conflicting actions of S-glutathionylation, S-nitrosylation and oxidation.

- Andrade FH, Reid MB, Allen DG & Westerblad H. (1998) *Journal of Physiology* **509**, 565-575.
Lamb GD & Posterino GS. (2003) *Journal of Physiology* **546**, 149-163.
Murphy RM, Dutka TL & Lamb GD. (2008) *Journal of Physiology* **586**, 2203-2216.
Posterino GS, Cellini MA & Lamb GD. (2003) *Journal of Physiology* **547**, 807-823.
Spencer T & Posterino GS. (2009) *American Journal of Physiology. Cell Physiology* **296**, C1015-1023.

Skeletal Muscle H₂O₂ and Insulin Sensitivity

T. Tiganis, Department of Biochemistry & Molecular Biology, School of Biomedical Sciences, Monash University, VIC 3800, Australia.

Reactive oxygen species (ROS) are thought to contribute to the progression of various human diseases. In type 2 diabetes, ROS are generated by mitochondria, as a by-product of oxidative phosphorylation and as a consequence of inflammation. There is direct evidence for ROS serving to suppress the insulin response and contribute to the development of insulin resistance, a key pathological feature of type 2 diabetes. Paradoxically, ROS generated by NADP(H) oxidases at the plasma membrane and endomembranes may also be required for normal intracellular signaling. A wide variety of physiological stimuli including growth factors, cytokines and hormones such as insulin promote the generation of ROS for the coordinated inactivation of protein tyrosine phosphatases (PTPs) and the promotion of tyrosine phosphorylation, as well as phosphatidylinositol 3-kinase and mitogen-activated protein kinase signaling. Thus, ROS have the potential to both promote and attenuate the insulin response. Our recently published studies (Loh *et al.*, 2009) have focused on the capacity of ROS to promote muscle insulin sensitivity through the inactivation of the PTP superfamily member PTEN, a lipid phosphatase that terminates signals generated by phosphatidylinositol-3-kinase.

Loh, K., Deng, H., Fukushima, A., Cai, X., Boivin, B., Galic, S., Bruce, C., Shields, B.J., Skiba B., Ooms L., Stepto, N., Wu, B., Mitchell, C.A., Tonks, N.K., Watt, M.J., Febbraio, M.A., Crack, P.J., Andrikopoulos, S., & Tiganis, T. (2009) Reactive oxygen species enhance insulin sensitivity. *Cell Metabolism* **10**, 260-272.

The role of ROS in insulin resistance

*D.E. James, Garvan Institute of Medical Research, 384 Victoria Street, Darlinghurst, NSW 2010, Australia.
(Introduced by Glenn McConell)*

A great deal is known about the cellular response to starvation *via* AMP-activated protein kinase (AMPK), but less is known about the adaptation to nutrient excess. Insulin resistance is one of the earliest responses to nutrient excess, but the cellular sensors that link these parameters remain poorly defined. It has been suggested that defects in the early elements of the insulin signalling cascade constitute the major cause of insulin resistance. However, we have recently described evidence in cell and animal models as well as in insulin resistant humans that this is not the case. On the other hand, mitochondrial superoxide production is a common feature of many different models of insulin resistance in adipocytes, myotubes, and mice. Moreover, insulin resistance was reversed by agents that act as mitochondrial uncouplers, ETC inhibitors, or mitochondrial superoxide dismutase (MnSOD) mimetics. Similar effects were observed with overexpression of mitochondrial MnSOD. Furthermore, acute induction of mitochondrial superoxide production using the complex III antagonist antimycin A caused rapid attenuation of insulin action independently of changes in the canonical PI3K/Akt pathway. These results were validated *in vivo* in that MnSOD transgenic mice were partially protected against HFD induced insulin resistance and MnSOD^{+/-} mice were glucose intolerant on a standard chow diet. These data place mitochondrial superoxide at the nexus between intracellular metabolism and the control of insulin action potentially defining this as a metabolic sensor of energy excess.

Periconceptual and early preimplantational undernutrition alters gene expression of metabolic and gluconeogenic regulating factors in the liver

S. Lie, J.L. Morrison, O. Wyss, S. Zhang and I.C. McMillen, Early Origins of Adult Health Research Group, Sansom Institute for Health Research, School of Pharmacy and Medical Sciences, University of South Australia, Australia.

Introduction: Maternal undernutrition during gestation can result in insulin resistance and glucose intolerance, leading to the development of type-2 diabetes. The effect of maternal undernutrition during the periconceptual period, however, has not been widely investigated. The metabolic master switch, AMP-Activated Protein Kinase (AMPK) and the master integrator of external signals, peroxisome proliferator-activated receptor γ co-activator 1 α (PGC-1 α) play critical roles in liver metabolism. More importantly, the capacity of the liver for gluconeogenesis which is regulated by phosphoenolpyruvate carboxykinase, PEPCK, is critical in maintaining glucose homeostasis.

Hypothesis: We hypothesise that periconceptual (PCUN) and early preimplantational (PIUN) undernutrition will result in a decrease in gene expression of the metabolic regulators, AMPK and PGC-1 α , as well as an increase in the gluconeogenic regulator, PEPCK in the fetal liver in late gestation.

Methods: Control ewes were fed 100% metabolisable energy (ME) from -45d to 6d after conception. Ewes in the PCUN group were fed 70% ME from -45d to 6d and ewes in the PIUN group were fed 70% ME from conception to 6d postconception. Liver samples were collected at 136-138d gestation. The mRNA expression of AMPK- α 1, AMPK- α 2, PGC-1 α and the mitochondrial and cytosolic forms of PEPCK (PEPCK-M, PEPCK-C) were analysed using Real Time-PCR. $p < 0.05$ was considered statistically significant.

Results: Hepatic mRNA expression of AMPK- α 1 was decreased in the PIUN singleton compared to the control and PCUN groups. There was no difference, however, in the expression of AMPK- α 2. The expression of PGC-1 α and the cytosolic form of PEPCK was decreased in the PIUN and PCUN groups compared to the control group, with no difference in the expression of the mitochondrial form of PEPCK.

Conclusion: Periconceptual and early preimplantational undernutrition may result in a dysregulation of hepatic energy metabolism and a decrease in gluconeogenesis. The decrease in AMPK- α 1 mRNA expression in the PIUN group may be due to a mismatch between the oocyte and the early embryo's energy status.

The effects of chronic moderate prenatal ethanol exposure on cardiovascular and renal artery function in adult rats

M. Tjongue,¹ M. Tare,¹ M.E. Probyn,² K.M. Moritz² and K.M. Denton,¹ ¹Department of Physiology, Monash University, VIC 3800, Australia and ²School of Biomedical Sciences, University of Queensland, QLD 4072, Australia.

Maternal alcohol consumption during pregnancy remains common in society today. Prenatal exposure to high levels of alcohol can cause developmental abnormalities. The effect of more moderate alcohol exposure on the offspring remains unclear. An adverse environment in early life can increase the risk of cardiovascular disease in adulthood. The aim of this study was to examine the effects of chronic moderate fetal alcohol exposure on arterial pressure and vascular function in adult rat offspring. Female rats were given a complete liquid diet containing either ethanol (6% v/v equating to 15% of total calories and a peak blood alcohol content of 0.03 – 0.05%) or an isocaloric equivalent during pregnancy. Male ($n = 6-9$) and female ($n = 7-8$) offspring were studied at 1 year of age. Mean arterial pressure (MAP) was recorded under basal conditions and during restraint stress *via* radiotelemetry. At *post mortem*, the kidneys were removed and the renal interlobar arteries were isolated. Segments of renal interlobar artery were mounted onto a wire myograph for testing of smooth muscle and endothelial function. Arteries were bathed in warmed, oxygenated physiological saline (PSS). Other segments of artery were mounted onto a pressure myograph and bathed in 0mM Ca²⁺ PSS containing 1mM EGTA, for the assessment of passive wall stiffness. Basal MAP and heart rate (HR) were not different between vehicle and alcohol-treated groups. MAP and HR increased significantly in response to restraint stress, however, the increase in MAP was lower in alcohol-treated groups of both sexes ($p = 0.001$). Constriction of the renal interlobar artery evoked by single pulses of perivascular nerve stimulation was smaller in alcohol-treated females ($p = 0.012$), but not in the males. Vasoconstriction evoked by angiotensin II and phenylephrine, and vasodilation evoked by the nitric oxide donor sodium nitroprusside, were not altered with alcohol treatment. Total endothelium-dependent relaxation and the relaxation due to endothelium-derived hyperpolarizing factor were not different between treatment groups. Interlobar arteries from alcohol-treated females were modestly more compliant ($p = 0.02$), but arterial stiffness was not different between treatment groups for the males. In conclusion, this study demonstrates that even moderate maternal alcohol consumption, equivalent to 2 standard drinks per day, during pregnancy does have lasting effects on the cardiovascular system of the offspring.

Gonadotropin-inhibiting hormone (GnIH) regulates spontaneous action potentials in anorexigenic proopiomelanocortin neurons and orexigenic neuropeptide Y cells

J.S. Jacobi, H.A. Coleman, A. Sali, H.C. Parkington, M.A. Cowley and I.J. Clarke, Department of Physiology, Monash University, Clayton, VIC 3800, Australia..

Energy homeostasis and reproduction are intimately related and the mechanisms for such a close connection are the subject of considerable attention. However, our understanding of the neurobiological basis for this phenomenon is still incomplete. Neuropeptide Y (NPY) is a potent orexigen that is produced by cells in the arcuate nucleus of the hypothalamus. In the same nucleus, cells express the proopiomelanocortin (POMC) gene that produces melanocortins which are anorectic. Gonadotropin-inhibiting hormone (GnIH) peptide is a recently discovered inhibitory regulator of reproduction that is released by neurons localized in the dorsomedial nucleus of the hypothalamus, which is a nucleus with a role in regulating appetite and energy balance. It has been reported that central injections of GnIH increase food intake in birds and rats. Since GnIH neurons provide input to subsets of NPY and POMC cells, the aim of this study was to determine the effects of GnIH on the electrical activity of these appetite regulating neurons of the arcuate nucleus.

We used mice in which NPY or POMC genes were tagged with a transgene for renilla and green fluorescent protein. Mice were killed, the brain was rapidly removed into an ice slurry, and 250 μm thick coronal slices were cut. Slices were mounted in a recording chamber on the platform of an upright microscope and continuously superfused with artificial cerebrospinal fluid (aCSF) at 32°C. GFP-expressing cells were identified using epifluorescence, and patch electrodes were positioned using infrared DIC optics. Patch-clamp recordings of spontaneous action potential activity were made in whole-cell current-clamp mode or in cell-attached mode.

GnIH inhibited the firing rate of POMC cells. Since these cells are anorexigenic this inhibition may be involved in the increase of food intake induced by GnIH. The GnIH regulation of NPY cells was more complex. In one group of NPY cells, GnIH inhibited spontaneous action potential activity and this effect was associated with a clear hyperpolarisation of the membrane potential. Another group of NPY cells showed no effect of GnIH. The combined presence of blockers of glutamatergic and GABAergic receptors decreased spontaneous action potential activity. Under these conditions, GnIH evoked an increase in action potential activity.

In conclusion, these data indicate that GnIH, in addition to having an important role in regulating reproductive function, is also a significant regulator of the appetite/energy expenditure system within the hypothalamus.

Maternal overnutrition during the periconceptional period and gender influences insulin signalling and glucose handling in lambs after birth

L.M. Nicholas,¹ L. Rattanatrak,¹ S. McLaughlin,¹ S.E. Ozanne,² B.S. Muhlhausler,¹ D. Kleeman,³ S. Walker,³ J.L. Morrison¹ and I.C. McMillen,¹ ¹Sansom Institute of Health Research, University of South Australia, SA 5000, Australia, ²Institute of Metabolic Science-Metabolic Research Laboratories, Addenbrooke's Hospital, Cambridge, CB2 0QQ, United Kingdom and ³Turrefield Research Centre, South Australian Research and Development Institute, SA 5000, Australia.

The increased prevalence of overweight and obesity amongst Australians aged 18 years and older is reflected in an increase in the number of women who are entering pregnancy obese (Callaway, O'Callaghan & McIntyre, 2009; Ryan, 2007; LaCoursiere *et. al.*, 2005). Maternal obesity before pregnancy is associated with an increased risk of obesity and metabolic disease in the offspring (Catalano *et. al.*, 2003). How the liver responds to insulin is an important contributor to the body's ability to maintain normal glucose levels throughout life (Postic, Dentin & Girard, 2004). Little is known, however, about the impact of maternal obesity or the impact of dieting before conception on how the liver of her offspring responds to insulin in order to maintain glucose homeostasis. The present study investigated whether maternal obesity during the periconceptional period (*i.e.* before and just one week after conception) resulted in changes in the expression of insulin signalling molecules and genes that control glucose output in the liver of postnatal lambs. This study also investigated the effects of dietary restriction in overnourished and normally nourished ewes on these measures of hepatic insulin sensitivity in the offspring.

Donor ewes were randomly allocated to one of 4 treatment groups. The CC group received a control diet of 100% metabolisable energy requirements (MER) for 4 months before conception. The CR group received a diet of 100% MER for 3 months followed by a restricted diet (70% MER) for 1 month. Ewes in the HH group, which is our model of maternal periconceptional overnutrition, was overnourished (~180% MER) for 4 months. The HR group, which is our model of dietary restriction in the overnourished ewe, was overfed for 3 months followed by a restricted diet of 70% MER for 1 month. After conception, single embryos were transferred into non obese 'recipient' ewes at 6-7 days after conception. Ewes lambed normally and tissues including the liver were collected at 4 months of age for analysis.

There was a lower ($p<0.05$) abundance of insulin signalling proteins Akt2, pAkt and pFoxO1 in the HH group and this effect was ameliorated in the HR group. Interestingly, expression of the gluconeogenic enzyme PEPCK (mitochondrial form) and 11 β HSD1 mRNA was lower ($p<0.05$) in the HH group and this effect was also abolished in the HR group. In addition, expression of the cytosolic form of PEPCK mRNA was lower ($p<0.05$) in CR, HH (male lambs) and HR groups.

In conclusion, periconceptional overnutrition appears to program decreased expression of insulin signalling molecules in the liver of the offspring which could contribute to the emergence of insulin resistance in later life. In contrast, periconceptional over- and under-nutrition differentially suppress the mitochondrial and cytosolic forms of the major gluconeogenic enzyme in the liver which may protect the lamb from the consequences of poor insulin signalling in the immediate term.

Callaway, L.K., O'Callaghan, M.J., & McIntyre, H.D. (2009). Barriers to addressing overweight and obesity before conception. *Medical Journal of Australia* **191**: 425-428.

Catalano, P.M., Kirwan, J.P., Haugel-de Mouzon, S., & King, J. (2003). Gestational diabetes and insulin resistance: role in short- and long-term implications for mother and fetus. *Journal of Nutrition* **133**: 1674S-1683S.

LaCoursiere, D.Y., Bloebaum, L., Duncan, J.D., & Varner, M.W. (2005). Population-based trends and correlates of maternal overweight and obesity, Utah 1991-2001. *American Journal of Obstetrics and Gynecology* **192**: 832-839.

Postic, C., Dentin, R., & Girard, J. (2004). Role of the liver in the control of carbohydrate and lipid homeostasis. *Diabetes and Metabolism* **30**: 398-408.

Ryan, D. (2007). Obesity in women: A life cycle of medical risk. *International Journal of Obesity* **31**: S3-S7.

The role of regulator of calcineurin 1 (RCAN1) in the regulation of glucose homeostasis

H. Peiris,¹ D. Mohanasundaram,² J. Brealey,³ C. Jessup,^{2,5} T. Coates,^{2,5} M. Pritchard⁴ and D. Keating,¹

¹Molecular and Cellular Neuroscience Group, Department of Human Physiology and Centre for Neuroscience, Flinders University, Adelaide, SA 5000, Australia, ²Central Northern Adelaide Renal and Transplantation Service, Royal Adelaide Hospital, North Terrace, Adelaide, SA 5000, Australia, ³Surgical Pathology, Electron Microscopy Unit, Royal Adelaide Hospital, North Terrace, Adelaide, SA 5000, Australia, ⁴Department of Biochemistry and Molecular Biology, Monash University, VIC 3800, Australia and ⁵School of Medicine, University of Adelaide, Adelaide, SA 5000, Australia.

Regulator of calcineurin 1 (RCAN1) is a gene located on chromosome 21 and is over expressed in the brains of Down syndrome (DS) patients. Our lab has previously shown that RCAN1 regulates exocytosis in adrenal chromaffin cells. As the incidence of diabetes is 5-10 times greater in the DS population we are investigating the effect of increased RCAN1 expression and its possible role in the pathogenesis of diabetes. Transgenic mice with a universal over-expression of RCAN1 were generated for this study. *In vivo* studies indicate that transgenic mice develop age-dependent diabetes characterized by increased fasting blood glucose levels of 5.8 ± 0.3 mmol/L (n=9) at 60 days old compared to 4.2 ± 0.2 mmol/L (n=9) in age-matched wild-type mice ($p < 0.05$). Glucose tolerance, measured by injecting 2mg glucose/g body weight, is also reduced in transgenic mice, with glucose values reaching peak levels of 27.5 ± 1.4 mmol/L (n=5) after 60 minutes compared to 19 ± 1.3 mmol/L (n=5) in wild-type mice ($p < 0.01$). Immunohistochemical analysis of pancreatic islets revealed that transgenic mice have a 70% reduction in islet area (n=4) at 100 days. Electron microscopy analysis reveals that transgenic mice have a 40% increase in empty secretory vesicles (n=3) at 120 days. Transgenic mice also have significantly decreased fasting blood insulin values at 120 days (n=6) when compared to age-matched wild-type mice. In islets of transgenic mice, expression of genes such as those mutated in hereditary forms of monogenic type 2 diabetes (MODY) and others related to β -cell survival and insulin production were downregulated. Our findings highlight a novel role of RCAN1 in regulating glucose homeostasis, islet growth, secretory vesicle loading and insulin release. Additionally expression of RCAN1 increased 2.5 fold ($p < 0.05$) when islets were exposed *in vitro* to 16.7 mM glucose for 6 days. This along with our previous findings provide the exciting proposition that RCAN1 may be involved in the β -cell failure and hypoinsulinemia that occurs in the later stages of type 2 diabetes.

Agonist interactions and selectivity in GABA_{A/C} receptors

B.A. Cromer, H.S. Tae and S. Petrou, Health Innovations Research Institute, School of Medical Sciences, RMIT University, Bundoora, VIC 3083, Australia and Howard Florey Institute, University of Melbourne, Parkville, VIC 3095, Australia.

Cys-loop ligand-gated ion channels constitute one of two major superfamilies of receptors mediating rapid chemical synaptic transmission in the central nervous system. They include cation selective channels that are receptors for excitatory neurotransmitters, acetylcholine and serotonin, and anion selective channels that are receptors for inhibitory neurotransmitters, γ -aminobutyric acid (GABA) and glycine. Recent structural information from snail acetylcholine binding proteins (AChBP), torpedo acetylcholine receptors and bacterial homologs have provided a good understanding of the overall structure of the superfamily and of specific details of acetylcholine-receptor interactions. For inhibitory receptors for GABA and glycine, however, we have a much more limited understanding of how receptors interact with and are selectively activated by particular agonists.

In this study, we have investigated interactions between GABA and receptor, using the homopentameric $\rho 1$ γ -aminobutyric acid receptor (GABA_C) as a model for the broader family of heteropentameric GABA_A receptors. We used homology modeling to identify a series of conserved charged residues at the GABA-binding site that we hypothesized formed a series of charge-charge interactions likely to be important for interaction with agonist, agonist selectivity and receptor activation. We have tested this hypothesis using site-directed mutagenesis in combination with two-electrode voltage clamp recording of recombinant receptors expressed in *Xenopus* oocytes. Preliminary results have revealed key determinants of agonist selectivity, particularly determining sensitivity to the size or length of the ligand, as well as receptor activation or gating. These results are consistent with our hypothesis and provide a basis for a more detailed understanding of agonist-receptor interactions in inhibitory Cys-loop ligand-gated ion channels.

Defining GABA_A receptor pharmacology and physiologies through the disruption of receptor protein interactions

M.L. Tierney,¹ V.A.L. Seymour,¹ J. Curmi,¹ W. Xu² and H.C. Chan,² ¹The John Curtin School of Medical Research, The Australian National University, Canberra, ACT 0200, Australia and ²Epithelial Cell Biology Research Center, School of Biomedical Sciences, Faculty of Medicine The Chinese University of Hong Kong, Shatin, Hong Kong.

GABA_A receptors are the dominant inhibitory neurotransmitter-gated ion channel in the central nervous system. We have identified a novel way in which these neuronal ion channels alter their electrical response. Interactions between neighbouring, clustered GABA_A receptors profoundly alter single-channel properties (conductance and kinetics), leading to a significant enhancement of channel activity ('cross-talk') (Everitt *et al.*, 2009). Interactions were identified using competitor peptides that mimic defined intracellular protein binding sites. Peptides were applied directly onto inside-out membrane patches pulled from newborn rat hippocampal neurons and single-channel currents were recorded. Combining the use of competitor peptides and single-channel recordings provided a visual insight into the dynamic nature of protein interactions that affect the activity of single GABA_A ion channels. Specifically, when applied to inside-out patches, a peptide mimicking the MA helix of the $\gamma 2$ subunit ($\gamma 381-403$) of the GABA_A receptor abrogated the potentiating effect of the drug diazepam on endogenous receptors by substantially reducing their conductance.

In addition to benzodiazepines, barbiturates, general anaesthetics and neurosteroids have all been shown to facilitate neuronal receptor cross-talk, that is, the drugs potentiate GABA-activated currents increasing both channel open probability and conductance. Such drugs however, are predicted to act on different GABA_A receptor subtypes. We hypothesized therefore, that modulation of ion permeation was a general mechanism through which all GABA_A receptor subtypes signal. Using a competitor peptide specific to δ -containing GABA_A receptors we tested our hypothesis. GABA currents were potentiated by the general anesthetic etomidate and competitor peptides were applied to neuronal patches. Addition of the δ MA peptide but not a scrambled version or the γ MA peptide abrogated the potentiating effects of etomidate. These data support our hypothesis and are aiding our understanding of the complex interplay between drugs and ion channels and also amongst the different GABA_A receptors subtypes themselves.

Everitt AB, Seymour VA, Curmi J, Laver DR, Gage PW, Tierney ML. (2009) Protein interactions involving the $\gamma 2$ large cytoplasmic loop of GABA_A receptors modulate conductance. *FASEB Journal* **23**: 4361-4369.

Developing activation mechanisms for GABA_A receptors

A. Keramidas, Queensland Brain Institute, QBI Building #79, St Lucia, QLD 4072, Australia.

The $\alpha 1\beta 2\gamma 2$ and $\alpha 3\beta 3\gamma 2$ are two synaptic isoforms of α -aminobutyric acid type A (GABA_A) receptor. They are found at different synapses, for example in the thalamus, where they mediate different inhibitory postsynaptic current profiles, particularly with respect to the rate of current decay. The kinetic characteristics of both isoforms were investigated by analysing single-channel currents over a wide range of GABA concentrations. $\alpha 1\beta 2\gamma 2$ channels exhibited briefer active periods than $\alpha 3\beta 3\gamma 2$ channels over the entire range of agonist concentrations and had lower intraburst open probabilities at subsaturating concentrations. Activation mechanisms were constructed by fitting postulated reaction schemes to data recorded at saturating and subsaturating GABA concentrations, simultaneously. Reaction mechanisms were ranked according to goodness of fit values to open and shut dwell histograms of single channel activity, and how accurately they simulated ensemble currents. The highest ranked mechanism for both channels consisted of two sequential binding steps, followed by three conducting and three nonconducting configurations. The equilibrium dissociation constant for GABA at $\alpha 3\beta 3\gamma 2$ channels was $\sim 3 \mu\text{M}$ compared with $\sim 19 \mu\text{M}$ for $\alpha 1\beta 2\gamma 2$ channels, suggesting that GABA binds to the $\alpha 3\beta 3\gamma 2$ channels with higher affinity. A notable feature of the mechanism was that two consecutive doubly liganded shut states preceded all three open configurations. The lifetime of the third shut state was briefer for the $\alpha 3\beta 3\gamma 2$ channels. The longer active periods, higher affinity, and preference for conducting states are consistent with the slower decay of inhibitory currents at synapses that contain $\alpha 3\beta 3\gamma 2$ channels. The reaction mechanism we describe accurately simulates real macropatch and synaptic currents mediated by the two GABA_A receptor subtypes and may be appropriate for the analysis of other GABA_A receptor isoforms. The mechanism may also be applicable for the rational investigation of the kinetic effects of therapeutic agents that activate and modulate GABA_A receptors, in addition to mutated channels that give rise to disease.

Understanding the molecular and pharmacological basis of selectivity of nicotinic acetylcholine receptor antagonists using reactive methyllycaconitine analogues

N.L. Absalom,¹ G. Quek,¹ J. Ambrus,² M.D. McLeod² and M. Chebib,¹ ¹Faculty of Pharmacy, University of Sydney, Camperdown, NSW 2006, Australia and ²Research School of Chemistry, Australian National University, Canberra, ACT 0200, Australia.

The nicotinic acetylcholine receptor (nAChR) mediates fast synaptic transmission between neural cells. The nAChR is a pentameric protein that contains a large extracellular domain, four transmembrane domains (M1-M4) where the second M2 lines the channel pore, two short M1-M2 and M2-M3 loops that move to gate the channel and a large intracellular M3-M4 loop. There is a large amount of subunit heterogeneity within the nAChR, which can be formed by specific combinations of α 2-10 and β 2-4 receptors. The expression patterns of receptor subtypes partly determine the physiological role of each nAChR subtype. Thus, pharmacological agents that can distinguish between receptor subtypes may have greater selectivity for certain physiological process, and may provide superior pharmacological agents. The α 7 homomeric is potently and selectively inhibited by the toxin methyllycaconitine (MLA) from the larkspur plant. Our aim was to identify the site of the receptor that conferred the binding selectivity to MLA on the α 7 receptor and compare this to the corresponding residues on the α 4 β 2 receptor. The α 7, α 4 or β 2 cRNA was injected into *Xenopus* oocytes that were removed from frogs anaesthetized with tricaine and ion channel function was measured by the two-electrode voltage clamp technique. For efficient expression of the α 7 nAChR, cRNA for the chaperone protein RIC-3 was co-injected. To prevent the large desensitization properties of the α 7 nAChR, a mutant L9'T DNA was created by site directed mutagenesis and all further mutations were studied with this background. The L9'T mutation markedly affected acetylcholine activation but not MLA sensitivity. When varying concentrations of ACh were applied to oocytes injected with α 7 or α 7L9'T after 3 minute incubation with a set concentration of MLA, the maximum response was the same as for the maximum response to ACh alone. This suggests that the ACh is competing for the same binding site with the MLA. Furthermore, the IC₅₀ of MLA is significantly reduced in the α 4 β 2 nAChRs, highlighting the selectivity. When this experiment was performed on oocytes injected with α 4 β 2 nAChRs, the ACh the maximum response with ACh and MLA was significantly lower than ACh alone, indicating that the MLA was also binding at a site different to the ACh-binding site. A previous published crystal structure of the acetylcholine binding protein bound to MLA identified residues that interact directly with the MLA molecule. We focused on two sites where MLA was bound, including the Q79 residue where several antagonists and agonists of the α 7 nAChR confer selectivity by interactions with this residue in the extracellular domain. We have mutated this residue to the lysine and threonine residues that are the homologous residues on the α 4 and β 2 receptors, respectively to create the Q79K L9'T and Q79T L9'T mutant receptors. We have also made the homologous reversal mutations on the α 4 and β 2 subunits to determine if the MLA inhibition is altered. A second approach was taken by modifying MLA to contain a cysteine-reactive MLA molecule that can tether to introduced cysteines on the target receptor. We applied this molecule to α 7 receptors with introduced cysteine residues and identified one residue, S188C L9'T, where the addition of the cysteine reactive MLA causes a permanent reduction in the current elicited by ACh. This indicates a strong association between this residue and the site of the cysteine reactive group in MLA binding. We have made the corresponding mutations in the α 4 and β 2 subunits to compare the residues that bind to MLA in nAChR subtypes. Here we show that the while the residues that bind to selective antagonists of nAChRs can be predicted with homology models, the mechanism by which these antagonists are selective are best understood by studies using a combination of site-directed mutagenesis and chemical modification.

Reciprocal regulation of expression of STIM1 and Orai1 proteins

L. Ma,¹ D.P. Wilson,¹ G.J. Barritt² and G.Y. Rychkov,^{1,1} ¹School of Medical Sciences, University of Adelaide, Adelaide, SA 5000, Australia and ²School of Medicine, Flinders University of South Australia, Adelaide, SA 5011, Australia.

Two proteins, stromal interaction molecule 1 (STIM1) and Orai1 constitute the minimum molecular components of the Ca²⁺ release-activated Ca²⁺ (CRAC) channel (Liou *et al.*, 2005; Roos, *et al.*, 2005; Vig, *et al.*, 2006). STIM1 is predominantly located in the membrane of the endoplasmic reticulum (ER) and functions as a molecular sensor of free ER Ca²⁺, whereas Orai1 is located on the plasma membrane and when activated by STIM1 forms the Ca²⁺ selective pore of the channel (Yeromin *et al.*, 2006). While activation of CRAC channels uniquely depends on the free Ca²⁺ concentration in the ER lumen, its inactivation is regulated by both the free ER [Ca²⁺] and the cytosolic [Ca²⁺]. Fast Ca²⁺-dependent inactivation (FCDI) is a feedback mechanism which limits Ca²⁺ entry through these channels at negative potentials and is regulated by Ca²⁺ binding to surface composed of residues from both Orai1 and STIM1 (Mullins *et al.*, 2009; Lee *et al.*, 2009). Previously we identified that FCDI of I_{CRAC} depends on the relative expression levels of the STIM1 and Orai1 proteins (Scrimgeour *et al.*, 2009). Herein we present data that suggests the presence of another Ca²⁺-dependent mechanism which regulates the activity of CRAC channels. Specifically, the expression of STIM1 and Orai1 are interdependent and also [Ca²⁺]-dependent.

Heterologous expression of STIM1 and Orai1 was conducted in HEK293T cells using the plasmid/DNA vectors pEX-GFP-Myc-Orai1, pCMV-Sport6-STIM1, pCMV-Sport6-Orai1, Sport6-Orai1 Δ 70-88 and pCIneo-hCIC-1 which were co-transfected at different ratios (between 1:8 and 8:1 of Orai1:STIM1) using PolyFect transfection reagent (Qiagen). The relative expression of STIM1 and Orai1-GFP proteins was determined using quantitative western blot analysis using anti-STIM1 and anti-GFP antibodies. GAPDH was used as an internal loading control.

Increasing the amount of Orai1 containing plasmid in the transfection mixture resulted in a significant decrease in STIM1 expression. In contrast, control experiments using expression of either, non-functional Orai1 Δ 70-88 or the unrelated CIC-1 protein had no effect on the expression levels of STIM1, identifying that the Orai1-STIM1 interaction was not a non-specific effect of competition in co-transfection. Depletion of intracellular Ca²⁺ stores, using thapsigargin, which activates Ca²⁺ entry through CRAC channels, increased the dependence of STIM1 expression on the Orai1. In contrast, inhibition of Ca²⁺ entry by 2-aminoethoxy-diphenyl borate (2-APB) or La³⁺ virtually abolished the interdependence of STIM1 and Orai1 expression.

These data indicate that the expression of STIM1 and Orai1 proteins is interdependent and is regulated in a Ca²⁺-dependent manner which may provide an important cellular feedback mechanism to enable medium to long term regulation of ER Ca²⁺ homeostasis.

Lee KP, Yuan JP, Zeng W, So I, Worley PF & Muallem S. (2009) *Proceedings of the National Academy of Sciences of the United States of America* **106**: 14687-92.

Liou J, Kim ML, Heo WD, Jones JT, Myers JW, Ferrell JE & Meyer Jr.T. (2005) *Current Biology* **15**: 1235-41.

Mullins FM, Park CY, Dolmetsch RE & Lewis RS. (2009) *Proceedings of the National Academy of Sciences of the United States of America* **106**: 15495-500.

Roos J, DiGregorio PJ, Yeromin AV, Ohlsen K, Lioudyno M, Zhang S, Safrina O, Kozak JA, Wagner SL, Cahalan MD, Velicelebi G & Stauderman KA. (2005) *Journal of Cell Biology* **169**: 435-45.

Scrimgeour N, Litjens T, Ma L, Barritt GJ & Rychkov GY. (2009) *Journal of Physiology* **587**: 2903-18.

Vig M, Peinelt C, Beck A, Koomoa DL, Rabah D, Koblan-Huberson M, Kraft S, Turner H, Fleig A, Penner R & Kinet JP. (2006) *Science* **312**: 1220-3.

Yeromin AV, Zhang SL, Jiang W, Yu Y, Safrina O & Cahalan MD. (2006) *Nature* **443**: 226-9.

Atrogin-1 regulation in human and mouse skeletal myotubes

R.J. Stefanetti and A.P. Russell, Centre for Physical Activity and Nutrition Research, School of Exercise and Nutrition Sciences, Deakin University, 221 Burwood Highway, Burwood, VIC 3125, Australia.

Atrogin-1, an E3 ubiquitin ligase, is increased in numerous models of muscle atrophy and is seen as a potential therapeutic target to combat muscle wasting. While previous rodent studies have consistently shown that under catabolic conditions, Atrogin-1 is regulated by FoXO transcription factors, studies in atrophic human skeletal muscle do not support a dominant role of FoXO. Our aim was to identify potential transcriptional regulators of Atrogin-1 in human and mouse myotubes. Human primary and C2C12 myotubes were infected with a c-MyC, C/EBPa or PPARd adenovirus for 48 h. Atrogin-1 mRNA levels were increased by 72% and decreased by 52% with PPARd and C/EBPa over-expression, respectively. mRNA analysis in human myotubes is in progress. At the protein level there was a 74% and 46% increase in Atrogin-1 with C/EBPa over-expression in mouse and human myotubes, respectively. c-MyC and PPARd over-expression increased Atrogin-1 protein by 46% and 62% in mouse myotubes respectively, while in human myotubes infection with c-MyC and PPARd decreased Atrogin-1 protein levels by 23% and 26% respectively. These preliminary results suggest that Atrogin-1 may be transcriptionally regulated by factors other than FoXO, and further highlight that Atrogin-1 regulation is species dependent. Future studies will determine direct transcriptional regulators of Atrogin-1 *via* luciferase assays.

NDRG2, a novel player in the control of skeletal muscle mass?

V.C. Foletta and A.P. Russell, Centre for Physical Activity and Nutrition Research, School of Exercise and Nutrition Sciences, Deakin University, 221 Burwood Highway, VIC 3125, Australia.

The N-myc downstream-regulated genes (NDRG1-4) represent a family of molecules linked to cell growth, differentiation and stress (Melotte *et al.*, 2010); however, how they function and their protein partners are poorly described. Recently, we identified that the knockdown of NDRG2 affected myoblast proliferation and differentiation (Foletta *et al.*, 2009). In addition, we identified that NDRG2 expression increased markedly with muscle differentiation and that its gene expression increased also following treatment with catabolic agents, and conversely, decreased under hypertrophic conditions in myotubes. Furthermore, the profile of NDRG2 gene expression closely matched the mRNA profiles of the E3 ligases atrogin-1/MAFbx and MuRF1, key regulators of the ubiquitin proteasome pathway and skeletal muscle mass. This outcome suggests that these three genes are regulated by related factors and that they may have connected roles during changes in muscle mass. Here, we sought to characterize further the potential relationship of these molecules in differentiated muscle cells.

Protein synthesis and degradation as measured by ³H-tyrosine incorporation and release, respectively, was assessed in mouse C2C12 myotubes following the knockdown of NDRG2 protein levels by siRNA under basal, 10 nM insulin and 1 μM dexamethasone treatments. Co-immunoprecipitation analyses of overexpressed NDRG2, atrogin-1 and MuRF1 proteins in C2C12 myoblasts in the presence or absence of the proteasome inhibitor MG132 also were performed.

A 20% increase in insulin-mediated protein synthesis ($p < 0.01$) was found in myotubes lacking NDRG2 although no effect on protein degradation was measured. Co-immunoprecipitation analyses also revealed an ability of NDRG2 to interact with both atrogin-1 and MuRF1. Moreover, the interaction between NDRG2 and atrogin-1 was enhanced by 20 μM MG132, but not for the NDRG2 and MuRF1 interaction, suggesting that the inhibition of atrogin-1 activity may promote NDRG2-atrogin-1 binding.

These data provide corroborative evidence of a relationship between NDRG2 and the ubiquitin proteasome regulators, atrogin-1 and MuRF1, and that NDRG2 may also impact on the control of skeletal muscle mass. Currently, we are characterising the signaling pathways through which NDRG2 may affect protein synthesis. These studies will help provide greater insight into the complex molecular mechanisms governing muscle mass regulation.

Melotte V, Qu X, Ongenaert M, van Crielinge W, de Bruine AP, Baldwin HS and van Engeland M. (2010). *FASEB Journal* **24**:1-14

Foletta VC, Prior M, Stupka N, Carey K, Segal DH, Jones, S, Swinton C, Martin S, Cameron-Smith D and Walder KR. (2009). *Journal of Physiology* **587**: 1619-34.

Multiple cell types express myokines following intense resistance exercise

P.A. Della Gatta,¹ J. Peake,² A.P. Garnham¹ and D. Cameron-Smith,¹ ¹School of Exercise and Nutrition Sciences, Deakin University, 221 Burwood Hwy, Burwood, VIC 3125, Australia and ²School of Human Movement Studies, The University of Queensland, St Lucia, QLD 4072, Australia.

Optimal repair of skeletal muscle following injury requires a significant and well orchestrated inflammatory response. The infiltration of leukocytes, and particularly monocytes/macrophages, in the hours/days following injury is a critical component in the repair of skeletal muscle (Chazaud *et al.*, 2009; Koh & Pizza, 2009). These cells are not only responsible for the clearance of cellular debris, but also the release of factors that help to control the myogenic program of stem cells (Chazaud *et al.*, 2009). While the appearance and functions of these cells have been widely investigated, the factors that are responsible for the recruitment and chemotaxis of leukocytes into skeletal muscle are still somewhat unknown. Our aim was to investigate the effect of a single bout of resistance exercise on the expression and localization of 2 major chemoattractive factors, monocyte chemoattractant protein 1 (MCP-1) and interleukin 8 (IL-8).

Eight young males (22.1±0.2yr) completed three sets of resistance exercise for the leg muscles (leg press, leg extension and squat). Two sets consisted of 8-12 repetitions at 80% 1-RM, whereas in the final set the subjects exercised until exhaustion. Muscle biopsies were obtained before exercise, and 2, 4 and 24 h after exercise. Expression of MCP-1 and IL-8 was analyzed *via* Multiplex analysis (protein) and PCR (gene). Immunohistochemistry was used to establish localization.

Large increases in both gene and protein expression of MCP-1 and IL-8 were evident 2 h following exercise completion, returning to resting levels by 24 h. Neither factor was prevalent within the cytoplasm of myofibres following exercise. MCP-1 was localized predominately to Pax7 and CD68 positive mononucleated cells, but not strictly confined to these cell types. The distribution of IL-8 immunoreactivity was different to that of MCP-1 and seemed to be in close proximity to collagen IV expressing cells.

Both MCP-1 and IL-8 have been identified as major regulators of muscle mediated leukocyte recruitment *in vitro* (Chazaud *et al.*, 2003; Peterson & Pizza, 2009). The present study indicated that both factors increased dramatically in response to a single bout of resistance exercise, which is in accordance with previous literature (Nieman *et al.*, 2004; Hubal *et al.*, 2008). The localization of these factors within a variety of cell types, and the contrasting pattern of expression, suggest a complex and multifaceted response occurs within the muscular microenvironment to regulate inflammation and muscular repair in response to resistance exercise.

- Chazaud B, Brigitte M, Yacoub-Youssef H, Arnold L, Gherardi R, Sonnet C, Lafuste P & Chretien F. (2009). Dual and beneficial roles of macrophages during skeletal muscle regeneration. *Exercise and Sport Sciences Reviews* **37**, 18-22.
- Chazaud B, Sonnet C, Lafuste P, Bassez G, Rimaniol AC, Poron F, Authier FJ, Dreyfus PA & Gherardi RK. (2003). Satellite cells attract monocytes and use macrophages as a support to escape apoptosis and enhance muscle growth. *Journal of Cell Biology* **163**, 1133-1143.
- Hubal MJ, Chen TC, Thompson PD & Clarkson PM. (2008). Inflammatory gene changes associated with the repeated-bout effect. *American Journal of Physiology. Regulatory, Integrated and Comparative Physiology* **294**, R1628-1637.
- Koh TJ & Pizza FX. (2009). Do inflammatory cells influence skeletal muscle hypertrophy? *Frontiers in Bioscience (Elite Ed)* **1**, 60-71.
- Nieman DC, Davis JM, Brown VA, Henson DA, Dumke CL, Utter AC, Vinci DM, Downs MF, Smith JC, Carson J, Brown A, McAnulty SR & McAnulty LS. (2004). Influence of carbohydrate ingestion on immune changes after 2 h of intensive resistance training. *Journal of Applied Physiology* **96**, 1292-1298.
- Peterson JM & Pizza FX. (2009). Cytokines derived from cultured skeletal muscle cells after mechanical strain promote neutrophil chemotaxis *in vitro*. *Journal of Applied Physiology* **106**, 130-137.

PGC-1 α and PGC-1 β regulate protein synthesis in C2C12 myotubes

E.L. Brown, P. Sepulveda, C.R. Wright, R. Snow and A.P. Russell, Centre for Physical Activity and Nutrition Research, School of Exercise and Nutrition Sciences, Deakin University, 221 Burwood Highway, Burwood, VIC 3125, Australia.

Skeletal muscle atrophy is characterised by increased rates of protein degradation and/or decreased rates of protein synthesis. Overexpression of peroxisome proliferator-activated receptor γ co-activator-1 α (PGC-1 α) or PGC-1 β can attenuate muscle atrophy, and this has been attributed to a decrease in protein degradation (Brault, Jespersen & Goldberg, 2010; Sandri *et al.*, 2006).

This study investigated the role of PGC-1 α and PGC-1 β in protein synthesis in C2C12 myotubes. Myotubes were infected with GFP, PGC-1 α , or PGC-1 β adenoviruses, and protein synthesis was measured at basal levels and with dexamethasone treatment, by the uptake of [³H]-tyrosine.

PGC-1 α or PGC-1 β overexpression resulted in a 25-28% increase in protein synthesis. Dexamethasone decreased protein synthesis by 15% in the GFP-infected myotubes. However, overexpression of PGC-1 α or PGC-1 β was able to prevent the dexamethasone-induced decrease. Treatment with LY294, an inhibitor of PI3K/Akt, did not prevent the PGC-1 α or PGC-1 β driven increase in protein synthesis. This effect was therefore independent of Akt, a major kinase involved in muscle growth.

Another potential mechanism for the PGC-1 α and PGC-1 β driven increase in protein synthesis may be *via* their regulation of microRNAs (miRNAs). The expression of miR-1 and miR-133a, two miRNAs that are thought to play a role in muscle hypertrophy, were downregulated by PGC-1 α or PGC-1 β overexpression. Further studies will determine if these two miRNAs are involved in the regulation of protein synthesis with PGC-1 α and PGC-1 β overexpression.

Brault JJ, Jespersen JG & Goldberg AL. (2010) Peroxisome proliferator-activated receptor γ coactivator 1 α or 1 β overexpression inhibits muscle protein degradation, induction of ubiquitin ligases, and disuse atrophy. *Journal of Biological Chemistry* **285**, 19460-71.

Sandri M, Lin J, Handschin C, Yang W, Arany ZP, Lecker SH, Goldberg AL & Spiegelman BM. (2006). PGC-1 α protects skeletal muscle from atrophy by suppressing FoxO3 action and atrophy-specific gene transcription. *Proceedings of the National Academy of Sciences USA* **103**, 16260-16265.

Properties and amounts of heat shock proteins in skeletal muscle

N.T. Larkins, R.M. Murphy and G.D. Lamb, Department of Zoology, La Trobe University, VIC 3086, Australia.

Heat shock proteins (HSP) are considered to be important in protecting and maintaining cellular homeostasis by binding to partially denatured proteins and acting as molecular chaperones. α B-crystallin, HSP25 and HSP72 are thought to protect key components in skeletal muscle such as SERCA pumps or actin. In the present study, we have measured the amounts, diffusibility and activation characteristics of these proteins in fast-twitch (*extensor digitorum longus*) and predominantly slow-twitch (*soleus*) fibres from rat skeletal muscle.

Male Long-Evans hooded rats (6-8 months old) were sacrificed using a lethal overdose of isoflurane with approval of the La Trobe University Animal Ethics Committee, and the *extensor digitorum longus* (EDL) and *soleus* (SOL) muscles were excised. Muscles were either used for obtaining skinned fibre segments or homogenized and the entire muscle homogenate analysed using a quantitative Western blotting technique. To determine the absolute amounts of α B-crystallin, HSP25 and HSP72 in unstressed muscle, known amounts of pure HSP25, HSP72 and α B-crystallin were run on Western blots alongside or with the muscle homogenates samples (Murphy *et al.*, 2009) (see Table). From these measurements α B-crystallin is almost 29 times more expressed compared to HSP72 and ~13 time more than HSP25 in SOL muscle. These measurements of the absolute amounts of HSPs present give insight into the importance of α B-crystallin as well as the binding limitations and physiological function of Hsps in skeletal muscle.

To measure diffusibility, individual fibre segments were mechanically skinned, removing the surface membrane and allowing proteins to diffuse out of the fibre and into the bathing solution. The skinned fibre segment and the matched bathing solution were run on Western Blots and the diffusibility of α B-crystallin, HSP25 and HSP72 could be determined.

In unstressed muscle between 50 – 90% of HSP25, HSP72 and α B-crystallin appeared in the bathing solution within 10 min, indicating these proteins are broadly in rapid equilibrium with the cytoplasm in quiescent fibres. When a muscle was exposed to a potent oxidative stress of 10 mM H₂O₂ whilst pinned at room temperature, or bubbled with 95% O₂ at an elevated temperature (~31°C) for more than 1 hour, the diffusibility of α B-crystallin, HSP25 and HSP72 remained the same as that of an unstressed muscle.

Diffusibility was also investigated after a muscle was heated to 40°C for 30 min whilst pinned under paraffin oil. HSP25 and α B-crystallin became almost completely bound within the fibre, whereas HSP72 showed no change in diffusibility from that of an unstressed muscle. However when the temperature was raised to 45°C, HSP72 was no longer diffusible and became bound within the fibre. When fibre segments from a 40°C heated muscle were washed in the presence of 10 mM DTT, HSP25 and α B-crystallin remained bound and did not become diffusible, indicating the bonds between HSP25 or α B-crystallin and the target site was not a simple disulfide bond.

	Amount (μ mol/kg muscle \pm SEM)	
	EDL	SOL
HSP72	1.0 \pm 0.0	4.3 \pm 0.1
HSP25	2.8 \pm 0.3	8.9 \pm 1.3
α B-crystallin	3.3 \pm 0.8	123.9 \pm 16.7

Murphy RM, Larkins NT, Mollica JP, Beard NA, Lamb GD. (2009) *Journal of Physiology* **587**(2): 443-60.

Knockdown of STARS alters protein synthesis and degradation

M.A. Wallace and A.P. Russell, Centre for Physical Activity and Nutrition Research, School of Exercise and Nutrition Sciences, Deakin University, 221 Burwood Hwy, Burwood, VIC 3125, Australia.

Background and Aim: Striated muscle activator of Rho signalling (STARS) is a muscle specific actin-binding protein (Arai *et al.*, 2002). We have recently shown that STARS is up-regulated in hypertrophied human skeletal muscle following resistance exercise and is decreased following atrophy-stimulating detraining (Lamon *et al.*, 2009). STARS mRNA is also reduced in sarcopenic mice (Sakuma *et al.*, 2008). These studies suggest that STARS may be involved in skeletal muscle protein synthesis and/or degradation; however this has not been determined. Therefore, the aim of this study was to establish the role of STARS in protein synthesis and degradation in C2C12 myotubes.

Methods: STARS over-expression and knockdown in C2C12 myotubes was achieved using adenoviral infection and siRNA transfection, respectively. Myotubes were also treated with insulin (100nM) to promote protein synthesis or dexamethasone (DEX) (10 μ M) to promote protein degradation. Protein synthesis and degradation was determined by the amount of radio-labelled ³H-tyrosine incorporation into and release from the myotubes, respectively.

Results: STARS over-expression did not influence basal protein synthesis or degradation, nor did it influence insulin stimulated or dexamethasone attenuated protein synthesis. However, knockdown of STARS significantly reduced basal and insulin stimulated protein synthesis by 25%. Additionally, knockdown of STARS significantly increased basal and dexamethasone-induced protein degradation by 20% and 50%, respectively.

Conclusion: These observations show that STARS is necessary to maintain the fine balance between basal protein synthesis and degradation. Furthermore, a reduction in STARS reduces the influence of anabolic stimuli and enhances the effect of catabolic stimuli. A minimum amount of STARS may be required to sustain a healthy level of protein turnover.

- Arai A, Spencer JA, Olson EN. (2002). STARS, a striated muscle activator of Rho signaling and serum response factor-dependent transcription. *Journal of Biological Chemistry* **277**: 24453-24459.
- Lamon S, Wallace MA, Léger B, Russell AP. (2009). Regulation of STARS and its downstream targets suggest a novel pathway involved in human skeletal muscle hypertrophy and atrophy. *Journal of Physiology* **587**: 1795-1803.
- Sakuma K, Akiho M, Nakashima H, Akima H, Yasuhara M. (2008). Age-related reductions in expression of serum response factor and myocardin-related transcription factor A in mouse skeletal muscles. *Biochimica et biophysica Acta*. **1782(7-8)**: 453-61.

Expression of STIM and Orai in liver disease

C.H. Wilson,¹ G.Y. Rychkov² and G.J. Barritt,¹ ¹Department of Medical Biochemistry, School of Medicine, Flinders University, Adelaide, SA 5001, Australia and ²Department of Physiology, School of Medicine, The University of Adelaide, Adelaide, SA 5001, Australia.

Liver disease is one of the leading causes of death in people with type II diabetes. Disruption in Ca²⁺ homeostasis has been detected in numerous liver diseases. In hepatocytes, Ca²⁺ regulates glucose homeostasis, protein synthesis and lipid metabolism amongst other functions. Store-operated calcium entry (SOCE) plays a key role in maintaining intracellular Ca²⁺ and SOCE plays an important role in growth and differentiation of hepatocytes. Defects in this process may lead to the development of liver disease ranging from non-alcoholic steatosis, cirrhosis and cancer. STIM and Orai1 proteins are key components of SOCE and STIM1 and Orai are required for SOCE in primary hepatocytes (Jones *et al.*, 2008). STIM1 and Orai1 isoforms, STIM2, Orai2 and Orai3 may also be involved in disease altered SOCE. We hypothesize that defects in Ca²⁺ homeostasis associated with liver disease are due to abnormal expression, localization, and interaction of Orai1 with STIM1. In hepatocytes isolated from genetically obese (*fa/fa*) Zucker rats, a model of obesity and insulin resistance that develop steatosis, we previously detected a significant decrease in the amplitude of ISOC activated by 25 μ M ATP compared to the ISOC of lean Hooded Wistar rats. To assess whether this observation was due to altered gene expression, the mRNA levels of STIM1, Orai1 and their isoforms STIM2, Orai2 and Orai3 were compared between primary hepatocytes of Zucker obese and lean control rats. In addition, gene expression was determined in cultured H4IIE rat liver cancer cells treated with or without 100 nM insulin/dexamethasone to influence differentiation. Hepatocytes were isolated from Zucker rats anaesthetized with xylazine/ketamine followed by collagenase perfusion of the liver. Gene expression was measured by relative quantitative polymerase chain reaction (qPCR) and expressed relative to B-actin. Results revealed no difference in expression of STIM1, STIM2, Orai1 and Orai3 in hepatocytes from obese and lean Zucker rats. This suggests that the observed difference in SOCE is due to changes in the distribution of STIM and Orai proteins, not altered expression. Orai2 is only expressed at low levels in liver tissue and was difficult to detect in all samples. From measurements obtained it appears that there is a small increase in Orai2 expression in hepatocytes from obese Zucker compared with lean Zucker rats, suggesting that this might contribute to the observed altered SOCE current. Insulin and dexamethasone treatment of H4IIE cells resulted in a significant ($p < 0.05$) decrease in the levels of STIM2 and Orai3 accompanied by a decrease in STIM1 level, and increase in Orai1 levels. Orai2 was not detected. These initial findings suggest that STIM and Orai expression is altered in liver cancer and indicates their possible involvement in cellular differentiation. The complete absence of Orai2 indicates its possible loss in cancer tissue. Future assessment of expression levels in diseased human liver tissue samples compared to normal tissue will test whether this finding is physiologically relevant. Moreover, immunofluorescence microscopy will help determine if altered distribution of STIM1 is responsible for changes in ISOC of obese Zucker rats hepatocytes. Further work will be needed to determine whether a change in distribution occurs in livers of Type II diabetes patients that might lead to disruption of liver Ca²⁺ homeostasis and development of liver disease.

Jones BF, Boyles RR, Hwang SY, Bird GS, Putney JW. (2008). Calcium influx mechanisms underlying calcium oscillations in rat hepatocytes. *Hepatology* **48(4)**: 1273-81.

Molecular mechanisms of paracetamol induced liver damage

E. Kheradpezhoh, ¹ G.J. Barritt ² and G.Y. Rychkov, ¹ ¹School of Medical Sciences, University of Adelaide, Adelaide, SA 5005, Australia and ²School of Medicine, Flinders University of South Australia, Bedford Park, SA 5042, Australia.

Paracetamol (acetaminophen) is the most commonly used analgesic and antipyretic drug that is available over the counter in many countries, including Australia. At the same time, paracetamol overdose is the most common cause of acute liver failure and the leading cause of liver failure requiring liver transplantation in developed countries (Chun *et al.*, 2009). Paracetamol overdose causes a multitude of interrelated biochemical reactions in liver cells producing multitude of outcomes. Among those are covalent modification and inhibition of enzyme activity, protein oxidation, lipid peroxidation, DNA fragmentation, and deregulation of Ca²⁺ homeostasis, each contributing to paracetamol-induced liver damage (Jaeschke & Bajt, 2006). It has been known for a long time that paracetamol overdose causes a Ca²⁺ raise in hepatocytes; however, the importance of Ca²⁺ in paracetamol-induced liver toxicity is not well understood, primarily due to lack of knowledge about the source of Ca²⁺ rise (Thomas, 1993).

In this work we investigated the molecular pathways of Ca²⁺ entry activated by paracetamol in hepatocytes. Primary rat hepatocytes were isolated by liver perfusion with collagenase under general anaesthesia (intraperitoneal injection of pentobarbitone 50 mg/kg body mass). The experiments were conducted on cells maintained in culture for 24-48h. Cytoplasmic Ca²⁺ concentration ([Ca²⁺]_{cyt}) was measured using Fura-2 with the aid of a Nikon TE-300 inverted fluorescence microscope. Measurements of ion currents were conducted by standard patch clamping in whole cell mode using a computer-based EPC-9 patch-clamp amplifier and PULSE software.

Fura-2 experiments showed that application of 5 mM acetaminophen to the bath caused slow increase in [Ca²⁺]_{cyt} reaching levels above 1 μM in 45 min. Application of paracetamol in the absence of Ca²⁺ in the bath solution did not cause any changes in [Ca²⁺]_{cyt} suggesting that it activates Ca²⁺ entry across plasma membrane through Ca²⁺ permeable channels. In patch clamping experiments incubation of hepatocytes with 5-10 mM paracetamol for 30-60 min resulted in activation of a large linear non-selective cation current, which was inhibited by 20 μM clotrimazole, 100 μM chlorpromazin, 100 μM 2-APB, 5 μM N-(p-aminocinnamoyl)anthranilic acid (ACA), and 100 μM La³⁺. Similar current was activated by treatment of hepatocytes with 100-500 μM of H₂O₂ for 15-30 min. The selectivity and pharmacological profile of the channels activated by paracetamol and H₂O₂ were consistent with those of the Transient Receptor Potential Melanostatin (TRPM) 2 channel. TRPM2 is a non-selective cation channel expressed in many tissues and is activated by ADP ribose and H₂O₂. We confirmed the expression of TRPM2 in primary rat hepatocytes by western blotting and RT-PCR. To ascertain the molecular identity of the channel mediating non-selective cation current activated by paracetamol, the expression of TRPM2 protein was suppressed by a specific siRNA. SiRNA-mediated knockdown of TRPM2 in rat hepatocytes resulted in almost complete elimination of the current activated by either paracetamol or H₂O₂. These results suggest that TRPM2 may play a significant role in paracetamol toxicity and oxidative damage in the liver.

Chun LJ, Tong MJ, Busuttill RW, Hiatt JR. (2009) *Journal of Clinical Gastroenterology* **43**, 342-349.

Jaeschke H & Bajt ML. (2006) *Toxicological Sciences* **89**, 31-41.

Thomas SHL. (1993) *Pharmacology and Therapeutics* **60**, 91-120.

Mitochondria-induced hyperpolarization in mouse locus coeruleus neurons is dependent on Ca²⁺ entry but not intracellular Ca²⁺ release

R.B. de Oliveira, F.S. Gravina, A.M. Brichta, R.J. Callister and D.F. van Helden, School of Biomedical Sciences and Pharmacy, University of Newcastle, NSW 2308, Australia.

Locus coeruleus (LC) neurons are known to play a fundamental role in brain function, impacting on many physiological processes such as regulation of sleep and vigilance, learning and memory, behavioural flexibility, and a range of other functions (for review see Sara, 2009). Mitochondria are intracellular organelles that appear to be involved in vast range of different pathways, including energy production, neuronal death, oxidative stress, neurodegenerative diseases and their role in buffering intracellular Ca²⁺ and resultant impact on Ca²⁺-dependent pathways (Ishii, Hirose & Iino, 2006; Lehninger, Nelson & Cox, 2008). In rat LC neurons, it has been demonstrated that mitochondrial disruption caused an increase in intracellular Ca²⁺ and activation of Ca²⁺-activated K⁺ channels and resultant membrane hyperpolarization (Murai *et al.*, 1997). Here, we demonstrate that the hyperpolarization caused by mitochondrial disruption in mouse LC neurons is dependent on external Ca²⁺ entry and not dependent on increases in cytosolic Ca²⁺ concentration ([Ca²⁺]_c). The methods used for euthanizing mice were approved by the Animal Care and Ethics Committee at the University of Newcastle. The brain was rapidly removed with a slice containing the LC then prepared, allowed to equilibrate and placed on the stage of an upright microscope in a bath perfused with artificial cerebrospinal fluid (ACSF) at 35°C (de Oliveira *et al.*, 2010). Recordings were made from LC neurons using patch electrodes in whole cell recording mode. Mitochondrial disruption with the protonophore CCCP (1 µM) caused hyperpolarization or outward current in current and voltage clamp modes, respectively. This outward current was likely to be dominantly generated by Ca²⁺ activated K⁺ channels of the SK type, as the conductance was largely blocked by Apamin (1 µM). The outward conductance was dependent on external Ca²⁺ entry, as determined using Ca²⁺-free (0.5 mM EGTA) ACSF and Co²⁺ ACSF (Co²⁺ substituted for Ca²⁺) solutions. This conductance was not inhibited when an internal pipette solution containing a high concentration of the Ca²⁺ buffer EGTA (15 mM) was used, suggesting that [Ca²⁺]_c was not involved in its activation. Ca²⁺ imaging demonstrated that CCCP increased intracellular Ca²⁺ in both ACSF and the Ca²⁺-free ACSF. The latter observation combined with the finding that the CCCP-generated outward conductance was not activated in Ca²⁺-free ACSF confirmed that increases in cytosolic [Ca²⁺]_c *per se* did not activate the outward conductance. Taken together, these results demonstrate that hyperpolarization induced by mitochondrial disruption using the protonophore CCCP causes Ca²⁺ entry and resultant Ca²⁺-activated K⁺ conductance that is independent of intracellular Ca²⁺ release from stores, but is dependent on external Ca²⁺ entry. This suggests that activation of this conductance occurs in a microdomain.

- de Oliveira RB, Howlett MC, Gravina FS, Imtiaz MS, Callister RJ, Brichta AM & Helden DF. (2010). Pacemaker currents in mouse locus coeruleus neurons. *Neuroscience* **170**(1): 166-77.
- Ishii K, Hirose K & Iino M. (2006). Ca²⁺ shuttling between endoplasmic reticulum and mitochondria underlying Ca²⁺ oscillations. *EMBO Reports* **7**: 390-396.
- Lehninger AL, Nelson DL & Cox MM. (2008). *Lehninger Principles of Biochemistry*. W.H. Freeman, New York.
- Murai Y, Ishibashi H, Koyama S & Akaike N. (1997). Ca²⁺-activated K⁺ currents in rat locus coeruleus neurons induced by experimental ischemia, anoxia, and hypoglycemia. *Journal of Neurophysiology* **78**: 2674-2681.
- Sara SJ. (2009). The locus coeruleus and noradrenergic modulation of cognition. *Nature Reviews. Neuroscience* **10**: 211-223.

Calcium influx-activating action of P-EPTX-Ar1a: an isolated neurotoxin from the venom of Irian Jayan death adder

J. Chaisakul,¹ H.C. Parkington,² M.A. Tonta,² H.A. Coleman,² N. Konstantakopoulos¹ and W.C. Hodgson,¹

¹Department of Pharmacology, Monash University, Clayton, VIC 3800, Australia and ²Department of Physiology, Monash University, Clayton, VIC 3800, Australia.

We have isolated a fraction from Irian Jayan death adder (*Acanthopis rugosus*) venom, that we have shown displays pre-synaptic neurotoxic activity in chick neuromuscular junction *via* phospholipase A₂ activity (Chaisakul *et al.*, 2010). We called this fraction P-EPTX-Ar1a. Past studies have reported that many pre-synaptic snake neurotoxins increase cellular calcium by hydrolyzing the plasma membrane and generating lysophosphatidylcholine and fatty acids (Rigoni *et al.*, 2007; Tedesco *et al.*, 2009). In this study, we investigated whether P-EPTX-Ar1a changes cytoplasmic calcium in rodent dorsal root ganglion cells (DRG).

DRGs were isolated from embryonic day (E) 19 Wistar rats or E18 Swiss mice. Cells were isolated by gentle trituration, in the absence of digestive enzymes, and the cells were plated onto 9mm poly-ornithine/laminin coated glass coverslips and rested for 2 h in DMEM/F12 containing 5% fetal calf serum, 0.5 ng/ml nerve growth factor, 1:100 dilution N2 hormone supplement and 2ng/ml glial-cell derived nerve growth factor. The cells were washed and incubated in the calcium fluorophore Fluo-4-AM at 22°C for 10 min. The cells were then continuously superfused with Hanks solution flowing at 1ml/min at 35°C, and the experiment started after a 10 min wash. The snake toxin was added to the superfusate for 4 min. In separate experiments, the patch clamp technique was used in whole cell mode to record the effects of P-EPTX-Ar1a on membrane currents in DRG cells.

P-EPTX-Ar1a, 74nM, caused a prompt increase in cytoplasmic calcium in approximately one third of DRG neurons. The smaller diameter DRG cells were more vulnerable than those of larger diameter. Bursts of cytoplasmic calcium continued to occur throughout the 4 min application of the snake toxin. Following removal of the toxin, calcium bursting abated slowly. DRG cells were then exposed to calcium-free Hanks solution for 1min prior to and during snake toxin exposure. In this situation the increase in cytoplasmic calcium in response to toxin application was delayed by about 3min. Normal (1.3mM) calcium was re-introduced during the washout period and this caused prolonged bursts in cytoplasmic calcium in 98±2% of toxin-sensitive cells. Furthermore, the increase in cytoplasmic calcium in this situation was so large (equal to or exceeding that evoked by exposure to 100 K solution for 10 s) that many cells promptly withdrew projections and discontinued association with the glass coverslip. The increase in cytoplasmic calcium induced by snake toxin was unaffected by nifedipine or ω-conotoxin, which block L-type and N-type voltage-gated calcium channels, respectively. However, the response was blunted by agatoxin. Pretreatment with tetrodotoxin, which blocks voltage-gated sodium channels 1.1-1.4, 1.6, 1.7, completely prevented both the immediate increase in cytoplasmic calcium induced by snake toxin in calcium-containing Hanks solution and to the large delayed response following restoration of extracellular calcium, as described above. P-EPTX-Ar1a induced an inward current in DRG cells.

Like many other snake toxins, P-EPTX-Ar1a increases cytoplasmic calcium in neurons. The response is very difficult to reverse and the extent of the increase in cytoplasmic calcium can be sufficient to cause cell death within minutes. The underlying mechanisms may involve alteration of the activity of ion channels.

Chaisakul J, Konstantakopoulos N, Smith AI, Hodgson WC (2010). Isolation and characterisation of P-EPTX-Ar1a and P-EPTX-Ar1a. *Biochemical Pharmacology* **80**: 895-902.

Rigoni M, Pizzo P, Schiavo G, Weston AE, Zatti G, Caccin P, Rossetto O, Pozzan T, Montecucco C (2007). *Journal of Biological Chemistry* **282**: 11238-11245.

Tedesco E, Rigoni M, Caccin P, Grishin E, Rossetto O, Montecucco C (2009). *Toxicon* **54**: 138-144.

Alcohol-induced pancreatic trypsinogen activation depends on calmodulin-sensitive inositol trisphosphate receptors types 2 and 3

J. Gerasimenko, Cardiff University, School of Biosciences, Biomedical Sciences Building, Museum Avenue, Cardiff CF10 3AX, UK. (Introduced by A/Prof. G. Rychkov)

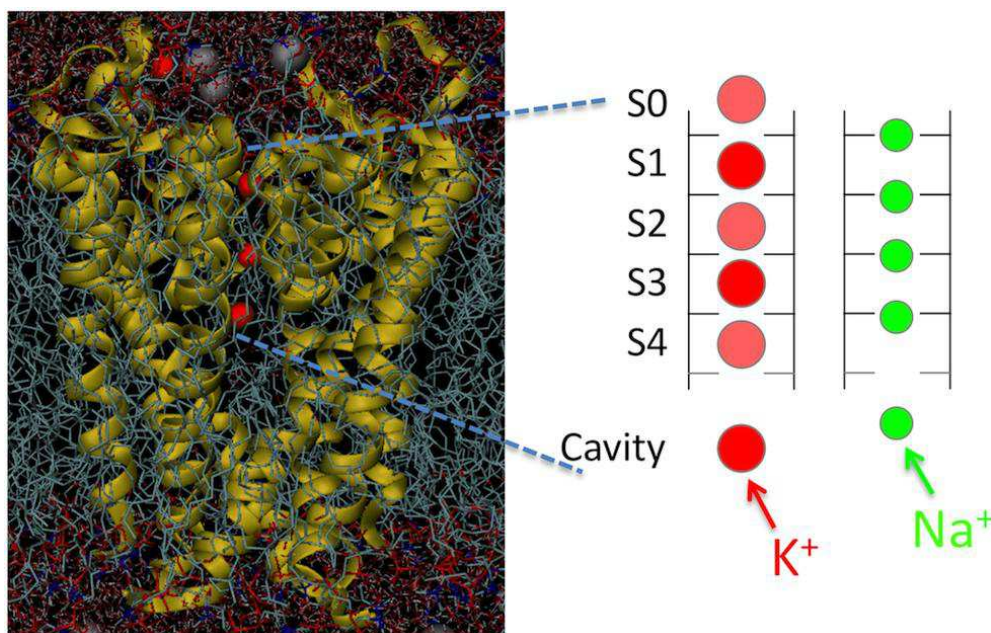
One of the major causes of acute pancreatitis is excessive alcohol intake; however the molecular mechanism of this severe inflammatory disease is not completely understood. Acute pancreatitis is generally initiated by premature trypsinogen activation in pancreatic acinar cells mediated by excessive intracellular calcium release from internal stores. We now show that in two-photon permeabilized mouse pancreatic acinar cells even a relatively low ethanol concentration elicits calcium release from intracellular stores and also induces intracellular trypsin activation. Adding the calcium sensor calmodulin (at a normal intracellular concentration) to the solution surrounding the permeabilized cells markedly reduced ethanol-induced calcium release and trypsin activation. Both ethanol-elicited calcium liberation and trypsin activation were significantly reduced in acinar cells from mice in which type 2 inositol trisphosphate receptors had been knocked out. Double knock out of inositol trisphosphate receptors of both types 2 and 3 further reduced ethanol-induced calcium release and trypsin activation to low levels. Thus the inositol trisphosphate receptor calcium release channels, that are responsible for normal pancreatic stimulus-secretion coupling, also play a major role in the toxic action of ethanol. Calmodulin provides a protective mechanism, regulating the sensitivity of the calcium release process.

Selective ion binding and its role in potassium channel selectivity

T.W. Allen, Department of Chemistry, University of California, Davis, One Shields Avenue, Davis, CA, 95616, U.S.A..

Ion channels catalyse rapid and selective ion movement across cell membranes to control electrical and chemical activity in the body. K^+ channels have the remarkable ability to pass K^+ ions at near diffusion-limited rates, while sensitively excluding Na^+ ions; a characteristic essential for membrane repolarization during action potentials. Since it was suggested, over 20 years ago (Neyton & Miller, 1988), that K^+ channel pores consisted of multiple K^+ -selective binding sites, and high resolution structures (Doyle *et al.*, 1998; Morais-Cabral *et al.*, 2001) subsequently revealed these sites, the prevailing view has been that K^+ channels select for K^+ ions *via* a mechanism of selective binding.

Recent molecular dynamics simulations (Figure, left), x-ray crystallography and patch clamping (Thompson *et al.*, 2009) have unveiled a putative Na^+ binding site within the K^+ channel selectivity filter, and new calculations (Kim & Allen, 2010) have demonstrated the existence of multiple such sites, leading us to question the hypothesis of selective permeation *via* selective binding. Each K^+ binding site (S0-S4, red balls in the Figure) consists of a cage of 8 carbonyl (or threonine OH for S4) oxygen ligands, made from two planar rings formed by the KcsA tetramer (only two subunits depicted as lines). Each of these sites is adjacent to one or two Na^+ binding sites, consisting of planar rings of 4 carbonyl oxygen atoms, as shown in the Figure (green balls). Free energy calculations indicate that these planar sites select for Na^+ over K^+ , and that the net selectivity for K^+ over Na^+ in the selectivity filter is much lower than previously calculated. These results suggest the need for a broader view of selectivity mechanisms, including possible kinetic entry barriers for Na^+ ions (Bezanilla & Armstrong, 1972), with fully-atomistic molecular dynamics simulations helping to reveal those barriers within the multiple-ion permeation process.



Bezanilla F & Armstrong CM. (1972). Negative conductance caused by entry of sodium and cesium ions into the potassium channels of squid axons. *Journal of General Physiology* **60**, 588-608.

Doyle D, Morais Cabral J, Pfuetzner R, Kuo A, Gulbis J, Cohen S, Chait B & MacKinnon R. (1998). The structure of the potassium channel: molecular basis of K^+ conduction and selectivity. *Science* **280**, 69-77.

Kim I & Allen TW. (2010). On the selective ion binding hypothesis for potassium channels. *In preparation*

Morais-Cabral JH, Zhou Y & MacKinnon R. (2001). Energetic optimization of ion conduction rate by the K^+ selectivity filter. *Nature* **414**, 37-42.

Neyton J & Miller C. (1988). Discrete Ba^{2+} block as a probe of ion occupancy and pore structure in the high-conductance Ca^{2+} -activated K^+ channel. *Journal of General Physiology* **92**, 569-586.

Thompson AN, Kim I, Panosian TD, Iverson TM, Allen TW & Nimigean CM. (2009). Mechanism of potassium-channel selectivity revealed by Na^+ and Li^+ binding sites within the KcsA pore. *Nature Structural and Molecular Biology* **16**, 1317-1324.

The induction and stabilization of transmembrane pores by peptides

A.E. Mark, School of Chemistry and Molecular Bioscience, The University of Queensland, St Lucia, QLD 4072, Australia.

Atomistic molecular dynamics simulation techniques have been used to examine the interaction of a range of pore-forming and cell-penetrating peptides with lipid membranes. Such systems are archetypical examples of self-organizing molecular systems leading to functional complexes. In general it had been assumed that the structures formed were highly regular. However, simulations of the spontaneous induction of transmembrane pores by the antimicrobial peptides Magainin and Melletin suggest that the pores are at least initially highly disordered casting doubt on the validity of current models (Leontiadou, Mark & Marrink, 2006; Sengupta *et al.*, 2008). In contrast in the case of the cell-penetrating peptides Penetrin and the TAT-peptide no spontaneous formation of transmembrane pores was observed. Instead, the simulations suggest that the peptides may enter the cell by micropinocytosis, whereby the peptides induce curvature in the membrane, ultimately leading to the formation of small vesicles within the cell that encapsulate the peptides (Yesylevskyy, Marrink & Mark, 2009).

Leontiadou, H, Mark, AE & Marrink, SJ, (2006) Antimicrobial peptides in action. *Journal of the American Chemical Society* **128**, 12156-12161.

Sengupta, D, Leontiadou, H, Mark, AE & Marrink, SJ.(2008) Toroidal pores formed by antimicrobial peptides show significant disorder. *Biochimica et Biophysica Acta - Biomembranes* **1778**, 2308-2317.

Yesylevskyy, S, Marrink, SJ & Mark, AE. (2009) Alternative mechanisms for the interaction of the cell-penetrating peptides Penetratin and the TAT peptide with lipid bilayers. *Biophysical Journal* **97**, 40–49.

Monitoring the conformational changes involved in MscL channel gating using FRET microscopy and simulation

B. Corry, School of Biomedical, Biomolecular and Chemical Sciences, University of Western Australia, Crawley, WA 6009, Australia.

Large scale conformational changes often play an essential role in the functioning of proteins, yet they can be hard to probe with experimental methods and take place over timescales that are difficult to simulate. We are using a combination of low resolution experimental techniques in combination with a variety of computational methods to try to understand the large structural rearrangements taking place in the gating of the mechanosensitive channel MscL. These bacterial channels open large pores in response to membrane tension in order to rescue the cell under osmotic shock. In this case we gain structural data on the protein in a natural environment using patch-clamp studies and confocal FRET microscopy. Combining this with existing EPR data as restraints in molecular and coarse grain simulations has allowed us to determine the likely structure of the open state of the pore. While there are many challenges to be overcome in this methodology, including careful approaches to labelling; control of the protein state; careful analysis of the orientation, geometry and number of fluorescent probes; and rigorous sampling of the conformational space; we believe that it provides a useful tool for studying the structures of a range of membrane proteins in natural environments.

Free energy simulations of Asp/Glu transporter GltPh

S. Kuyucak and T. Bastug, School of Physics, University of Sydney, NSW 2006, Australia.

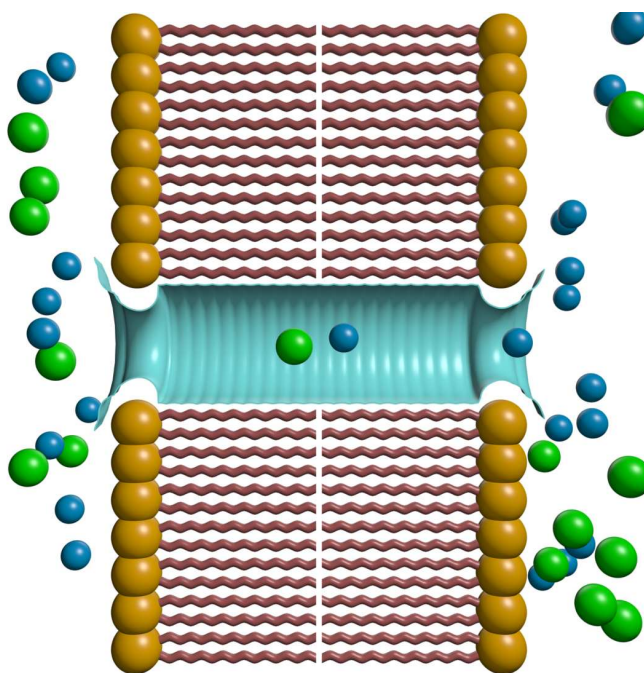
Glutamate is the dominant excitatory neurotransmitter in the brain. Its extracellular concentration is kept at the nanomolar level by glutamate transporters – membrane proteins that continuously pump glutamate back to the neurons using the existing ionic gradients. Because small changes in glutamate concentration have major effects in signaling in the brain, glutamate transporters are key targets for treatment of various neurological conditions. Here we use the recently determined bacterial transporter structure GltPh in MD simulations to delineate the basic steps involved in glutamate transport and provide a structural basis for the transport mechanism. We have confirmed the binding sites Na1, Na2 and Asp, suggested by the experimental structure, and found a third Na ion binding site (called Na3), which is critical for the functioning of the transporter. This also strengthens the case for constructing homology models for human glutamate transporters (EAAT1-5) from the GltPh structure. Our proposed binding site for Na3 is completely consistent with the structural data, which is not the case for other proposed sites.

We have calculated the binding free energies for Na ions and Asp in various configurations and thus determined the order of binding as Na3, Na1, Asp, Na2 (following the notation used in the crystal structure). To understand the selectivity of GltPh for Asp, we have performed free energy perturbation calculations for the transformation Asp to Glu and found a selectivity free energy barrier of 4-5 kcal/mol consistent with the experimental observations. This is basically caused by steric interactions - the larger sidechain of Glu does not quite fit in the binding site. Once we understand the operation of the bacterial transporter, we will create a homology model for the mammalian glutamate transporter EAAT1 and investigate similarities and differences in the transport mechanism with the bacterial one, following steps similar to above.

Mimicking biological ion channels using nanotubes

T.A. Hilder, D. Gordon and S.H. Chung, Computational Biophysics Group, Research School of Biology, Australian National University, Canberra, ACT 0200, Australia.

Biological ion channels are selectively permeable to specific ionic species, and regulate the flow of ions across the cell membrane. They maintain the resting membrane potential, generate propagated action potentials in nerves and control a wide variety of cell functions. We report that hollow nanotubes constructed from carbon atoms, and with hydrogen, carbonyl or carboxylic acid terminated ends, have the ability to mirror some of the important functions of various biological ion channels. In particular, these carbon nanotubes (CNTs), embedded in a lipid bilayer (illustrated in Figure), are selectively permeable to cations or anions, depending on their terminated ends and diameter. They broadly mimic some of the permeation characteristics of the antibiotic gramicidin, chloride channels, and the mutant glycine receptor.



Using a combination of molecular and stochastic dynamics simulations (see Gordon *et al.*, 2009 for details), we characterize certain properties of these engineered nanotubes, such as the free energy profiles encountered by charged particles, the current-voltage-concentration profiles and the overall conduction mechanism. We demonstrate that CNTs can be designed such that they are selective to either cations or anions by modifying their surface chemistry. In particular, we discuss three CNTs with a length of approximately 36 Å and varying surface chemistry, namely (i) with a radius of 4.53 Å and terminated with carbonyl groups (see Hilder *et al.*, 2010 for details); (ii) with a radius of 4.53 Å and terminated with hydrogen and with two regions near the entrance and exit of the nanotube exohydrogenated (outside surface hydrogenation); and (iii) with a radius of 5.08 Å and terminated with carboxylic acid. These CNTs are shown to broadly mimic the permeation characteristics of (i) the CIC-1 chloride channel and GABA_A but with conduction rates 4 times and 2 times larger, respectively (see Hilder *et al.*, 2010 for details); (ii) the antibiotic gramicidin but with a potassium current 6 times larger; and (iii) the mutant glycine receptor in which anions chaperone sodium across the channel (illustrated in Figure) but with a sodium conductance 7 times larger. These synthetic nanotubes may lead to a host of pharmaceutical products to assist in treatments such as antibacterial, cancer and cystic fibrosis in addition to potential applications as sensitive biosensors.

Hilder, T.A., Gordon, D. and Chung, S.H. (2010) *Biophysical Journal*, **99**: in press.

Gordon, D., Krishnamurthy, V. and Chung, S.H. (2009) *Journal of Chemical Physics*, **131**: 134102.

Multi-drug efflux by P-glycoprotein; why has this protein not been stopped yet?

R. Callaghan,¹ R. Ford,² M. O'Mara³ and I.D. Kerr,⁴ ¹Nuffield Department of Clinical Laboratory Sciences, John Radcliffe Hospital, University of Oxford, Oxford OX3 9DU, United Kingdom, ²Faculty of Life Sciences, Manchester Inter-disciplinary Biocentre, University of Manchester, Manchester M1 7DN, United Kingdom, ³Molecular Dynamics Group, School of Chemistry and Molecular Biosciences, University of Queensland, Brisbane, QLD 4072, Australia and ⁴Molecular Dynamics Group, School of Chemistry and Molecular Biosciences, University of Nottingham, Queen's Medical Centre, Nottingham NG7 2UH, United Kingdom,.

Several ATP-Binding Cassette (ABC) transporters confer resistance to chemotherapy used in the treatment of cancer, bacterial infections and numerous parasitic infections. These proteins confer resistance by preventing the attainment of sufficient intracellular concentrations of cytotoxic drugs through active efflux. This efflux based resistance mechanism is simple, yet highly effective and a widely used strategy. The efflux pumps share the ability to bind, and translocate, a large number of functionally and chemically unrelated drugs. Consequently, the transporters have been collectively grouped as multidrug efflux pumps and share a common structural organisation. Each fully functional efflux pump contains two transmembrane domains (TMD) and two cytosolic nucleotide binding domains (NBD). The TMDs constitute the drug recognition sites and the translocation pathway through the membrane, whilst the NBDs provide energy for translocation (against large concentration gradients) from ATP hydrolysis.

P-glycoprotein (P-gp or ABCB1) is the archetypal multidrug efflux pump from the ABC family and has been established to confer resistance in numerous solid and blood-borne cancers. Given its prevalence and burden to chemotherapy, this protein has been the subject of intensive investigation for over three decades. Its astonishing ability to interact/translocate over 200 compounds has been suggested as a biological enigma. The research in our laboratories has a central objective to provide a molecular mechanism of drug translocation by P-gp. We have utilised biochemical, pharmacological and biophysical approaches to reach this objective and focussed on three specific areas:

How does P-gp bind so many compounds? Convention dictates that substrate binding requires high affinity, directional and selective chemical interactions with the protein. Should this be upheld by P-gp it may require the presence of multiple drug binding sites. Alternatively, the protein may have evolved a binding site capable of mediating the translocation of substrates without the requirement of specific interactions. We have adopted a pharmacological strategy to explore the nature of multi-drug binding by P-gp and two related drug efflux pumps. P-gp does indeed interact with substrates/inhibitors with high affinity and at multiple pharmacologically distinct sites. Moreover, the sites form a complex allosteric communication network.

What is the mechanism coupling drug binding with energy provision? P-gp is able to hydrolyse nucleotide in the absence of any bound substrate and was initially suggested to be an uncoupled transporter. However, the presence of drugs increases the rate of hydrolysis several-fold in a manner suggestive of coupling between domains. Furthermore, there are numerous two-way communication pathways between the drug binding sites and NBDs. We have detailed the involvement and nature of these pathways during the translocation process.

What topographical alterations occur during drug translocation? Structural and biophysical approaches have demonstrated large conformational changes within the TMDs in response to events at the NBDs. It is also clear that TM helices 6 and 12 are intimately involved in propagating this inter-domain coupling. We have demonstrated a number of local topographical changes in TM6/12 and that the two helices mediate their effects in a drug specific manner, indicating multiple communication routes.

Data from these research investigations have been assimilated into a potential translocation mechanism for P-gp, which may form a template for multidrug transport by ABC proteins.

Metabolic regulation in exercise: mechanisms and experimental models

E.A. Richter, Molecular Physiology Group, Department of Exercise and Sport Sciences, University of Copenhagen, 13 Universitetsparken DK-2100, Denmark.

During exercise utilization of glucose and fatty acids as well as of glycogen and intramuscular lipids is increased. In skeletal muscle exercise elicits changes in molecular signaling that partly control these changes in fuel utilization; however, the knowledge of this intricate interplay between different molecular signaling pathways is quite limited. In addition, the results of the various experiments are often hard to reconcile because they depend heavily upon whether the results are obtained *in vitro* or *in vivo* and whether experiments have been performed in cells, animals or humans.

The AMP activated protein kinase (AMPK) has received much attention as a master regulator of metabolism in cells, including muscle cells during exercise. AMPK activity is increased in contracting muscle in an intensity dependent manner, but to a smaller extent in women than in men when exercising at the same relative intensity. This is likely due to a higher proportion of oxidative type 1 fibers in muscles in women, and a lesser disturbance of energy status during exercise. Studies with various transgenic and knockout models of AMPK deficiency have yielded conflicting results as to the importance of AMPK for regulation of glucose uptake during exercise, whereas lipid metabolism quite clearly is not regulated by AMPK. In addition, results obtained *in vitro* sometimes do not agree with results obtained *in vivo* likely reflecting the enormous complexity of the *in vivo* whole body exercise response compared to the reductionist models *in vitro*. Finally, the obvious rather large differences between mouse and man are likely also of importance for interpretation of experimental findings.